167
6-3-76

DR-137

GENERAL ATOMIC

GA-A13833
UC-77

THORIUM UTILIZATION PROGRAM

QUARTERLY PROGRESS REPORT
FOR THE PERIOD ENDING FEBRUARY 29, 1976

Prepared under
Contract E(04-3)-167
Project Agreement No. 53
for the San Francisco Operations Office
U.S. Energy Research and Development Administration

GENERAL ATOMIC PROJECT 3225

DATE PUBLISHED: MARCH 31, 1976

DISCLAIMER

QUARTERLY REPORT SERIES*

GA-A13178 - June 1974 through August 1974

GA-A13255 - September 1974 through November 1974

GA-A13366 - December 1974 through February 1975

GA-A13510 - March 1975 through May 1975

GA-A13593 - June 1975 through August 1975

GA-A13746 - September 1975 through November 1975

*Prior to GA-A13178, the Thorium Utilization Program was reported in the Base Program Quarterly Progress Report.

ABSTRACT

This publication continues the quarterly series presenting results of work performed under the National HTGR Fuel Recycle Program (also known as the Thorium Utilization Program) at General Atomic Company. Results of work on this program prior to June 1974 were included in a quarterly series on the HTGR Base Program.

The work reported includes the development of unit processes and equipment for reprocessing of High-Temperature Gas-Cooled Reactor (HTGR) fuel and the design and development of an integrated line to demonstrate the head end of HTGR reprocessing using unirradiated fuel materials. Work is also described on the development of the conceptual design of recycle facilities to identify the requirements of large-scale recycle of HTGR fuels and to incorporate the results of these studies in guidance of development activities for HTGR fuel recycle.

INTRODUCTION

This report covers the work performed by General Atomic Company under U.S. Energy Research and Development Administration Contract E(04-3)-167, Project Agreement No. 53. The work done under this project agreement is part of the program for development of recycle technology for High-Temperature Gas-Cooled Reactor (HTGR) fuels described in the "National HTGR Fuel Recycle Development Program" (ORNL 4702).

The objective of the program is to provide the necessary technology, development, engineering, and demonstration of the steps required in the economic recycle of HTGR fuels utilizing thorium as a fertile material. Work at General Atomic Company is concentrating on the development of reprocessing methods (Subtask 110 of the National Program), reprocessing pilot plant support (Subtask 120), refabrication pilot plant support (Subtask 220), and engineering and economic studies (Subtask 310).

The objectives of Subtask 110, Reprocessing Development, are to develop the necessary technology for the construction and operation of a prototype reprocessing facility which will process irradiated fuel materials and to provide the capability for commercial recycle of HTGR fuels. The output of this subtask includes (1) definition of process flowsheets, (2) development of equipment components, and (3) definition of operating data.

The objectives of Subtask 120 are to perform process review studies to provide reference reprocessing flowsheet definition; evaluate development activities within Subtasks 110 and 310 to determine the need for reference flowsheet revision; and assess the development status of key reprocessing equipment systems.

The objectives of Subtask 220 are to perform process review studies to provide reference refabrication flowsheet definition; evaluate development

activities within Subtasks 110 and 310 to determine the need for revision of the reference flowsheet; and identify additional development requirements.

The objectives of Subtask 310 are to guide the development program from the viewpoint of overall recycle needs and to obtain an economical HTGR fuel recycle method for early recovery and use of bred U-233. Alternate methods and options for reprocessing and refabrication are evaluated, and recommendations are made for possible further experimental development.

This report has been published using customary units only. Conversion to dual dimensioning or SI units only will be made gradually to minimize the impact on costs and schedule.

CONTENTS

FIGURES

FIGURES (Continued)

FIGURES (Continued)

FIGURES (Continued)

TABLES

TABLES (Continued)

TABLES (Continued)

1. SUMMARY

Work on the Program proceeded in the last quarter essentially as scheduled with significant progress in all areas. Minor delays have been encountered but the major milestones for the year are still expected to be met.

Eight summary reports containing design calculations for the UNIFRAME size reduction system were distributed to program participants and ERDA at a design readiness review meeting. Installation is on schedule with the main machine frame and stationary jaws already assembled.

Installation of bunker assemblies and the electrical control system for the materials transfer system on the prototype reprocessing line is now under way. Thermal effects due to discharge of hot burner products into the transport systems are being re-examined to ensure successful operation.

Fabrication of both prototype burner vessels is nearing completion; installation of heating and cooling systems and vessel shrouding is under way. A definition of control modes, operating procedures, and operating cycles for these burners is provided.

Installation of the rebuilt 20-cm primary burner has been completed. Shakedown tests of the induction heating system have verified wall heatup to 900°C using the empty burner tube. Inert and fresh feed bed heatup and startup testing awaits final instrumentation connections with the Diogenes semiautomatic controller.

The experimental plan for the rebuilt 20-cm primary burner includes confirmation of the prototype design configuration and control functions developed to date, as well as continuing development investigation of

alternate fines recycle modes and control functions that may improve the process simplicity and economics.

Cold fluidization studies were performed in a simulated 20-cm glass primary burner to investigate primary burner fluidization characteristics. Twenty beds ranging in size from 10 to 40 kg and in composition from -3/16 in. fresh feed (17 wt % particles) to 100% particles were fluidized at 0 to 4.5 ft/sec. Work was performed with the actual distributor (90° perforated cone with 1/2-in. diameter vertex) that had been used on the 20-cm primary burner prior to the recent rebuild of the system.

Fabrication of the prototype secondary burner is nearing completion. Fourteen of nineteen major assemblies are completed. Manufacturing difficulties encountered in the construction of this system and their resolution are discussed in this report. Further studies on the secondary burning process have been completed and were presented at a design readiness review meeting for ERDA and other program participants.

Seventeen steam jet transfer runs were made in studies to test jet configurations for transferring leacher slurries. The tests were made using a mixture of water and SiC hulls or simulated whole fuel particles. All runs using a submerged jet were successful. Runs using an elevated jet with dilution water injected into the jet suction experienced excessive jet pluggage.

No feed adjustment runs were made during the past quarter in the pilot plant equipment. Additional sample analyses were obtained on runs made the previous quarter and the data gathered were reanalyzed. The reanalyses indicate that there is no significant difference between steam and water as stripping agents.

Sixteen bench-scale feed adjustment runs were made during the quarter. In continuous runs (continuous feed and continuous product removal) at a 135° B.P. using leacher solution diluted with an equal volume of water and steam sparging, it was not possible to achieve acid deficiency. It was

possible, however, to achieve acid deficiency in continuous operation with undiluted leacher solution when formic acid was continuously added. Runs with 1BT feed (thorium product from the partition solvent extraction column) demonstrated acid deficiency can be achieved on a continuous basis with (1) no steam or formic acid addition at a pot temperature of 135°C or (2) water and formic acid addition at a pot temperature of 125°C. It was not possible to render concentrated 1BT acid deficient continuously without formic acid addition.

Bench-scale studies were initiated to determine the limiting temperature for abrupt reactions between highly degraded solvent ("red-oil") and thorium nitrate. Preliminary findings suggest that the current diluent (NPH) is more resistant to "red-oil" formation than the diluents used in prior studies by other investigators.

Solvent extraction runs 49 and 50 were completed during the quarter. These runs represented the first cycle of the acid-Thorex flowsheet. Each of the runs was made using the facilities in the pilot plant five-column system. The runs included the addition of nonradioactive and radioactive zirconium. Dibutyl phosphate (DBP) was added to the 1A column to simulate solvent degradation.

The results of these two runs confirm that feed made up from leached, burned fertile kernels gives poorer Zr-95 decontamination in solvent extraction (a factor of 2 to 5) than does feed prepared from purchased thorium nitrate. Further work is under way to resolve whether this observed difference will be significant with high radiation solvent damage in the first cycle of the HRDF.

A number of fixtures have been designed and fabricated to aid in the construction and assembly of unit operations in the prototype line and to demonstrate techniques which will be required for remote disassembly of operating equipment in a production-scale reprocessing facility. These fixtures are actually to be employed in a semiremote fashion in which manual manipulations are presently required but for which manipulators and other

remotely operated devices could be used to perform similar operations in a large-scale facility. Progress in the manufacture of these fixtures is described.

A critical review of current development activities and engineering studies has been completed to provide a basis for reconfirmation of the reference flowsheet and to identify additional development requirements. Studies of specific facility requirements in a large-scale recycle facility are continuing; this report includes an evaluation of the activity in recovered thorium and its impact on long-term storage and refabrication requirements.

An evaluation of disposal methods for irradiated graphite reflector blocks has been performed. Shipping by truck appears to be more economical than by rail for transportation of irradiated reflector blocks. Final disposal by burial will be more economical than handling in a reprocessing facility if the reflector elements are not classified as transuranic-bearing wastes. If reflector blocks are classified as transuranic waste, processing would be economically feasible.

2. FUEL ELEMENT CRUSHING

2.1. INTRODUCTION

A size reduction system, designated UNIFRAME (Fig. 2-1), has been proposed for reducing spent HTGR fuel and control rod elements to a suitable feed for fluidized-bed burning to separate the fuel and graphite for subsequent fissile material recovery. The design and procurement of a full-scale prototype of this system are under way.

The UNIFRAME system comprises five major equipment items, arranged in an array that utilizes gravity flow, eliminates the need for intraequipment material transport devices, and provides a continuous size reduction process without recycle.

The major equipment items are:

1. Primary crusher: an overhead eccentric jaw crusher for reducing the elements to <6-in. ring-sized fragments.

2. Secondary crusher: an overhead eccentric jaw crusher for further reduction of the fragments to <2-in. ring-sized fragments.

3. Tertiary crusher: a double-roll crusher for final reduction of the fragments to <3/16-in. ring-sized product.

4. Screener: a vibratory screener-separator for separating the acceptable product from any oversized fragments.

5. Oversize crusher: an eccentrically mounted single-roll crusher for reduction of oversize fragments to acceptable product size.

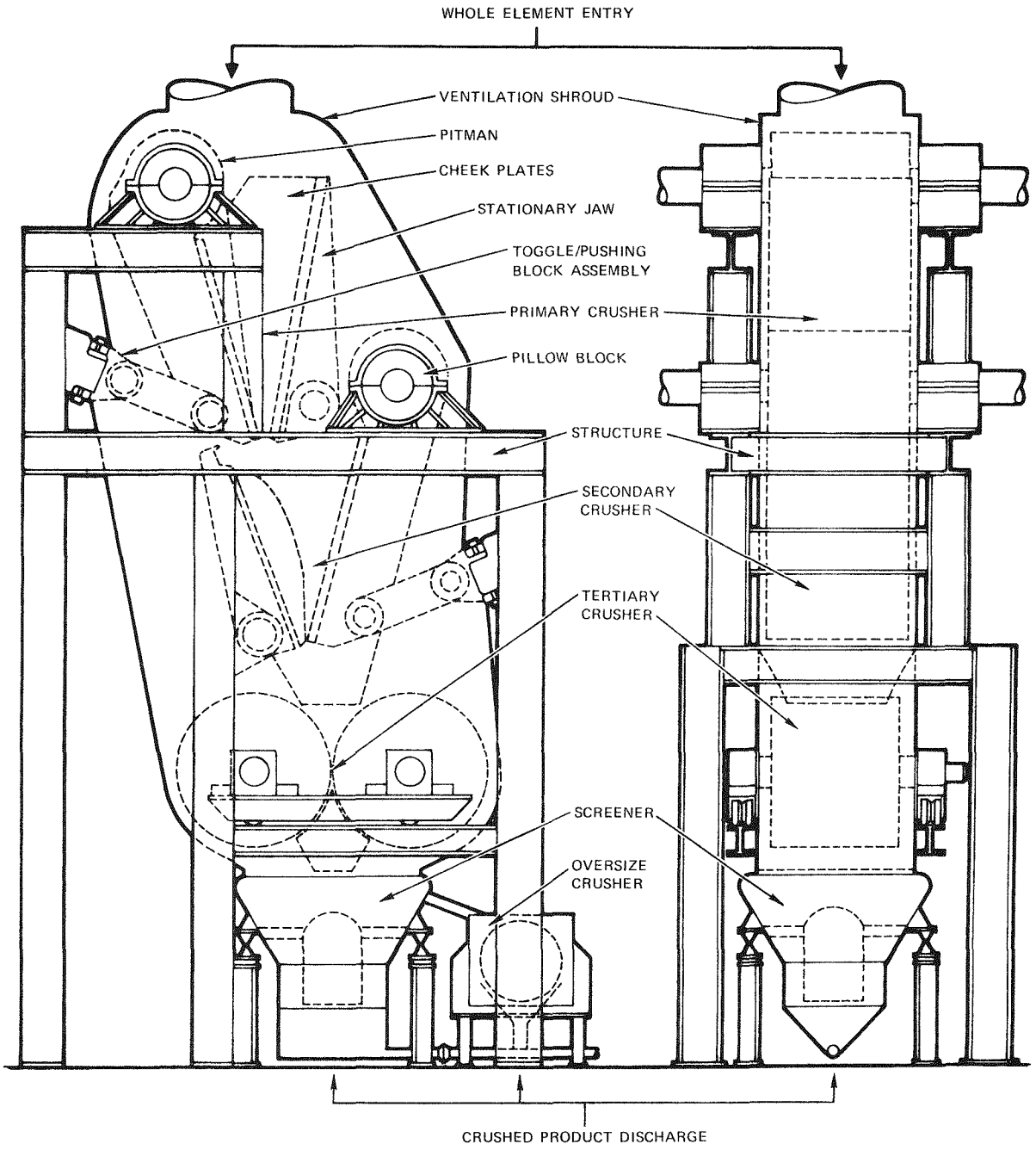

Fig. 2-1. UNIFRAME size reduction system

The components of the UNIFRAME system have been categorized into five subsystems to provide a logical plan for the design efforts. These subsystems are:

1. Structural: the special framework replacing standard machine frames to enable an efficient array of the equipment.

2. Ventilation: the enclosure that provides containment and collection of radioactive materials and dusts while minimizing the surfaces exposed.

3. Lubrication: the standard and special lubrication and bearings for equipment that make it more reliable and compatible with the radioactive environment and the remote operation requirements.

4. Drive: the standard and special drive components required to make the UNIFRAME system compatible with remote operation requirements and the radioactive environment.

5. Mechanical: the standard and special components required to make the major equipment items compatible with the structural, ventilation, and remote operation requirements.

2.2. DOCUMENTATION

To date the following control documents have been issued.

Document No.	Title
DC-521002, Issue A	Design Criteria - Fuel Element Size Reduction System
SD-521001, Issue A	System Description - Fuel Element Size Reduction System

Document No.	Title
PF-521001	Process Flow Diagram - Fuel Element Size Reduction System
PI-521001	Piping & Instrumentation Diagram - Fuel Element Size Reduction System

During February a presentation of the UNIFRAME project status was made to ERDA, ACC-ICPP, and ORNL. For this presentation, the following reports were written and distributed.

1. Project Summary Report
2. Primary Crusher Report
3. Secondary Crusher Report
4. Tertiary Crusher Report
5. Oversize Monitoring System Report
6. Ventilation Subsystem Report
7. Drive Subsystem Report
8. Structural Subsystem Report

Abstracts of each of these reports are given below.

2.1.1. Project Summary Report

This report presents, in summary form, the general status of design, procurement, and installation; the performance characteristics of the system; and a time schedule for evolutionary improvements in design.

2.1.2. Primary Crusher Report

This report presents the design criteria for the primary crusher and a discussion of the design features which satisfy these criteria. A summary of supporting calculations is provided.

2.1.3. Secondary Crusher Report

This report presents the design criteria for the secondary crusher and a discussion of the design features which satisfy these criteria. A summary of supporting calculations is provided.

2.1.4. Tertiary Crusher Report

This report presents the design criteria for the tertiary crusher and a discussion of the design features which satisfy these criteria. A summary of supporting calculations is also provided.

2.1.5. Oversize Monitoring System Report

This report describes the design of that portion of the UNIFRAME system between the tertiary crusher and the pneumatic transport system. This portion of the UNIFRAME system, termed the oversize monitoring system, consists of the vibratory screener/separator, rate sensor, and oversize pulverizer. As the name suggests, the purpose of the oversize monitoring system is to monitor the performance of the UNIFRAME system and to prevent any oversize tertiary crusher product from entering the transport system and reaching the primary burner feed hopper.

2.1.6. Ventilation Subsystem Report

The purposes of the ventilation subsystem are: (1) to provide the means for confining the crushed materials and dusts, (2) to prevent the spread of radioactive materials to the environs outside the UNIFRAME system, and (3) to demonstrate the ability to minimize material losses in an experimental program, thus ensuring optimal accountability of special nuclear materials in future hot cell applications. This report describes the design features of the subsystem and how they satisfy the above criteria.

2.1.7. Drive Subsystem Report

The UNIFRAME drive system for the pilot plant is composed of the necessary drives for powering the three size reduction stages, the screener, and the oversize crusher. It is not prototypical to the drive system for the hot demonstration facility.

The primary, secondary, and tertiary crusher drives are mounted on a common structure, which is anchored to the floor apart from the monolithic foundation of the UNIFRAME. The drives for the screener and for the oversize crusher are separate and independent, with the screener drive totally enclosed within the screener structure. This drive is discussed in detail in the screener report. The oversize crusher drive is identical to that recommended by the crusher manufacturer. In all cases, the drives are powered by single speed, alternating current, electric motors.

2.1.8. Structural Subsystem Report

This report describes the design of the support structure which replaces the standard machine frames. In addition, it presents the structural analysis methods, the design factors, and the reliability and maintainability incorporated into the design.

2.3. CURRENT STATUS

2.3.1. Major Equipment Items and Subsystem Designs

Design of all of the major equipment items and the subsystems is complete with the exception of the ventilation enclosure. This enclosure will be field constructed; therefore, approved drawings will be issued on the as-built construction.

2.3.2. Procurement

All components of the UNIFRAME system have been received except the structural steel for the drive stand.

2.3.3. Installation

The following items have been installed:

1. Foundation
2. Foundation pads
3. UNIFRAME machine frame
4. Primary crusher stationary jaw
5. Secondary crusher stationary jaw

Work has begun on installation of the tertiary crusher and its support frame.

The primary and secondary pitman assemblies were prefitted at the frame fabricator's facility for locating the pillow blocks and match-drilling the pushing block - pushing beam assemblies.

3. SOLIDS HANDLING

Testing of the pneumatic transport test system was interrupted for modifications to the system to enable testing the secondary burner product removal system.

A study of the thermal effects of hot burner products on the pneumatic transfer system was begun.

Procurement of the equipment for the prototype pneumatic transfer systems is nearing completion. Installation of the electrical control system is continuing, and installation of the bunker assemblies has been started.

A design readiness review meeting was held with ERDA, ICPP, and ORNL on the prototype solids handling system and the classification system.

Installation of the pneumatic classifier will coincide with installation of the pneumatic transport system.

Solids properties testing is continuing, with a majority of the particulate systems tested. The need for such testing is recognized to be important because of the need for functionally correct and reliable storage and flow of particulate material in the head-end flowsheet.

3.1. PNEUMATIC TRANSPORT

Transfer of the particulate solids between and around the unit operation in the head-end prototype reprocessing system will be pneumatic transport. With respect to this mode of material transfer, there is an ongoing evaluation of the criteria, equipment, and operation.

A study of thermal effects in the pneumatic conveying systems in the pilot plant has commenced. Products of both the primary and secondary burners, at elevated temperatures, will enter a stream of conveying gas at ambient temperatures. Since the discharge of both burners will be batch as opposed to continuous, the heat transfer to conveying lines, bunkers, and filters will be predominantly transient rather than steady state.

It is important to know what happens to the heat leaving the burners for the following reasons:

1. Prevention of excessive particle breakage.

2. Prevention of overloading the blowers.

3. Calculation of heat release to building.

4. Prevention of disturbance to downstream operations (e.g., pneumatic classification).

Hot cell operation will add extra dimensions since the fuel blocks will be at a raised temperature and fission product decay will be a source of extra heat. Consequently, more of the handling systems will be involved.

The first system to be studied in detail is the primary burner product removal system. Thermo-physical data on burned-back BISO and TRISO particles have been used to assess the heat content of flows of various rates and compositions leaving the burner. The temperature of the conveying gas affects the velocity, which in turn governs the particle breakage and the pressure drop. The heat not removed in the conveying system must be reduced to acceptable levels in the systems that follow prior to pneumatic classification.

3.1.1. Pneumatic Transport Test System

Upon completion of the testing of the crushed graphite (Ref. 3-1), the test system was remodeled for testing of the secondary burner product removal system. The remodeling encompassed not only the piping of the system to accommodate the radioactive material (Fig. 3-1) but also the electronics. Since the flow of material from the secondary burner is a function of the bed weight, a method for recording the process variables (absolute pressure and pressure drop) was needed. Four two-pen recorders, which receive their input from pressure transducers, were mounted into a central control cabinet. In addition to these instruments, the remaining electrical controls were relocated in the cabinet. The installation of the central control cabinet is nearing completion, with testing of the secondary burner product following immediately after the checkout testing.

3.1.2. Prototype Pneumatic Transport System

3.1.2.1. Description

The prototype pneumatic transport system has been designed to link the unit operations in the head-end to produce an integrated process. As a result, the transport system encompasses both the feeding and product withdrawal interfaces for each unit operation. To optimize each operation, hence the process as a whole, surge bunkers were specified where needed. To facilitate the design and description of the transport system, it was broken down into eleven subsystems which are described in Table 3-1 and shown in Fig. 3-1.

3.1.2.2. Design

Design of the prototype pneumatic transport system was completed during the fourth quarter of 1975, and has been documented in eleven design calculation reports (one for each subsystem).

TABLE 3-1
SOLIDS HANDLING SUBSYSTEMS

Subsystem	Title	Function
1	Crusher product removal	Removes crusher product from the bottom of the UNIFRAME crushers and feeds the material to the product bunker
2	Crusher product bunker	Provides surge capacity between the UNIFRAME and the primary burner
3	Primary burner feed bunker	Feeds material to the primary burner on demand
4	Primary burner product removal	Aids in the removal and transfer of fuel particles from the primary burner to the product bunker
5	Primary burner product bunker	Provides surge capacity between the primary burner and the pneumatic classifier and allows recycle to the primary burner
6	Air classifier feed bunker	Feeds material to the pneumatic classifier for separation of fertile and fissile fuel particles
7	Air classifier product bunker	Receives the separated fuel particles
8	Air classifier filter vessel	Provides secondary filtration for the pneumatic classifier
9	Particle crusher feed bunker	Feeds fuel particles to the particle crusher
10	Secondary burner product removal	Aids in the removal and transfer of material from the secondary burner to the product bunker
11	Secondary burner product bunker	Provides surge capacity between the secondary burner and the dissolver-leacher

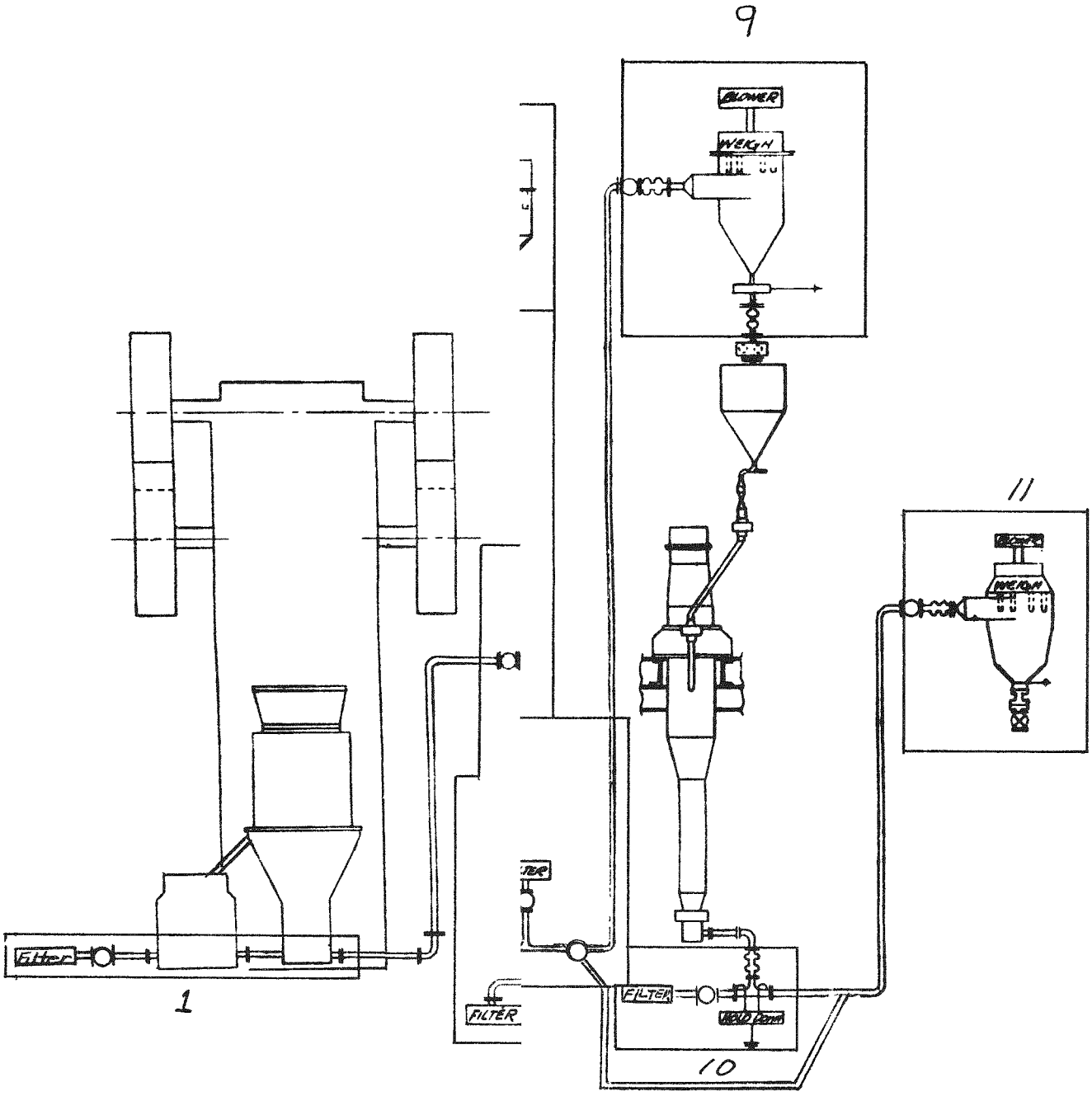

Fig. 3-1. Pneumatic transport system

3.1.2.3. Procurement

Aside from the weigh system and the bunker assemblies, all items for the pneumatic transport system have been received. The load cells, their support pads, and the cable for the weigh system have been received. The arrival of the remaining equipment (printer, displays, and force computers) will be staggered through April. The cages and bunkers have been received, leaving only the blow-back assemblies which should arrive by early March.

3.1.2.4. Installation

Installation of the electrical control system began last quarter. The relay cabinet is now completely installed and will be connected to the control room when it is completed. At this point, the control room/relay cabinet will be checked out prior to connecting the relay cabinets to the field components.

Installation of the bunker assemblies has begun.

3.1.2.5. Documentation

Using the Design Calculation Reports as a basis, the control documentation for the solids handling system is being prepared. Table 3-2 gives the status of these documents.

3.2. PNEUMATIC CLASSIFICATION

The prototype pneumatic classifier will be installed along with subsystems 6, 7, and 8 of the prototype pneumatic transport system.

3.3. SOLIDS PROPERTIES TESTING

3.3.1. "Cold" Testing

The measurement of flow properties of different materials found in the cold head-end process has continued with crusher fines. The "rat-hole"

TABLE 3-2
SOLIDS HANDLING SYSTEM DOCUMENT STATUS

Document	Document No.	Status
Design Criteria: Solids Handling	(DC-520101)	In review
Process Flow Diagram	(PF-520101)	In review
Piping and Instrumentation Diagram	(PI-520101)	Issue A
Operating Procedures: Solids Handling	(OP-520101)	--
Maintenance Manual: Solids Handling	(MM-520101)	--
Interim Design Report: Solids Handling		--
Project Report: Solids Handling	(DR-520101)	--
Plant Arrangement	(PA-500001)	Issue B
Equipment Assembly	(5201002)	Issue A
Equipment Detail Drawings in Chronological Order	(5201003)	Issue A
System Description: Solids Handling	(SD-520101)	In writing
Implementation Specification: Bunkers	(IS-520101)	--
Implementation Specification: Blowers	(IS-520102)	--
Implementation Specification: Filters	(IS-520103)	--

(reported in Ref. 3-1) which occurred during a run on the 8-in. primary burner was caused by the accumulation of the fine fraction of the crusher product in the bunker. The mechanism of segregation was probably the suspension of fines around the filters in the bunker until transport of the batch was completed. The fines were then deposited on the mass of crusher product and when most of the material had been discharged, the fines were close to the outlet and formed a "rat-hole." Samples were taken and tested in the Jenike shear cell. The results from the testing of -710 μm crusher fines are shown in Fig. 3-2.

The intersection of the flow function (FF) and the flow factor (ff) is a measure of the minimum outlet required. Based on operating experience with the 8-in. primary burner, this intersection corresponds to a diameter of 272 in. This point, given in Fig. 3-2, is outside the range of shear cell measurements. The minimum stress in the Jenike shear cell corresponds to the weight of the ring, the top, and the powder inside the ring. The minimum consolidation load is approximately three times larger. It is not possible, therefore, to measure flow properties at stresses corresponding to very small dimensions with a Jenike shear cell. In many cases, the shape of the flow function is unambiguous (Fig. 3-3), which gives the results obtained with primary burner fines and superfines. (Primary burner fines have a characteristic upper size limit of 44 μm with 20% of the particles having a size less than this limit; primary burner superfines have a characteristic upper size limit of 44 μm with 80% of the particles having a size less than this limit.) The crusher fines tested here, however, give a flow function which becomes steeper as the stress level increases. This is probably due to particle breakage at larger stresses and the result is relatively greater strength. Extrapolation of such results to lower stresses can be difficult, and as a backup machine for this sort of case, a small gravity flow rig is available (Fig. 3-4). A small hopper, with an aerated cone, discharges into a small vessel through

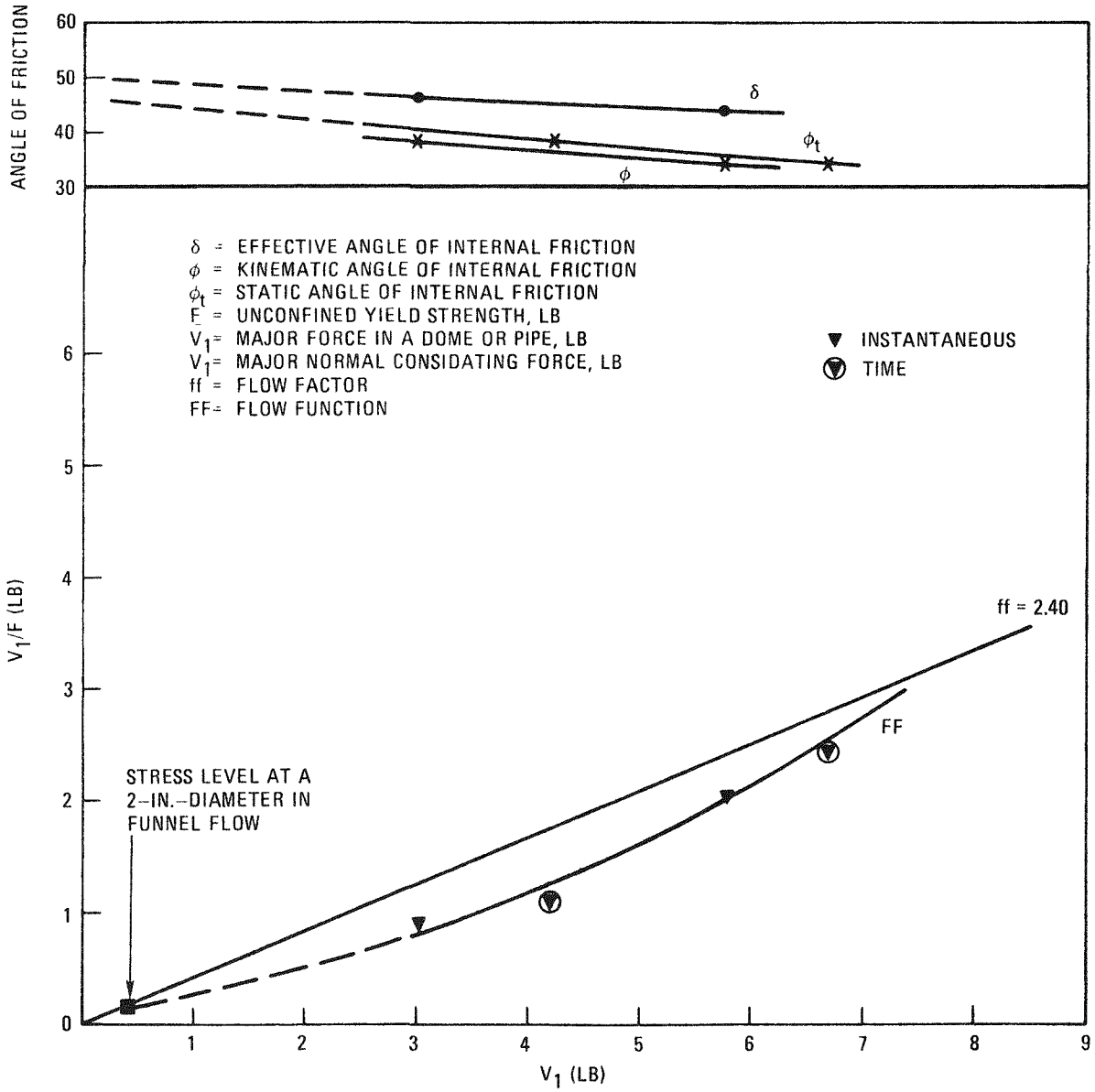

Fig. 3-2. Results of tests of crusher fines

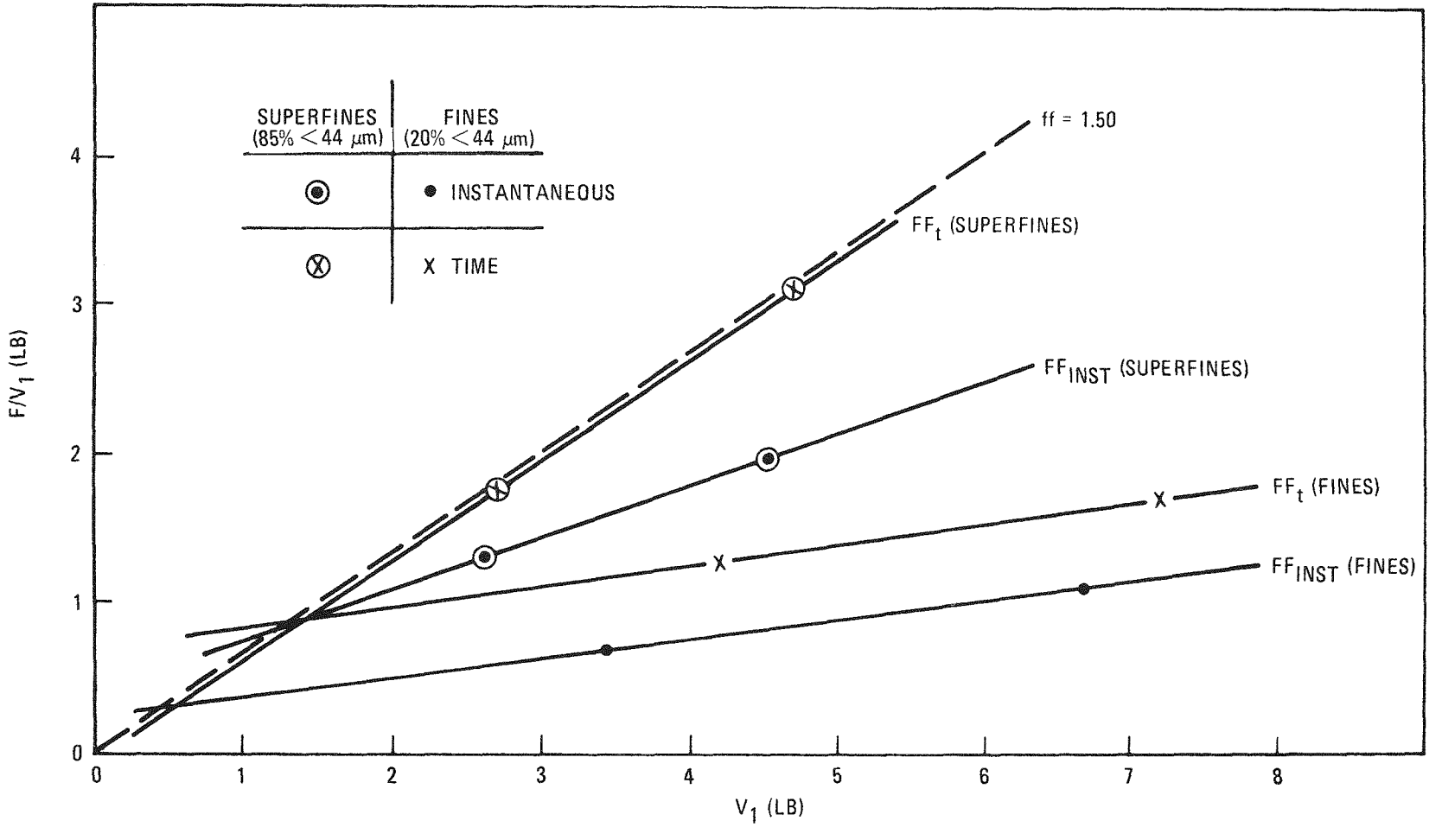

Fig. 3-3. Flow functions for primary burner fines

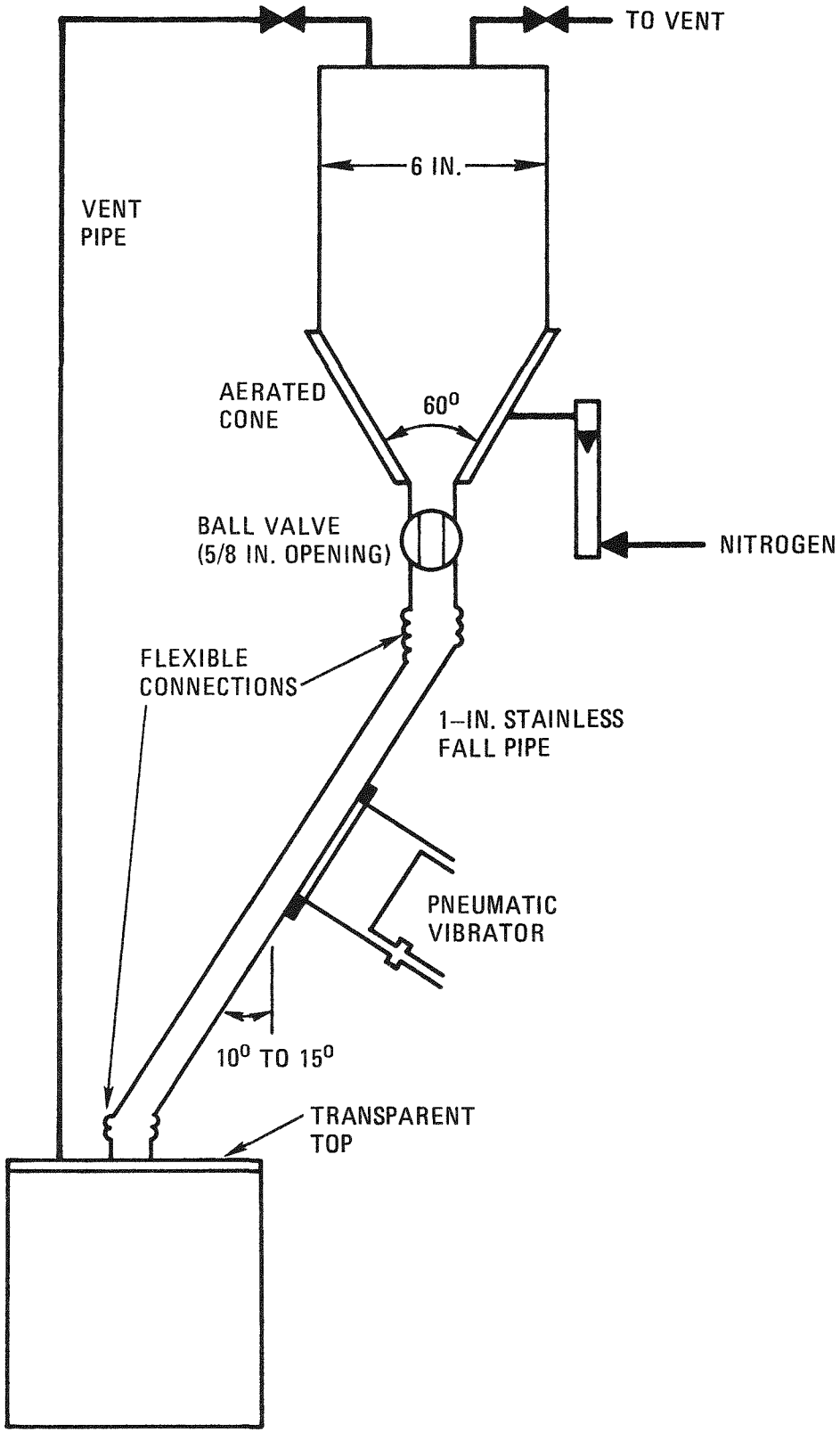

Fig. 3-4. Gravity flow test apparatus

a vibrated pipe. This equipment was used, without the fall pipe, with crusher fines in order to assess the amount of aeration gas required to obtain steady flow. Testing showed that a superficial gas velocity of 0.2 in./sec was sufficient.

The results with burner fines (Fig. 3-3) demonstrate the effect of particle size on cohesion. The superfines are so named because of their significantly smaller size:

Primary burner fines: 20% < 44 μm
Primary burner superfines: 85% < 44 μm

Gravity flow of superfines, even instantaneously, can be difficult to achieve unless they remain fluidized or aerated.

3.3.2. "Hot Testing"

Hot cell criticality constraints require the use of an amount of secondary burner product which is smaller than that required for a Jenike shear cell. A small shear cell has therefore been constructed and is being used with secondary burner product. A comparison between the results from the two sizes of shear cell is required in order to assess the effect of irradiation on flow properties.

REFERENCE

3-1. "Thorium Utilization Program Quarterly Progress Report for the Period Ending November 30, 1975," ERDA Report GA-A13746, General Atomic Company, December 31, 1975.

4. FLUIDIZED-BED COMBUSTION

Fabrication of both prototype burner vessels was completed in February. Installation of the heating/cooling system and vessel shrouding is under way. The cooling blower and induction heating system has been completed. The 20-cm primary burner installation is completed and shakedown testing is under way. This unit will be utilized to verify design parameters and to study alternate fines feeding and control modes.

Two Interim Development Reports were issued during the quarter (Refs. 4-1, 4-2). These reports document design bases for the prototype burners. Emphasis was placed upon the individual components with detailed discussions of the evolution of the current design and operating philosophy.

4.1. BURNER CONTROL SYSTEM

The system for controlling the 40-cm fluidized-bed crushed fuel element (primary) burner and the 20-cm fluidized-bed crushed particle (secondary) burner has been defined for at least the initial stages of the development program. The major control functions are described in Tables 4-1 and 4-2. The major differences in the methods of control of the burners involve post-ignition bed temperature control and bed inventory control. These differences exist primarily because of differences in burner feed material characteristics and because primary burner operation is semicontinuous while secondary burner operation is batch.

Piping and instrumentation (P&I) diagrams have been released for both the primary and secondary prototype burner systems (Figs. 4-1 and 4-2, respectively).

TABLE 4-1
MAJOR CONTROL FUNCTIONS OF PRIMARY BURNER

FUNCTION	METHOD OF CONTROL	TYPE OF SENSOR	BASIS FOR SELECTION
BED HEATING	INDUCTION HEATER CASCADED TO BED/VESSEL/SUSCEPTOR TEMPERATURE	TYPE-K THERMOCOUPLES	• BETTER CONTROL • ALLOWS INDEPENDENT FLUIDIZATION CONTROL • LONGER BURNER LIFE • EASIER TO MAINTAIN • BETTER SAFETY, RELIABILITY
POST-IGNITION BED TEMPERATURE CONTROL	ADJUST OXYGEN FLOW	TYPE-K THERMOCOUPLES	• FAST RESPONSE
OXYGEN FLOW	EQUAL-% (LINEAR) CONTROL VALVE	SWIRLMETER	• HIGH ACCURACY • WIDE RANGEABILITY
FLUIDIZING GAS FLOW	EQUAL-% (LINEAR) CONTROL VALVE TO HOLD TOTAL GAS FLOW CONSTANT	SWIRLMETER	• HIGH ACCURACY • WIDE RANGEABILITY • PREVENTS BED STAGNATION
VESSEL COOLING	ADJUST COOLING AIR FLOW	TYPE-K THERMOCOUPLES/ ANNUBAR PITOT TUBE	• AVOID CRITICALITY
COMBUSTION OFF-GAS OXYGEN CONCENTRATION	REDUCE OXYGEN FLOWS	PARAMAGNETIC OXYGEN ANALYZER	• OXYGEN DELETERIOUS TO OFF-GAS TREATMENT SYSTEM • MINIMIZE EXPLOSION HAZARD • PREVENT HIGH FILTER TEMPERATURES • CO/CO_2 AMBIGUOUS
BED INVENTORY	START/STOP FEED/PRODUCT FLOWS	DIFFERENTIAL PRESSURE TRANSMITTER	• CONTROL BED LEVEL • CONTROL DISENGAGEMENT HEIGHT • MINIMIZE PARTICLE CARRYOVER

TABLE 4-1 (Continued)

FUNCTION	METHOD OF CONTROL	TYPE OF SENSOR	BASIS FOR SELECTION
FEED RATE	VARIABLE SPEED ROTARY VALVE	TACHOMETER	• ALLOWS CONTROL AND FEED RATE ESTIMATION
PRODUCT RATE	REMOTE-MANUAL ON/OFF	FEED/PRODUCT BUNKER LOAD CELLS	• ALLOWS LOW-CARBON PRODUCT • CONTROLS TRANSPORT LOADING TO MINIMIZE BREAKAGE
FINES RECYCLE	DUAL PARALLEL HOPPER PRESSURIZED RECYCLE TO BURNER	LOAD-CELL	• 20-CM PRIMARY BURNER EXPERIENCE

TABLE 4-2
MAJOR CONTROL FUNCTIONS OF SECONDARY BURNER

FUNCTION	METHOD OF CONTROL	TYPE OF SENSOR	BASIS FOR SELECTION
BED HEATING	INDUCTION HEATER CASCADED TO BED/VESSEL/SUSCEPTOR TEMPERATURE	TYPE-K THERMOCOUPLES	• BETTER CONTROL • ALLOWS INDEPENDENT FLUIDIZATION CONTROL • LONGER BURNER LIFE • EASIER TO MAINTAIN • BETTER SAFETY, RELIABILITY
POST-IGNITION BED TEMPERATURE CONTROL	ADJUST COOLING AIR FLOW	TYPE-K THERMOCOUPLES	• ADEQUATE RESPONSE • SAME MODE OF CONTROL DURING RUN • PROVEN BY 10-CM SECONDARY BURNER OPERATION
OXYGEN FLOW	EQUAL-% (LINEAR) CONTROL VALVE	SWIRLMETER	• HIGH ACCURACY • WIDE RANGEABILITY
FLUIDIZING GAS FLOW	EQUAL-% (LINEAR) CONTROL VALVE TO HOLD TOTAL GAS FLOW CONSTANT	SWIRLMETER	• HIGH ACCURACY • WIDE RANGEABILITY • PREVENTS BED STAGNATION
VESSEL COOLING	ADJUST COOLING AIR FLOW	TYPE-K THERMOCOUPLES/ ANNUBAR PITOT TUBE	• AVOID CRITICALITY
COMBUSTION OFF-GAS OXYGEN CONCENTRATION	REDUCE OXYGEN CONTROL BY CASCADE FLOW CONTROL	PARAMAGNETIC OXYGEN ANALYZER	• OXYGEN DELETERIOUS TO OFF-GAS TREATMENT SYSTEM • MINIMIZE EXPLOSION HAZARD • PREVENT HIGH FILTER TEMPERATURES • CO/CO_2 AMBIGUOUS
BED INVENTORY	NONE	DIFFERENTIAL PRESSURE TRANSMITTER	-
FEED RATE	BATCH	KNOWN WEIGHT	-
PRODUCT RATE	REMOTE-MANUAL ON/OFF	PRODUCT BURNER LOAD CELL	• ALLOWS LOW-CARBON PRODUCT

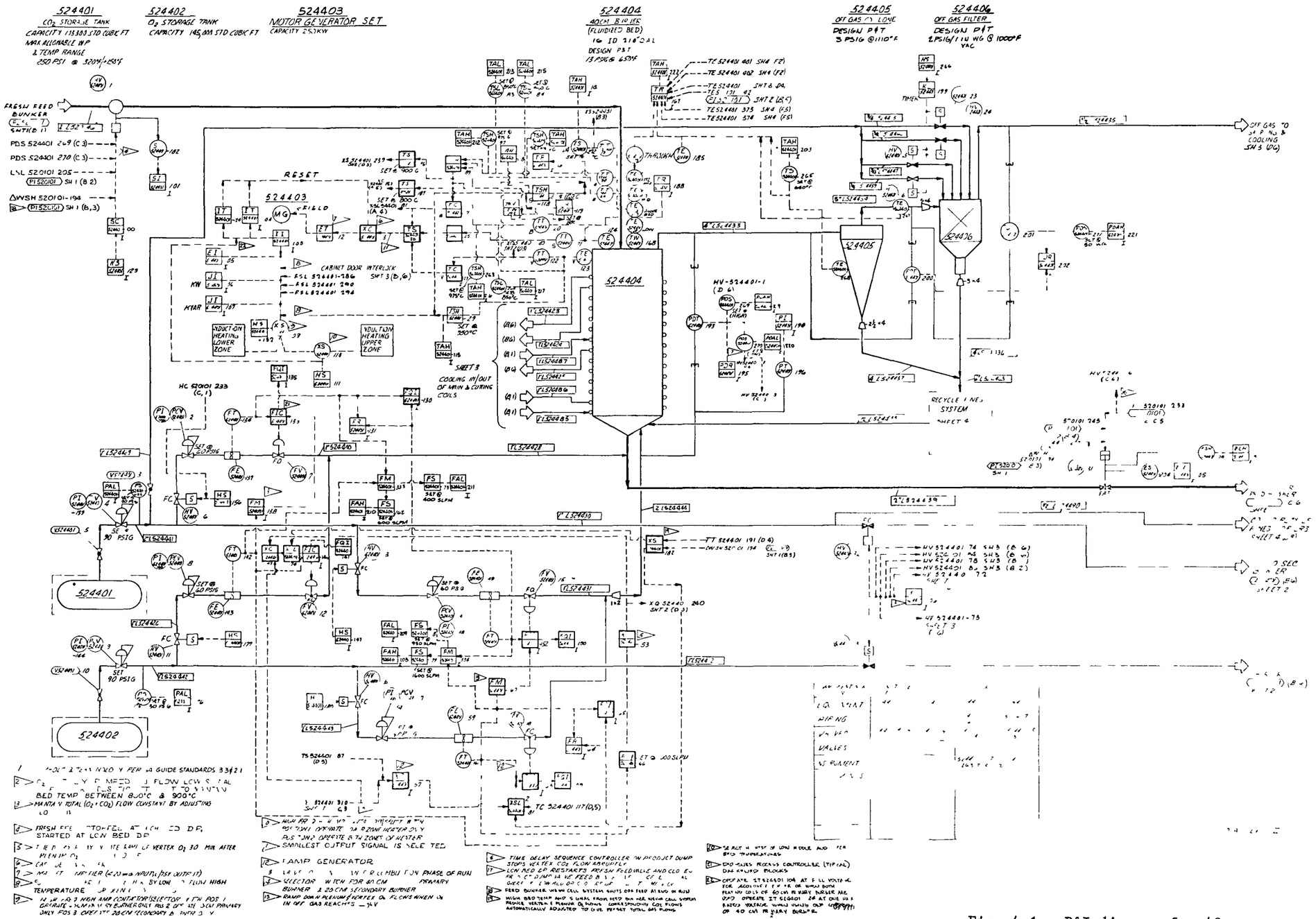

Fig. 4-1. P&I diagram for 40-cm prototype fluidized bed crushed fuel element burner (Sheet 1 of 4)

524411
COOLING AIR BLOWER

CAPACITY: 8000 SCFM
HEAD: 6.0 PSI
MOTOR HP: 150 (MAX.)

524412
EXHAUST AIR COOLER
DUTY: 1.5813 X 10⁶ BTU/HR
AREA: 512 SQ. FT.
DESIGN P & T
SHELL: PSIG @ °C
TUBE: PSIG @ °C

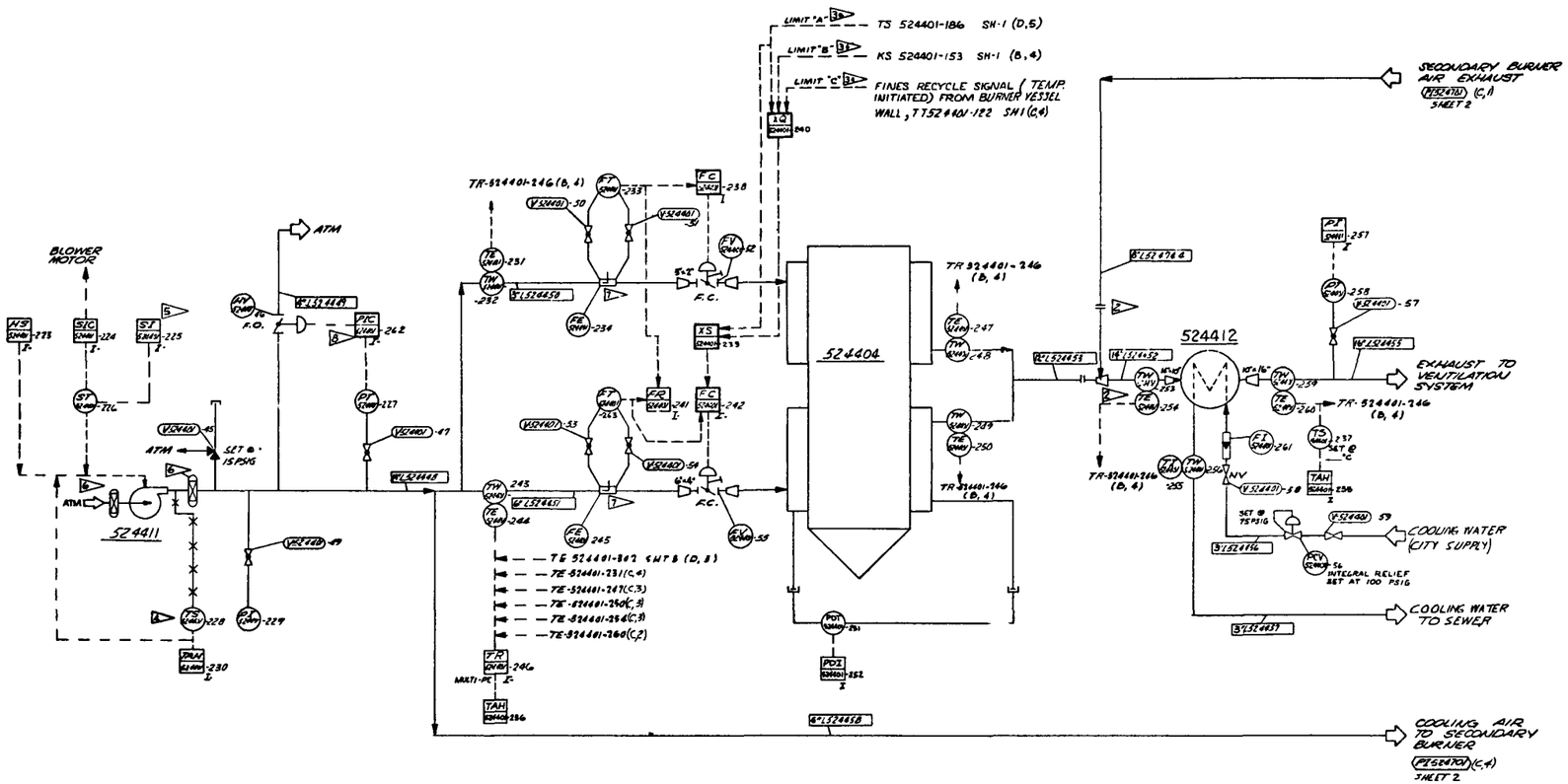

NOTES:

1. SYMBOLS & TERMINOLOGY PER ISA GUIDE STANDARDS S-5 & 2-1
2. PROVIDE FLANGES FOR POSSIBLE BLINDING IF COOLING JACKETS LEAK.
3. a-INITIATE COOLING AIR FLOW WHEN MAX. BED TEMP REACHES 300°C, FLOW IS INCREASED RAPIDLY TO LIMIT "A" ( ).
   b-WHEN VERTEX OXYGEN FLOW IS INITIATED, AIR FLOW INCREASES RAPIDLY TO LIMIT "B" ( ).
   c-WHEN FINES RECYCLE FLOW IS INITIATED THE FLOW CHANGES RAPIDLY (UP/DOWN) TO LIMIT "C" ( )
   -IF BED TEMP. DROPS BELOW 900°C, COOLING AIR IS SHUT OFF
4. TWO POSITION SWITCH: ALARM SETTING @ 150°C, TRIP BLOWER @ 180°C.
5. TACHOMETER FOR RPM READOUT
6. FILTER - SILENCER
7. ANNUBAR FLOW-AVERAGING PITOT TUBE. LOCATE IN LINE WITH MINIMUM OF 7 UPSTREAM DIAMETERS AND 3 DOWNSTREAM DIAMETERS OF STRAIGHT PIPE
8. DIGGENTS PROCESS CONTROLLER (TYPICAL) DARKENED BLOCKS

COMPONENT NUMBERS NOT USED ON THIS SHEET		NUMBERS USED
EQUIPMENT	524418 THRU 524426	524401 THRU 524412
PIPING	524454	524448 THRU 524458
VALVES	524401-42 THRU 524401-71 (48)	524401-45 THRU 524401-53
INSTRUMENTS	524401-175 THRU 524401-196	524401-185 THRU 524401-262

Fig. 4-1. P&I diagram for 40-cm prototype fluidized bed crushed fuel element burner (Sheet 2 of 4)

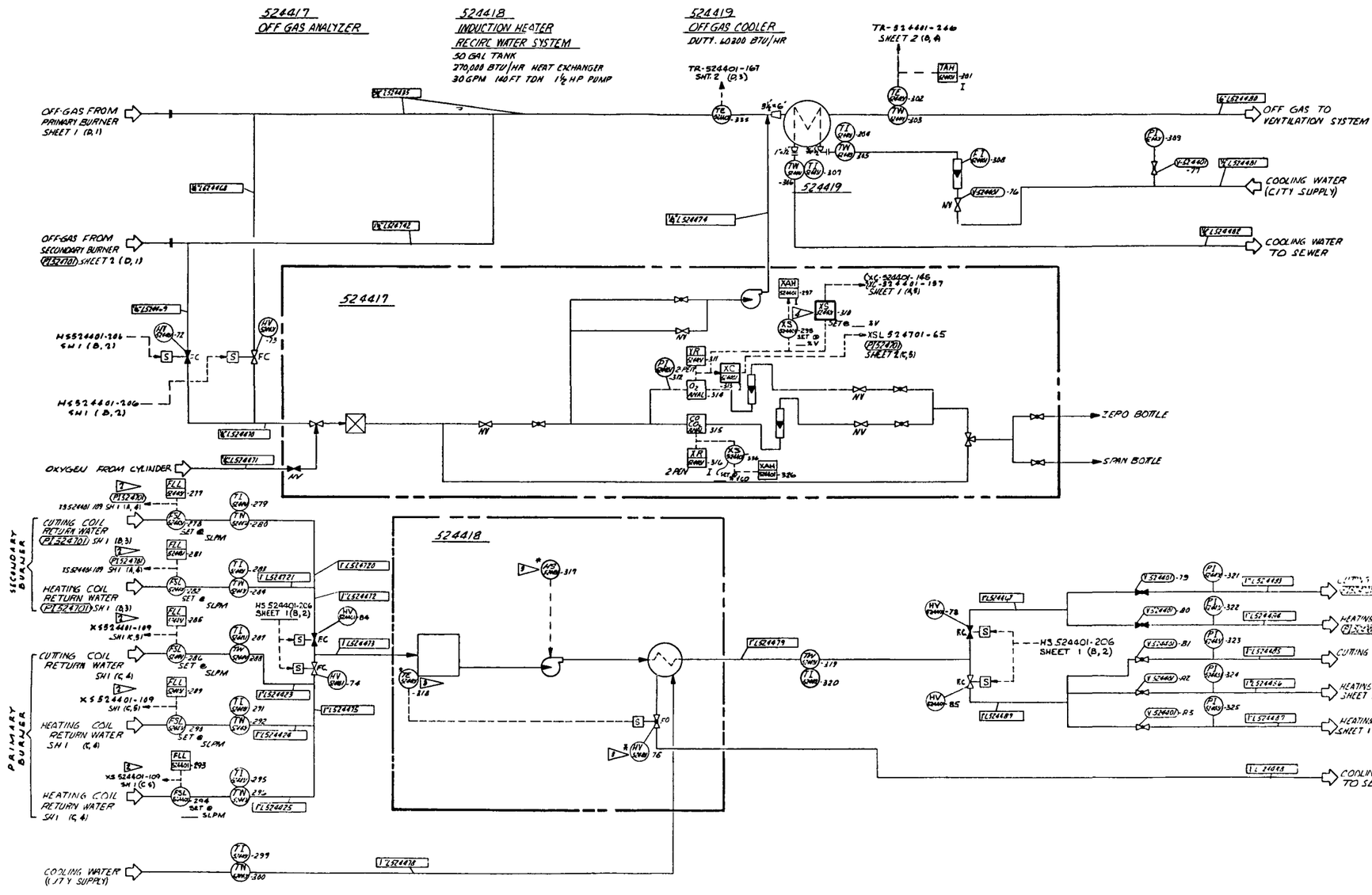

NOTES

1. SYMBOLS & TERMINOLOGY PER GA GUIDE STANDARDS 3-5 & 2-1
2. TURN OFF POWER TO INDUCTION HEATING COIL ON LOW FLOW
3. VENDOR ITEM INSTALLED
4. DIOGENES PROCESS CONTROLLER (TYPICAL) DARKENED BLOCKS

COMPONENT NUMBERS NOT USED ON THIS SHEET		NUMBERS USED
EQUIPMENT		524417 THRU 524419
PIPING		524403 THRU 524489
VALVES	524411 86 THRU 524414-92	524415 72 THRU 524441 85
INSTRUMENTS	524414 337 THRU 524401-341	524418 317 THRU 524419 321 - 325, 336

Fig. 4-1. P&I diagram for 40-cm prototype fluidized bed crushed fuel element burner (Sheet 3 of 4)

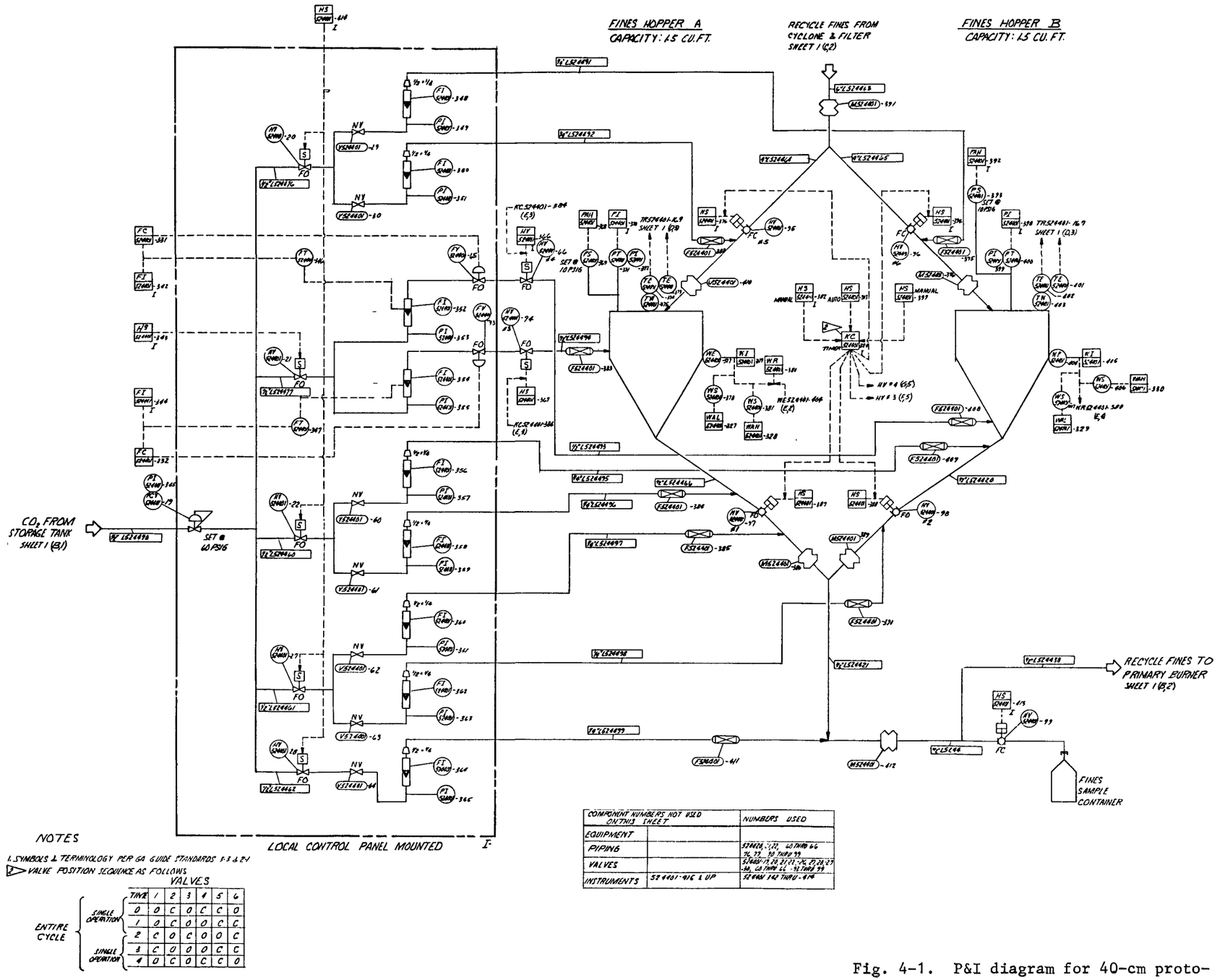

TIME	1	2	3	4	5	6
0	0	C	0	C	C	0
1	0	C	0	0	C	C
2	C	0	C	0	0	C
3	C	0	0	0	C	C
4	0	C	0	C	C	0

Fig. 4-1. P&I diagram for 40-cm prototype fluidized bed crushed fuel element burner (Sheet 4 of 4)

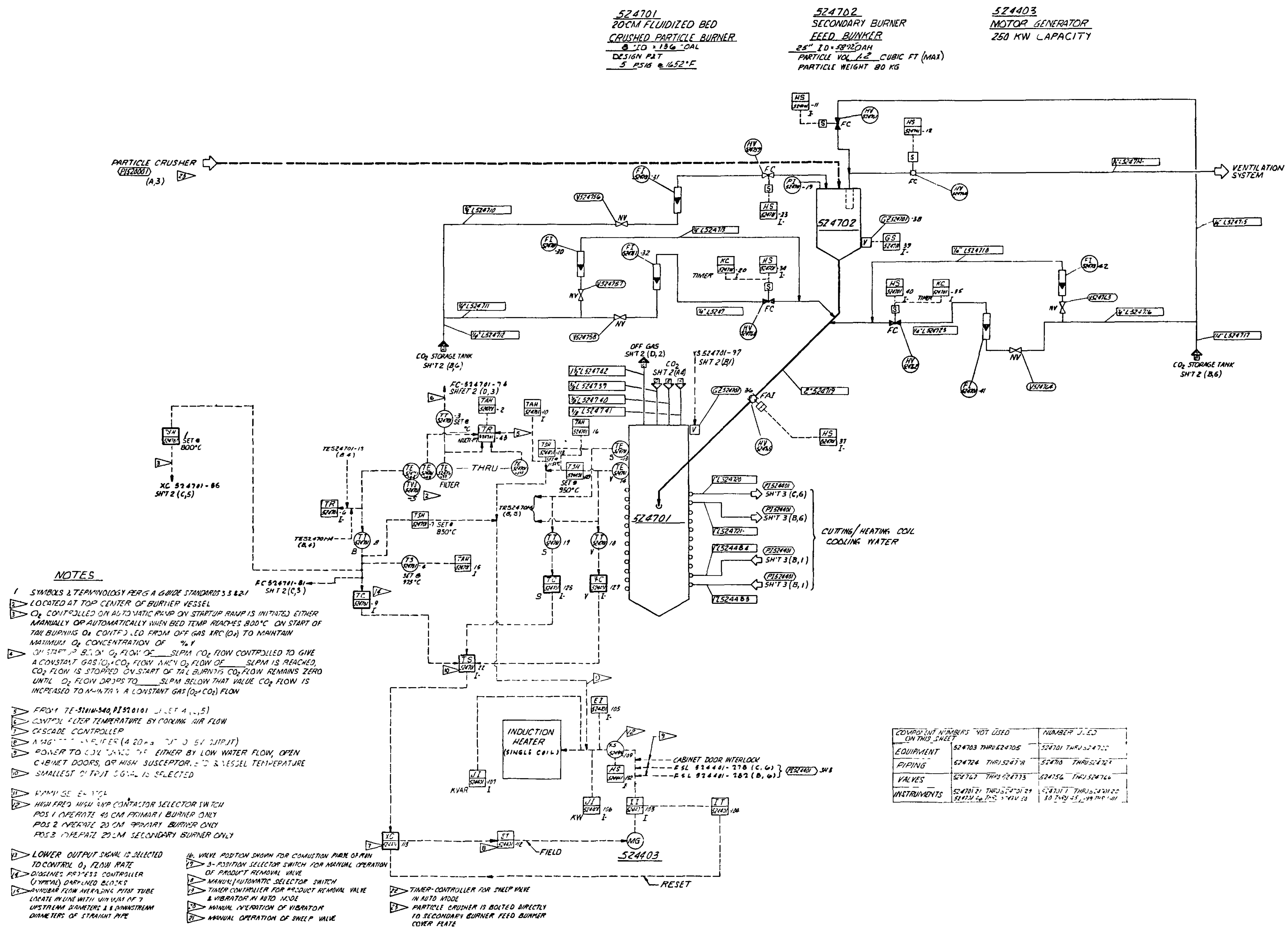

Fig. 4-2. P&I diagram for 20-cm prototype fluidized bed crushed particle burner (Sheet 1 of 2)

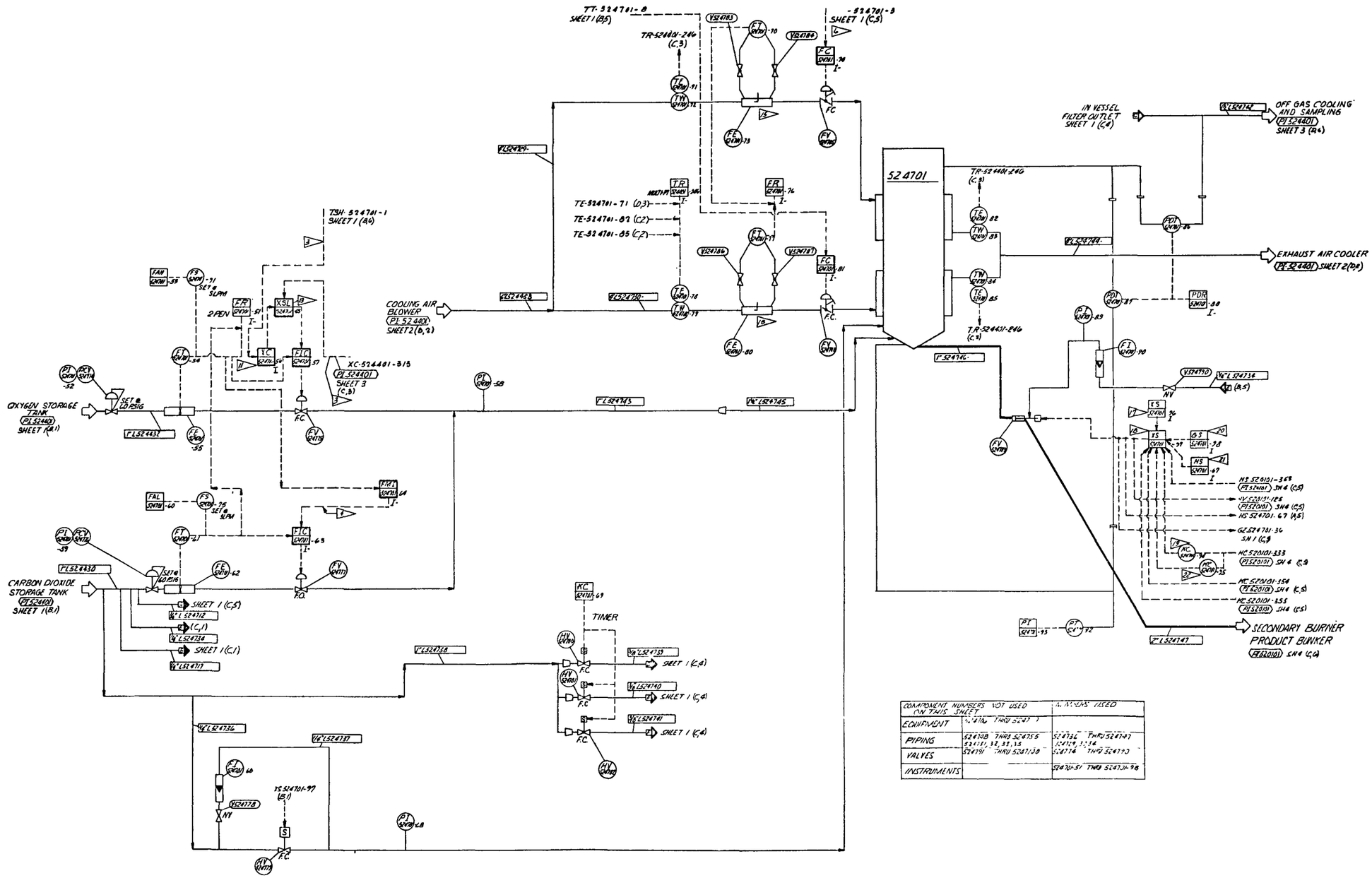

COMPONENT NUMBERS NOT USED ON THIS SHEET		NUMBERS USED
EQUIPMENT	-4 THRU 524701	
PIPING	524708 THRU 524755 524731, 32, 33, 35	524732 THRU 524747 524759, 1754
VALVES	524791 THRU 524730	524776 THRU 524790
INSTRUMENTS		524701-51 THRU 524734-98

Fig. 4-2. P&I diagram for 20-cm prototype fluidized bed crushed particle burner (Sheet 2 of 2)

Operating procedures have been established for both burners. The sequence of operational events for the primary and secondary burners is given in Tables 4-3 and 4-4.

4.1.1. Burner System Failure Analysis

A fault tree analysis and failure mode and effects analysis have been conducted to determine the nature of upset events caused by failure of burner system components and to determine what remedial action should be taken. Alarms and safety interlocks have been defined. The results of this analysis are given in Table 4-5.

4.2. PROTOTYPE (40-cm) PRIMARY BURNER

4.2.1. Primary Burner Operating Cycle

Based on the latest information available on heat transfer (Ref. 4-3), fluidization (Ref. 4-4), and commercial reprocessing flowsheets (Ref. 4-5), an operating cycle has been developed for the 40-cm prototype primary burner.

The following model describes the cycle:

1. Heat removal limitations require a 4-1/2-ft fresh feed bed or a 5-1/2-ft particle bed to attain the design burn rate (48 kg/hr-°C).

2. Bed heights are determined using 20-cm glass tube data.

3. Initial startup of each 6 to 12 day campaign is with fresh feed to either the top of the first coil (see case A, Fig. 4-3a) or the second coil (see case B, Fig. 4-3b).

TABLE 4-3
PRIMARY BURNER OPERATION

FIRST CAMPAIGN STARTUP

1. TURN ON POWER
2. ESTABLISH CO_2 FLOWS
3. LOAD BURNER WITH INITIAL BED
4. OPEN O_2 ISOLATION VALVES
5. TURN ON INDUCTION HEATER

FIRST AND INTER-CAMPAIGN

1. INITIATE O_2 FLOW TO PLENUM
2. REDUCE CO_2 FLOW TO PLENUM
3. TURN OFF INDUCTION HEATER
4. START FLOW OF COOLING AIR
5. INITIATE O_2 FLOW TO VERTEX
6. REDUCE CO_2 FLOW TO VERTEX
7. START FINES RECYCLE (AS APPROPRIATE)
8. ADJUST COOLING AIR FLOW
9. START FRESH FEED ON DEMAND
10. STOP FRESH FEED ON DEMAND
11. STOP FINES RECYCLE ON HIGH ABOVE-BED TEMPERATURE
12. REDUCE COOLING AIR FLOW
13. REDUCE O_2 FLOW ON HIGH OFF-GAS CONCENTRATION
14. INCREASE CO_2 FLOWS
15. DUMP BED TO LOW LEVEL
16. RE-ESTABLISH BED WITH FRESH FEED

FINAL TAIL BURN

1. STOP FRESH FEED BY LOAD-CELL SYSTEM
2. REDUCE O_2 FLOWS
3. INCREASE CO_2 FLOWS
4. INCREASE COOLING AIR FLOW
5. SHUT OFF O_2 ON HIGH OFF-GAS CONCENTRATION
6. INCREASE CO_2 FLOWS TO SHUTDOWN LEVEL
7. DUMP ENTIRE BED

TABLE 4-4
SECONDARY BURNER OPERATION

STARTUP

1. TURN ON POWER
2. ESTABLISH CO_2 FLOW
3. LOAD BURNER WITH CRUSHED PARTICLES
4. TURN ON INDUCTION HEATER

COMBUSTION

1. INITIATE O_2 FLOW
2. REDUCE CO_2 FLOW
3. TURN OFF INDUCTION HEATER
4. START FLOW OF COOLING AIR

SHUTDOWN

1. REDUCE COOLING AIR FLOW
2. REDUCE O_2 FLOW ON HIGH OFF-GAS CONCENTRATION
3. TURN ON INDUCTION HEATER
4. TURN OFF O_2
5. INCREASE CO_2 FLOW TO SHUTDOWN LEVEL

TABLE 4-5
UPSET EVENTS AND REMEDIAL ACTIONS FOR PROTOTYPE BURNERS

UPSET EVENT	REMEDIAL ACTION
I. BED TEMPERATURE EXCURSION	I. (a) ALARM HIGH BED, VESSEL, SUSCEPTOR TEMPERATURES (b) TRIP INDUCTION HEATER POWER (SAFETY INTERLOCK) (c) ALARM LOW CO_2 FLOW (d) ALARM HIGH O_2 FLOW (e) INCREASE CO_2 AND/OR DECREASE O_2 AND/OR INCREASE COOLING AIR FLOWS (AUTO OR MANUAL) (f) REMOTE-MANUALLY INITIATE BURNER SHUTDOWN
II. REDUCTION OR LOSS OF FLUIDIZING GAS	II. (a) ALARM LOW FLOW (b) REMOTE-MANUALLY DECREASE O_2 FLOW (c) REMOTE-MANUALLY INITIATE BURNER SHUTDOWN
III. REDUCTION OR LOSS OF COOLING AIR	III. (a) ALARM HIGH VESSEL, BED TEMPERATURES (b) TRIP INDUCTION HEATER POWER (SAFETY INTERLOCK) (c) DECREASE O_2 OR INCREASE CO_2 FLOW (AUTO OR MANUAL) (d) REMOTE-MANUALLY INITIATE BURNER SHUTDOWN
IV. PLUGGING OR RECYCLE FINES TRANSPORT LINES (PRIMARY BURNER ONLY)	IV. (a) ALARM HIGH FINES HOPPER PRESSURE (b) ALARM HIGH FINES HOPPER LEVEL (WEIGHT) (c) TERMINATE RECYCLE FINES FLOW

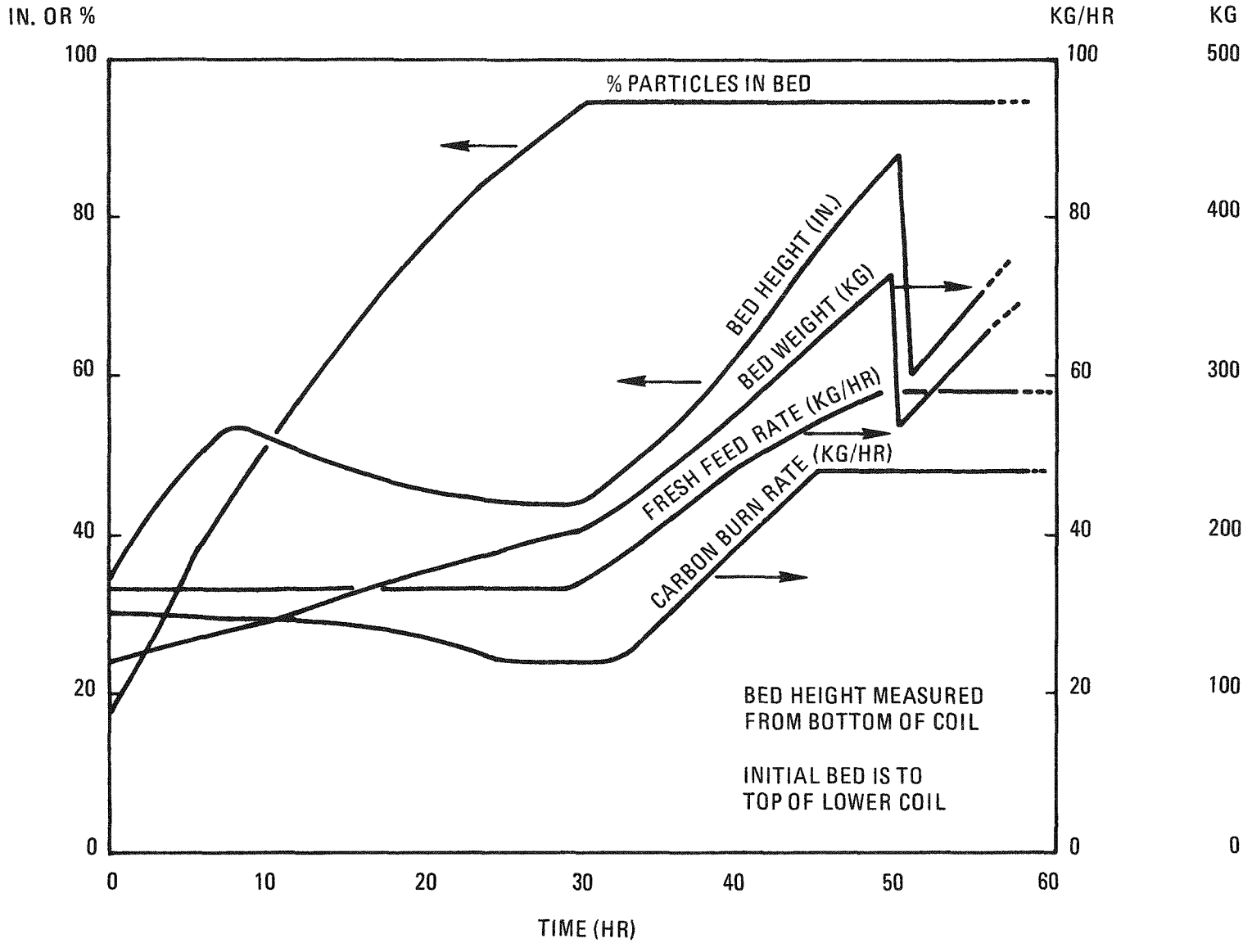

Fig. 4-3a. Case A: 40-cm primary burner operating cycle with feed to the top of the first coil

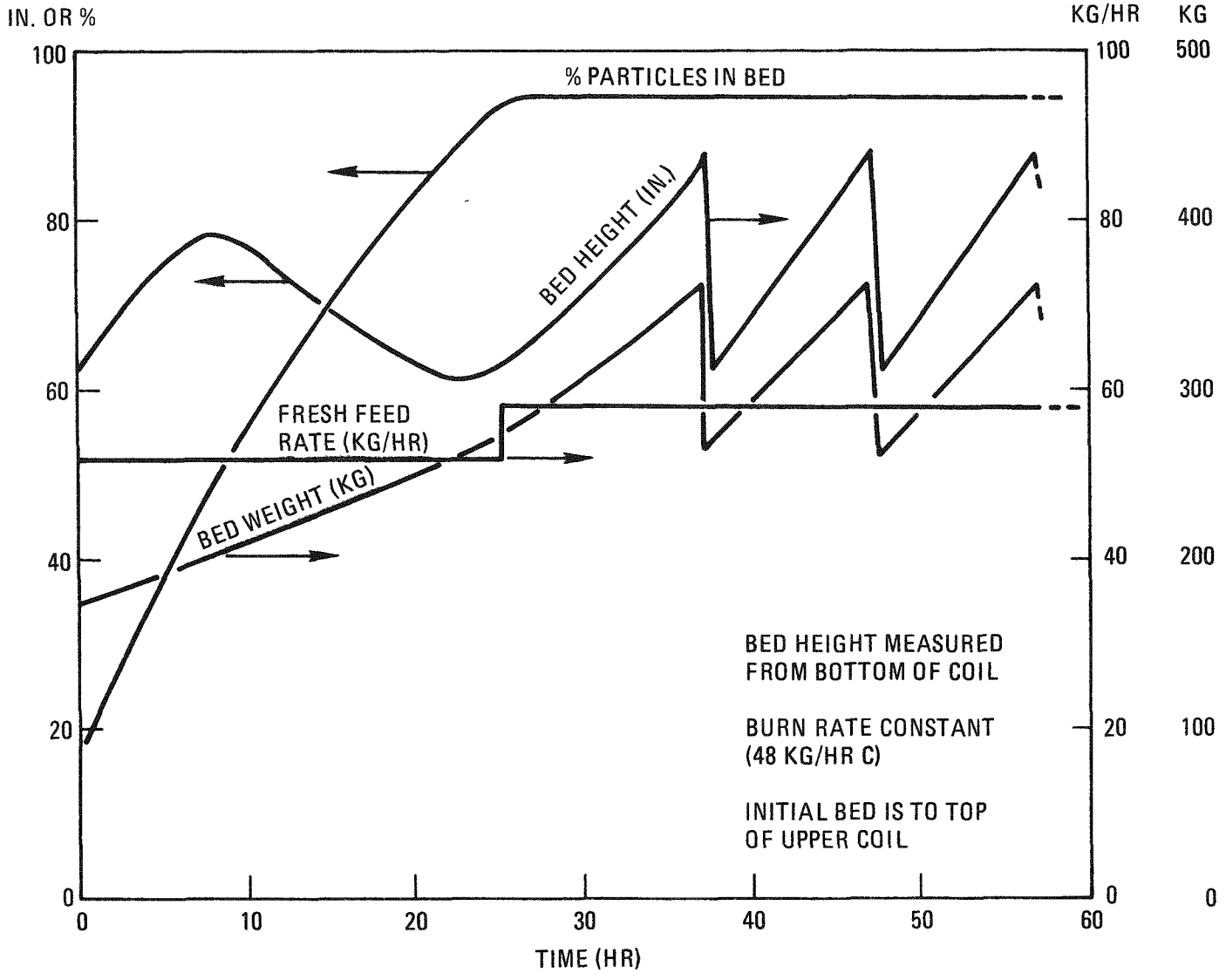

Fig. 4-3b. Case B: 40-cm primary burner operating cycle with feed to the top of the second coil

4. The initial fresh feed bed is converted to a low (5%) carbon particle bed of approximately the same height by adding fresh feed at less than the burn rate. This low carbon bed is then fed at the burn rate to build it up to 1 ft higher than the induction coil (7-ft bed).

5. When the 7-ft bed is attained, fresh feed is stopped and burning is continued until O_2 is detected in the off-gas.

6. Product removal follows to yield a 5-1/2-ft particle bed. This 7-ft to 5-1/2-ft cycle of bed height is repeated until the end of the campaign.

4.2.2. Primary Burner Cooling System Design

4.2.2.1. Pin Length Reduction From 0.5 to 0.4 in.

Based on the result of the dimensional envelope check at Clark and Wheeler (Ref. 4-6), it is concluded that the 1/4-in. Hastelloy-X tube can be used as is without modification to the tube diameter (except grinding the weld seams flush). The minimum assembly clearance available between the pin envelope and the susceptor is 5/32 in. with the present tube ovality and camber. In order to re-establish the original design radial clearance of 1/4 in., it would be desirable to remove 0.1 in. from the pin length, making the pin 0.4 in. long. The new pin fin will be 0.4 in. x 3/16-in. O.D. with the same pin pattern as before. The 1/4-in. radial clearance is felt to be a necessity, especially since the susceptor has a tendency to warp under frequent thermal cycling.

The effect of pin length reduction on heat transfer is approximately a 3.5% reduction in the heat transfer rate if the cooling air flow remains constant. On the other hand, a 10% increase in air flow can compensate for the reduction in heat transfer effectiveness. The present blower has the capability to handle the 10% increase in flow.

The primary function of the pin fin is to increase heat transfer effectiveness in the limited 6-ft burner surface. Thermal analysis was made to determine the effect of cutting the pin by 0.1 in. Table 4-6 compares the reference design (0.5-in. pin length) (case I) heat transfer and flow parameters with the proposed shorter pin design (case II). For the same cooling air flow, the decrease in heat removal effectiveness through the burner wall is only 3.5%, despite a 20% reduction in actual fin surfaces. This relatively small effect is partially due to the increase in fin efficiency for a shorter pin: 74% in case II versus 65% in case I. The higher mean fin temperature is responsible for this efficiency increase.

The 6% increase in frontal cross section for flow due to the shorter pin is accompanied by a 22% reduction in pressure drop through the shroud.

Case III is a better solution to the problem. By increasing the cooling flow by approximately 10%, the design removal rate can be maintained even with the shorter 0.4-in. fin. The pressure drop through the shroud would be approximately 12% less than for case I.

The present cooling blower has the capability to deliver 2400 scfm at 12 psig and there is more than sufficient margin to compensate for this loss of heat transfer effectiveness. In addition, fines elutriation from the burner provides another yet unaccounted for source of cooling. Fresh feed addition also provides a slight cooling effect. The upper jacket potentially can remove approximately 10% of the heat from the vessel at 500 scfm, thus adding extra margin to the cooling system.

4.2.2.2. Effects of Burner Tube Ovality and Bow

By ERDA request, the consequences of the burner tube "as-built" ovality and bow have been assessed. Using pessimistic assumptions and

TABLE 4-6
COMPARISON OF HEAT TRANSFER EFFECTIVENESS FOR DIFFERENT PIN LENGTHS

	Case I	Case II	Case III
Pin fin dimension	1/2 x 3/16 in. O.D. (original design)	0.4 x 3/16 in. O.D. (proposed change)	0.4 x 3.16 in. O.D. (proposed change)
Heat removal rate, Btu/hr	1.28×10^6	1.24×10^6	1.28×10^6
Process parameters			
Cooling air flow, scfm	1470	1470	1600
Shroud ΔP, psi	4.2	3.3	3.7
Inlet velocity, ft/sec	98	97	100
Inlet flow, ft^3/min	1278	1344	1389
Outlet velocity, ft/sec	299	276	291
Outlet flow, ft^3/min	3890	3812	4032
Heat transfer parameters			
Cooling air temperature, °C			
Exit	490	475	454
Inlet	50	50	50
Burner wall temperature, °C			
Bed	900	900	900
Inner wall	632	641	632
Bare wall	595	605	595
Mean fin	454	498	486
Mean outer wall	500	539	527
Fin efficiency	0.65	0.74	0.74
Heat transfer coefficient, $Btu/ft^2-hr-°F$			
Fin	65	63	65
Bare tube	24	23	24
Effective outer wall	95	85	88
Bed wall	106	106	106
Overall	47	44.5	45
Physical dimensions			
Frontal flow cross section, ft^2	0.217	0.23	0.23
Bare surface, ft^2	21.78	21.78	21.78
Fin surface, ft^2	44.17	35.31	35.31

conversative calculations, it is concluded that:

1. A maximum circumferential temperature gradient of 100°C could develop.

2. The temperature gradient of 100°C would be accompanied by a maximum (and self-limiting) thermal deflection of 0.175 in.

3. The design heat removal can still be achieved by increasing the cooling air delivery.

4. An axial maximum thermal stress of 12.3 ksi could develop, which is well within the criteria for elastic shakedown. Consequently, neither fatigue nor creep-fatigue effects are likely.

4.2.2.2.1. Circumferential Temperature Variation in Burner Tube due to Ovality and Bow. Figure 4-4 illustrates the idealized (axisymmetric) geometry of the heat transfer zone surrounding the fluidized bed which was assumed for the initial design. Circumferential tolerances of the gap dimension were not considered in the original design nor in a subsequent design modification which reduced pin length from 0.5 to 0.4 in.

To calculate tube wall circumferential ΔT, two "worst case" models were analyzed. Both cases assume that the burner and susceptor tubes are assembled with maximum measured diameters (long axis of ellipse) at right angles, as shown in Fig. 4-5. In addition, the centerlines of the tubes are given an initial eccentricity, ΔR. Case A represents the worst case cold installed condition with an initial eccentricity of 0.205-in. Case B represents the worst possible operating condition, where the pin fins actually touch the susceptor on one side, requiring an initial $\Delta R = 0.455$ in. Both the maximum and minimum gaps are shown in Fig. 4-5. The assumed thermal models are very conservative since (1) worst case dimensions are all stacked, (2) the worst case condition is assumed to exist along the entire length (Z-axis) of the cooling zone, and (3) no circumferential mixing is assumed to average cooling air bulk temperature.

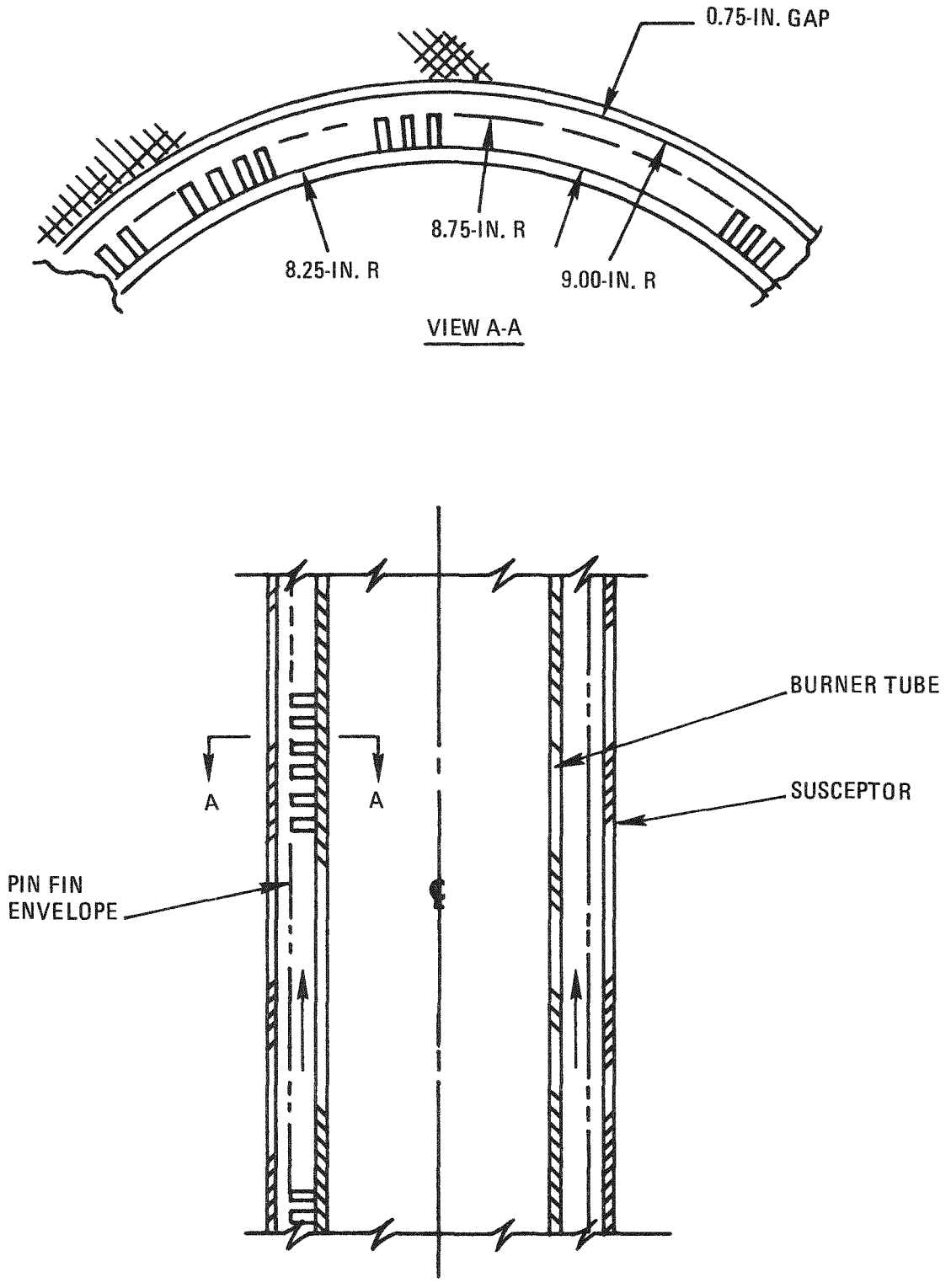

Fig. 4-4. Design geometry for cooling section of the primary burner

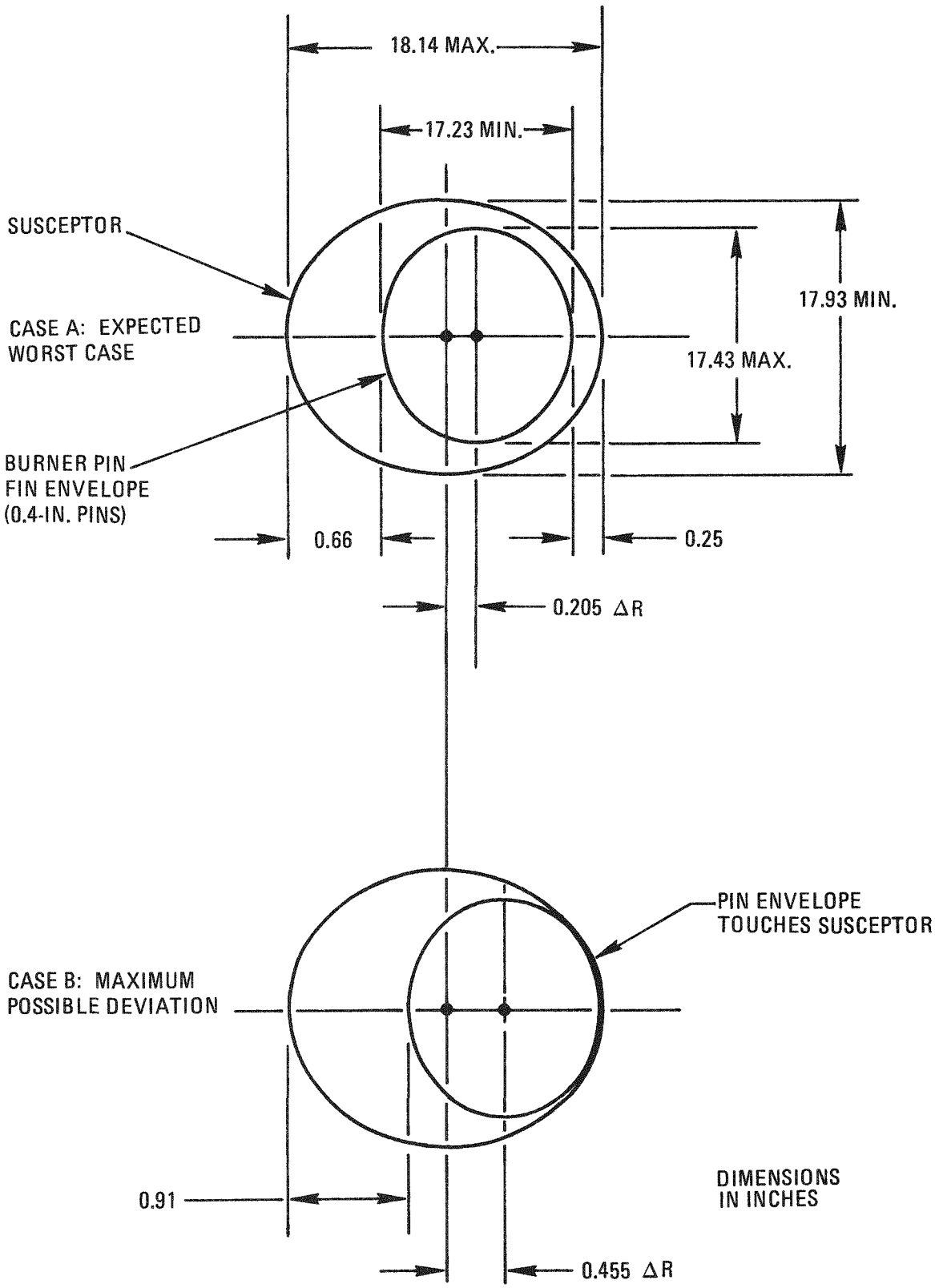

Fig. 4-5. Thermal models of the primary burner

Based on these models, the circumferential temperature gradients for the two cases are presented in Figs. 4-6 and 4-7. A summary of the analysis approach is outlined in Table 4-7. The predicted maximum circumferential ΔT values of 80°C for case A and 235°C for case B are surprisingly high and are indicative of a higher sensitivity to circumferential gap tolerances than was thought possible.

4.2.2.2.2. Structural Effects. Based on the results of the thermal model, structural considerations can be addressed. The following must be determined:

1. Structural effects that will result from the temperature gradient.

2. Whether the thermally induced growth will be self-limiting (stable) or destructive (unstable).

To determine (1), item (2) must first be determined. In the previous section, the hypothetical "worst case" ΔT was presented as a function of the eccentricity of the burner-susceptor pair. Figure 4-12 shows a curve of ΔT versus ΔR based on the two points calculated in the thermal model. This curve is considered "hypothetical" since the assumed worst case eccentricity cannot exist for the full length of the cooling zone as the one-dimensional calculation implies. Since the burner is centered in the susceptor at the bottom of the cooling section shroud, the actual worst case misalignment for a straight tube occurs when the top of the burner is offset by the maximum amount, ΔR_{max} (see Fig. 4-13a). The actual average ΔT should then correlate more closely to a model based on $\overline{\Delta R} = \Delta R_{max}/2$. A more severe condition can be visualized as in Fig. 4-13b. Here the initial camber (represented by a burner radius of curvature R) is positioned so as to maximize the axial average eccentricity. For this case, $\overline{\Delta R} = 0.67$ ΔR_{max}. An "actual worst case" thermal response curve is shown in Fig. 4-12, based on a ratio of $\overline{\Delta R}/\Delta R_{max} = 0.67$. The question of self-limited

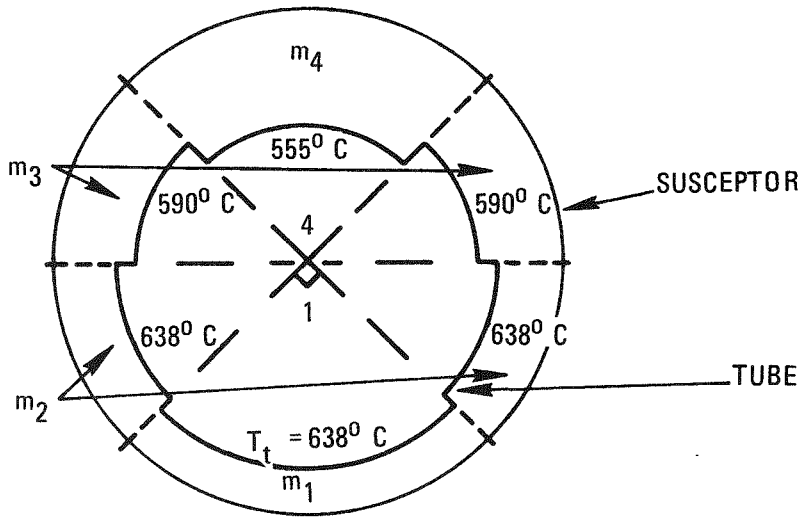

T_t = TUBE OUTER WALL TEMPERATURE
PIN FIN = 0.4 IN.

	QUADRANT 4	QUADRANT 3	QUADRANT 2	QUADRANT 1	TOTAL
Δr_i, AVERAGED ANNULAR GAP (TUBE-SUSCEPTOR), IN.	0.99	0.76	0.63	0.63	/
MASS FLOW, LB/MIN	m_4 = 49.7 (41%)	m_3 = 30.1 (25%)	m_2 = 20.1 (17%)	m_1 = 20.1 (17%)	m_t = 120 (100%)
HEAT TRANSFER RATE, BTU/HR	0.37×10^6	0.32×10^6	0.28×10^6	0.28×10^6	1.24×10^6 (97% OF DESIGN)
SHROUD ΔP, PSI	3.8	3.8	3.8	3.8	4.8

Fig. 4-6. Circumferential temperature variation for expected worst case (case A)

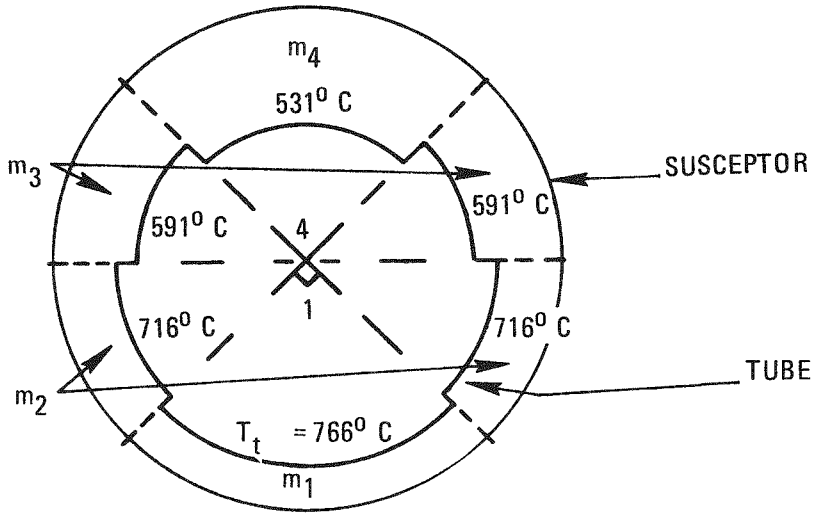

T_t = TUBE OUTER WALL TEMPERATURE
PIN FIN = 0.4 IN.

	QUADRANT 4	QUADRANT 3	QUADRANT 2	QUADRANT 1	TOTAL
Δr_i, AVERAGED ANNULAR GAP (TUBE-SUSCEPTOR), IN.	1.24	0.85	0.51	0.41	/
MASS FLOW, LB/MIN	m_4 = 69.5 (58%)	m_3 = 32.8 (27%)	m_2 = 10.8 (9%)	m_1 = 7.1 (6%)	m_t = 120 (100%)
HEAT TRANSFER RATE, BTU/HR	0.39×10^6	0.32×10^6	0.24×10^6	0.15×10^6	1.1×10^6 (86% OF DESIGN)
SHROUD ΔP, PSI	3.0	3.0	3.0	3.0	3.0

Fig. 4-7. Circumferential temperature variation for maximum possible deviation (case B)

TABLE 4-7
CIRCUMFERENTIAL TEMPERATURE VARIATION IN THE PRIMARY BURNER VESSEL DUE TO OVALITY AND BOW

1. Geometry for thermal model (Fig. 4-5)
   a. Case A - expected worst case (cold installed condition)
   b. Case B - maximum possible deviation (worst possible operating condition)
   c. Based on actual measured dimensions
2. Analysis approach (Case A geometry is used as an example in the following approach.)
   a. Establish flow distribution around burner tube
      (1) Approximate annular gap by dividing susceptor envelope into four quadrants (Fig. 4-6)
      (2) Calculate fin section performance for each annular cross section based on entire section and concentric arrangement (Fig. 4-8)
      (3) For a given shroud ΔP, find annular mass flow, M_t, by summing contribution from each quadrant:

$$M_t = (M_1 + M_2 + M_3 + M_4) \text{ X } 1/4$$

$$= m_1 + m_2 + m_3 + m_4$$

      (4) Determine shroud ΔP at design M_t (Fig. 4-9)
      (5) At design shroud ΔP, find mass flow for each quadrant (Fig. 4-8)
   b. Knowing the flow distribution, establish heat transfer and tube temperature of each quadrant (Fig. 4-8)
      (1) Total heat transfer across tube wall:

$$Q_t = (Q_1 + Q_2 + Q_3 + Q_4) \text{ X } 1/4$$

3. Conservative assumptions
   a. Worst case dimensions are stacked
   b. Worst condition exists along the entire 6 ft
   c. No circumferential mixing to average air bulk temperature (Fig. 4-3)
4. Case B calculation is summarized in Figs. 4-7, 4-10, and 4-11

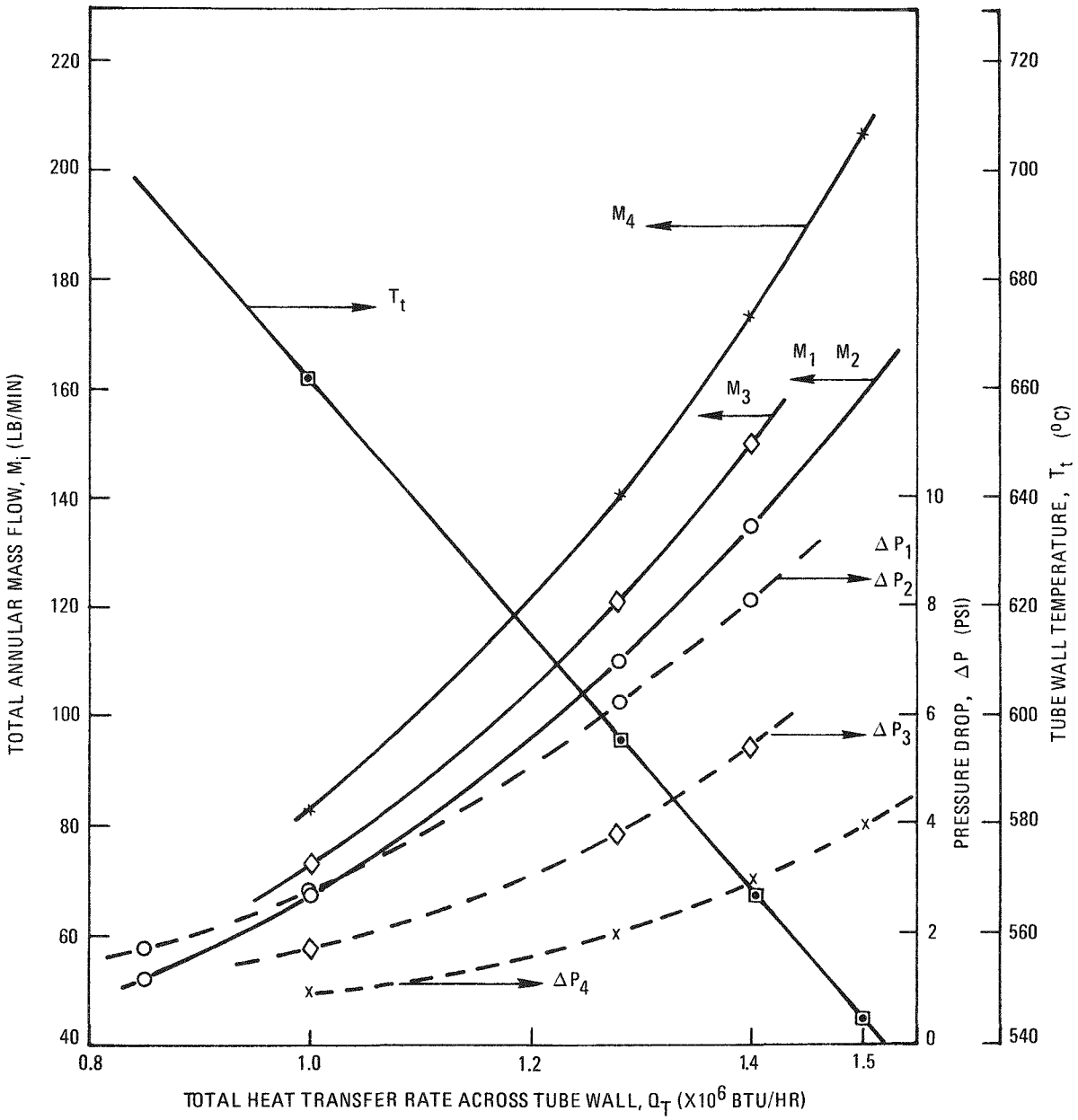

Fig. 4-8. Performance of fin section for annular cross sections corresponding to case A geometry (case A: expected worst case)

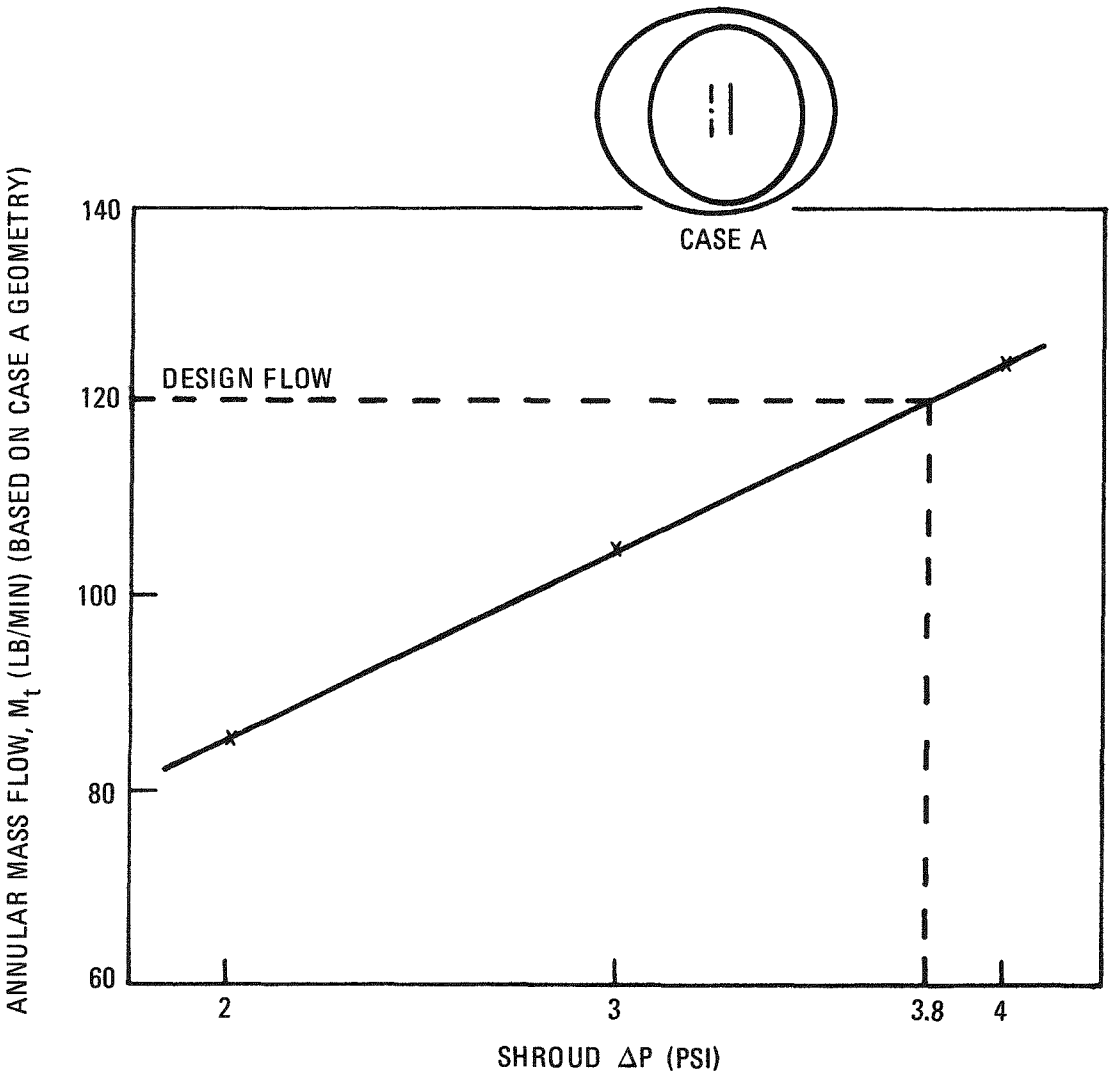

Fig. 4-9. Annular mass flow for case A as a function of shroud pressure drop

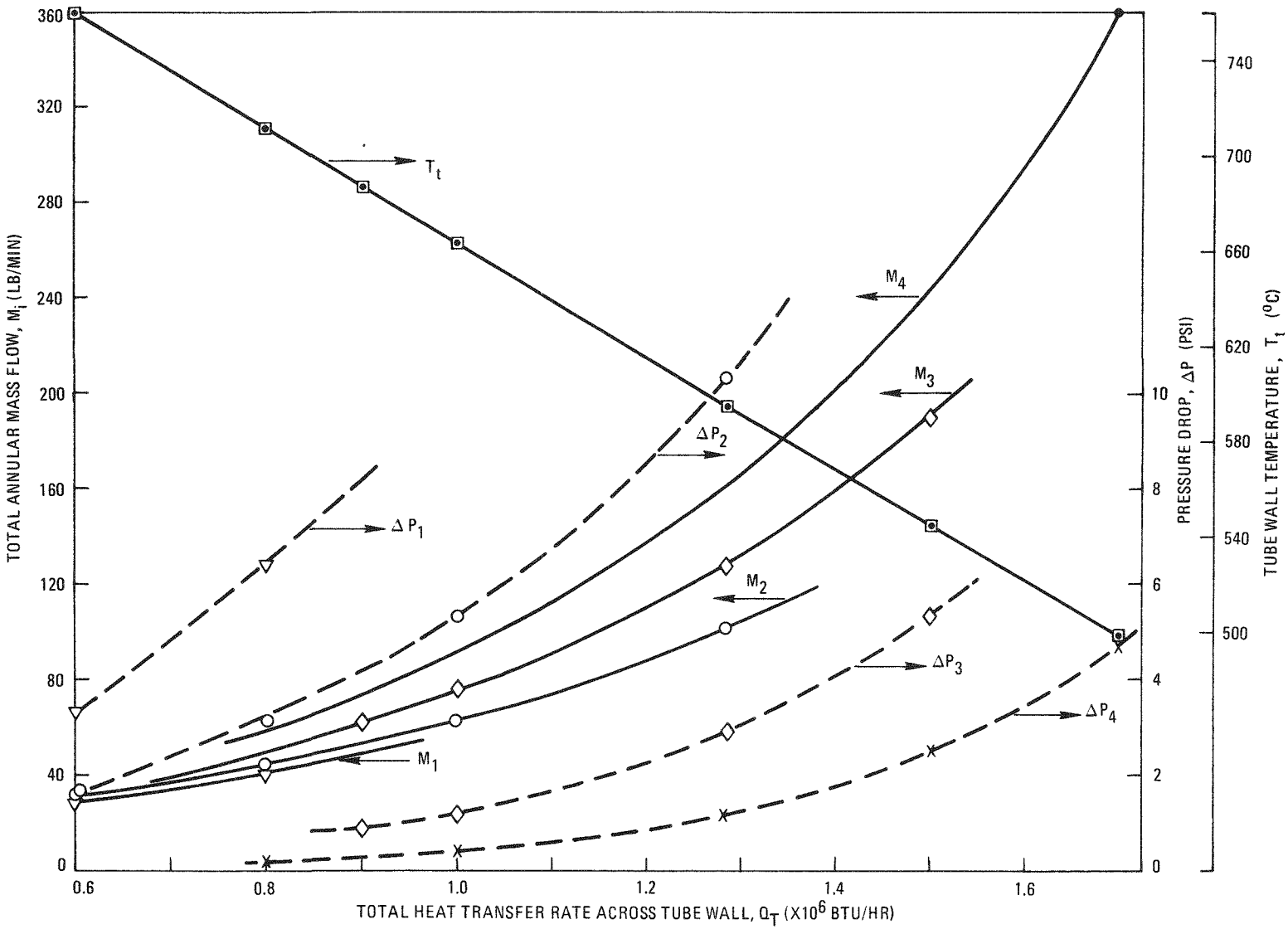

Fig. 4-10. Performance of fin section for annular cross sections corresponding to case B geometry (case B: maximum possible deviation)

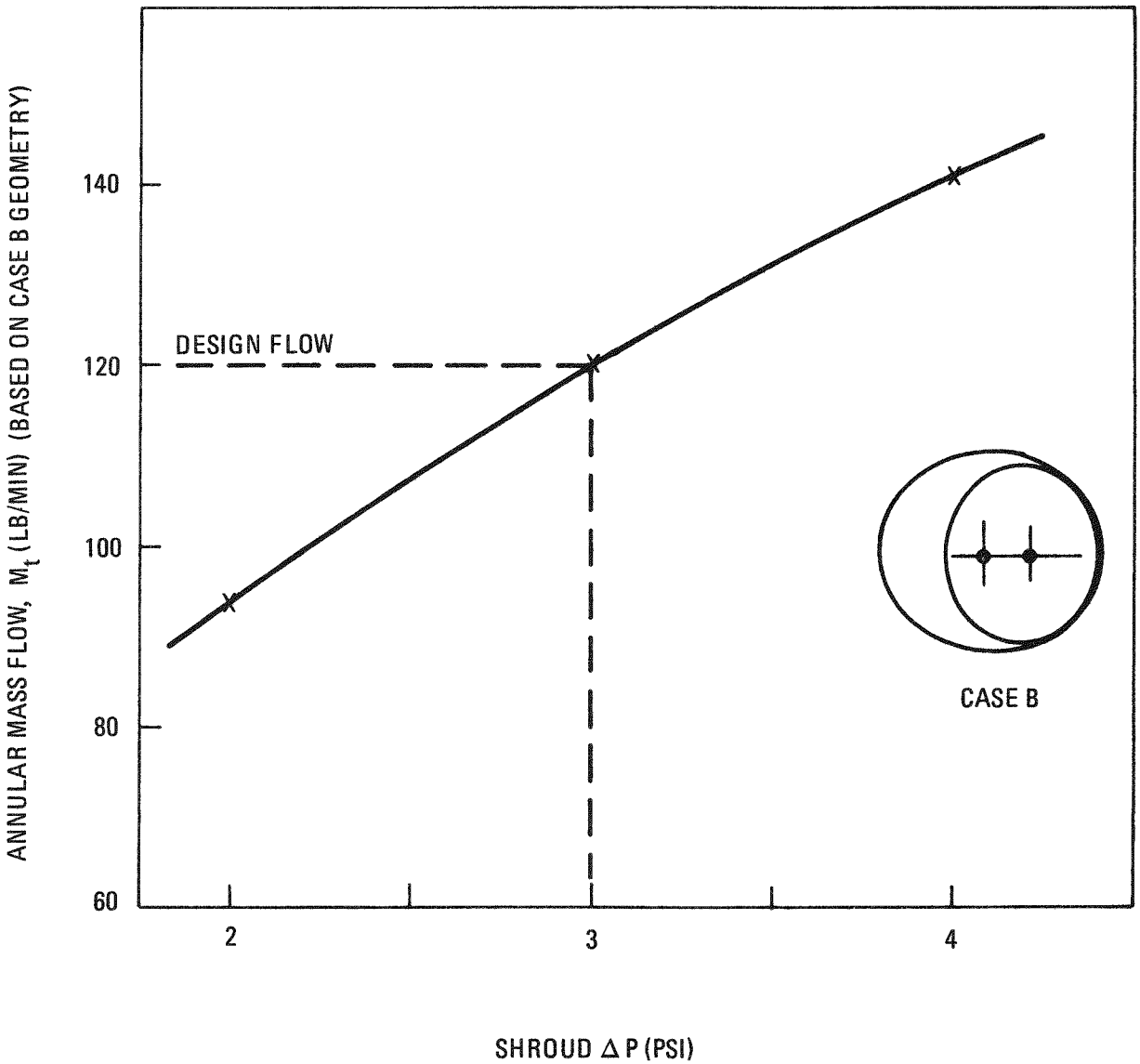

Fig. 4-11. Annular mass flow for case B as a function of shroud pressure drop

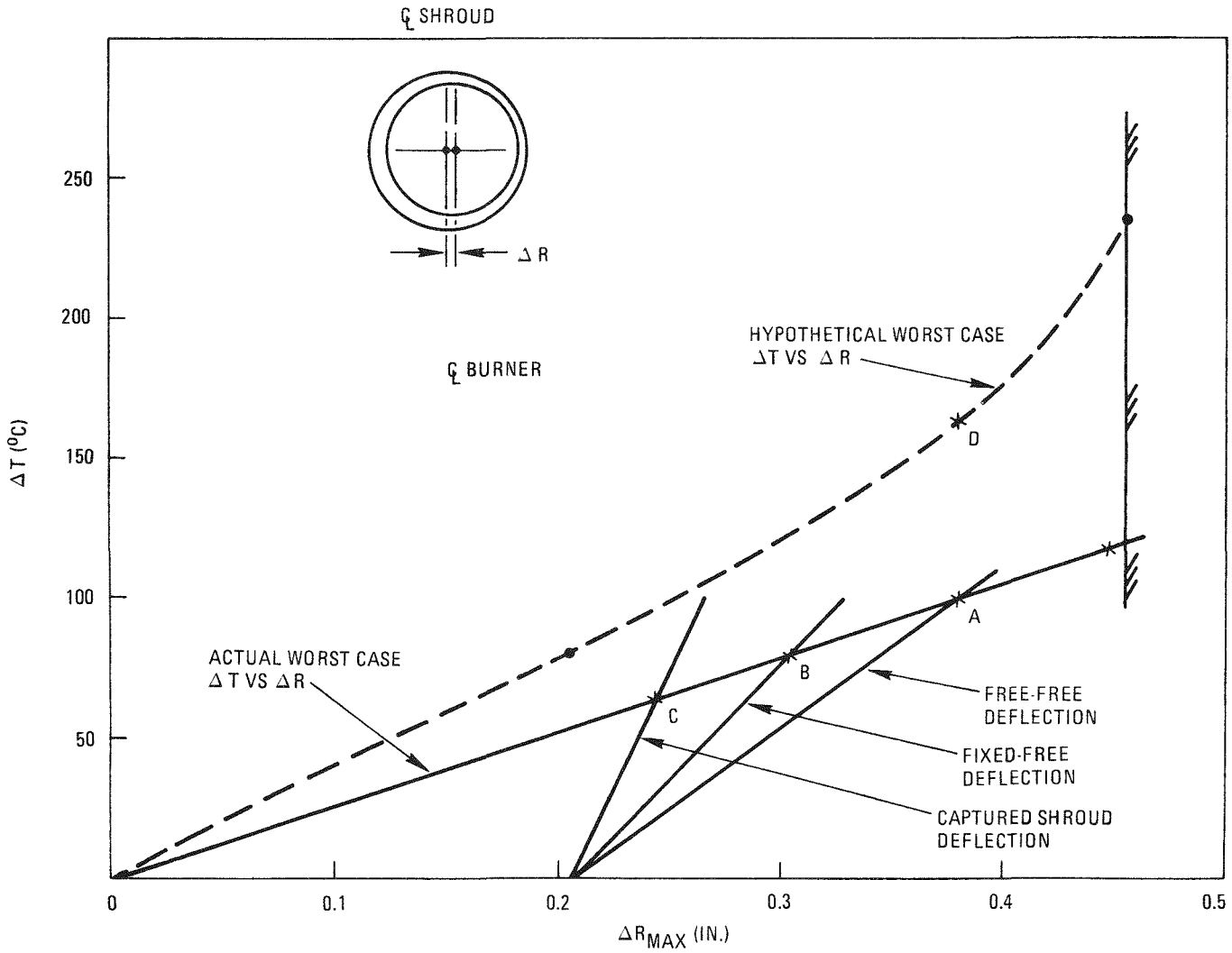

Fig. 4-12. Structural-thermal response of burner tube

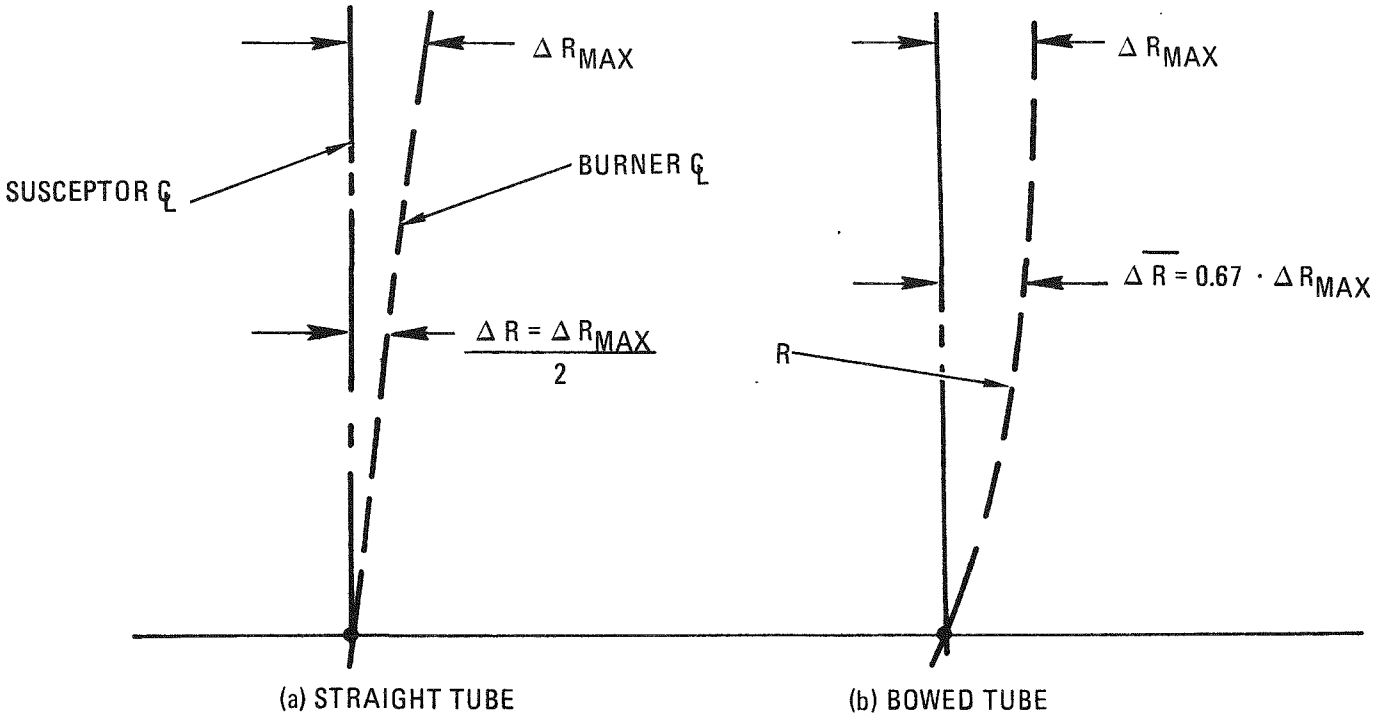

Fig. 4-13. Average gap relations

growth can now be answered by calculating the thermal deflection of the burner tube as a function of ΔT and plotting the resultant curve. This procedure was followed for three distinct cases:

1. Free-free support - current burner configuration. Burner is free to rotate at both ends.

2. Fixed-free support - the top of the burner is fixed while the bottom is free to rotate. This condition is readily achieved by bolting or clamping the burner support plate to the support beams.

3. Captured shroud - the burner cooling shroud is captured to the burner by the addition of a two-axis restraint (spacers) between the burner and shroud.

Thermal deflection was calculated by assuming that the circumferential temperature gradient is sinusoidal. The lateral temperature gradient is therefore linear, which produces a deflection curve of constant curvature. The deflection shapes corresponding to the three cases are shown in Fig. 4-14. The burner displacement, ΔR_{max}, is then the sum of the initial eccentricity and the additional thermal displacement between the shroud centerline and burner centerline.

The curves so calculated are shown in Fig. 4-12. The three curves intersect the thermal response curve at points A, B, and C, corresponding to cases, 1, 2, and 3, respectively, which indicates that all three cases demonstrate self-limiting growth. Stabilized values of maximum displacement and temperature gradient are given in Table 4-8.

Conservatively, the current design with as-received components might develop a worst-case burner tube ΔT of 100°C (212°F) and attain a maximum lateral eccentricity of 0.38 in. relative to the cooling shroud.

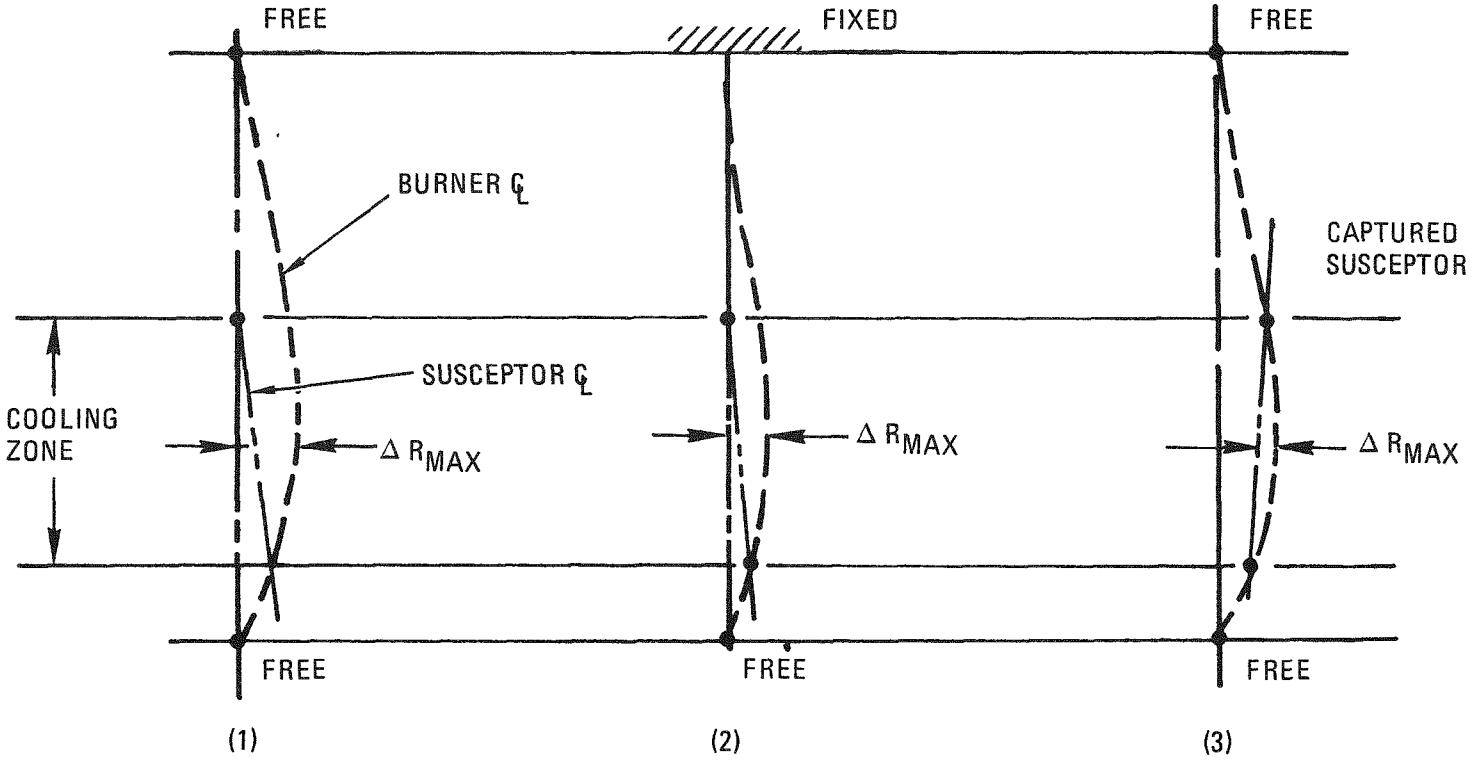

Fig. 4-14. Deflection shapes for three support arrangements

TABLE 4-8
BURNER DISPLACEMENT AND TEMPERATURE GRADIENTS FOR SEVERAL SUPPORT ARRANGEMENTS

Support Arrangement	Initial Eccentricity (in.)	Max. Thermal Deflection (in.)	Total Eccentricity (in.)	Max. ΔT (°C)
Free-free	0.205	0.175	0.38	100
Fixed-free	0.205	0.100	0.305	80
Captured-shroud	0.205	0.040	0.245	64

Other than the bending deflection, the only other effect of note is a thermal stress which develops in the tube as a result of a skewed temperature distribution. As shown in Fig. 4-15, the temperature distribution is not sinusoidal (balanced) as conservatively assumed for deflection calculations. The resulting thermal stress was calculated for an axial peak ΔT of 160°C (point D, Fig. 4-12). As shown in Fig. 4-15, the axial average maximum stress is 12.3 ksi and occurs on the diameter which is perpendicular to the diameter of the maximum ΔT. Since this maximum stress is less than 3 S_m (= 33.9 ksi at 648°C) and σ_y (= 27 ksi at 648°C), elastic shakedown will occur and neither fatigue nor creep-fatigue is likely to be a significant phenomenon.

4.2.3. Primary Burner Vessel Fabrication

The vessel fabricator's inspection plans required for pin fin fabrication were approved. Weld procedures, record and operator qualification tests, material certification for weld tests, and weld test data were approved for construction by Quality Assurance.

Fabrication of the burner assembly was started by Monarch Machine Corporation on January 14, 1976. As of mid-February, the lower Grayloc Hastelloy-X coupling was successfully welded to the burner tube and passed inspection by radiography. The thermal support skirt was also finished. At present the fabricator is awaiting delivery of the new Hastelloy-X Grayloc upper hub (P/N 5244019-1), which must be welded on the vessel before proceeding to the pin welding phase. The Hastelloy-X upper hub was shipped in February.

As required by the pin fin specification, pin samples were made on the same holding fixture that will be used for stud welding pins on the vessel. The holding fixture can index pin location to within ±0.005 in. by means of an indexing disc for radial location and an indexing rail for axial location. Figure 4-16 shows the holding fixture setup. Figures 4-17 and 4-18 describe the stud welder in action in making a pin sample.

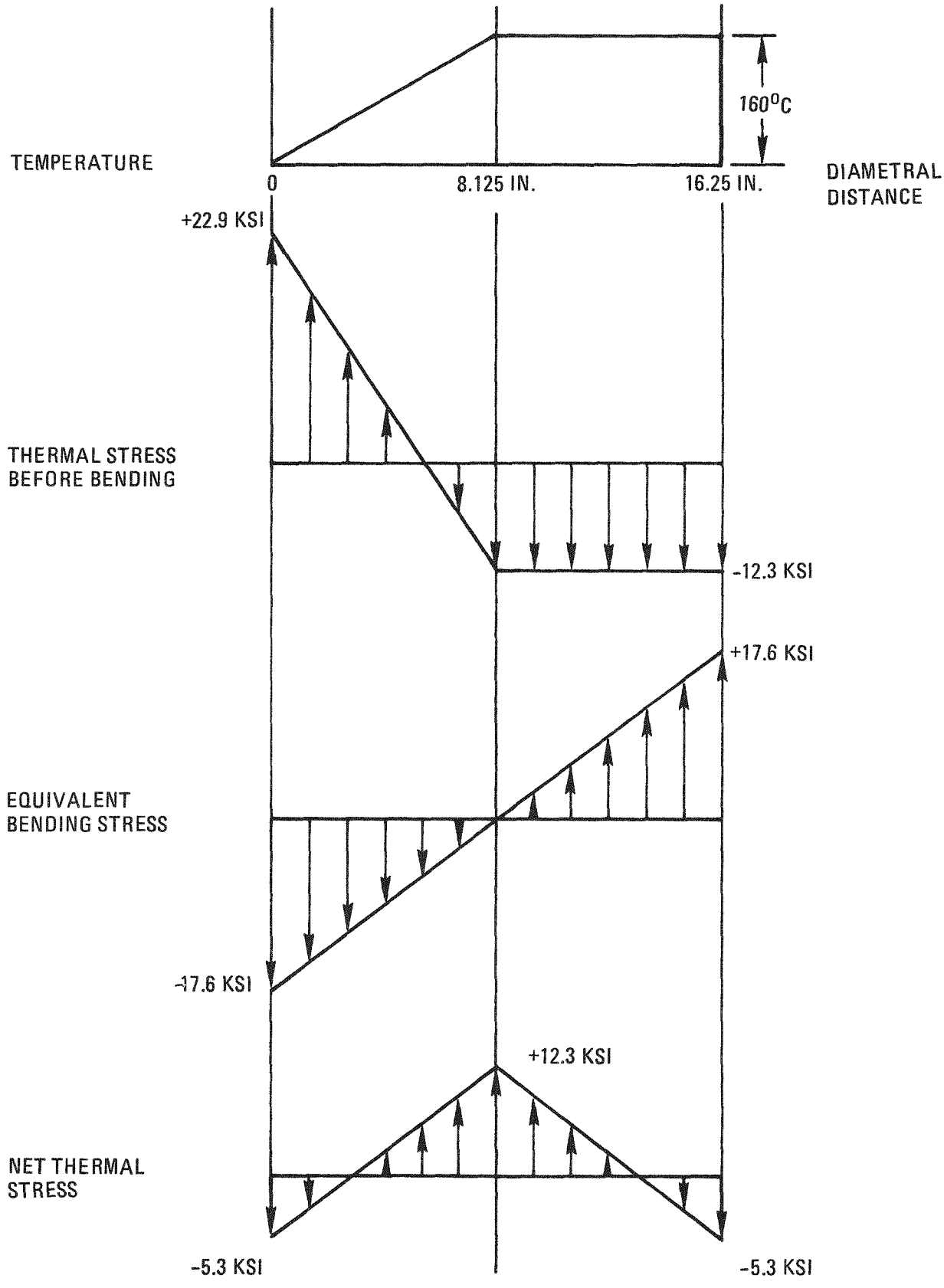

Fig. 4-15. Burner tube maximum thermal stress due to peak lateral temperature gradient

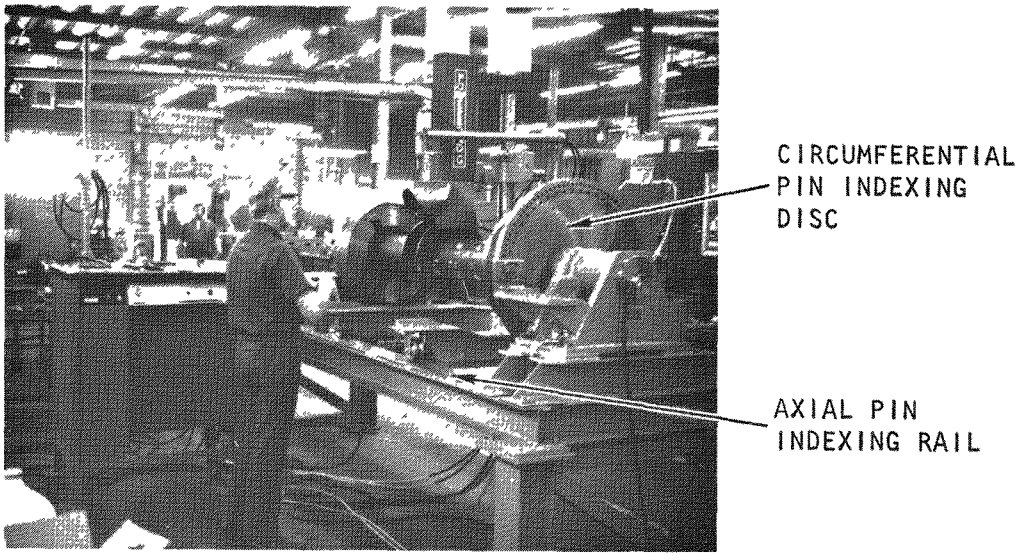

Fig. 4-16. Pin welder and holding fixture for primary burner

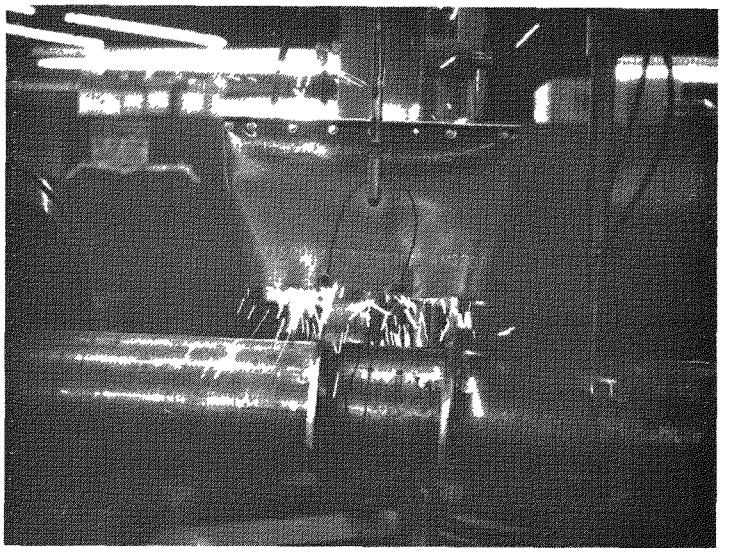

Fig. 4-17. Cooling pin welding in progress for primary burner

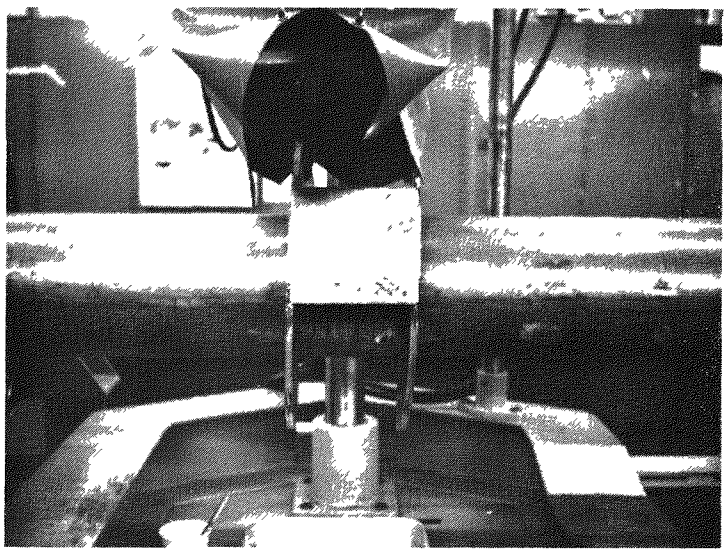

Fig. 4-18. Finished pin sample for primary burner

4.2.4. Heating and Cooling System Installation for Primary Burner

The heating and cooling system components are progressing toward final assembly and installation. With the help of the susceptor-ceramic trunnion holding fixture, the heater section is being assembled in a sequence as shown in Fig. 4-19. The assembly is expected to be installed by the end of February.

4.2.5. Installation of Auxiliary Systems for Primary Burner

The prototype burner induction heating system has been installed (Fig. 4-20). It has been checked and approved by the motor-generator manufacturer and is currently operable.

Piping and component installation continues in the prototype burner instrument cabinets (Fig. 4-21). This will soon be phasing into interconnecting piping between the burners and the cabinets.

Prototype burner plenum carts are now being assembled. All parts have been received (Fig. 4-22) and most of them have been painted. The carts will be installed in the pit after assembly.

The cooling air blower is installed in the blower vault (Fig. 4-23). Instrumentation and control cable connections are under way with preoperational testing expected in March.

4.2.6. Prototype Fines Recycle for Primary Burner

All major components are scheduled for delivery in February with the exception of the hopper support system, which is scheduled to arrive in early March. Assembly and installation of this equipment will be done by GA technicians.

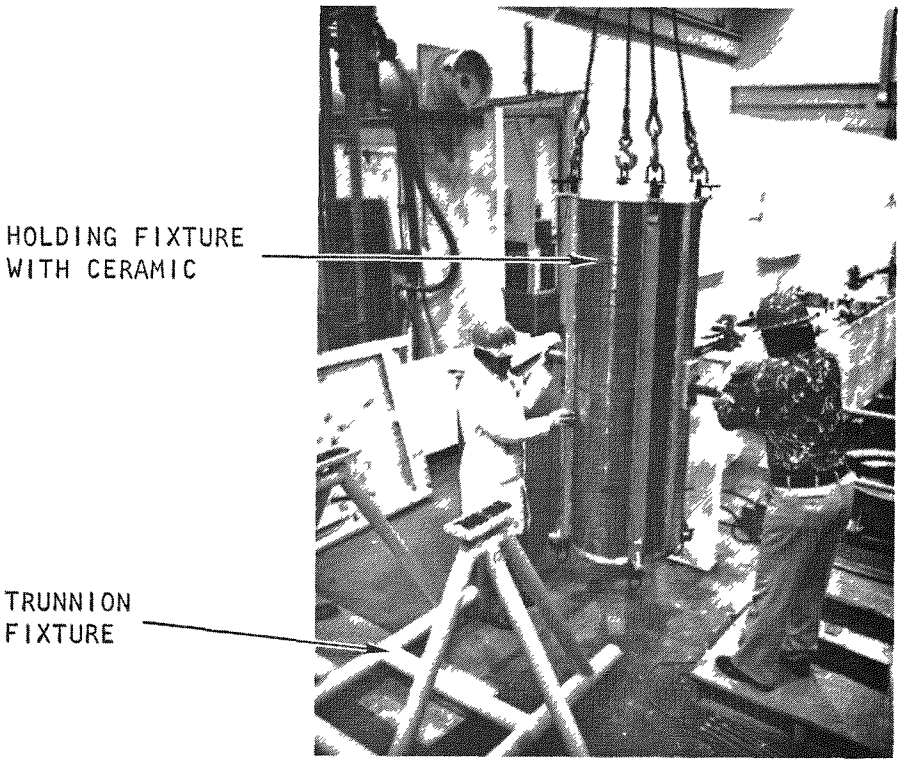

(a) Ceramic insulation is picked up with holding fixture and transferred to trunnion fixture

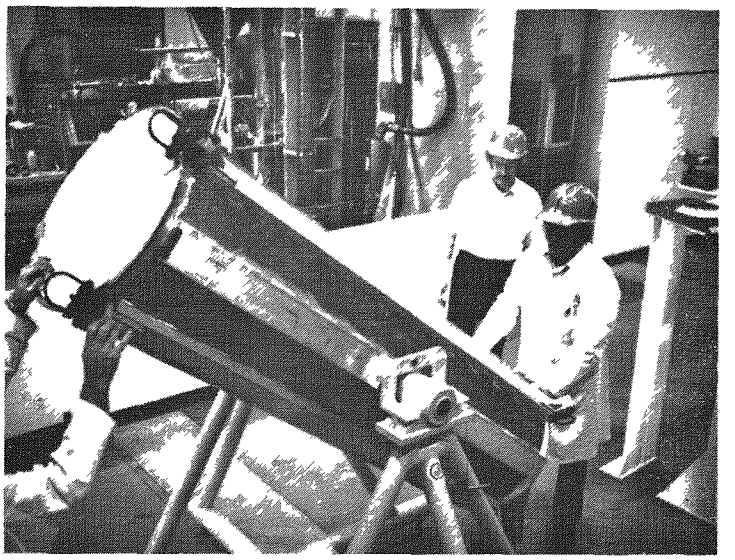

(b) Fixture is rotated so that ceramic insulation is bottom-side up

Fig. 4-19. Sequence for assembly of 40-cm primary burner heater section

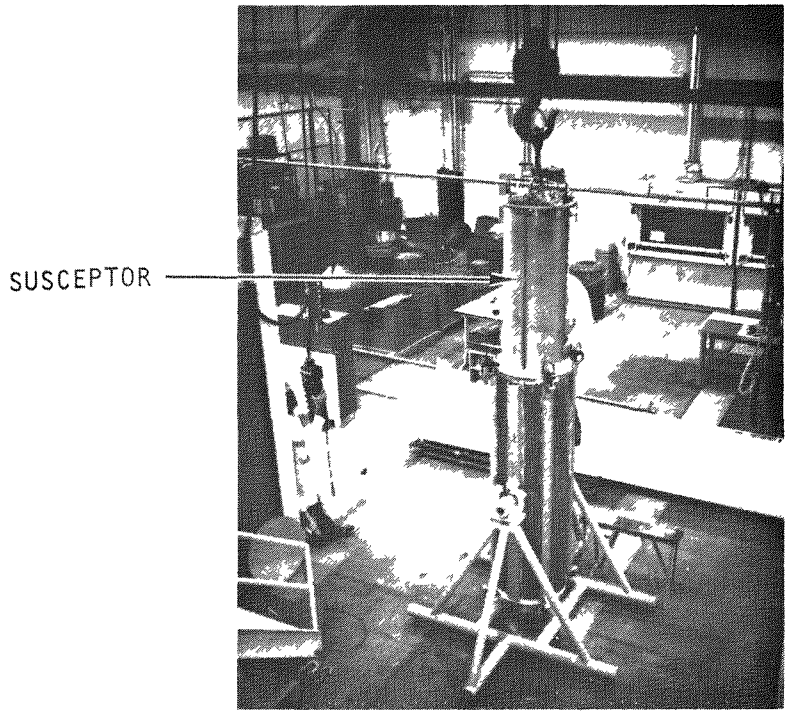

(c) Susceptor is inserted into the ceramic insulation with the susceptor lifting fixture

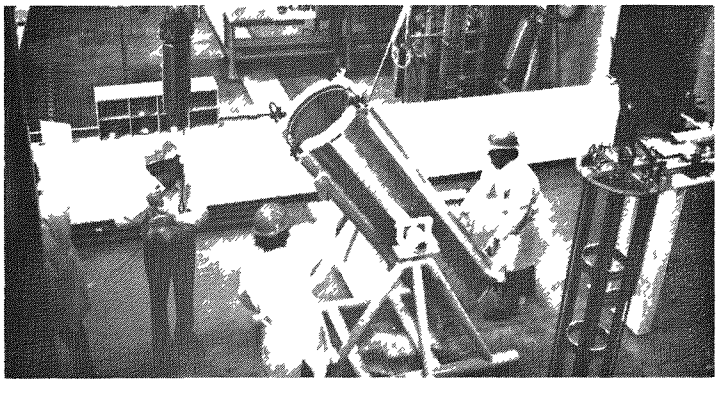

(d) Susceptor-ceramic assembly is rotated so that it is right-side up

Fig. 4-19. Sequence for assembly of 40-cm primary burner heater section

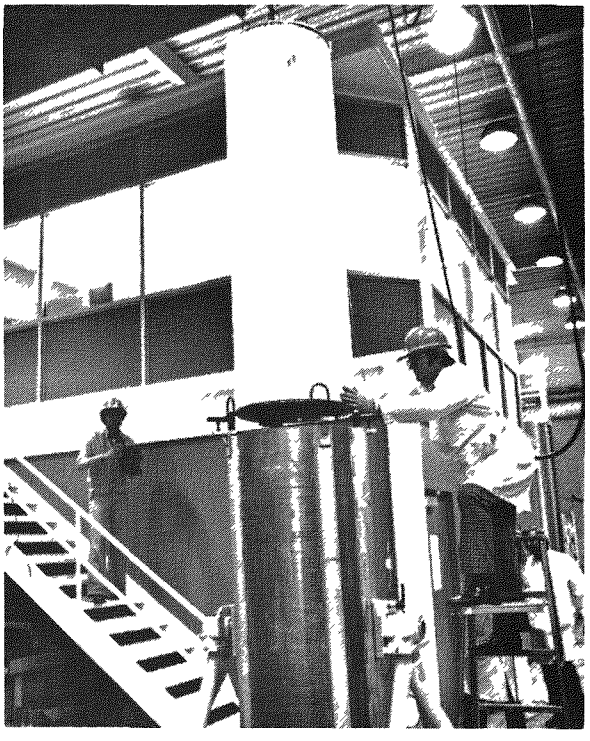

(e) Ceramic-susceptor assembly is picked up by the susceptor flange with the lifting fixture

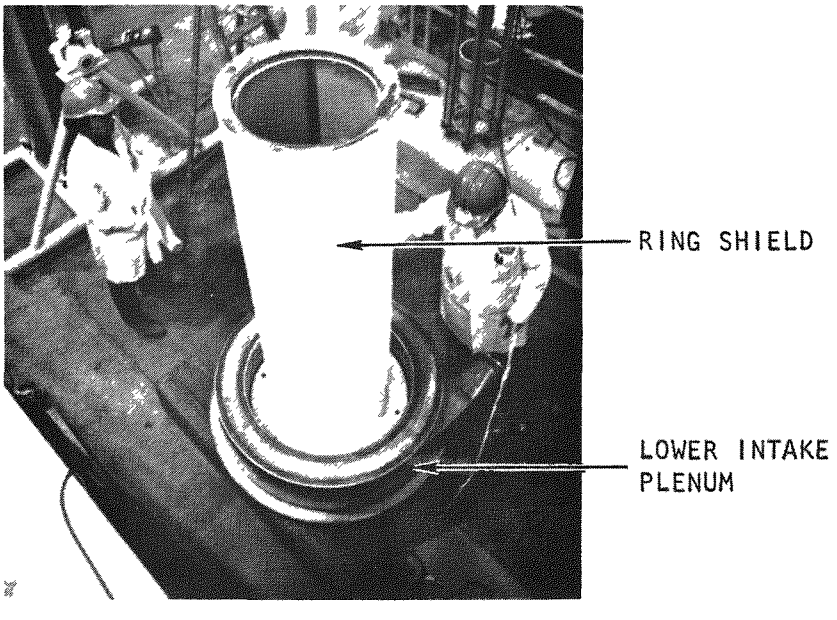

(f) Susceptor-ceramic assembly is positioned on lower intake plenum

Fig. 4-19. Sequence for assembly of 40-cm primary burner heater section

(g) Induction coil is slipped over the ceramic insulation

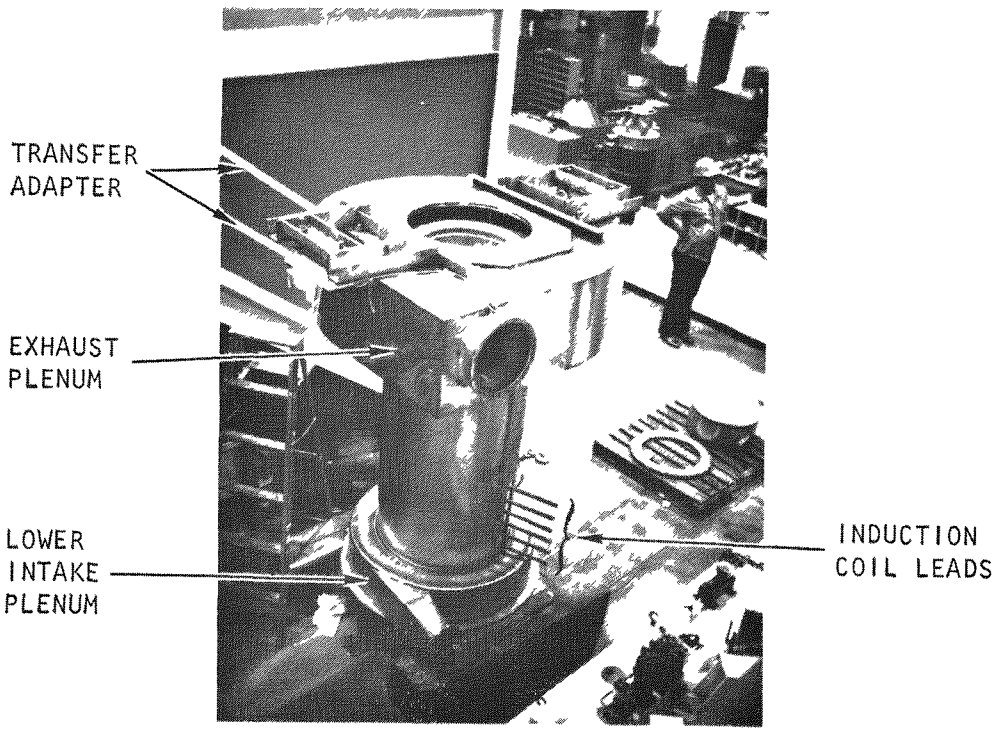

(h) Completed primary burner heater assembly

Fig. 4-19. Sequence for assembly of 40-cm primary burner heater section

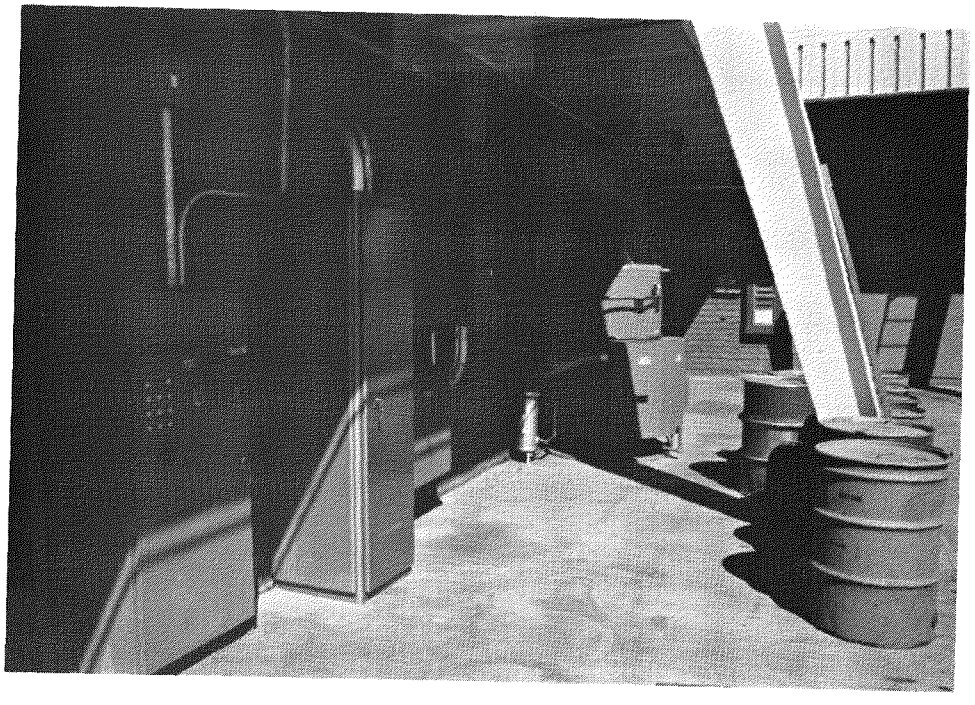

Fig. 4-20. Induction heater installation for the prototype burners

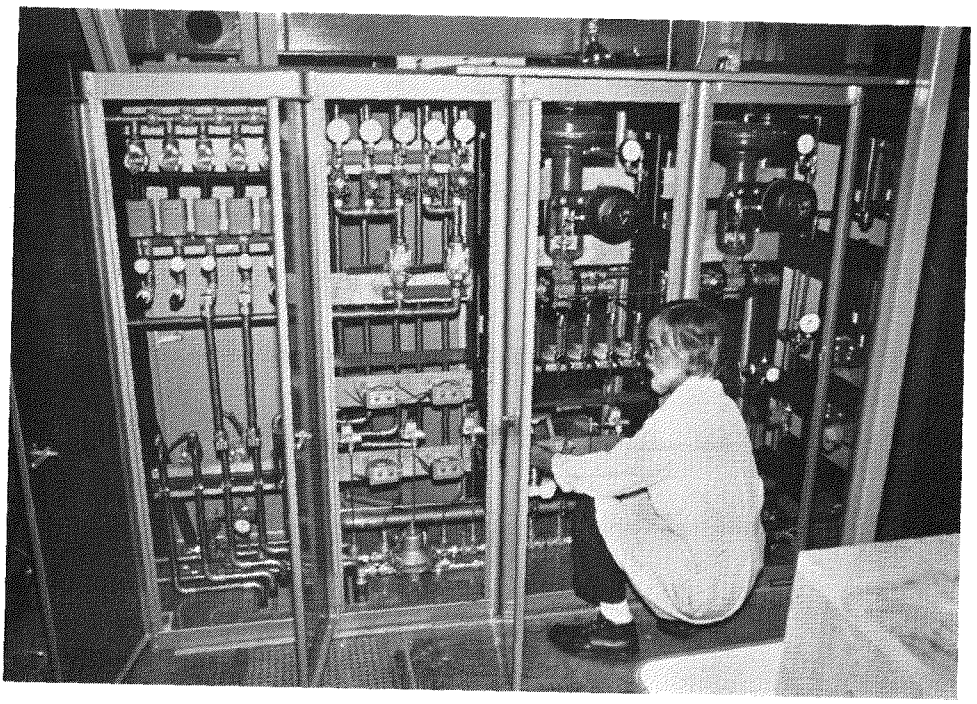

Fig. 4-21. Piping and control valve cabinet for the prototype burners

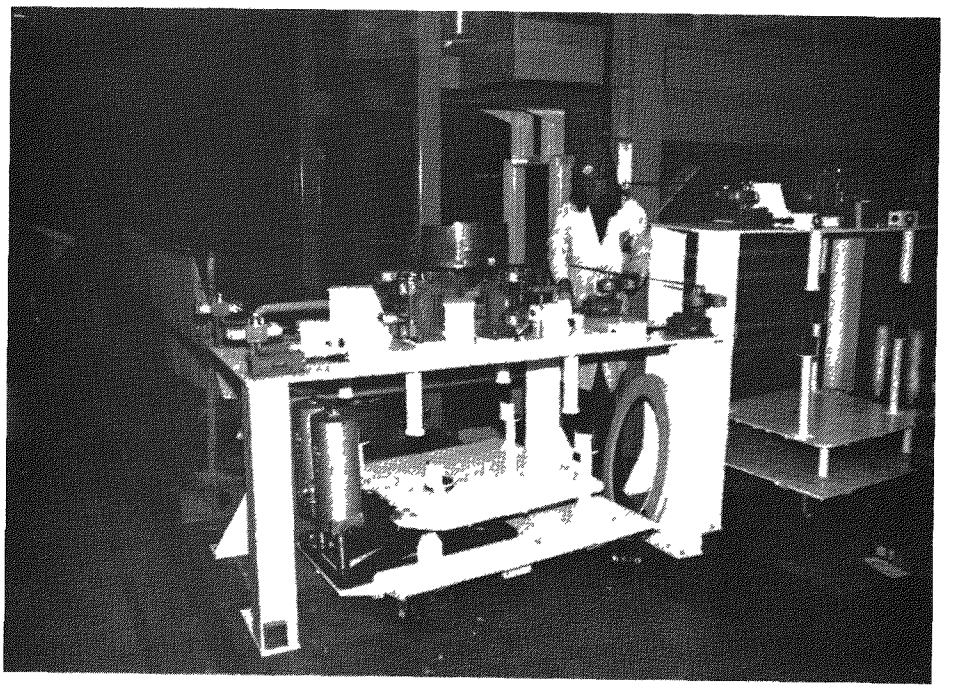

Fig. 4-22. Plenum carts for the 40-cm primary burner

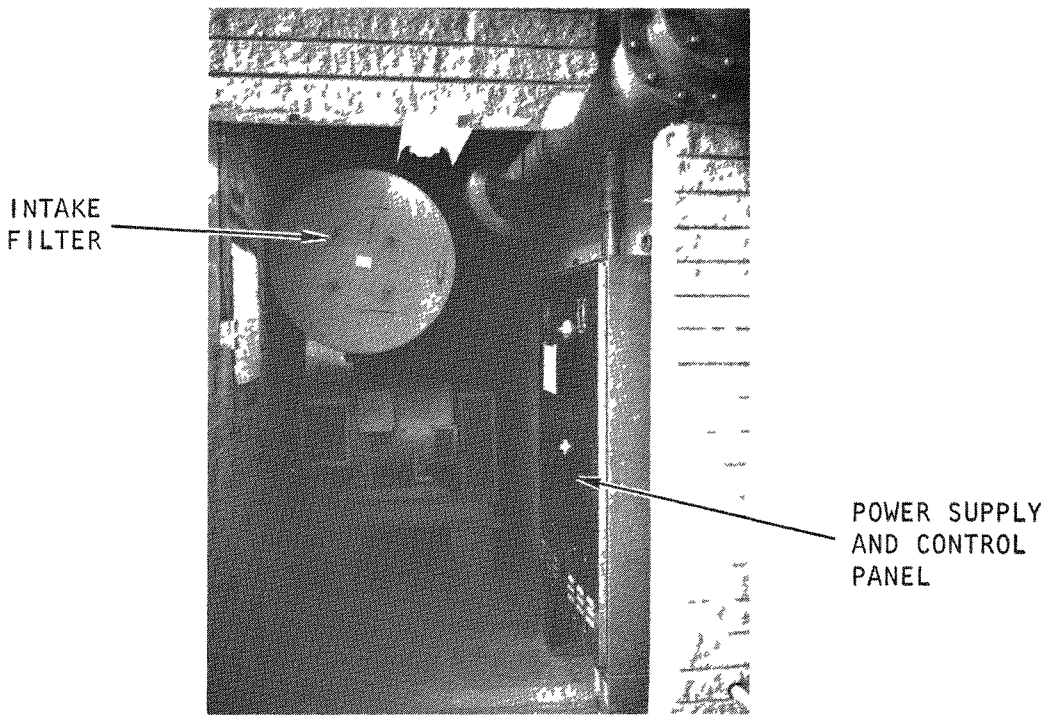

Fig. 4-23. Cooling air blower installation in blower vault for the prototype burners

4.3. 20-CM PRIMARY FLUIDIZED-BED BURNER

4.3.1. Burner Installation

Installation of the rebuilt 20-cm primary burner has been completed. Shakedown tests of the induction heating system have verified wall heatup to 900°C using the empty burner tube. Inert and fresh feed bed heatup and startup testing awaits final instrumentation connections with the Diogenes semiautomatic controller.

The experimental plan (Ref. 4-7) for the rebuilt 20-cm primary burner includes confirmation of the prototype design configuration and control functions developed to date, as well as continuing development investigation of alternate fines recycle modes and control functions that may improve the process simplicity and economics.

4.3.2. Fluidization Studies (Ref. 4-8)

Cold fluidization studies were performed in a simulated 20-cm glass primary burner to investigate primary burner fluidization characteristics. Twenty beds ranging in size from 10 to 40 kg and in composition from -3/16 in. fresh feed (17 wt % particles) to 100% particles were fluidized at 0 to 4.5 ft/sec. Work was performed with the actual distributor (90° perforated cone with 1/2-in.-diameter vertex) that had been used on the hot 20-cm primary burner prior to the recent rebuild of the system. The objectives of these experiments were:

1. Determination of maximum bed or slug height (H_{max}) as a function of bed composition and fluidization velocity.

2. Determination of bubbling or slugging characteristics.

3. Investigation of effects of vertex gas flow rate on bed mixing characteristics and H_{max}.

4. Determination of bed mixing characteristics as a function of bed composition, bed weight, and velocity.

5. Comparison of experimental H_{max} with predicted data.

6. Investigation of effects of distributor design.

7. Determination of product removal rates under normal operating conditions.

Maximum bed (slug) heights, H_{max}, were plotted as a function of gas velocity and bed composition (wt % fertile TRISO particles) (Figs. 4-24a through 4-24d) and were found to agree well with values predicted by the following relation (Ref. 4-9):

$$\frac{H_{max}}{H_{mf}} = \frac{V - V_{mf}}{0.35(gD)^{1/2}} + 1 \quad ,$$

where H_{max} = maximum bed (slug) height, in.,
H_{mf} = bed (slug) height at minimum fluidization, in.,
V = superficial gas velocity, ft/sec,
V_{mf} = superficial gas velocity at minimum fluidization, ft/sec,
D = column diameter, ft,
g = gravitational constant, ft/sec^2.

It was generally found that H_{max}/H_{mf} was at its maximum when V_{mf} was at its minimum (Fig. 4-25).

As the fluidization velocity was increased through each bed, a transition from static to spouting to good fluidization and complete mixing occurred in some beds, whereas no spouting occurred in other beds. Spouting is dependent on many interrelated factors such as particle size, size distribution, gas-inlet diameter, cone angle, gas flow rate, and bed depth.

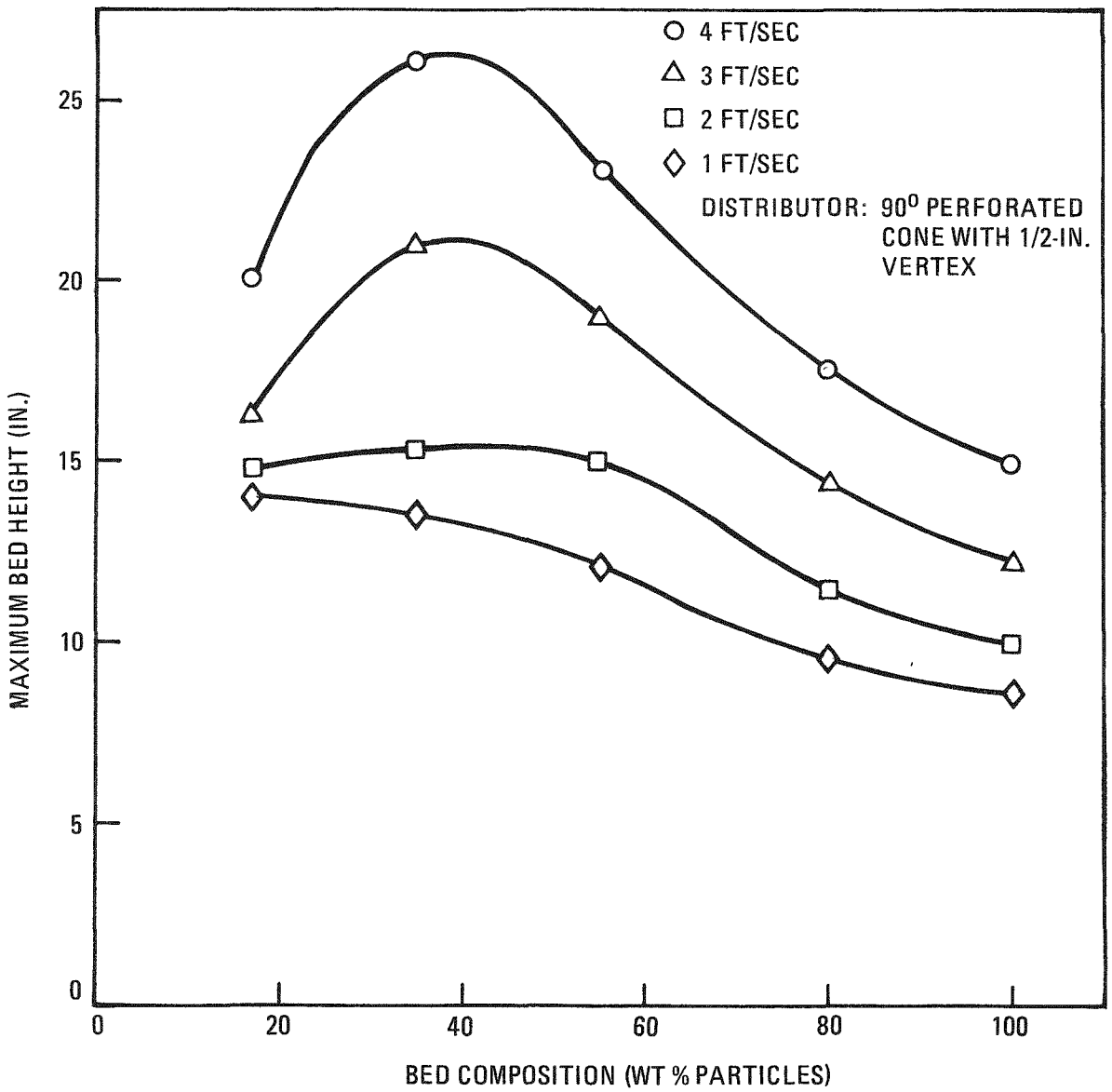

Fig. 4-24. Maximum bed height versus bed composition for the primary burner: (a) 10-kg beds

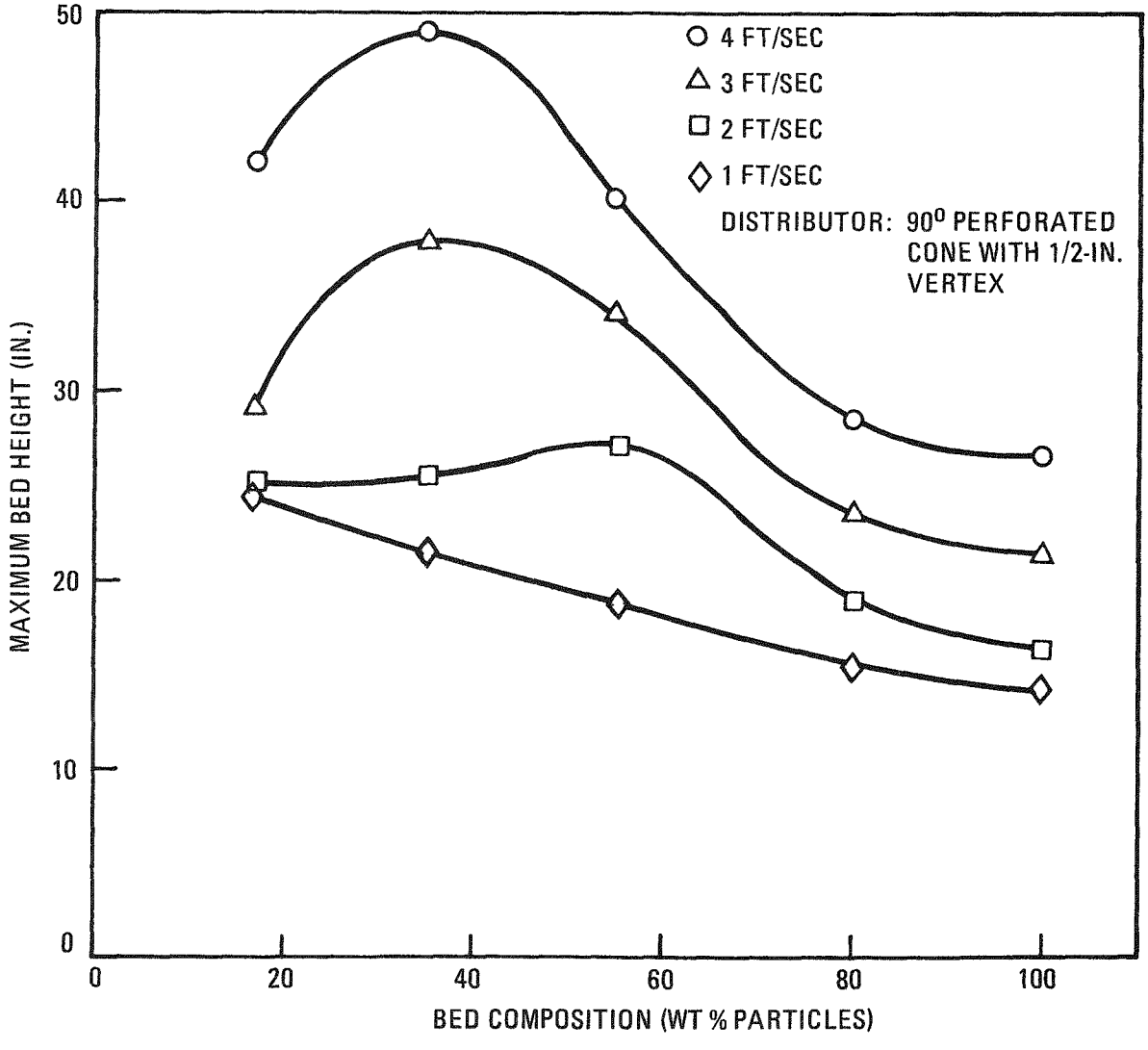

Fig. 4-24. Maximum bed height versus bed composition for the primary burner: (b) 20-kg beds

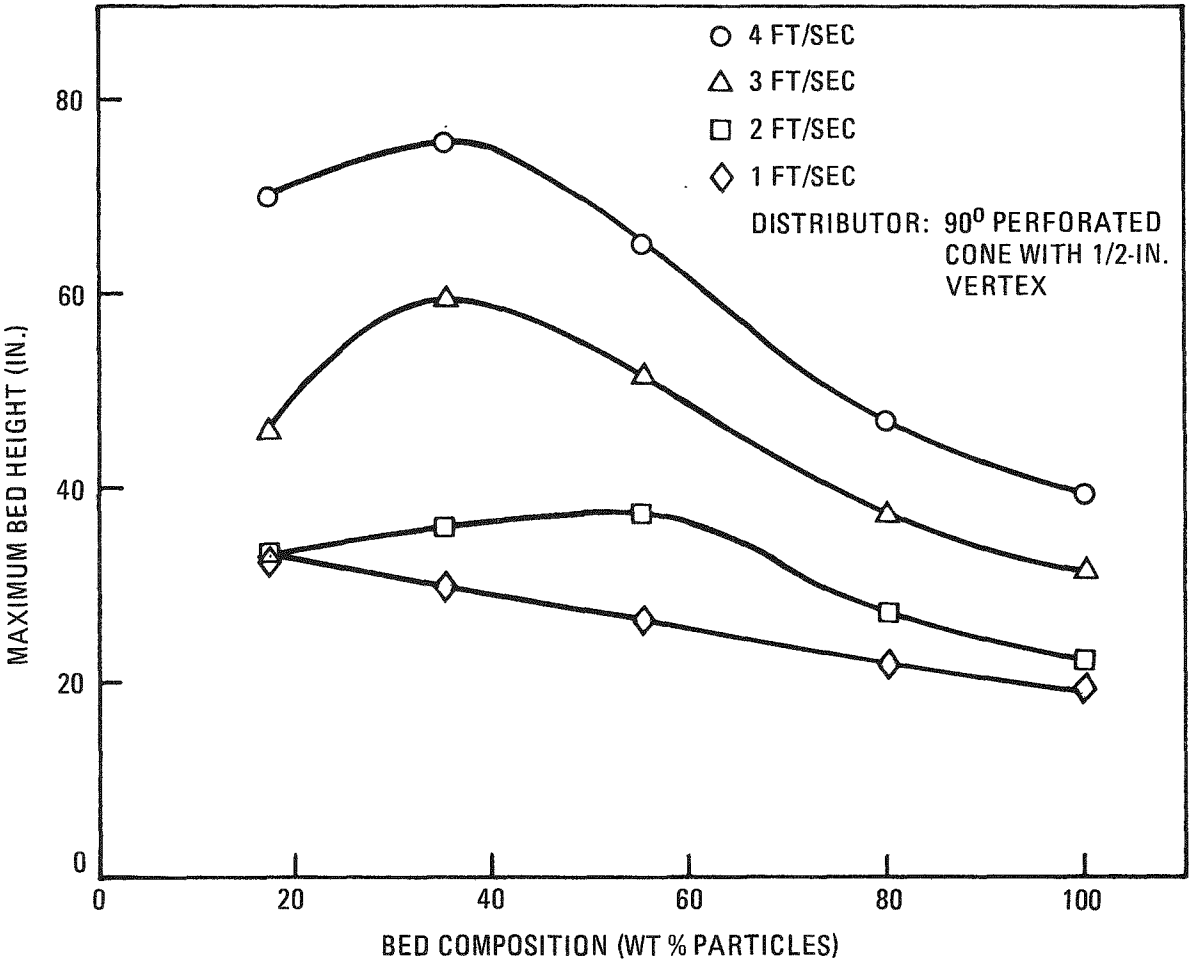

Fig. 4-24. Maximum bed height versus bed composition for the primary burner: (c) 30-kg beds

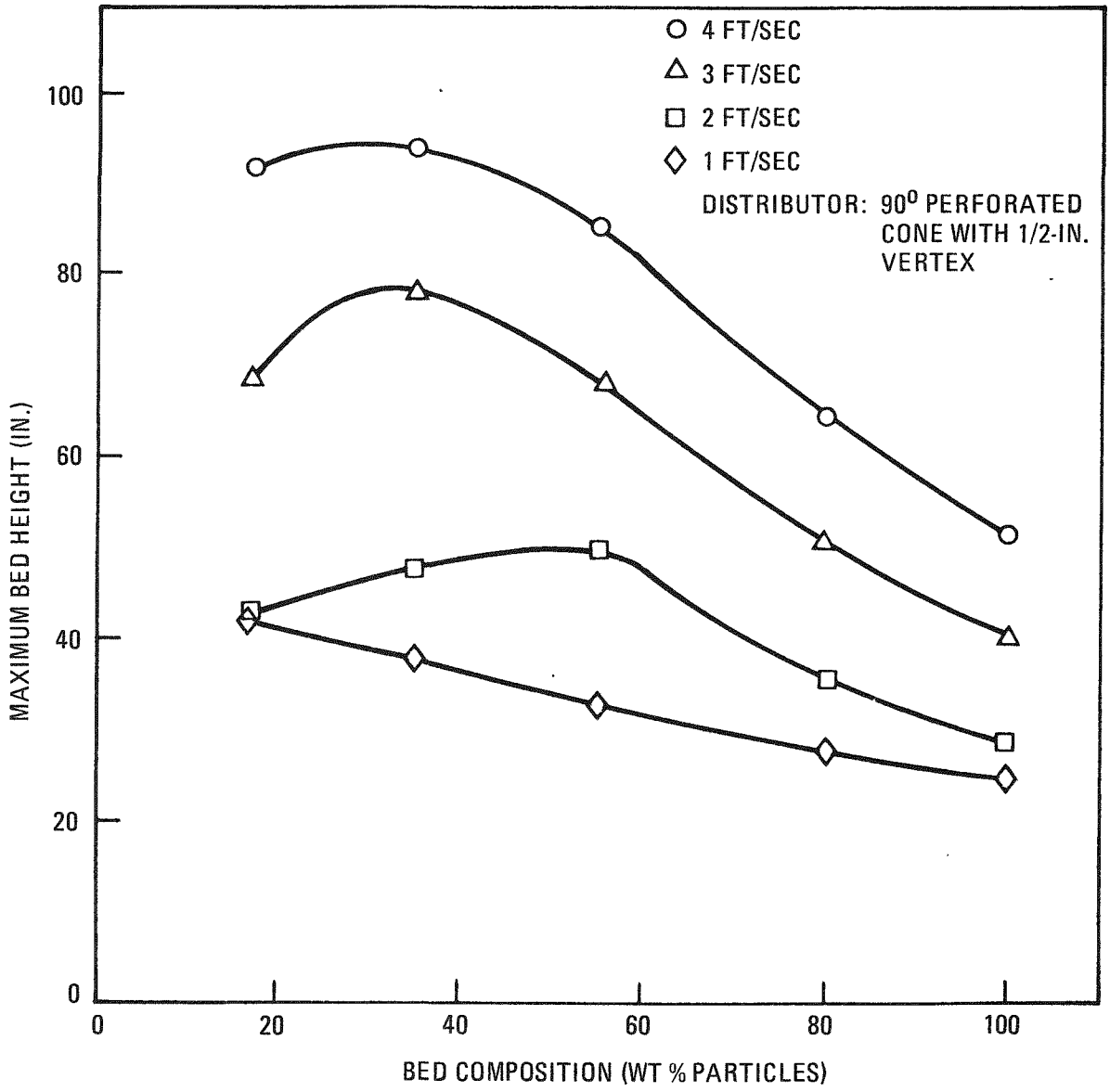

Fig. 4-24. Maximum bed height versus bed composition for the primary burner: (d) 40-kg beds

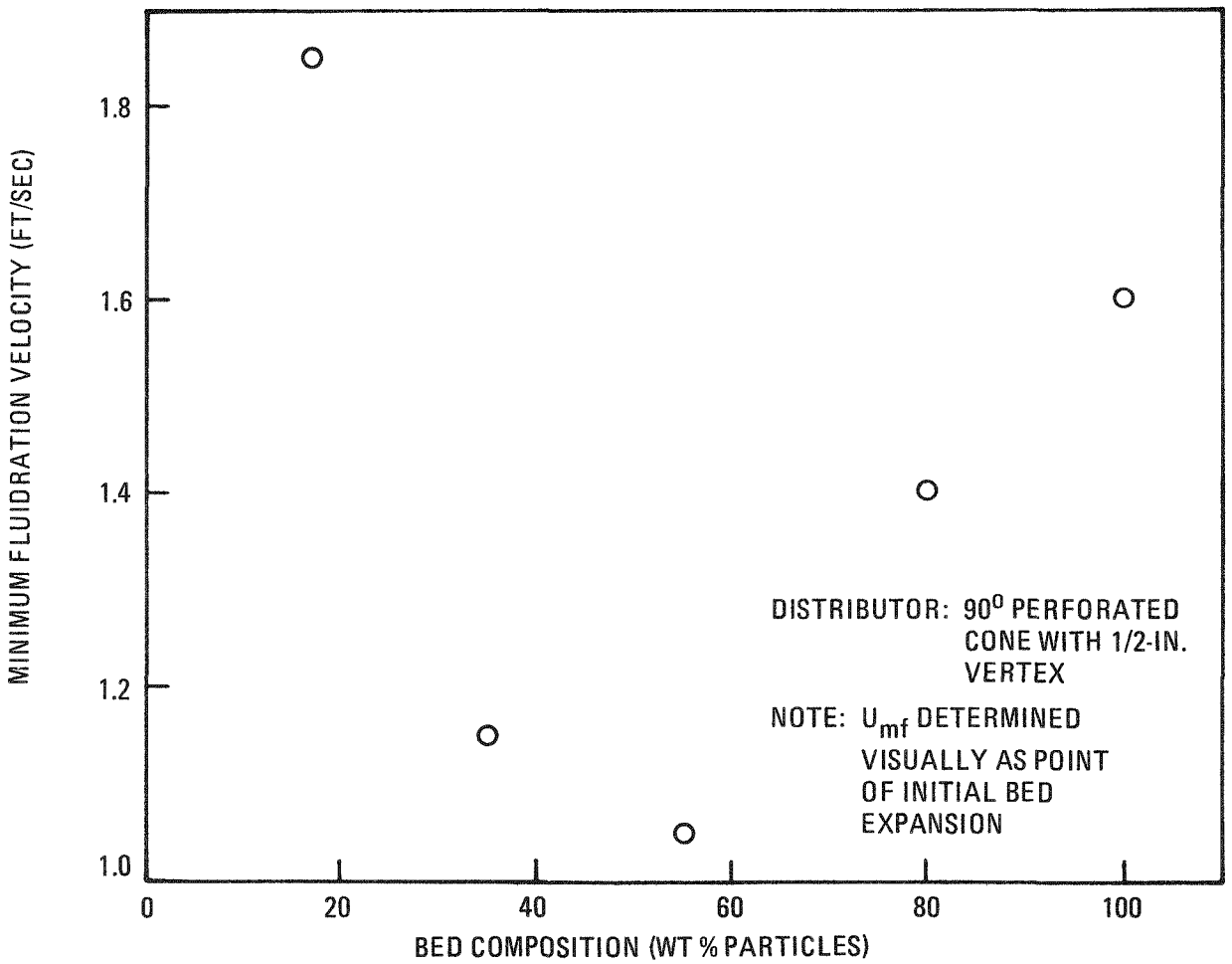

Fig. 4-25. U_{mf} versus bed composition for the primary burner

In this work, spouting was generally experienced in the smaller beds (10 to 20 kg), particularly in the lower particle beds, whereas it was not as evident in the larger 30- to 40-kg beds. The minimum spouting velocity increased as the bed weight increased and decreased as the vertex gas flow rate increased. Slugging generally occurred in beds of 20 kg or larger with sufficient fluidizing velocity. There appeared to be no discernible pattern to the observed slugging characteristics with respect to the height and frequency. Typical slug characteristics were such that a large slug approaching H_{max} seldom occurred; the majority of slugs were $<<H_{max}$.

Bed mixing characteristics were determined and plotted as functions of bed composition, superficial gas velocity, bed weight, and vertex gas flow rate (Figs. 4-26a and 4-26b). Bed compositions with low particle percentages were the most difficult to fluidize as V_{cm} (minimum velocity for complete and uniform bed mixing) dropped off very quickly as the bed became richer in particles. In beds of high particle percentage, V_{cm} decreased as the bed weight decreased, whereas in beds of low particle percentage, the reverse was true. In addition, the effect of vertex gas flow rate on V_{cm} was quite significant except in the high particle beds (Figs. 4-26c and 4-26d). In all cases, the general bed mixing pattern as velocity increased was to achieve a significantly better quality of mixing in the upper one-third to one-half of a bed than below. As the fluidization velocity approached that required for complete mixing, this discrepancy between upper and lower mixing gradually decreased until V_{cm} was achieved. This type of behavior was analogous to that previously reported (Ref. 4-8) in work with a different distributor (60° cone, 1-in.-diameter vertex).

Distributor design effects on bed fluidization characteristics were found to be significant as seen by comparison with work using a different distributor (Ref. 4-8). The major differences appeared to be a greater tendency to spout, a lower H_{max} at the same velocity, and a higher V_{cm} at a given bed composition for operation with the smaller 1/2-in. vertex and shallower 90° cone angle. Product removal through the 1/2-in. vertex was

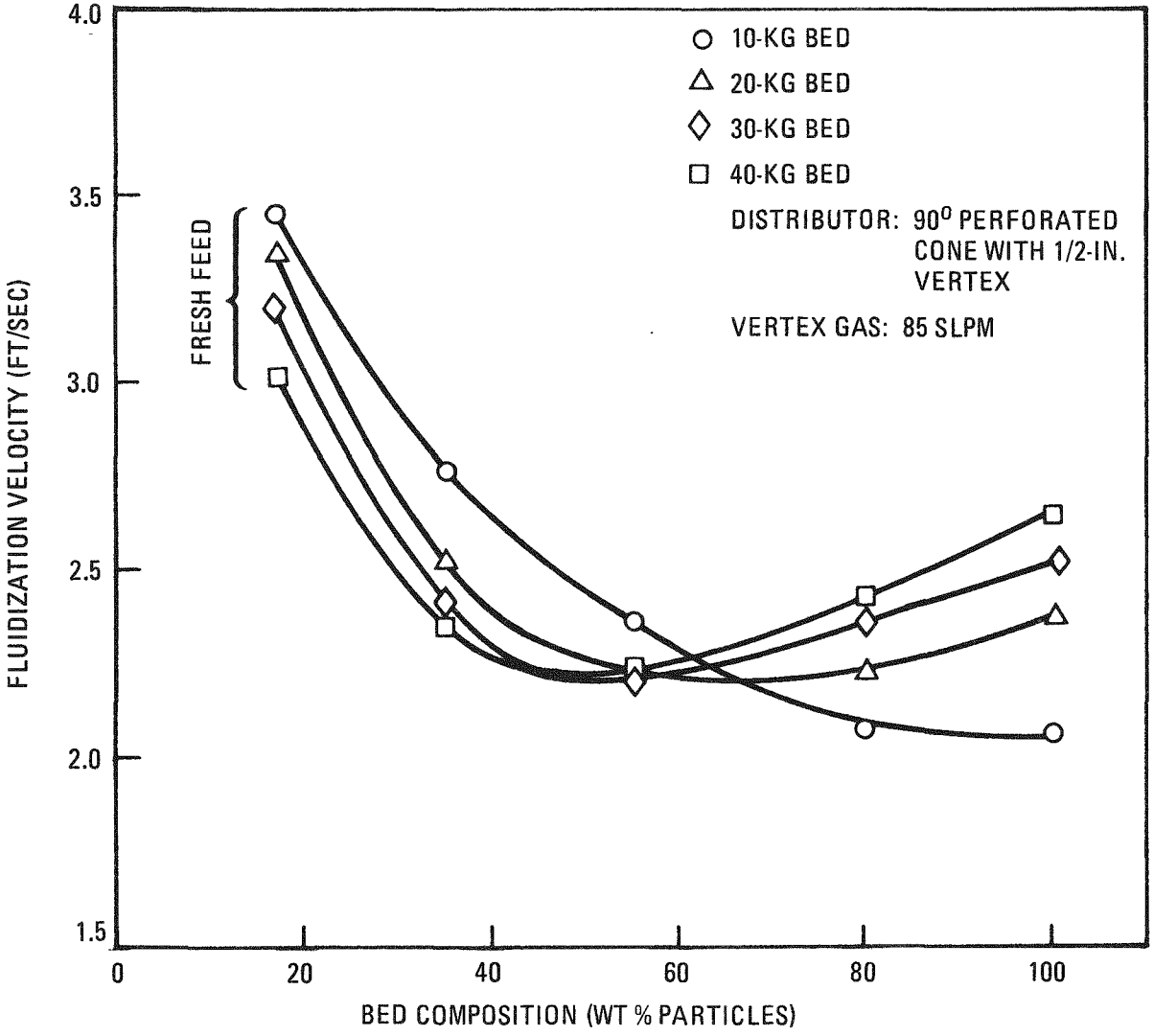

Fig. 4-26. Conditions for onset of complete and uniform bed mixing for primary burner: (a) 85 slpm vertex gas

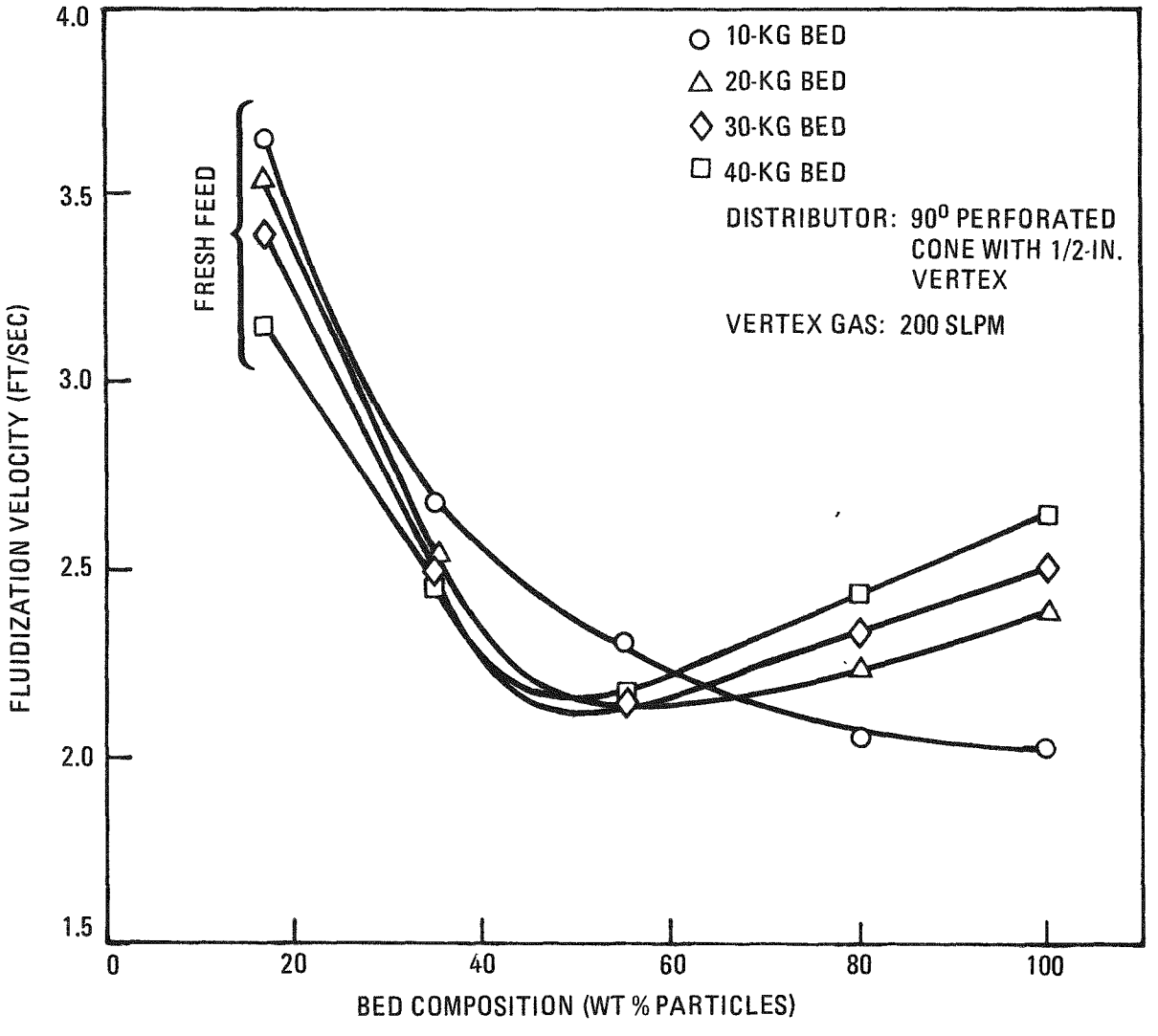

Fig. 4-26. Conditions for onset of complete and uniform bed mixing for primary burner: (b) 200 slpm vertex gas

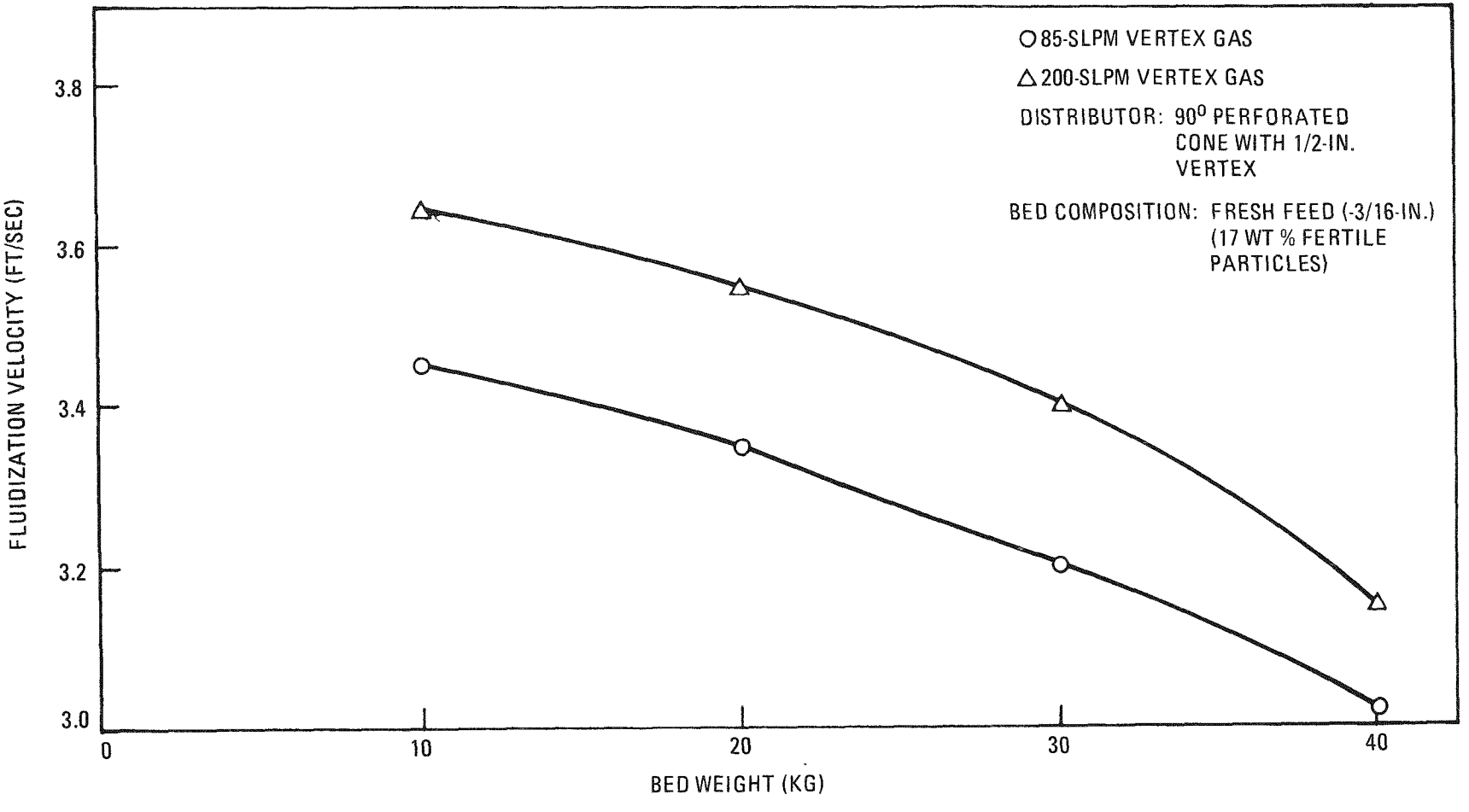

Fig. 4-26. Conditions for onset of complete and uniform bed mixing for primary burner: (c) 85 and 200 slpm vertex gas, fresh feed (-3/16 in., 17 wt % fertile particles)

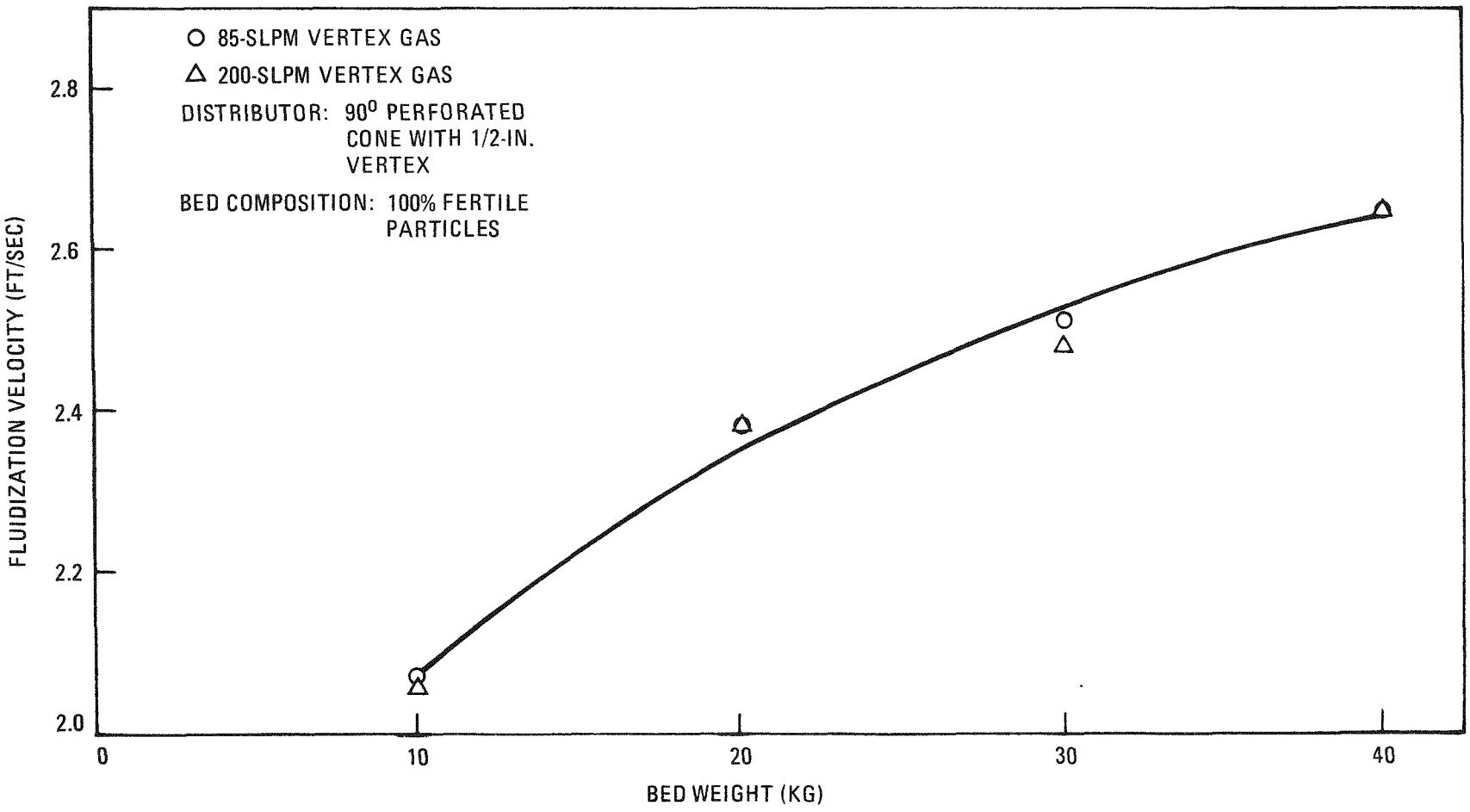

Fig. 4-26. Conditions for onset of complete and uniform bed mixing for primary burner: (d) 85 and 200 slpm vertex gas, 100% fertile particles

easily achieved using the 100% particle bed with rates of ∿18 kg/min. However, bridging occurred often in the other beds containing varying percentages of graphite. It is concluded from this work that a 1/2-in. vertex should not be used for product removal. The prototype primary burner has a 1-in. vertex which will not bridge with graphite.

All of this work was performed without recycle of fines. Since fines recycle is employed during most of a typical primary burner operating cycle, an understanding of the effect of a fines recycle stream on fluidization characteristics would be useful. If it is assumed that a continuously recycling fines stream to the distributor vertex and through the bed mixes uniformly with the larger bed material before elutriation, then the result is a bed with a significantly changed size distribution and a lower mean particle size (d_{sv}). In addition, bed viscosity significantly decreases as more and more fines pass through the bed. Thus, any change in fluidization behavior would be due to those properties which change with mean particle size, notably V_{mf}, bed expansion, and solids mixing rates. The last two increase with decreasing mean particle size at equal values of $(V - V_{mf})$. At constant superficial velocity, V, V_{mf} would be expected to decrease as the mean particle size, d_{sv}, decreases. $(V - V_{mf})$, which has been shown to correlate with maximum bed (slug) height, bubbling, and mixing, would increase as d_{sv} decreases. Thus, at constant V, fines recycle through the bed would probably result in significantly higher slug heights and better overall mixing. This is consistent with previous operating experience in the hot 20-cm primary burner where it was shown that fines recycle through the bed resulted in significant fuel particle elutriation (Ref. 4-10). This shows that cold data are applicable to hot operation and that future hot operation can be guided somewhat by these data.

4.4. 20-CM PROTOTYPE SECONDARY BURNER

Fabrication of the entire burner system is nearly complete. Fourteen major assemblies out of a total of nineteen have been completed. The heater assembly is ready for the hydrostatic test of the induction heating

coil. Difficulties in welding Hastelloy-X material have delayed burner vessel fabrication. All burner vessel subassemblies were completed in February (Table 4-9).

Installation of the burner support framework and the upper bonnet insulation assemblies has been completed. Work on the cooling/insulation shrouds is continuing. Installation of the auxiliary systems, i.e., induction heating motor-generator and the control system, cooling air blower and ducting system, burner off-gas ventilation system, and the burner remote cart system, is progressing on schedule.

Further studies on the process, such as the steady-state heat transfer, the overall mass and energy balance, and the operating cycle, have been made; results were presented as part of an ERDA design readiness review.

The process flow diagrams for the secondary burner and the interfacing solids handling systems have been reviewed. P&I level instrumentation and the control loop modifications to the Diogenes digital control unit are continuing; the cognizant engineer for the prototype secondary burner has been certified to operate the Diogenes unit.

4.4.1. Burner System Fabrication

Fabrication of the entire burner system is near completion. During the course of the fabrication, a number of manufacturing difficulties, which can be categorized as follows, were encountered:

1. Material distortion due to welding.
2. Material shrinkage due to welding.
3. Overly tight tolerances.
4. Material availability.

TABLE 4-9
FABRICATION STATUS

Major Assembly No.	Name	Scheduled Completion Date	Percent Completed as of Feb. 29, 1976
5247007-1	Vessel Assembly	Complete	100
5247010	Vessel Mounting Support Assembly	2/20/76	100
5247013	Upper Cap Assembly	2/20/76	100
5247025	Heater Assembly	2/17/76	95
5247040	Left Half Bonnet Assembly	Complete	100[a]
5247041	Right Half Bonnet Assembly	Complete	100[a]
5247048	Upper Intake and Exhaust - Left	Complete	100
5247049	Upper Intake and Exhaust - Right	Complete	100
5247050	Upper Intake and Exhaust - Fixed	Complete	100
5247053	Insulated Shroud	Complete	100
5247070	Lower Intake Plenum - Fixed	Complete	100[a]
5247071-1	Lower Intake Plenum - Right	Complete	100[a]
5247071-2	Lower Intake Plenum - Left	Complete	100[a]
5247075	Spool Hub Assembly	2/20/76	90
5247081	Feed Line Hub Assembly	Complete	100
5247090	Tube Assembly	2/20/76	100
5247096	Support Frame	Complete	100[a]
5247102	Support Arm Assembly	Complete	100[a]
5247103	Support Arm Plate	Complete	100[a]

[a] Items installed in the pilot plant.

The burner vessel, especially the lower spool piece, involves a substantial amount of welding. In many cases the material distortion was so large (Figs. 4-27 and 4-28) that the surfaces had to be remachined, resulting in thinner products. In some cases the final thickness was less than required by structural considerations and a new piece had to be made from a thicker stock.

Weld shrinkage caused a similar effect, weld distortion. When the shrinkage was local as shown in Fig. 4-28, the piece had to be resurfaced. In one special case with the lower spool hub assembly, the Hastelloy-X filler metal was not ductile enough to allow welding per the design. The welds on the insert cracked due to excessive thermal contraction combined with the rigidity of the welded pieces. The problem has been alleviated by using an Inco-82 filler metal instead of Hastelloy-X, based on a stress analysis showing that the substitution does not weaken the parts structurally. The weld shrinkage on the tube was within the design tolerance.

The material distortion for sheet metal was too severe to meet the specified tolerances. Skip welding has been used as much as possible in order to minimize the material warpage. Tolerance for the noncritical areas has been relieved, and machined pieces have been substituted in place of welded sheet metal pieces for critical areas.

In some instances the material specified was either not available or too costly to purchase in small amounts. Except for the critical items, such as the main burner vessel, the original materials have been replaced with equivalent materials in order to minimize the delay in fabrication.

To date during the fabrication period, a total of 65 Engineering Change Orders have been issued to alleviate the aforementioned difficulties as well as to improve the design as follows:

1. Structurally reinforce the burner support framework.

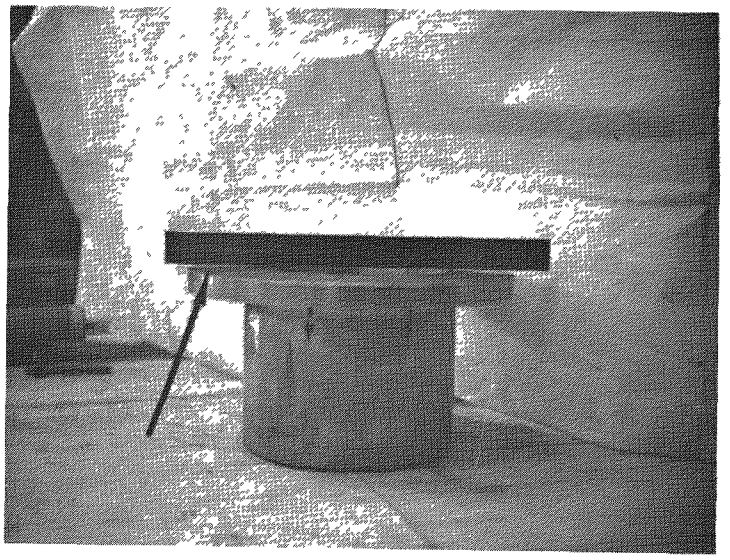

Fig. 4-27. Lower hub of secondary burner vessel showing distortion of the flange due to a circumferential weld

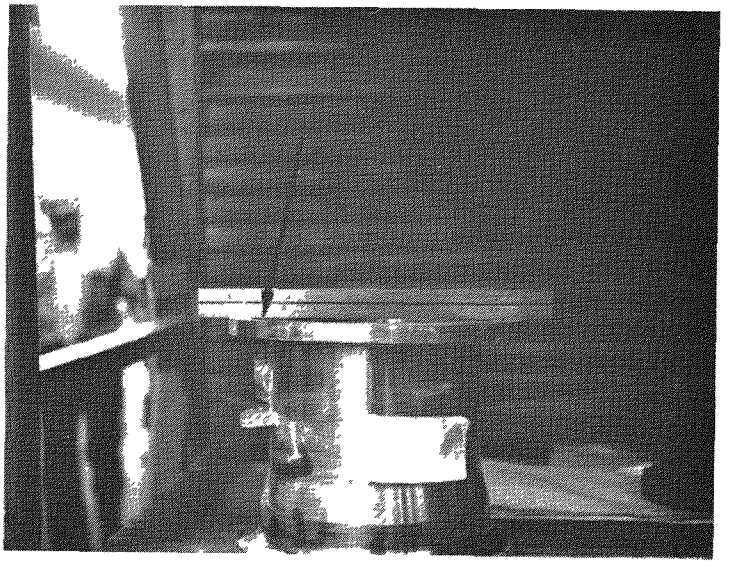

Fig. 4-28. Spool hub subassembly of secondary burner vessel showing extensive material shrinkage on one side due to welding of the insert

2. Ease the fabrication by eliminating unnecessary or noncritical requirements and by relieving design tolerances for noncritical items.

3. Utilize the same burner holding fixtures as the prototype primary burner by slightly modifying the secondary burner support plate.

Considering the above difficulties encountered, the following recommendations are made for future design and fabrication work:

1. Use skip welding instead of full welds as much as possible to reduce warpage.

2. Allow as large a tolerance as possible for the sheet metal work to accommodate warpage. If the piece is critical in dimensions, use a machined piece instead.

3. If the part involves both machining and welding, welding has to be done before the machining. If this is not possible, use thicker material so that the piece can be resurfaced after welding.

4. Tubes and pipes should be purchased longer than the design dimension in order to accommodate the weld shrinkage and to compensate for the irregularity of the mating piece, especially if the mating piece is a long-lead item which has to be accepted as is despite discrepancy from the design dimensions.

4.4.2. Burner Installation

The burner support framework (5247096) has been installed per the Initial Installation Procedure - 8-in. Secondary Burner (IP-524701) as shown in Figs. 4-29 and 4-30.

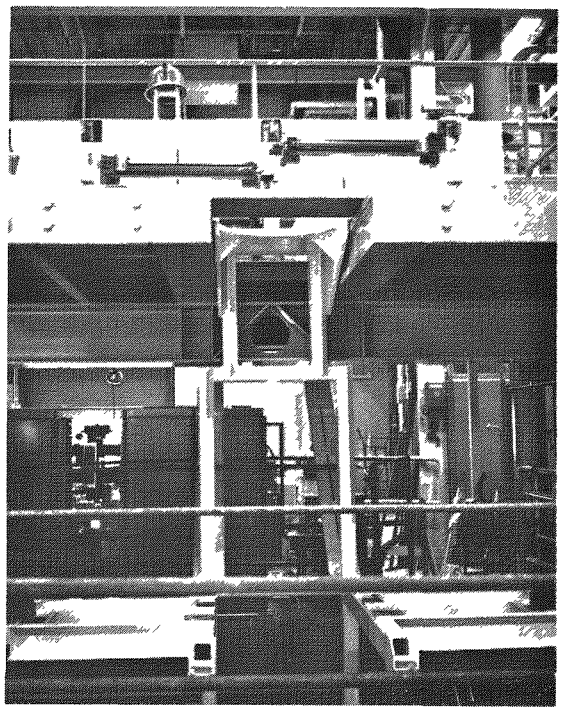

Fig. 4-29. Upper portion of the secondary burner support framework (5247096)

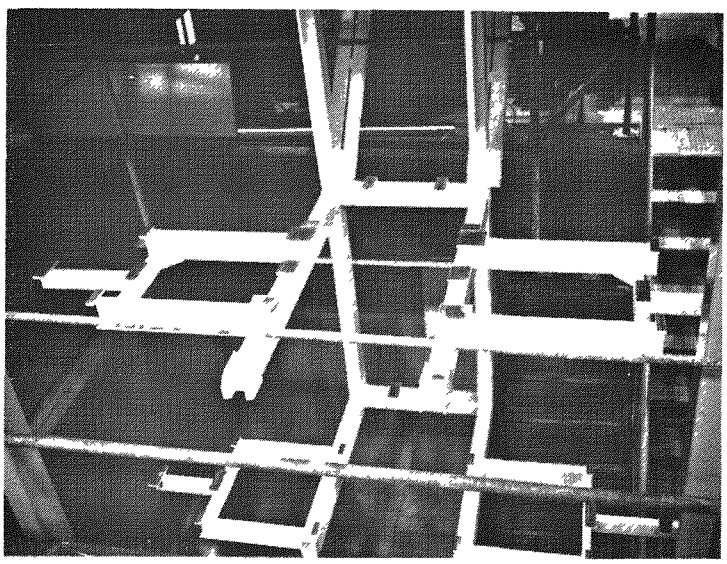

Fig. 4-30. Lower portion of the secondary burner support framework (5247096)

Installation of the upper insulation bonnets (5247041 and 5247040) has been completed; the subassembly stage is shown in Figs. 4-31 and 4-32. Work on the upper intake and exhaust plenum shrouds (5247048, -049, and -050), the lower intake plenum shrouds (5247070 and -071), and the spool shroud assembly (5247077) is continuing (Figs. 4-33 and 4-34). Figure 4-33 also shows the remotely operated De-Staco clamps actuated by air cylinders to lock the shroud sections. The skip weldings mentioned previously are shown in Fig. 4-34.

Installation of the auxiliary systems such as the induction motor-generator and its control systems, cooling air blower and ducting, the burner off-gas ventilation system, and the burner remote cart system are progressing on schedule. The burner remote cart support system is shown in Fig. 4-35.

4.4.3. Steady-State Heat Transfer

During the main burn period following the initial startup period, the total heat generation far exceeds the heat loss through the off-gas and the natural convection at the insulation surfaces. The total heat generation at steady state at the optimum operating conditions (Ref. 4-11), i.e., at 900°C and 60 cm/sec fluidizing velocity, is designed to be removed by forced air cooling. The heat duty for the upper and lower cooling jackets has been distributed in proportion to the estimated overall UA ΔT as shown in Fig. 4-36.

Based on this heat distribution, the upper and lower cooling jackets have been designed. A simplified heat balance model has been set up and solved by iterative trial and error calculations. The results for both the upper and lower cooling jackets are shown in Figs. 4-37 and 4-38.

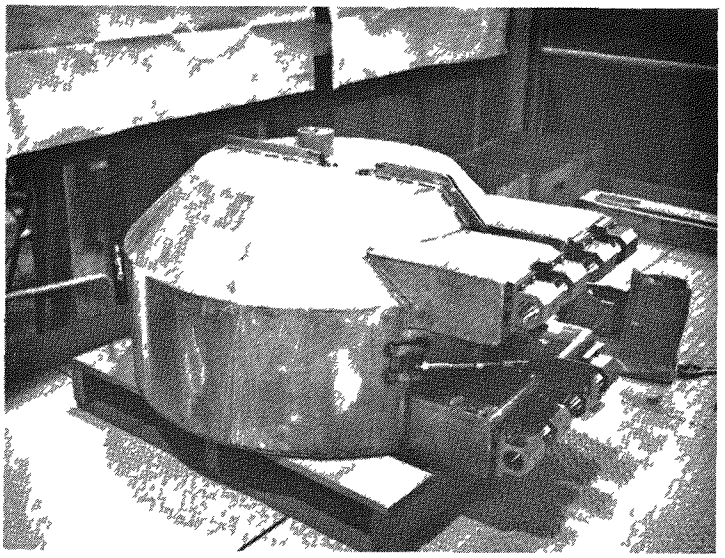

Fig. 4-31. Upper insulation bonnets for secondary burner (5247-040 & -041) ready to mount on the frame

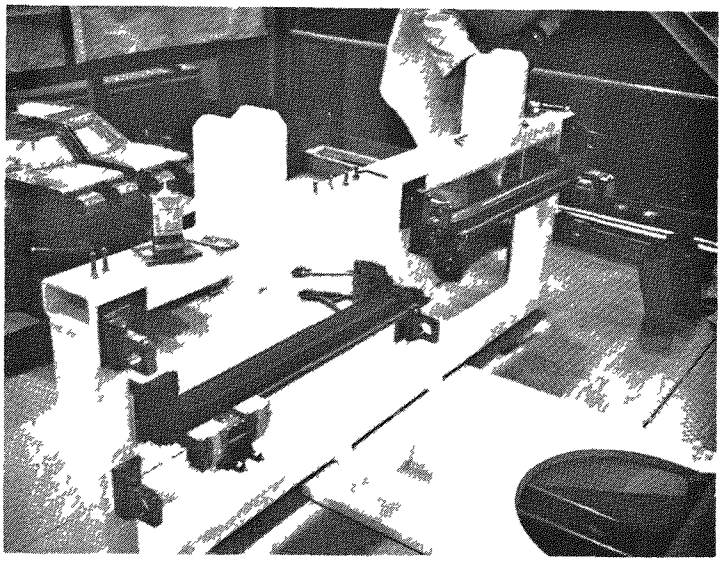

Fig. 4-32. Air motors and rod guides mounted on the framework for the installation of upper insulation bonnets (secondary burner)

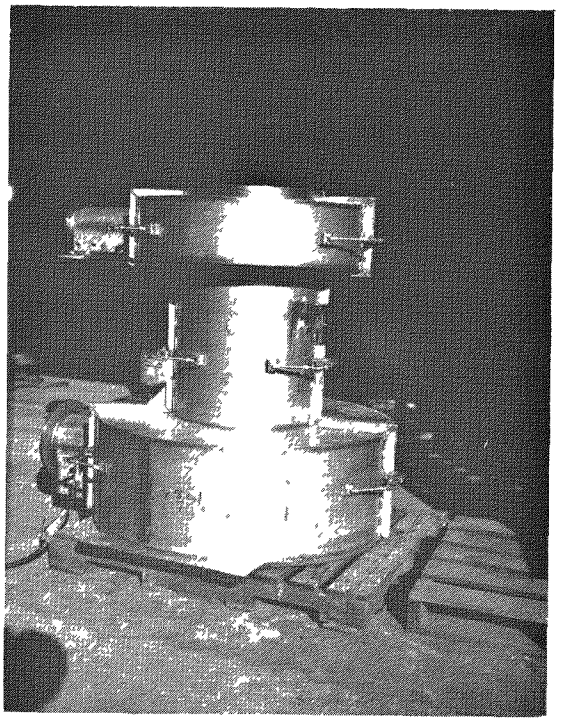

Fig. 4-33. Secondary burner upper intake and exhaust plenum shrouds ready to install

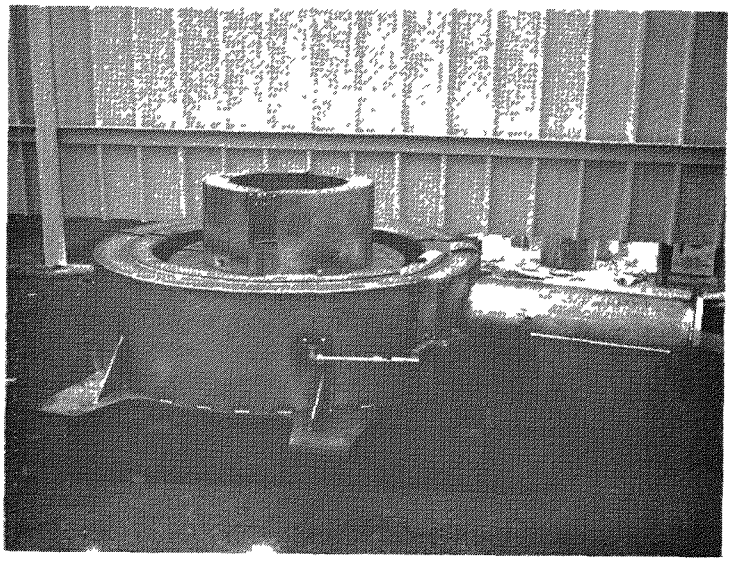

Fig. 4-34. Lower intake plenum shroud and the spool shroud assembly for secondary burner

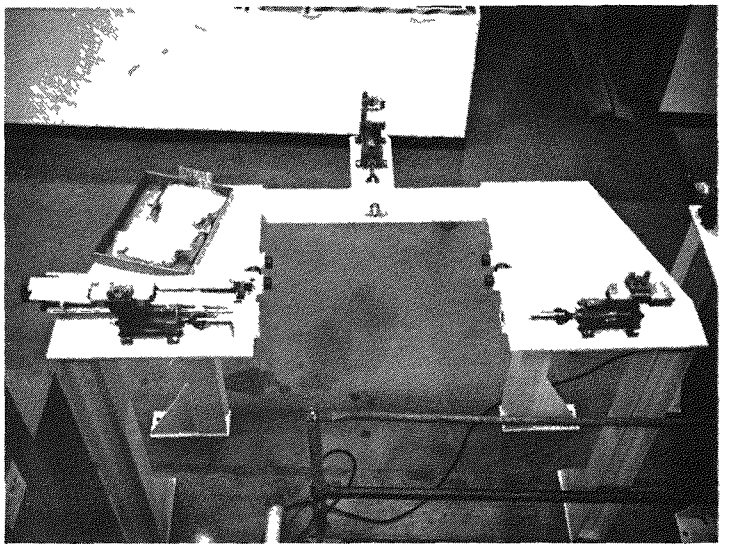

Fig. 4-35. Secondary burner remote cart support system

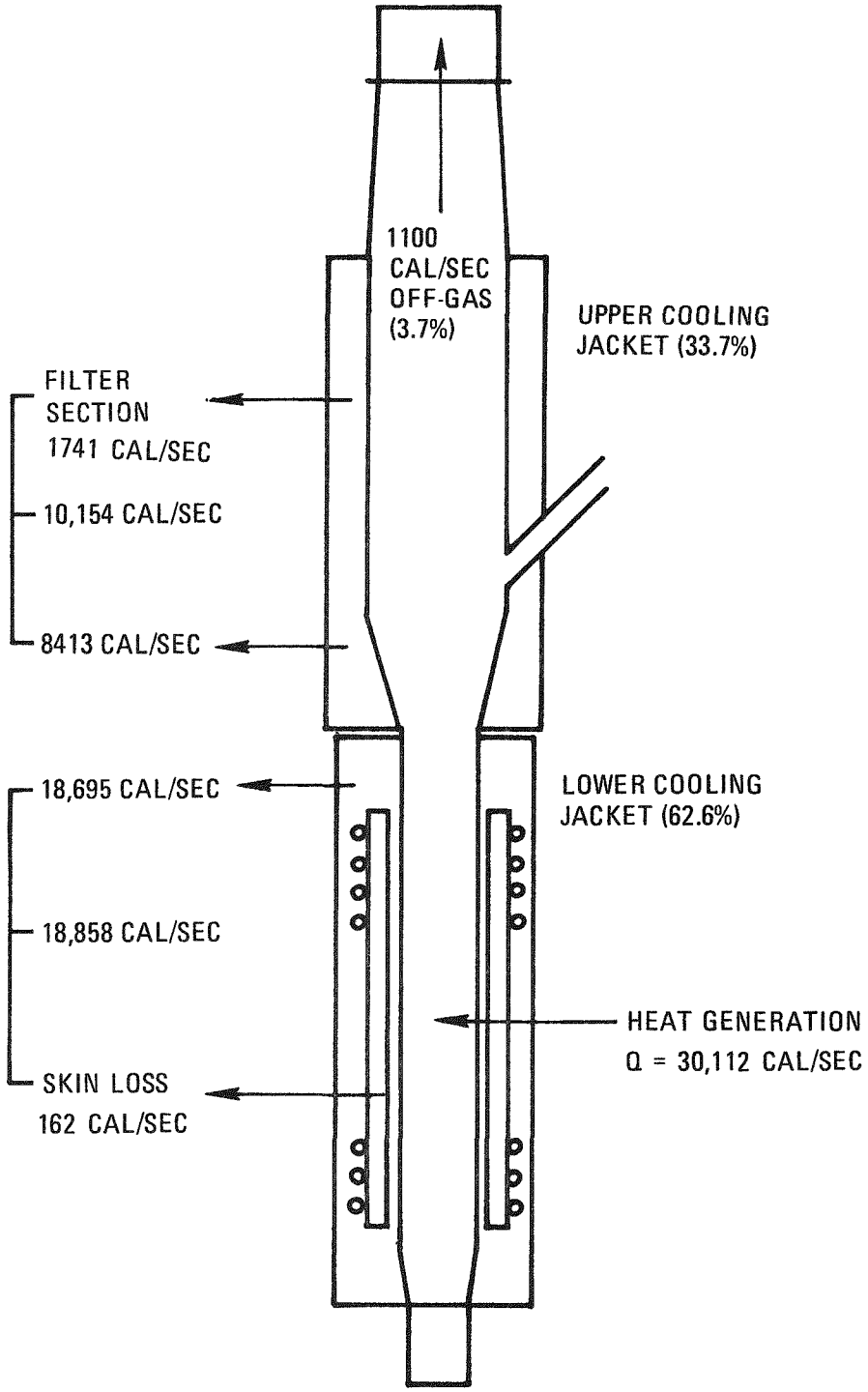

Fig. 4-36. Overall steady-state heat balance during operation of secondary burner

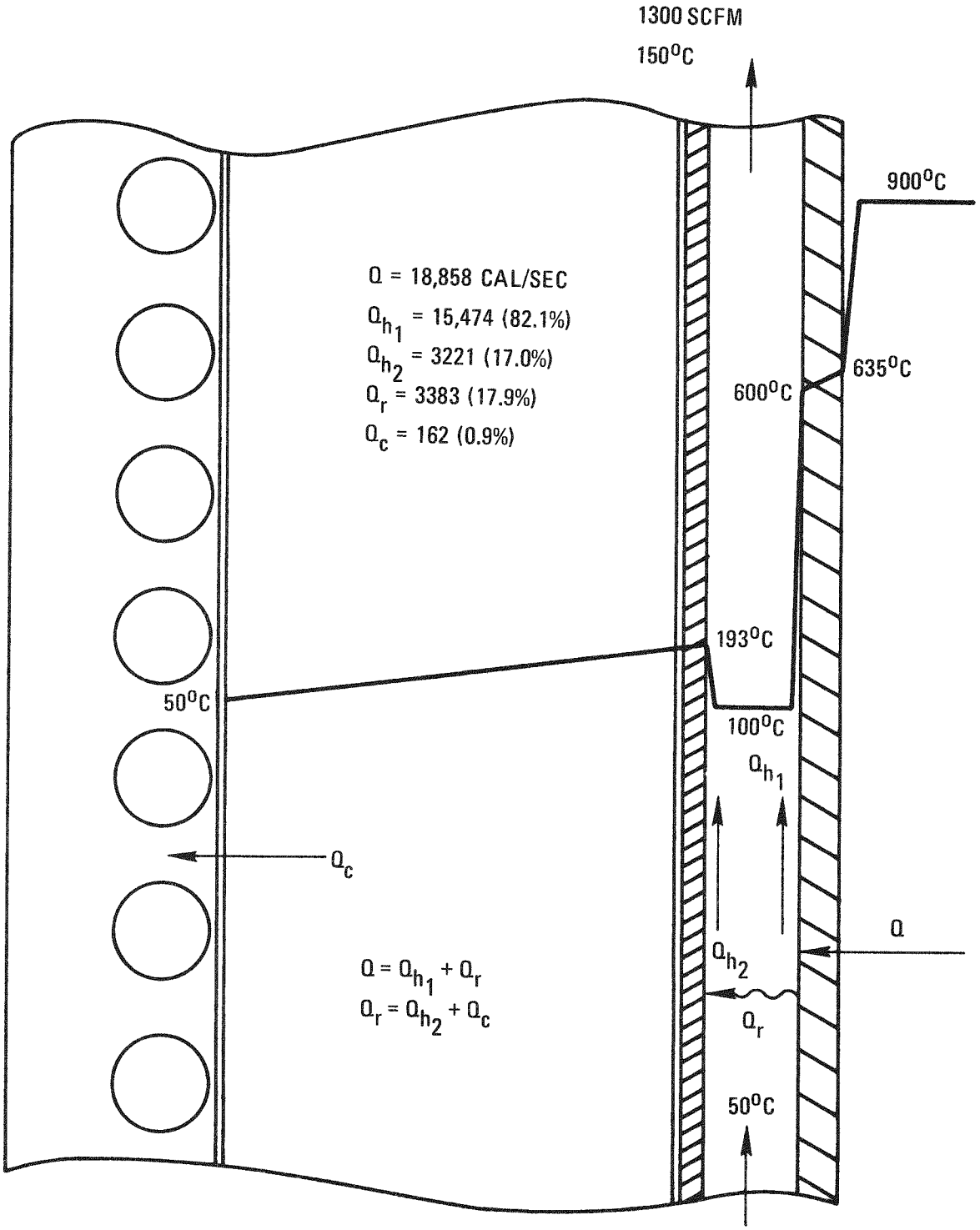

Fig. 4-37. Lower cooling jacket for secondary burner

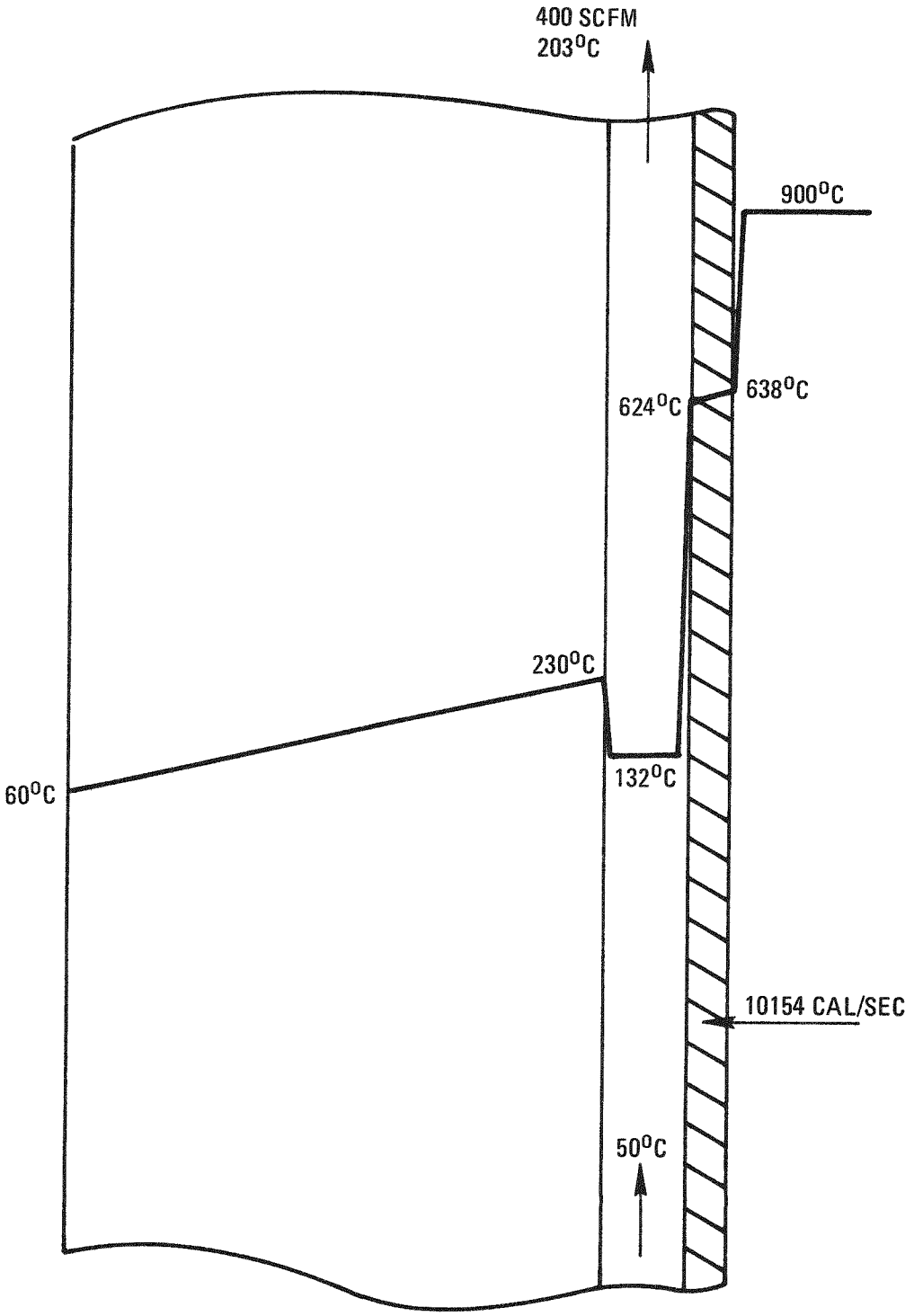

Fig. 4-38. Upper cooling jacket for secondary burner

4.4.4. Operating Mode

The prototype secondary burner is a batch-operated burner with an average capacity of 1 block (FSV-type fuel, fissile or fertile particles) per hour. The operation cycle is shown in Table 4-10. With this operation cycle the overall material and energy balance for one batch cycle has been estimated, as shown in Fig. 4-39. The numbers are conservative estimates only and will be updated after sufficient experimental runs are made on this burner.

TABLE 4-10[a]
OPERATION CYCLE

	Time (hr)
Preparation and feeding	0.5
Startup and ignition[b]	1.0
Main burn	2.0
Tail burn[c]	1.0
Soaking[d]	1.0
Product removal and downtime	0.5
Total	6.0

[a] Batch operation; charge = 61 kg fertile particles (≡ 6 FSV blocks).

[b] Design criteria DC-524701.

[c] Tail burn is also part of soaking cycle.

[d] Further information expected from ORNL.

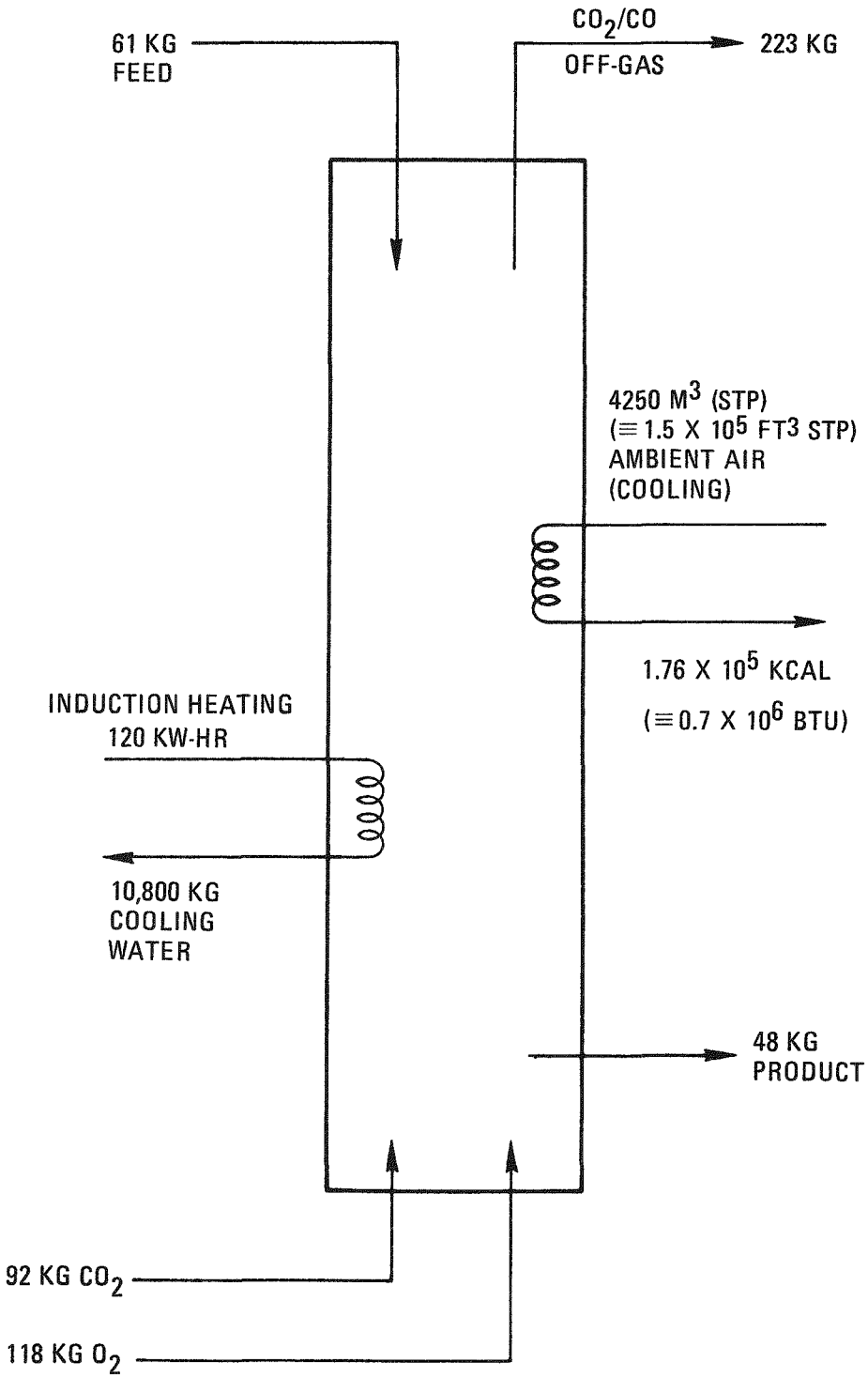

Fig. 4-39. Overall material and energy balance for secondary burner (basis: per batch cycle)

REFERENCES

4-1. Stula, R. T., D. T. Young, and H. H. Yip, "Interim Development Report for Primary Burning," ERDA Report GA-A13546, General Atomic Company, January 5, 1976.

4-2. Rickman, W. S., "Interim Development Report for Secondary Burning," ERDA Report GA-A13540, General Atomic Company, December 25, 1975.

4-3. Yip, H. H., General Atomic, private communication.

4-4. Stula, R. T., "Fluidization Studies in the Cold 20-cm Glass Primary Burner," General Atomic unpublished data, January 9, 1976.

4-5. Carney, H. C., and V. H. Pierce, "Burner Cyclical Operation in a Commercial HTGR Reprocessing Facility," General Atomic unpublished data, July 23, 1975.

4-6. Johanson, N. W., "Dimensional Envelope of Prototype Primary Burner Tube," General Atomic unpublished data, October 21, 1975.

4-7. Young, D. T., R. T. Stula, and J. S. Rode, "Experimental Plan: 20-cm Primary Burner," General Atomic unpublished data, January 8, 1976.

4-8. "Thorium Utilization Program Quarterly Progress Report for the Period Ending August 31, 1975," ERDA Report GA-A13593, General Atomic Company, September 30, 1975.

4-9. Davidson, J. F., and D. Harrison, Fluidization, Academic Press, New York (1971).

4-10. "Thorium Utilization Program Quarterly Progress Report for the Period Ending November 30, 1975," ERDA Report GA-A13746, General Atomic Company, December 31, 1975.

4-11. "Thorium Utilization Program Quarterly Progress Report for the Period Ending November 30, 1974," USAEC Report GA-A13255, General Atomic Company, February 15, 1975.

5. AQUEOUS SEPARATIONS

5.1. SUMMARY

Seventeen steam jet transfer runs were made in studies to test jet configurations for transferring leacher slurries. The tests were made using a mixture of water and SiC hulls or simulated whole fuel particles. All runs using a submerged jet were successful. Runs using an elevated jet with dilution water injected into the jet suction experienced excessive jet pluggage.

No feed adjustment runs were made during the past quarter in the pilot plant equipment. Additional sample analyses were obtained on runs made the previous quarter and the data gathered were reanalyzed. The reanalyses indicate that there is no significant difference between steam and water as stripping agents. Analyses of the condensed overheads show that some fluoride is volatized from the solution. Typically the condensate contained 1.5×10^{-3} molar free fluoride. Corrosion measurements show corrosion rates for 304L stainless steel average 0.4 mm/yr (16 mils/yr) and 1.5 mm/yr (60 mils/yr) in the liquid and vapor phases, respectively. The volatized fluoride would account for the higher corrosion rates obsered in the vapor phase.

Sixteen bench-scale feed adjustment runs were made during the quarter. In continuous runs (continuous feed and continuous product removal) at a 135°C B.P. using leacher solution diluted with an equal volume of water and steam sparging, it was not possible to achieve acid deficiency. It was possible, however, to achieve acid deficiency in continuous operation with undiluted leacher solution when formic acid was continuously added. Runs with 1BT feed (thorium product from the partition solvent extraction

column) demonstrated acid deficiency can be achieved on a continuous basis with (1) no steam or formic acid addition at a pot temperature of 135°C or (2) water and formic acid addition at a pot temperature of 125°C. It was not possible to render concentrated 1BT acid deficient continuously without formic acid addition.

Bench-scale measurements on the distribution coefficient of zirconium in the acid-Thorex system indicate the presence of carbide in the feed to the feed adjustment step significantly increases the zirconium distribution coefficient in the 1A column. Thus, the feed adjustment operation does not obviate the deleterious effects caused by carbide reactions with nitric acid in the leacher.

Bench-scale studies were initiated to determine the limiting temperature for abrupt reactions between highly degraded solvent ("red-oil") and thorium nitrate. Preliminary findings suggest that the current diluent (NPH) is more resistant to "red-oil" formation than the diluents used in prior studies by other investigators.

5.2. LEACHING

5.2.1. Preliminary Testing of Dilution Water and Submerged Jet Concepts for Leacher Product Removal

Previous steam jet transfer testing for leacher product removal was based upon a suction-lift design (Refs. 5-1 through 5-3). The suction produced by a steam jet was used to lift slurry out of a tank through 2.4- and 3.4-meter vertical tubes. Those tests have shown a rather low confidence level of 75% for avoiding pluggage of SiC hulls in the suction tubes. In an effort to find a more reliable transfer method, alternative designs were considered; two concepts were given preliminary testing.

The first alternative concept was to inject clear liquid into the slurry at the base of the suction tube to a steam jet. This liquid serves to dilute the slurry as it enters the suction tube, thereby reducing the

potential for pluggage, which is characteristic of more concentrated slurries. The second concept was to submerge a steam jet with an open suction into the bottom of the slurry holding tank. This would eliminate the need for a suction tube.

5.2.2. Experimental

The steam jet transfer apparatus was modified to demonstrate the dilution water concept as shown in Fig. 5-1. Water was injected at the base of the suction tube using a rotary pump. When purge air was used to keep lines clean prior to a run, the discharge valves for the jet and the pump were closed to direct the air into the holding tank.

The submerged jet concept was demonstrated by the apparatus shown in Fig. 5-2. Details of the modified jet are shown in Fig. 5-3. Note that there is no suction tube to plug. Four relatively large slots in the jet body allow the slurry to enter the jet. Purge air was used to keep the slurry from filling the steam nozzle prior to a run. The purge air is shut off and the steam is turned on simultaneously at the start of a run.

The slurry used for all runs was made up of about 7 kg of either SiC hulls or glass beads in about 50 liters of water. The glass beads were used to simulate whole fuel particles. In order to demonstrate the most severe conditions for transfer, the slurry was allowed to settle in the holding tank for several hours prior to most runs. The slurry was sparged immediately prior to run 55 only. Each run consisted of removing the slurry from the holding tank using one of the two jet configurations. Slurry samples of the discharge stream were taken periodically throughout the runs by briefly collecting the entire flow. Operating conditions and performance data for runs demonstrating the dilution water and submerged jet concepts are given in Tables 5-1 and 5-2, respectively. Variations in the slurry concentration of the discharge stream throughout several runs are plotted in Figs. 5-4 and 5-5.

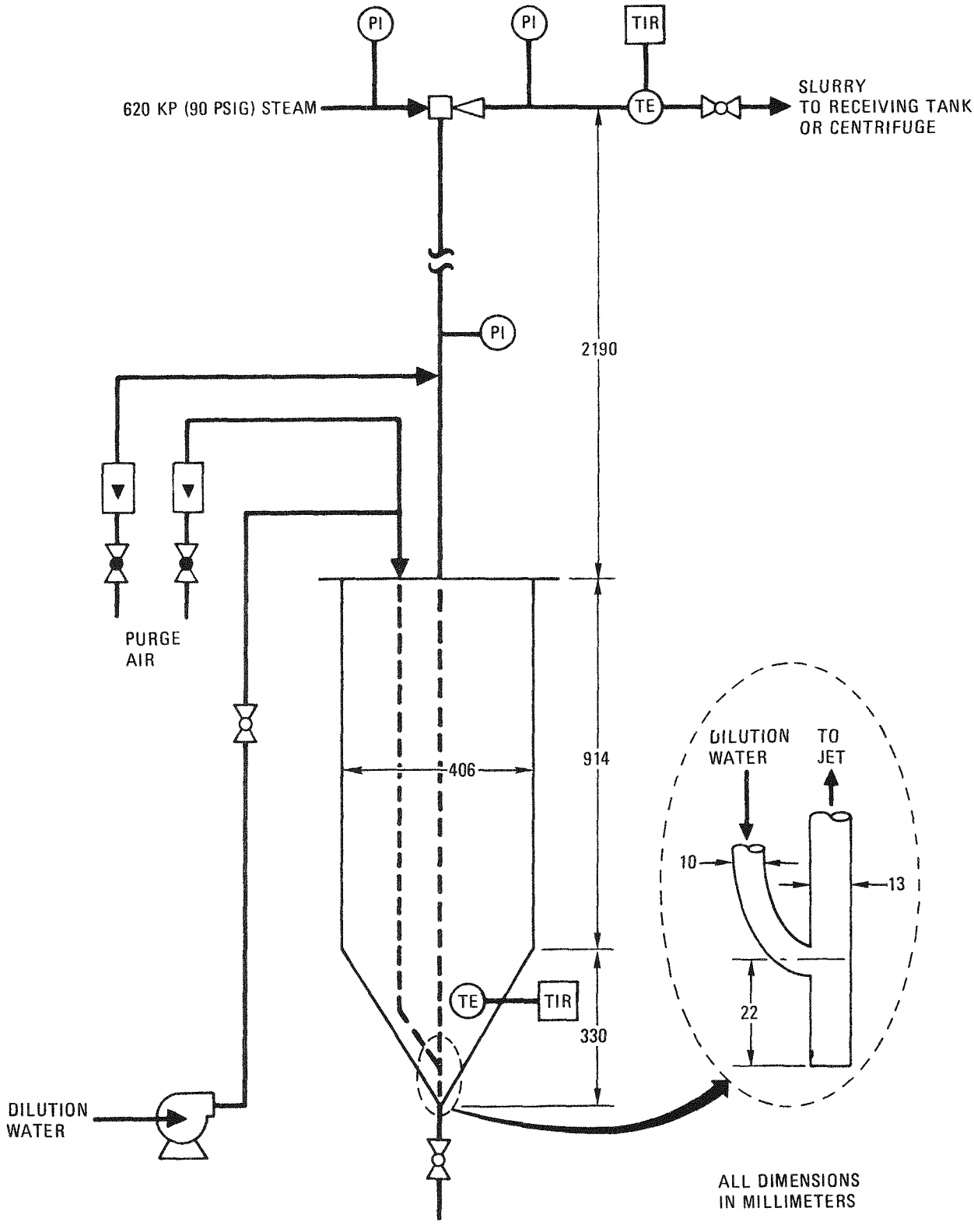

Fig. 5-1. Steam jet transfer apparatus for dilution water concept

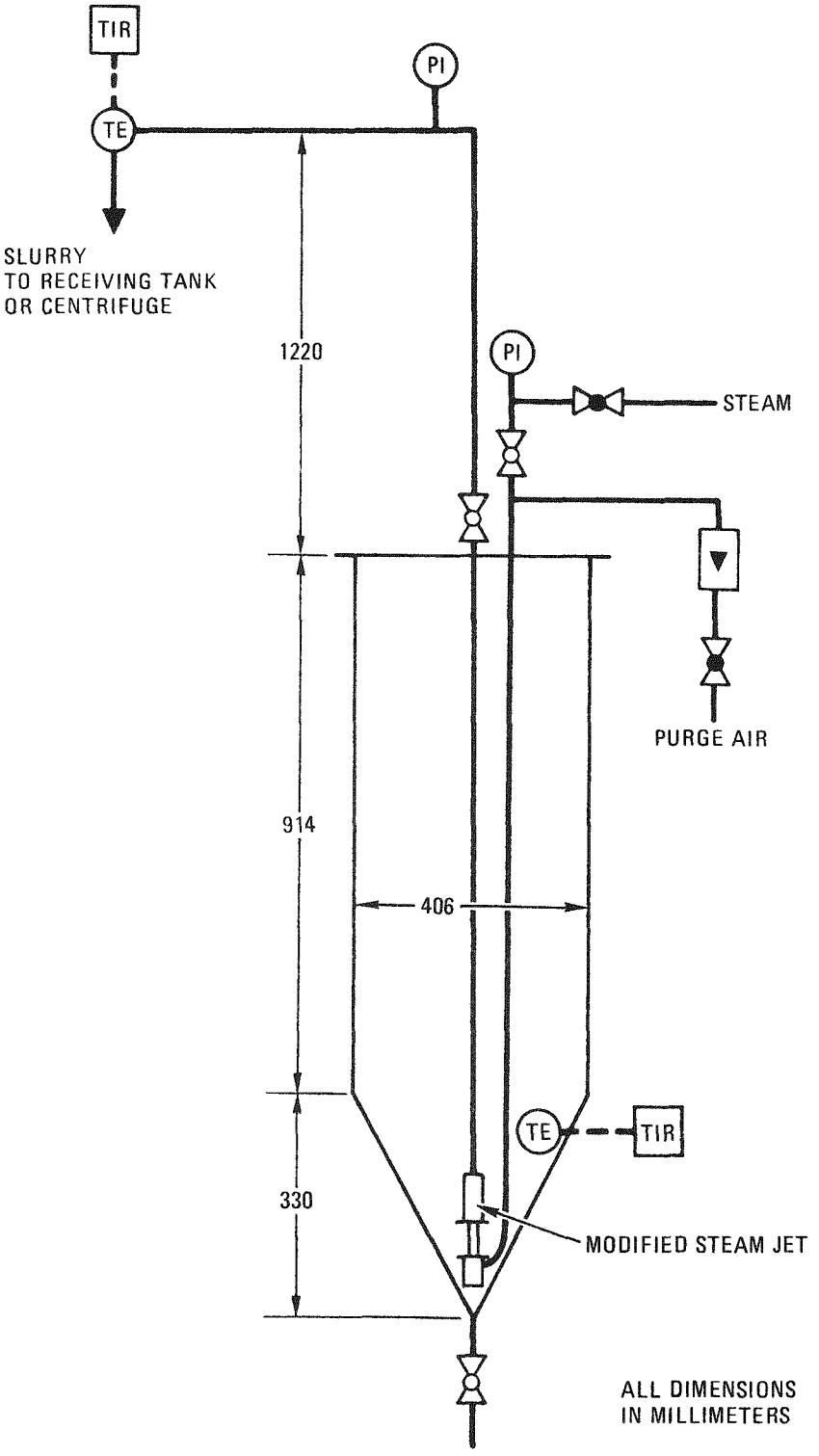

Fig. 5-2. Steam jet transfer apparatus for submerged jet concept

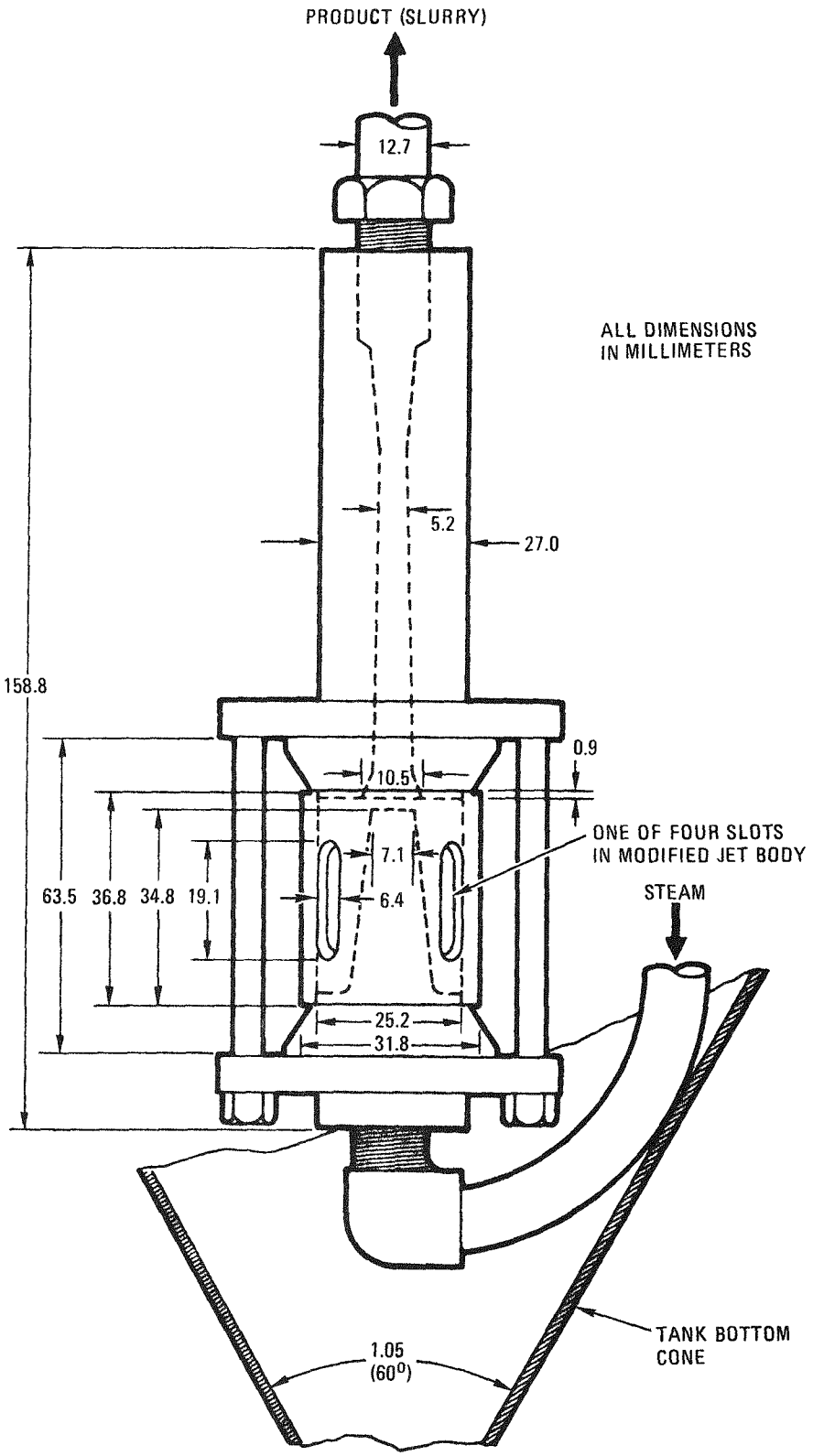

Fig. 5-3. Steam jet transfer modified jet for submerged, open suction service

TABLE 5-1
OPERATING CONDITIONS AND TRANSFER CHARACTERISTICS OF DILUTION WATER CONCEPT RUNS

Run	Slurry Temp (°C)	Dilution Water		Solids	Purge Air (slpm)	Transfer Time (min)	Total Flow Rate (ℓ/min)	Rate of Removal from Holding Tank (ℓ/min)	Temp. Rise (°C)
		Flow (ℓ/min)	Temp (°C)						
45	20	3.0	∿20	SiC	0	8.6	8.8	5.6	22
46	∿20	2.8	∿20	glass	0	7.6	9.6	6.8	--
47	∿20	1.0	∿20	SiC	0	(d)	--	--	--
48	∿20	2.0	∿20	SiC	0	(e)	--	--	--
50	26	1.0	∿20	SiC	0.9	8.7	7.6	6.6	27
52	∿20	1.0	∿20	SiC	0.9	(e)	--	--	--
53	∿20	2.0	∿20	SiC	0.9	(e)	--	--	--
54	21	4.0	∿20	SiC	0.9	(f)	--	--	--
55	20	3.0[a]	∿20	SiC	0.9[c]	17.6	5.8	2.8[i]	39
56	19	1.8	∿20	SiC	0.9	10.5[g]	6.9	5.1	28
59	32	5.0[b]	60	SiC	0.9	8.4	9.0	4.0[i]	26
61	34	5.0	65	SiC	0.9	(h)	--	--	--

(a) Dilution water turned off after 6.5 minutes.

(b) Dilution water turned off after 4.5 minutes.

(c) Sparged slurry at 7.6 slpm through bottom valve prior to run.

(d) Flow stopped due to pluggage 28 seconds after start of transfer.

(e) Flow would not start due to pluggage.

(f) Flow of solids stopped after 5.2 minutes. Clear dilution water was still being carried over in spurts indicating that plug was at base of suction tube below dilution water entry.

(g) First attempt to transfer using only 1 ℓ/min dilution water resulted in pluggage. Dilution water increased to 1.8 ℓ/min resulted in successful second attempt.

(h) Flow stopped due to pluggage after 1.5 minutes. Dilution water was being pumped into holding tank indicating plug was in suction tube between jet and dilution water entry.

(i) Prior to turning off dilution water.

TABLE 5-2
OPERATING CONDITIONS AND TRANSFER CHARACTERISTICS OF SUBMERGED JET RUNS

Run	Slurry Temp (°C)	Solids	Purge Air (slpm)	Transfer Time (min)	Flow Rate (ℓ/min)	Temp Rise (°C)
49	26	SiC hulls	0.9	4.0	12.5	13
51	18	SiC hulls	4.7	4.1	12.2	14
57	20	Glass beads	0.9	4.2	12.1	13
58	28	SiC hulls	0.9	3.9	13.2	10
60	23	SiC hulls	0.9	4.0	12.5	10

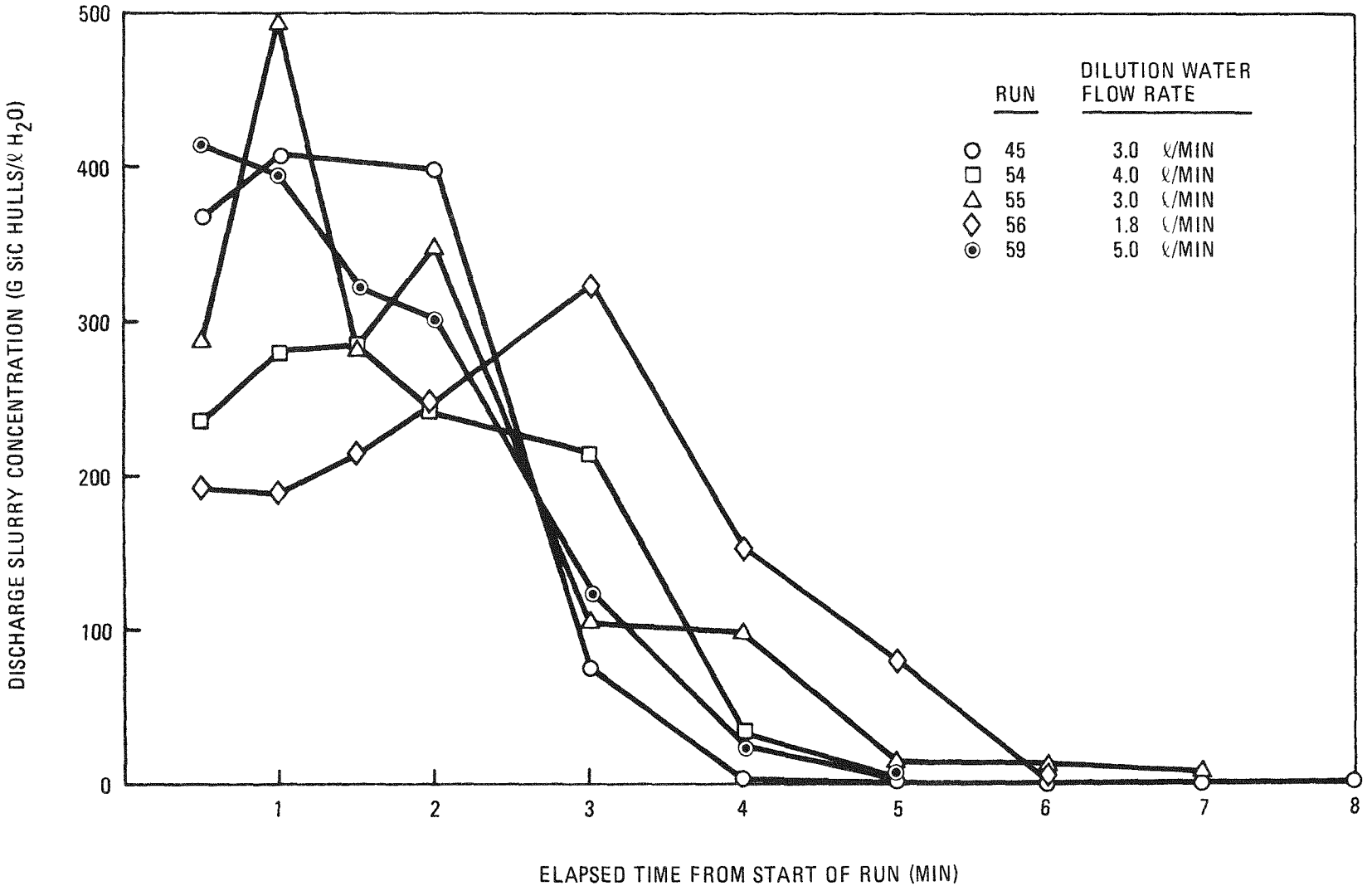

Fig. 5-4. Discharge slurry concentrations for dilution water runs

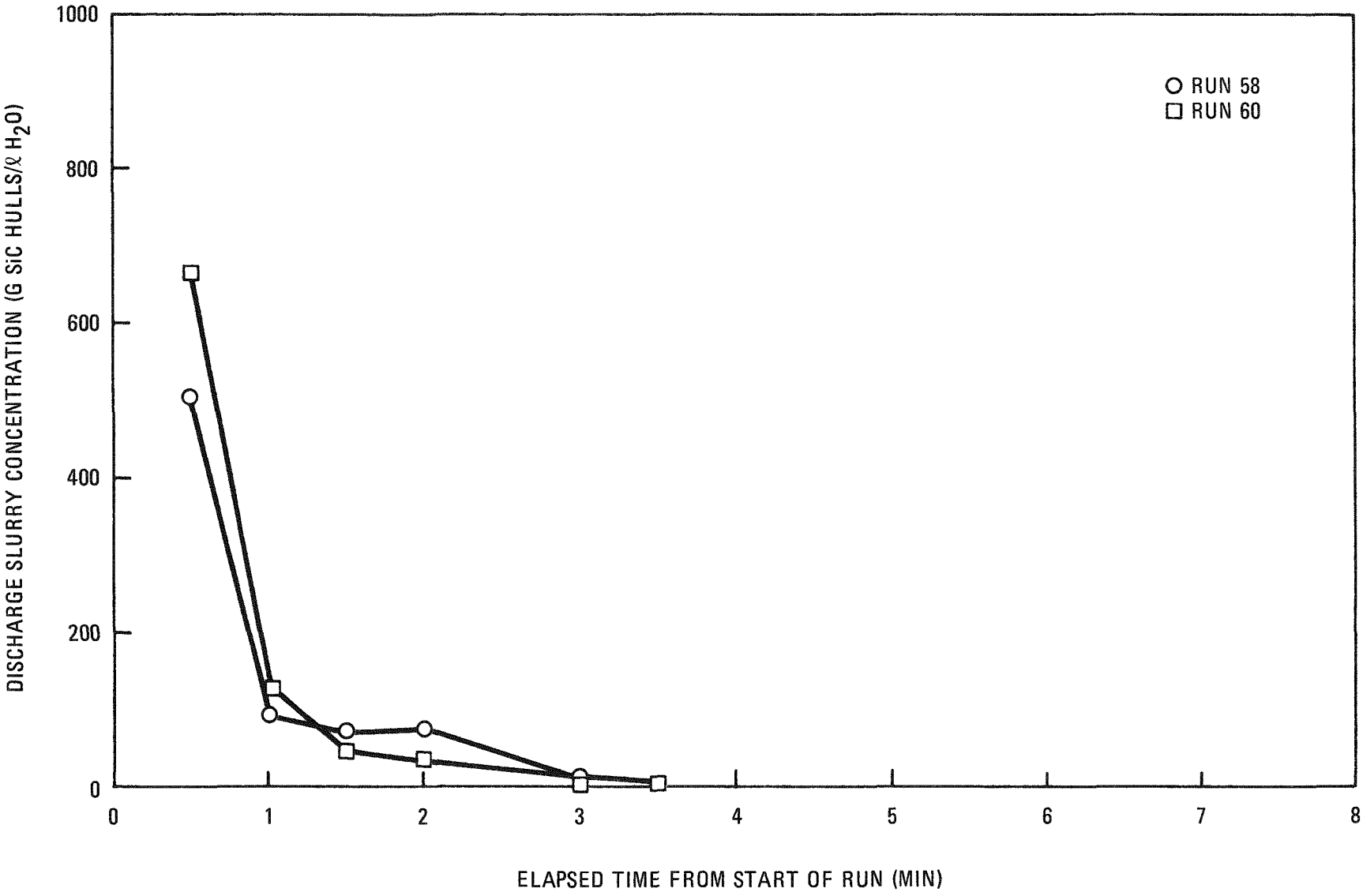

Fig. 5-5. Discharge slurry concentrations for submerged jet runs

5.2.3. Discussion

The dilution water concept described above as an alternative method for leacher product removal via steam jet transfer was found to be unreliable. Although the conditions of testing were extreme to demonstrate the worst case, the test runs showed a reliability of only 50%. A higher confidence level could be expected for more diluted and better mixed slurries. Confidence in the reliability of this concept was lost by the lack of reproducibility of the results. Runs 50 and 52, runs 53 and 56, and runs 59 and 61 were made under identical, respective conditions. Runs 50, 53 and 61 resulted in plugs while runs 52, 56, and 59 did not. Varying the dilution water flow rate did not reduce the plugging incidents. One run plugged and another was successful at a dilution water flow rate of 1 liter/min (about 12% of the total flow). One run also plugged and another was successful at a dilution flow rate of 5 liters/min (about 62% of the total flow).

Preliminary testing of the submerged jet resulted in no plugging incidents under the same extreme conditions used to test the dilution water concept. The reliability and reproducibility of the submerged jet performance was excellent. The observed flow rates were about 35% greater and temperature rises were about 7°C lower than could be obtained from the same jet requiring a 2.4-meter suction lift (Ref. 5-3), indicating efficient utilization of energy with the submerged jet. Transferring a slurry of glass beads and water with the submerged jet also showed excellent flow characteristics in contrast to the sputtering flow found in transferring glass bead slurries through 2.4- and 3.4-meter suction tubes (Ref. 5-3).

In the submerged jet configuration, an air purge through the steam line is necessary to keep the slurry out of the steam nozzle prior to the start of a run. It was found that a purge rate of 0.9 slpm was sufficient to keep the steam nozzle clear but would not create an airlift carrying liquid up the 2.4-meter discharge line. Therefore, a valve in the discharge line would not be required to prevent liquid transfer prior to leacher product removal.

An air purge was found to be necessary for both the suction tube and the dilution tube of the dilution water configuration. When no purge was provided, freely settling slurry entered these tubes and formed a plug which the dilution water flow could not remove.

Disadvantages of using a submerged jet in commercial leachers include: (1) the highly corrosive environment which could lead to frequent jet replacement, although remote replacement of submerged jets should be relatively simple, and (2) the inability of an open suction jet to completely empty a leacher. The configuration of a submerged jet may require special design and manufacturing in order to enable the jet to empty a leacher almost completely.

5.2.4. Conclusions and Recommendations

Preliminary testing has shown that a submerged, open-suction steam jet is a reliable and efficient method of leacher product removal. Detailed testing of submerged jets is required to establish effects of slurry temperature, slurry composition, slurry concentration, motive steam pressure, and discharge height upon transfer characteristics. In addition, testing of various submerged jet configurations is required to optimize the completeness of slurry removal from a vessel using a submerged jet.

No further work is planned for the concept of adding liquid to the base of a jet suction tube to dilute the slurry since that concept was found to be unreliable.

5.3. FEED ADJUSTMENT

5.3.1. Revised Analyses for Runs 11, 13, and 14

In the previous quarterly report (Ref. 5-3) it was reported that the analyses for acid content of the concentrate for run 13 was suspect. The concentrate samples for runs 11, 13, and 14 were resubmitted for analysis; the results are given in Fig. 5-6.

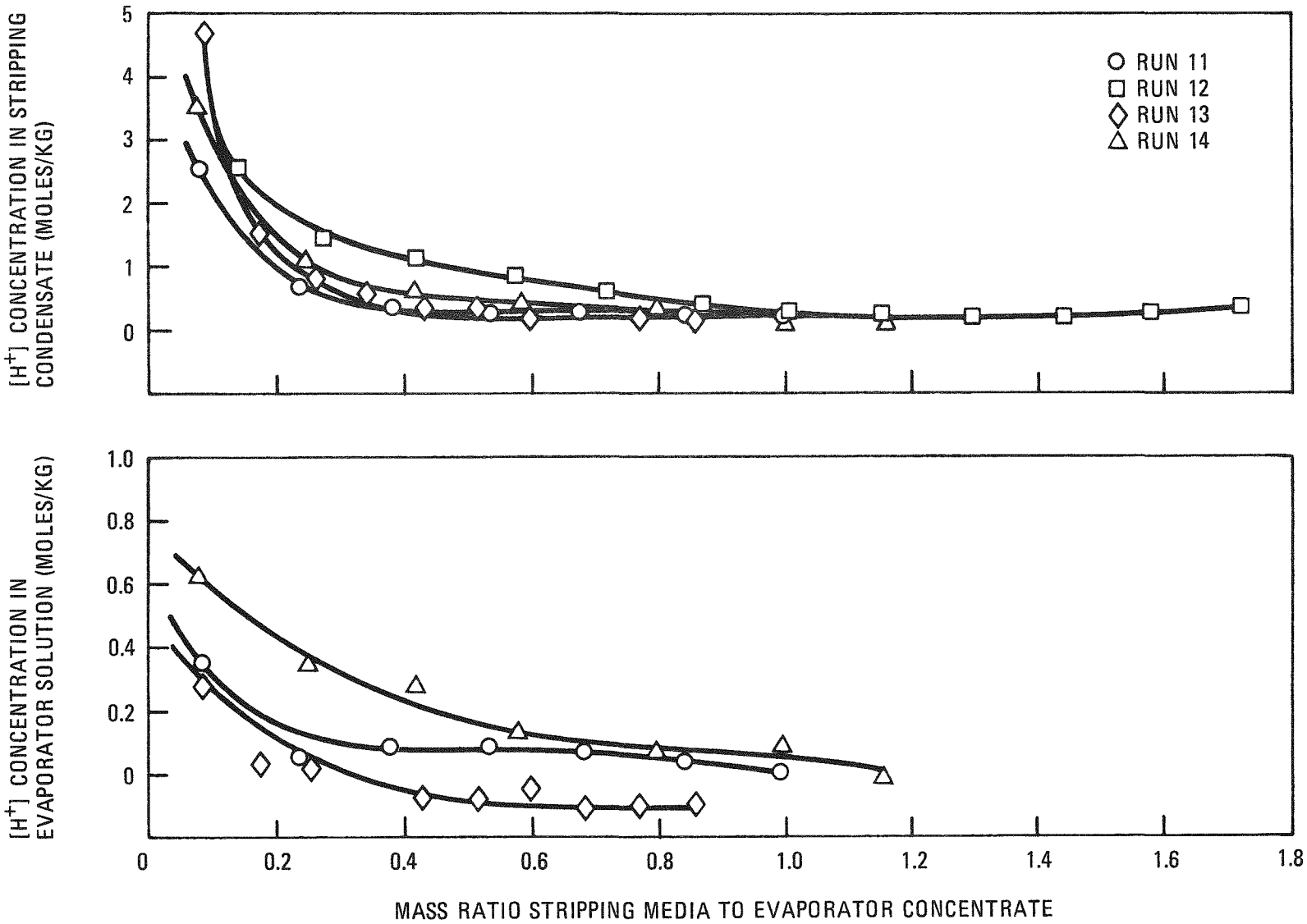

Fig. 5-6. Acidity of concentrate and condensate as a function of stripping mass used (revised analyses for concentrate)

The original analytical results indicated that acid deficiency had not been achieved in any of the runs. The resubmitted results for Run 11 show lower acid contents than the original analyses, but acid deficiency still was not reached. For Run 13 the resubmitted results show acid deficiency had been reached. For Run 14 there was essentially no change in the analyses.

The lack of acid deficiency in Runs 11 and 14 may be explained by the fact that the stripping temperature in those runs was allowed to drop during water addition. The stripping temperature will provide the vapor pressure difference, which is the driving force for transferring acid from the liquid to the vapor phase. The experimental trend for average stripping temperature versus mass ratio of stripping agent to concentrate required for acid deficiency is given in Fig. 5-7. Although it was previously reported that steam may have been a better stripping agent than water because steam appeared to require less mass to achieve acid deficiency, it is now evident that there is no difference between steam and water as stripping agents.

5.3.2. Entrainment in Feed Adjustment System

Initially the feed preparation system deentrainment tower was filled with 1.27 cm (0.5 in.) Intalox saddles to remove entrained moisture from the evaporator/stripper vapor. It was found, however, that the large heat sink of the saddles caused the vapor to condense in the tower at startup. The condensed liquid formed a block in the tower which led to overpressurizing the evaporator/stripper. The saddles were removed and the deentrainment function was left to the space in the empty tower.

The amount of entrainment was still very low after removal of the saddles. Table 5-3 shows that normally less than 0.04% of the thorium in the original feed was carried over in the condensate by entrainment, although run 13 showed 0.21% of the thorium entrained in the overhead

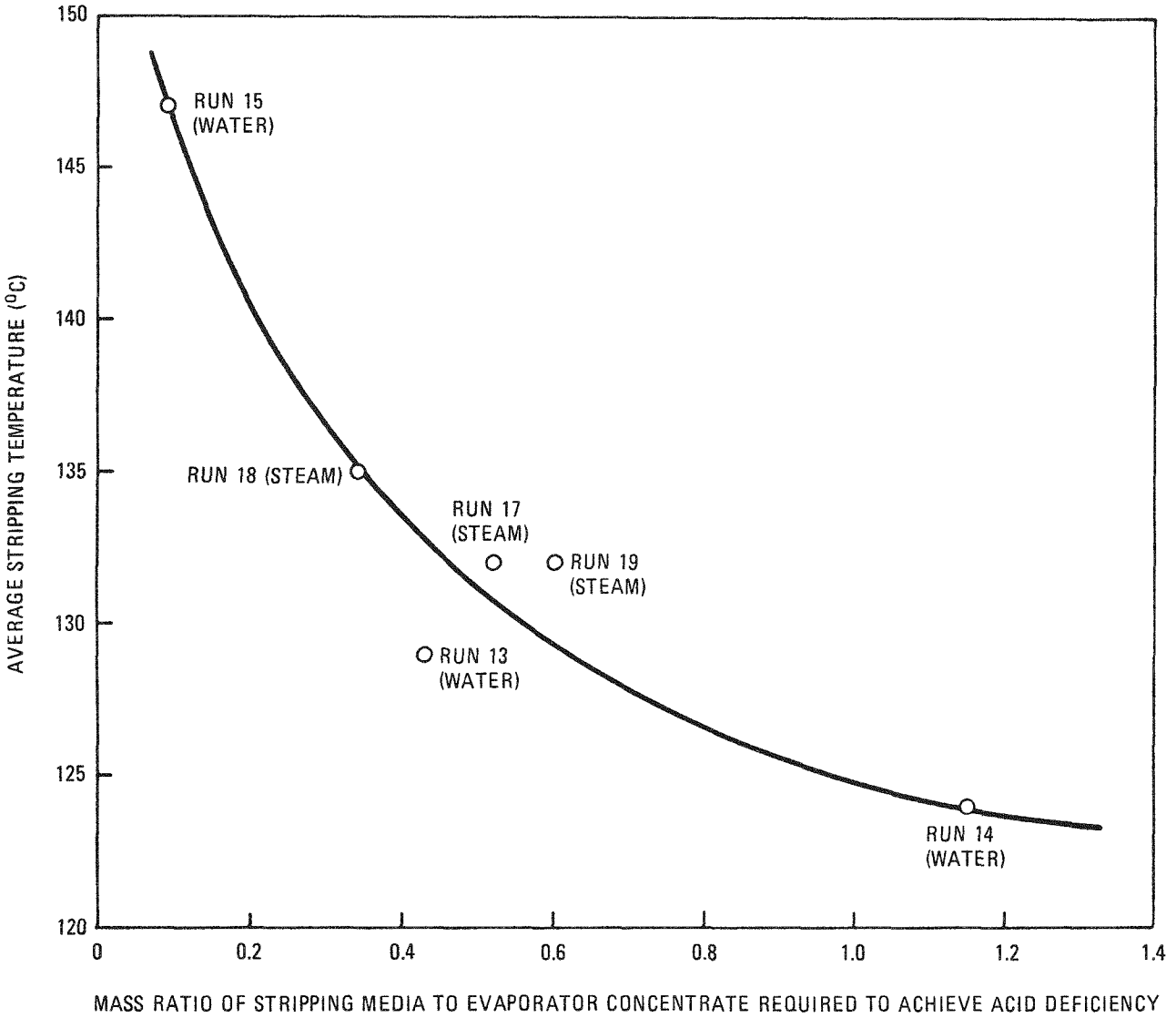

Fig. 5-7. Effect of stripping temperature upon mass of stripping agent required

TABLE 5-3
ENTRAINMENT OF THORIUM IN THE VAPOR FROM THE
FEED ADJUSTMENT SYSTEM

Run	Mass Thorium (g)			Thorium Entrained (%)	
	Overhead Condensate	Strip Condensate	Feed	Overhead	Strip
11	1.8	--	10160	0.018	--
12	2.5	--	7554	0.033	--
13	19.0	--	9060	0.210	--
14	0.5	--	12720	0.004	--
15	0.9	--	13730	0.007	--
16	0.2	--	10250	0.002	--
17	0.3	20.1	15030	0.134	0.002
18	0.7	0.6	12980	0.005	0.005
19	1.0	1.9	13210	0.015	0.007

condensate and run 17 showed 0.13% in the steam strip condensate. The relatively high entrainments found in runs 13 and 17 apparently were not related to the boildown rates, liquid levels, or stripping rates of those runs. Possible explanations are:

1. The feed for run 13 was the product from leacher runs containing carbide added to the ash. This could have promoted foaming.

2. Run 17 contained a greater mass of thorium than any other run.

It was concluded that entrainment is not a significant problem in the pilot plant system.

5.3.3. Fluoride Volatization

It is important to know the fluoride concentration of the vapor in the feed adjustment system because fluoride is very corrosive in acidic vapors. The composition of condensate for both the boildown and stripping steps is given in Table 5-4. These compositions are representative of the vapor and, as shown below, have not been significantly affected by entrained liquid being carried over. Variations in the operating conditions did not affect the amount of fluoride volatized, although, as expected, higher fluoride contents in the feed and concentrate give higher fluoride concentrations in the vapor.

The amount of fluoride which was entrained can be determined from the thorium-to-fluoride ratio of the feed and of the condensate. It is known that thorium is nonvolatile, and any thorium in the condensate came from entrainment. The mole ratios of thorium to fluoride in the feed, product, boildown condensate, and stripping condensate for runs 11 through 19 are given in Table 5-5. This table shows that normally less than 1% of the fluoride present in the condensate came from entrainment. The fluoride concentrations given in Table 5-4, therefore, are accurate for free, volatized fluoride and they are not biased significantly from entrainment.

TABLE 5-4
ANALYTICAL RESULTS FOR SAMPLES OF COMPOSITED STREAMS
IN FEED ADJUSTMENT SYSTEM

	H^+ (M)	Th (M)	F (M)	Al (M)	ρ (g/ml)
Run 11					
Feed	7.5	0.68	0.030	0.078	1.512
Product	0.20	2.0	0.094	0.17	1.806
Boildown condensate	8.6	1.5×10^{-4}	3.5×10^{-4}	$<2.4 \times 10^{-4}$	1.306
Strip condensate	--	--	--	--	--
Run 12					
Feed	8.9	0.44	0.030	0.084	1.439
Product	-0.13	1.6	0.12	0.28	1.651
Boildown condensate	5.9	1.7×10^{-4}	7.9×10^{-4}	$<2.4 \times 10^{-4}$	1.288
Strip condensate	0.86	--	--	--	1.006
Run 13					
Feed	7.9	0.59	0.053	0.085	1.484
Product	0.16	1.5	0.19	0.26	1.826
Boildown condensate	10.8	1.7×10^{-3}	2.5×10^{-3}	2.9×10^{-4}	1.321
Strip condensate	2.25	--	--	--	1.064
Run 14					
Feed	7.0	0.90	0.045	0.087	1.562
Product	0.13	2.1	0.090	0.19	1.772
Boildown condensate	9.0	4.7×10^{-5}	1.4×10^{-3}	1.2×10^{-4}	1.284
Strip condensate	1.08	--	--	--	1.041
Run 15					
Feed	6.7	0.99	0.057	0.078	1.622
Product	-0.14	1.95	0.11	0.14	1.796
Boildowm condensate	8.9	7.8×10^{-5}	1.2×10^{-3}	9×10^{-6}	1.289
Strip condensate	1.88	--	9.4×10^{-4}	--	1.044
Run 16					
Feed	6.5	1.3	0.048	0.043	1.678
Product	-0.017	2.2	0.10	0.097	1.864
Boildown condensate	9.6	3.3×10^{-5}	1.5×10^{-3}	4.8×10^{-5}	1.290
Strip condensate	--	--	--	--	--
Run 17					
Feed	7.1	1.1	0.064	0.091	1.637
Product	-0.46	2.6	0.145	0.22	2.019
Boildown condensate	8.4	3.2×10^{-5}	1.4×10^{-3}	4.6×10^{-5}	1.250
Strip condensate	2.0	1.8×10^{-3}	1.5×10^{-3}	7.9×10^{-5}	1.069
Run 18					
Feed	7.6	0.99	0.057	0.086	1.652
Product	-0.55	2.3	0.105	0.125	1.888
Boildown condensate	8.9	7.9×10^{-5}	1.7×10^{-3}	5×10^{-5}	1.301
Strip condensate	2.0	5.6×10^{-5}	9.5×10^{-4}	4×10^{-5}	1.089
Run 19					
Feed	7.2	0.97	0.054	0.044	1.575
Product	-0.36	2.3	0.127	0.061	1.889
Boildown condensate	9.7	1.0×10^{-4}	1.7×10^{-3}	4.7×10^{-5}	1.271
Strip condensate	1.1	1.6×10^{-4}	9.3×10^{-4}	3.8×10^{-5}	1.034

TABLE 5-5
ENTRAINMENT OF FLUORIDE IN THE FEED ADJUSTMENT SYSTEM

Run No.	Mole Ratio Th/F				% of F in Condensate That Was Entrained	
	Feed	Product	Overhead Composite	Strip Composite	Overhead Composite	Strip Composite
11	22.5	21.4	0.431	--	1.96	--
12	14.7	13.7	0.212	--	1.50	--
13	11.3	10.8	0.499	--	4.51	--
14	19.8	23.7	0.034	--	0.16	--
15	17.5	18.1	0.066	--	0.37	--
16	26.2	21.9	0.022	--	0.09	--
17	17.1	17.7	0.023	1.23	0.13	7.06
18	17.4	21.7	0.047	0.059	0.24	0.30
19	18.1	18.2	0.063	0.172	0.35	0.95

5.3.4. Corrosion Studies

Corrosion coupons of 304L stainless steel were installed in the liquid and vapor phases of the pilot plant solvent extraction feed adjustment system. Three types of coupons were prepared. Two sets of coupons were made from a section of 6-in. schedule 10 pipe. The coupons were cut in half and welded using 308 ELC rod. One set had about 30% weld penetration on one side and the other side was not welded. The other set had 100% weld penetration from one side. The third set of coupons was made from 0.5-in. tubing with a wall thickness of 0.035 in. These coupons were also cut in half and welded using 308 ELC rod.

The coupons were exposed during feed adjustment runs 10 through 19. They were exposed during the boildown step for a total of 51 hr and to the stripping operation for a total of 35 hr, which gives a total hot exposure time of 86 hr. In addition, the coupons were exposed for approximately 185 hr at room temperature; however, this time was not included in the corrosion rate calculations since rates are substantially less at lower temperatures and would give low rates. The measured corrosion rates are given in Table 5-6.

Corrosion rates in the vapor phase were found to be quite high with an average of 1.53 mm/yr (60.2 mils/yr) for the three coupons. Corrosion rates in the liquid phase were found to be an average of about 0.40 mm/yr (15.9 mils/yr). The high corrosion rates in the vapor phase are undoubtedly due to the volatile fluoride ion since it would no longer be complexed by the nonvolatile aluminum III and thorium IV ions. Since the fluoride ion is complexed by aluminum III and thorium IV in the boiling liquid, liquid phase corrosion rates are lower.

5.4. BENCH-SCALE INVESTIGATIONS

5.4.1. Bench-Scale Feed Adjustment

A feed adjustment step is necessary prior to heavy metal - fission product solvent extraction separation. During the feed adjustment

TABLE 5-6
CORROSION RATES IN SOLVENT EXTRACTION FEED ADJUSTMENT SYSTEM

Coupon and Location	Corrosion Rate [mm/yr (mils/yr)]
6-in. pipe, 30% weld penetration, liquid	0.417 (16.43)
0.5-in. tube, liquid	0.330 (12.98)
6-in. pipe, 100% weld penetration, liquid	0.463 (18.22)
6-in. pipe, 30% weld penetration, vapor	1.80 (70.96)
0.5-in. tube, vapor	1.15 (45.36)
6-in. pipe, 100% weld penetration, vapor	1.63 (64.24)

operation, the thorium-Thorex leacher solution (nominally 9M in $[H^+]$) is treated to yield a weak acidic or acid deficient solution. Improved solvent extraction decontamination factors are realized at lower feed acidity, and solvent degradation effects are less pronounced.

A previous study (Ref. 5-2) has demonstrated that acid deficiency can be achieved on a batch basis by evaporation to a specified temperature followed by steam sparging. However, attempts to produce an acid deficient feed on a continuous basis were not successful with a 1M thorium-Thorex feed solution.

R. H. Rainey of ORNL (Ref. 5-4) has suggested the use of diluted thorium-Thorex feed solutions in an effort to achieve acid deficiency on a continuous basis. Bradley and Goodlett (Savannah River Plant) have used formic acid treatment for the denitration of nitric acid solutions (Ref. 5-5). Consequently, experiments were conducted to evaluate both feed dilution and formic acid treatment as possible routes to acid deficiency during feed adjustment. Since it is known that acid deficiency can be achieved on a batch basis by evaporation and steam sparging (Ref. 5-2), feed adjustment experiments with diluted feeds were conducted only on a continuous basis. Both batch and continuous formic acid denitration experiments were performed.

Feed adjustment experiments were performed utilizing a three-neck (300 ml) flask, a downdraft condenser, and a thermometer. A measured volume of 1M thorium-Thorex solution was placed in the flask and evaporated to ∿30% of the original volume (135°C B.P.). Steam sparging was conducted until 167% of the boiled-down product volume was collected in the distillate (sample analytical results confirmed acid deficiency at this point). Continuous operation was begun by introducing feed solution of known

dilution at a constant rate from a buret attached to the flask side arm. Steam sparging was continued during feed addition, and samples of boiler pot product were continuously withdrawn and diluted with water for $[H^+]$ analysis. Sample data were used to calculate the $[H^+]$ of the boiler pot product prior to dilution.

The equipment used for feed dilution experiments was employed in the denitration studies. A measured volume of 1M thorium-Thorex solution was placed in the flask and evaporated to ∿30% of the original volume (135°C B.P.). Steam sparging was conducted until 167% of the boiled-down product volume was collected in the distillate (sample analysis confirmed acid deficiency at this point). Formic acid (88%) in controlled amounts was added to the molten thorium nitrate dihydrate product from a buret during steam sparging.* Following formic acid treatment, a second steam sparging was conducted to remove residual formic acid. The resultant treated product was sampled and diluted for chemical analysis.

Continuous formic acid denitration was attempted by adding 1M thorium-Thorex feed and formic acid during steam sparging. As with batch experiments, the boiler pot temperature was maintained at 135°C during continuous operation.

Data obtained from feed dilution experiments are presented in Table 5-7. As illustrated in this table, acid deficiency was not attained on a continuous basis with feed dilutions as great as 1 part water to 1 part feed. Studies using feeds of greater than 1:1 dilution were not made, as resultant large distillate volumes would be prohibitive in a practical application. Data from several continuous runs in which boric acid and cadmium were added to the 1M thorium-Thorex solution in order to monitor neutron poison volatility are not included in Table 5-7. These data were deleted because the analytical values for $[H^+]$ were found to be negatively

*In some experiments formic acid was added by sparging with steam - formic acid mixtures.

TABLE 5-7
SUMMARY OF CONTINUOUS FEED ADJUSTMENT, RUNS 1 THROUGH 3

Run No.	Steam Rate (ml/min)[a]	Feed Rate (ml/min)	Free $[H^+]$ of Boiler Product (M)	Avg Feed Residence Time (min)[b]	Avg Batch Residence Time (min)[c]	Evaporation Rate (ml/min)[a]	Feed Dilution
1	1.03	0.43	+0.15, +0.50	140	0.97	1.17	1 feed/1 H_2O
2	1.14	0.43	+0.69, +0.78	70	1.67	1.27	3 feed/1 H_2O
3	0.77	0.50	+0.06, +0.20	60	1.27	2.33	None

[a] As determined by measuring volume of distillate produced.

[b] Volume of boiler solution/feed rate.

[c] In steam sparging from 135° to acid deficiency on a batch basis, 50 ml was collected in the distillate. The time required to collect this amount determined the rate of sparging, and this rate divided into the volume of the boiler solution determined the average batch residence time. The feed rate was always set to give an average feed residence time greater than the average batch residence time.

biased by the presence of boric acid in samples. Boric acid possibly interferes on addition of the KF complexing agent used to reverse the hydrolysis of metal ions prior to enthalpimetric titration of free acidity as follows:

$$H_3BO_3 + xF^- \rightarrow BF_x(OH)_{3-x} + xOH^- \quad .$$

Data from formic acid denitration studies are contained in Tables 5-8 and 5-9. Analytical results for $[H^+]$ indicate acid deficiency was achieved in all batch formic acid denitration experiments. Nitrogen dioxide evolution was observed on addition of formic acid to molten thorium nitrate dihydrate at 135°C, giving further evidence of a denitration reaction. The following general equations are given for the reaction of formic acid with molten thorium nitrate:

1. $Th(NO_3)_4 + HCO_2H \xrightarrow{\Delta} Th(NO_3)_2(OH)_2 + 2NO_2 + CO_2$

2. $Th(NO_3)_4 + 2HCO_2H \xrightarrow{\Delta} Th(OH)_4 + 4NO_2 + 2CO_2$

The mechanism of the reaction is not clear at the present time; however, the reaction product probably has the following general formula:

$$Th(NO_3)_{4-x}(OH)_x \quad .$$

From reaction 2, it is apparent that 1 mole of $Th(NO_3)_4$ requires 2 moles of formic acid for complete denitration with NO_2 as a product.* Following evaporation of 100 ml of 1M thorium-Thorex solution to 135°C, the boiler pot contains 48.0 g of $Th(NO_3)_4$ or 0.1 mole. For complete denitration of 0.1 mole of $Th(NO_3)_4$, 0.2 mole or 9.2 g HCO_2H would be required. The following volumes of formic acid (88%) were calculated as necessary for the

*More HCO_2H would be required if NO is a reaction product.

TABLE 5-8
DATA SUMMARY FOR FORMIC ACID DENITRATION - BATCH OPERATION

Run No.	Boiler Product $[H^+]$ Following 1st Steam Sparge (M)	Volume HCO_2H Added (ml)	Boiler Product $[H^+]$ Following 2nd Steam Sparge (M)	HCO_2H Addition Rate (ml/hour)
1	+0.10	0.10	-1.37	1.0
2	-0.44	0.50	-3.59	1.0
3	-0.37	0.50	-1.47	3.0
4	-0.05	0.50	-1.31	1.0
5	--	2.65	-1.56	10.0
6	--	0.40[a]	-0.26	--

[a]Formic acid added by steam sparging with a steam-formic acid mixture.

TABLE 5-9
DATA SUMMARY FOR FORMIC ACID DENITRATION - CONTINUOUS OPERATION

Run No.	HCO_2H Vol (ml, total)	Steam Rate (ml/min)[a]	Feed Rate (ml/min)	Free $[H^+]$ of Boiler Product (M)	Avg Feed Residence Time (min)[b]	Avg Batch Residence Time (min)[c]	Evaporation Rate (ml/min)[a]
I	0.40[d]	5.0	0.41	+0.04, +0.07	73.2	6.0	4.4
II A	4.2	4.6	0.56	-1.56, -1.70	107.1	13.0	3.5
II B	7.3	4.6	0.79	-1.98, -1.91	75.9	4.5	3.5

[a] As determined by measuring volume of distillate produced.

[b] Volume of boiler solution/feed rate.

[c] In steam sparging from 135°C to acid deficiency on a batch basis, 50 ml was collected in the distillate. The time required to collect this amount determined the rate of sparging, and this rate divided into the volume of the boiled pot solution determined the average batch residence time. The feed rate was always set to give an average feed residence time greater than the average batch residence time.

[d] Formic acid added by steam sparging with a steam-formic acid mixture.

indicated denitration of 100 ml of 1M thorium-Thorex solution:

Volume HCO_2H (ml)	Percent Denitration
8.7	100
6.5	75
4.4	50
2.2	25

Examination of the data contained in Table 5-8 reveals that the degree of denitration attained required considerably less than the amount of formic acid calculated from stoichiometry. The reason for the deviation from stoichiometry is unknown. Supplemental experiments have ruled out a negative bias due possibly to residual formic acid in analytical samples (as was the case with boric acid).

Experiments conducted with 1BT feed (thorium product from the partitioning cycle) indicate that $-[H^+]$ is readily attainable on a direct continuous feed addition basis at 135°C. The addition of water to the 135°C boiler pot (as an auxiliary stripping medium) was not required. Also, currently available data show acid deficient boiler pot product was obtained at 125°C when 1% by volume HCO_2H was present in the 1BT feed and with water addition to the pot. Direct continuous experimentation with 1TC feed solution (thorium intercycle concentrator product) at 135°C failed to produce an acid deficient boiler pot product. A dilution or formic acid treatment is therefore indicated for continuous operation with 1TC feed and resultant adjustment to acid deficiency.

Analysis of feed adjustment data for 1BT and 1TC feeds is incomplete and results will be reported next quarter.

5.4.2. Effects of Carbide Carbon in Solvent Extraction Feed

Bench-scale experiments were performed to study the effect of: (1) evaporation to 135°C and (2) evaporation to 135°C with steam sparging on

zirconium decontamination values in the presence of carbide carbon. The work of Swanson of BNWL (Ref. 5-6) indicates that zirconium decontamination factors are significantly reduced during Purex solvent extraction processing of solutions containing carbide carbon. The lower zirconium decontamination factors are apparently the result of the formation of zirconium complexes with ligands formed from the reaction of heavy metal carbides and nitric acid.

The current flowsheet for the solvent extraction separation of heavy metals from fission products in HTGR fuel reprecessing specifies removal of excess nitric acid by evaporation to 135°C followed by steam sparging, should acid deficiency be required. Small amounts of carbide carbon are usually present in aqueous leachates prepared for solvent extraction as a result of whole particle breakage during feed dissolution or incomplete combustion during head-end burning operations. Therefore, it is of importance to assess the effect of evaporation and steam sparging on resultant zirconium decontamination factors in the presence of reaction products of carbide carbon and nitric acid.

Swanson (Ref. 5-6) discusses the effect of carbide carbon at a concentration of 400 μg carbon/g of uranium metal. In the referenced work, uranium metal was dissolved to yield a U concentration of 0.72 M with a resulting carbon content of 6.8 mg/100 ml. In the present study, U-Th mixed carbide fissile particles* (∿2% carbide carbon) were crushed under water and added to ^{95}Zr-Nb "spiked" 1M thorium-Thorex solution to yield a solution containing ∿23.5 mg C/100 ml or 1000 μg C/g heavy metal. For control purposes a sample with no added carbon was included. Solvent extraction feed solutions (with and without carbide addition) were prepared from 100-ml aliquots of 1M thorium-Thorex solution (Zr-95 present) by: (1) evaporation to 135°C and (2) evaporation to 135°C with steam sparging until 50 ml of steam condensed in the distillate. Following adjustment of the boiler pot product to 0.4M Th^{+4} and 1M H^{+}, an initial extraction with

*Sample TD-1067-JSL.

30% TBP-NPH was performed in a separatory funnel. A scrub solution containing 0.25M Th^{+4} and 1M H^{+} was used for all subsequent contacts. Gamma spectrometry, with NaI scintillation detection, was utilized for measurement of total sample ^{95}Zr-Nb activity in the organic and aqueous products following phase separation.

The experimental design is given in Fig. 5-8, and ^{95}Zr-Nb gamma spectrometry data appear in Tables 5-10 and 5-11.

The apparent increase in K values (distribution coefficients) calculated for a given sample is probably due to an increasing ratio of organic soluble complexing agent to zirconium at low zirconium concentration levels. Therefore, it is concluded that evaporation to 135°C with steam sparging does not obviate the deleterious effect of carbide carbon in solvent extraction feed solutions.

Additional experimentation, with Ge-Li counting of samples and phase separation by centrifugation, is suggested for more accurate calculation of K values for Zr-95. Also, solvent extraction runs indicate that graphite carbon, which is more likely to be in the burner ash, produces as significant a Zr-95 scrubbing lowering as does the carbide carbon. Bench-scale tests of graphite carbon and silicon carbide effects on Zr-95 scrubbing and possible flowsheet changes to overcome these effects are included in future planned work in this area.

5.4.3. Degraded Solvent - Uranium, Thorium Nitrate Reactions

Bench-scale testing was initiated during the quarter in an effort to define the conditions required for abrupt reactions of nitric acid degraded solvent ("red-oil") containing uranium-thorium nitrate salts in order to set limits for maximum temperature in HRDF concentrators. Initial experiments were conducted with 30% TBP/NPH and thorium or uranyl nitrate salts. Samples prepared to contain TBP/heavy metal nitrate weight ratios of 0.06,

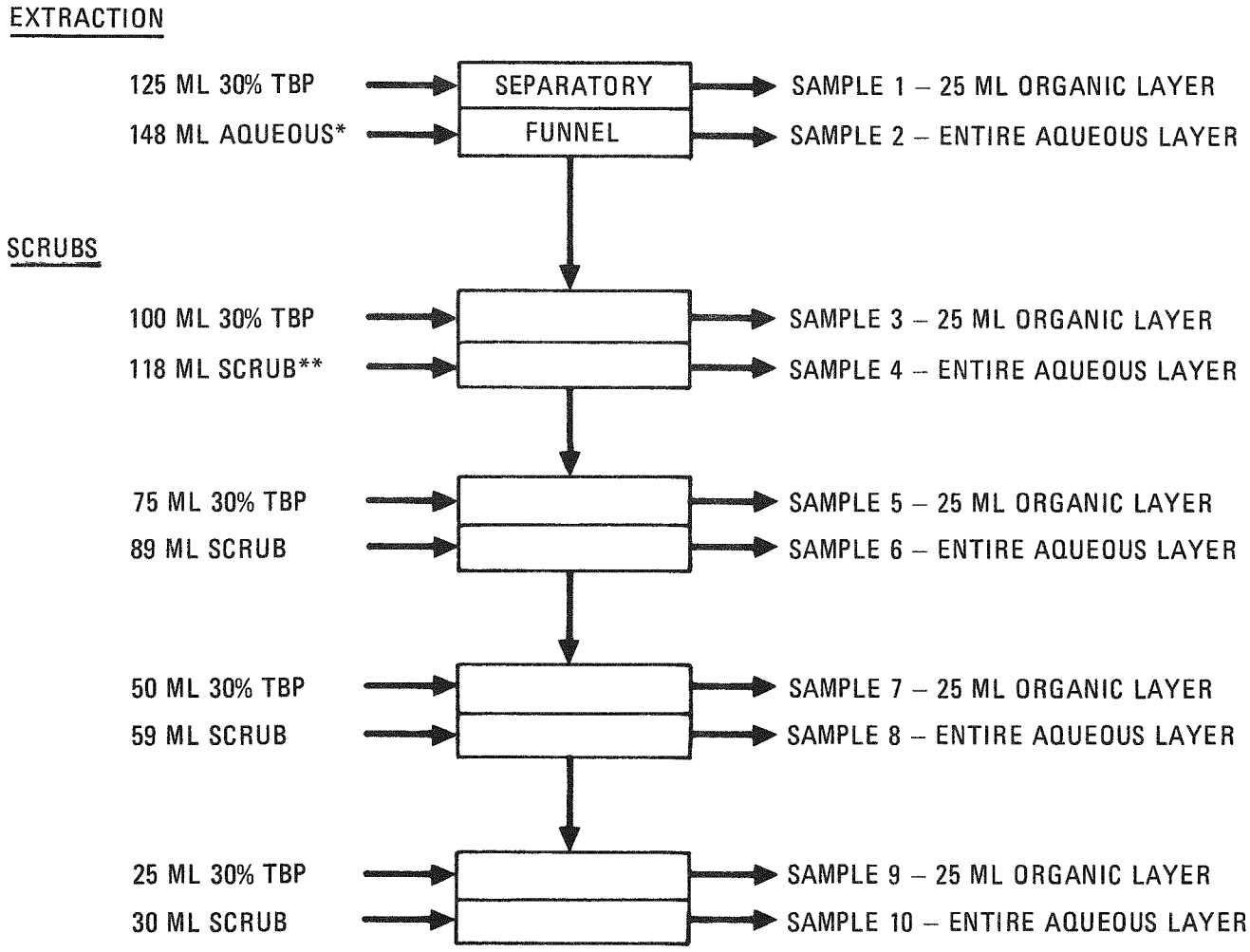

*0.4 M Th^{+4}, 1.0 M H^+ – FEED SOLUTION.
**0.25 M Th^{+4}, 1.0 M H^+ – SCRUB SOLUTION

Fig. 5-8. Experimental design - Zr-95 distribution studies in Thorex extraction column

TABLE 5-10
DATA SUMMARY FOR ^{95}Zr-Nb CARBIDE STUDIES - EVAPORATION TO 135°C ONLY

Sample No.[a]	Dilution	$\frac{\text{Counts}}{\text{Unit Time}}$	$\left(\frac{\text{Counts}}{\text{Unit Time}} \times \text{Dilution Factor}\right)$	Calculated K value[b]
1	None	100	100	0.013
2	1/25	300	7500	
3	None	5	5	0.033
4	1/25	6	300	
5	None	3.7	3.7	0.23
6	None	16	16	
7	None	3.7	3.7	0.46
8	None	8	8	
9	None	11	11	0.68
10	None	16	16	
1A	None	100	100	0.023
1B	1/25	170	4250	
1C	None	18	18	0.144
1D	1/25	5	125	
1E	None	10	10	0.883
1F	None	12	12	
1G	None	9	9	1.50
1H	None	6	6	
1I	None	11	11	2.20
1J	None	5	5	

[a] Samples 1 through 10 are control without carbide addition. Samples 1A through 1J are with carbide added.

[b] $K = \frac{\text{Conc. } ^{95}Zr \text{ organic layer}}{\text{Conc. } ^{95}Zr \text{ aqueous layer}}$ = distribution coefficient.

TABLE 5-11
DATA SUMMARY FOR ^{95}Zr-Nb CARBIDL STUDIES - EVAPORATION TO 135°C WITH STEAM SPARGING

Sample No.[a]	Dilution	$\frac{\text{Counts}}{\text{Unit Time}}$	$\left(\frac{\text{Counts}}{\text{Unit Time}} \times \text{Dilution Factor}\right)$	Calculated K value[b]
1	None	33	33	0.011
2	1/25	120	3000	
3	None	1.5	1.5	0.035
4	1/25	1.7	42.5	
5	None	0.7	0.7	0.18
6	None	4.0	4.0	
7	None	0.7	0.7	0.23
8	None	3.0	3.0	
9	None	12	12	4.0
10	None	3	3	
1A	None	36	36	0.020
1B	1/25	70	1750	
1C	None	4.3	4.3	0.14
1D	1/25	1.2	30.0	
1E	None	2.0	2.0	0.40
1F	None	5.0	5.0	
1G	None	1.6	1.6	0.53
1H	None	3	3	
1I	None	13	13	4.33
1J	None	3	3	

(a) Samples 1 through 10 are control without carbide added. Samples 1A through 1J are with carbide added.

(b) $K = \frac{\text{Conc. } ^{95}Zr \text{ organic layer}}{\text{Conc. } ^{95}Zr \text{ aqueous layer}}$ = distribution coefficient.

0.15 (literature minimum value for abrupt reaction with the TBP-$Pu(NO_3)_4$ system), and 0.21 were heated to 250°C in open cups. The following experimental observations were recorded:

1. System $UO_2(NO_3)_2$ - TBP is more reactive than system $Th(NO_3)_4$ - TBP.

2. Temperature in excess of 190°C was required for abrupt reaction with both systems.

Attempts to prepare nitric acid degraded solvent ("red-oil") during the refluxing of solvent - heavy metal - HNO_3 mixtures were not successful. The fact that "red-oil" was not found under reflux conditions more rigorous than described in earlier work (Ref. 5-7) leads to speculation that the diluent currently in use [normal paraffin hydrocarbon (NPH)] is considerably more resistant to nitration than the Shell Spray Base previously used. Additional experiments are currently being conducted because verification of this finding would impact the whole question of "red-oil" formation in the concentrator.

REFERENCES

5-1. "Thorium Utilization Program Quarterly Progress Report for the Period Ending May 31, 1975," ERDA Report GA-A13510, General Atomic Company, August 15, 1975.

5-2. "Thorium Utilization Program Quarterly Progress Report for the Period Ending August 31, 1975," ERDA Report GA-A12593, General Atomic Company, September 30, 1975.

5-3. "Thorium Utilization Program Quarterly Progress Report for the Period Ending November 30, 1975," ERDA Report GA-A13746, General Atomic Company, December 31, 1975.

5-4. Rainey, R. H., "Continuous Solvent Extraction Feed Adjustment," ORNL unpublished data, June 8, 1975.

5-5. Bradley, R. F., and C. B. Goodlett, "Denitration of Nitric Acid Solutions by Formic Acid," Dupont Savannah River Plant Report DP-1299, June 1972.

5-6. Swanson, J. L., "Improved Zirconium Decontamination in Purex Process," USAEC Report BNWL-1573, Battelle Northwest Laboratories, May 1971.

5-7. Wagner, R. M., "Investigation of Explosive Characteristics of Purex Solvent Decomposition Products (Red-Oil)," General Electric Report HW-27492, March 17, 1953.

6. SOLVENT EXTRACTION

6.1. SUMMARY

Solvent extraction runs 49 and 50 were completed during the quarter. These runs represented the first cycle of the acid-Thorex flowsheet (Fig. 6-1). Each of the runs was made using the facilities in the pilot plant five-column system. The flowsheet under investigation is related to HTGR fuel reprocessing. The runs included the addition of nonradioactive and radioactive zirconium. Dibutyl phosphate (DBP) was added to the 1A column to simulate solvent degradation.

The results of these two runs confirm that feed made up from leached, burned fertile kernels gives poorer Zr-95 decontamination in solvent extraction (a factor of 2 to 5) than does feed prepared from purchased thorium nitrate. Further work is under way to resolve whether this observed difference will be significant with high radiation solvent damage in the first cycle of HRDF.

6.2. PROCESS MODIFICATIONS

The headpot on the 1SP airlift system was modified to eliminate the foaming which had been observed in earlier runs. The hole size in the nozzle plates in the 1BX column was increased from 1/8-in. (0.32 cm) diameter to 3/16-in. (0.48 cm) diameter to test capacity effects.

The 1BSU stream was added to the 1SP (which goes to the bottom of the 1BX column) rather than 3 ft below the 1A column feed point as in previous runs.

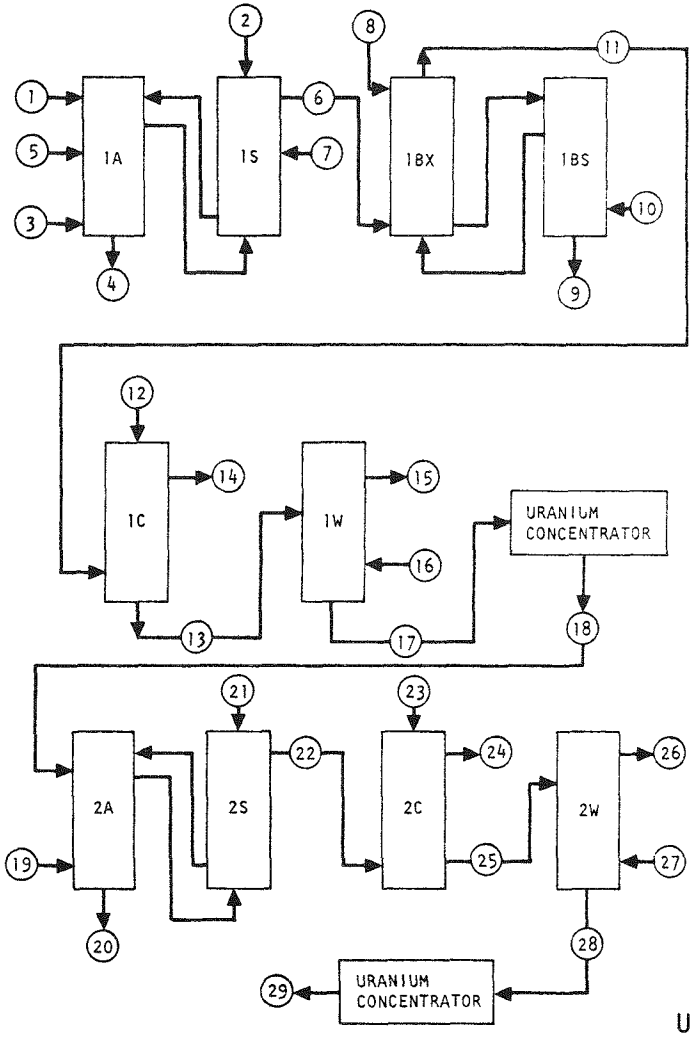

COLUMN STREAM	STREAM NO.	FLOW (L/DAY)	COMPOSITION U (G/L)	Th (G/L)	HNO_3 (M)
1AF	1	725	14	348	<1.0
1AS	2	754			0.01
1AX	3	7250		(30% TBP)	
1AW	4	1903		(FISSION PRODUCTS)	
1AA	5	234			13.0
1SP	6	7250	1.4	35	
1AIS	7	190			5.0
1BX	8	4350			0.2
1BT	9	4350	Trace	102	
1BS	10	1300		(30% TBP)	
1BU	11	8550	1.19		
1CX	12	4300			0.01
1CU	13	4300	2.37		
1CW	14	8550		(30% TBP)	TO 10
1WW	15	430		(NPH)	
1WS	16	430		(NPH)	
1WU	17	4300	2.37		
2AF	18	43.6	233		
2AX	19	858		(5% TBP)	
2AW	20	294		(WASTE)	
2AS	21	243			2.0
2SP	22	858	11.8		
2CX	23	430			0.01
2CW	24	858		(ORGANIC)	
2CU	25	430	23.6		
2WW	26	43		(NPH)	
2WS	27	43		(NPH)	
2WU	28	430	27.5		
U PRODUCT	29	43.6	233		

Fig. 6-1. Partition flowsheet

The thorium in the feed for run 49 was prepared in the pilot plant feed system. Run 50 feed was prepared from purchased thorium nitrate. These differences in feed allowed comparison of feed effects between the runs. The solvent was also treated by passing through a bed of macroreticular anion exchange resin (Amberlyst A-26*) prior to use in run 50.

6.3. RESULTS AND DISCUSSION

Table 6-1 contains the stream analyses and flow rates for each run. Tables 6-2 and 6-3 contain percent loss and heights equivalent to a theoretical stage (HETS) at the indicated percentage of flooding frequency. Table 6-4 contains the column and cartridge descriptions.

For both runs two columns were used for the extraction-scrub operation (1A-1S) and one column each for partition (1BX), partition-scrub (1BS), and urnaium strip (1C) operations. Runs 49 and 50 were similar to Runs 47 and 48, which were reported in Ref. 6-1.

In run 49 solids contained in the 1AF feed were visible in the extraction section (below 1AF inlet point) of the 1A column. A slight reduction from the normal pulse frequency was required to avoid flooding in the 1A column. The solids in run 49 feed were normal for pilot plant leaching and feed adjustment processing of Fort St. Vrain fertile fuels, and no solid materials were added.

In runs 47 and 48 the 1BSU stream was added to the 1A column 3 ft (0.91 m) below the 1AF inlet. The change to add the 1BSU stream to the 1SP stream in runs 49 and 50 was made because the amount of zirconium in the 1BSU is low; therefore, the overall system zirconium arithmetric decontamination factor (DF) is not decreased by addition to the 1SP stream. The other flow rates in the 1A-1S system were maintained at previous rates.

---

*Trade name.

TABLE 6-1
ANALYTICAL DATA AND FLOW RATES FOR SOLVENT EXTRACTION RUNS 49 AND 50[a]

Stream	Stream No.	U (g/liter)	Th (g/liter)	HNO_3 (M)	95-ZrNb (cpm)	Flow (ml/min)	Relative Flow	95-Zr (μCi/ml)
				Run 49				
1AF	1	37.3	347.0	0.90	1925 {Zr = 2.23g/ℓ}	99 (85)	100 (100)	0.0638
1CX	--	--	[F^-=0.0014M]	0.011	--	578 (589) (587)	584 (693) (691)	--
1BX	--	--	[F^-=0.0037M]	0.22	--	698 (696) (700)	705 (819) (824)	--
1AX	--	--	--	[30%TBP]	--	985 (1022) (1002)	995 (1202) (1179)	--
1BS	--	--	--	[30%TBP]	--	188 (139) (201)	190 (164) (236)	--
1AS	--	--	--	0.94	--	175 (190) (190)	177 (224) (224)	--
1AA	--	--	--	~15	--	24 (22.7) (31.1)	24 (27) (37)	--

TABLE 6-1 (Continued)

Stream	Stream No.	U (g/liter)	Th (g/liter)	HNO_3 (M)	95-ZrNb (cpm)	Flow (ml/min)	Relative Flow	95-Zr (μCi/ml)
1AW	--	9.6×10^{-3} (8.9×10^{-3}) --	4.58×10^{-2} (2.74×10^{-2}) (3.21×10^{-2})	1.18 (1.87) (1.94)	650 (550) (530)	--	--	--
1AP	--	3.2 (2.7) (3.1)	39.5 (39.1) (33.3)	0.25 (0.27) (0.26)	18 (19) (17)	--	--	2.02×10^{-3} (1.65×10^{-3}) (1.74×10^{-3})
1SR	--	0.49 (0.46) (0.42)	77.6 (86.7) (77.2)	1.20 (1.30) (1.39)	60.5 (77) (82.5)	--	--	4.79×10^{-3} (6.66×10^{-3}) (6.49×10^{-3})
1SP	--	3.1 (2.5) (2.7)	22.9 (35.5) (26.0)	0.20 (0.20) (0.21)	2.4 (3.0) (2.2)	--	--	4.44×10^{-4} (4.24×10^{-4}) (1.28×10^{-4})
1BU	--	2.6 (2.6) (2.1)	2.44×10^{-3} (7.0×10^{-4}) (3.2×10^{-3})	0.08 (0.10) (0.10)	0.35 (0.2) (0.07)	--	--	--
1BXT	--	0.73 (0.38) (0.22)	40.6 (51.5) (45.2)	0.40 (0.43) (0.39)	3 (3) (3)	--	--	--
1BSU	--	3.6 (2.9) (2.6)	15.0 (29.5) (17.2)	0.19 (0.16) (0.19)	0.15 (0.5) (0.4)	--	--	--

TABLE 6-1 (Continued)

Stream	Stream No.	U (g/liter)	Th (g/liter)	HNO_3 (M)	95-ZrNb (cpm)	Flow (ml/min)	Relative Flow	95-Zr (μCi/ml)
1BT	--	2.8×10^{-3} (8.3×10^{-3}) (1.3×10^{-3})	34.6 (45.4) (39.6)	0.39 (0.39) (0.39)	2.7 (3.6) (2.7)	--	--	9.07×10^{-5} (5.42×10^{-4}) (1.65×10^{-4})
1CU	--	7.0 (5.7) (4.0)	3.0×10^{-3} (1.2×10^{-3}) (1.4×10^{-3})	0.057 (0.049) (0.046)	0.6 (0.35) (0.35)	--	--	1.04×10^{-4} (6.7×10^{-5}) (2.39×10^{-5})
1CW	--	3.2×10^{-3} (5.3×10^{-4}) (7.3×10^{-3})	5.5×10^{-3} (1.9×10^{-3}) (1.5×10^{-3})	$<10^{-3}$ ($<10^{-3}$) ($<10-3$)	<0.03 (0.05) (0.02)	--	--	--
1A-DBP	--	--	--	[DBP = 3.0g/ℓ]	--	-- (9.8) (15.5)	-- (11.5) (18.2)	--
				Run 50				
1AF	--	33.7	375.9	0.87	7480 [Zr = 2.59g/ℓ]	111 (108) (108)	100 (100) (100)	0.287
1CX	--	--	[F^-=0.002M]	0.011	--	567 (603) (594)	510 (558) (550)	--
1BX	--	--	[F^-=0.0049M]	0.23	--	689 (705) (687)	621 (653) (636)	--

TABLE 6-1 (Continued)

Stream	Stream No.	U (g/liter)	Th (g/liter)	HNO_3 (M)	95-ZrNb (cpm)	Flow (ml/min)	Relative Flow	95-Zr (μCi/ml)
1AX	--	--	--	(30%TBP)	--	983 (986) (988)	886 (913) (915)	--
1BS	--	--	--	(30%TBP)	--	204 (190) (179)	184 (176) (166)	--
1AS	--	--	--	0.90	--	173 (181) (189)	156 (168) (175)	--
1AA	--	--	--	~15	--	29 (25.8) (24.2)	26 (24) (22.4)	--
1AW	--	5.6×10^{-3} (2.3×10^{-3}) (1.5×10^{-3})	0.68 (0.27) (0.10)	1.87 (1.49) (1.50)	2530 (2420) (2310)	--	--	--
1AP	--	3.3 (2.2) (2.5)	53.2 (76.5) (55.7)	0.17 (0.12) (0.14)	17.6 (14.3) (17.6)	--	--	1.82×10^{-3} (1.27×10^{-3}) (1.54×10^{-3})
1SR	--	0.62 (0.56) (0.53)	114.2 (144.9) (143.9)	1.08 (0.90) (0.88)	70 (65) (70)	--	--	7.5×10^{-3} (6.4×10^{-3}) (7.6×10^{-3})
1SP	--	3.5 (2.6) (2.5)	27.3 (31.3) (33.2)	0.18 (0.18) (0.17)	5.28 (4.4) (5.5)	--	--	1.53×10^{-4}) (3.32×10^{-4}) (4.03×10^{-4})

TABLE 6-1 (Continued)

Stream	Stream No.	U (g/liter)	Th (g/liter)	HNO_3 (M)	95-ZrNb (cpm)	Flow (ml/min)	Relative Flow	95-Zr (μCi/ml)
1BU	--	2.4 (1.8) (1.5)	2.4×10^{-3} (1.24×10^{-3}) (2.8×10^{-3})	0.02 (0.03) (0.02)	0.26 (0.50) (0.60)	--	--	--
1BXT	--	0.68 (0.40) (0.54)	49.6 (59.9) (55.1)	0.38 (0.36) (0.37)	8 (7) (8)	--	--	--
1BSU	--	1.9 (1.7) --	21.4 (22.7) --	0.11 (0.12) --	0.3 (0.3) --	--	--	--
1BT	--	6.7×10^{-4} (7.6×10^{-4}) (1×10^{-3})	48.9 (44.7) (53.0)	0.37 (0.36) (0.36)	9.6 (8.8) (7.2)	--	--	7.92×10^{-4} (9.25×10^{-4}) (4.89×10^{-4})
1CU	--	5.6 (5.9) (4.6)	1.5×10^{-3} (1.13×10^{-2}) (4.7×10^{-3})	0.02 (0.02) (0.02)	0.3 (1.1) (0.9)			3.13×10^{-5} (4.00×10^{-5}) (3.10×10^{-5})
1CW	--	3×10^{-4} (3.6×10^{-4})	2.4×10^{-3} (2.5×10^{-3})	5.9×10^{-3} $(<5\times10^{-4})$	<0.02 (<0.02)	--	--	--
1A-DBP	--	--	--	[3.0 g/ℓ, DBP]	--	-- (6.2) (20)	-- (5.7) (18.5)	--

(a) The data in parentheses correspond to a second and third set of operating conditions.

TABLE 6-2
HETS, PERCENT LOSS, Zr DECONTAMINATION FACTOR, AND FLOODING DATA, RUN 49[a]

Column	Purpose	Vol Velocity (gal/hr/ft^2)	Superficial Velocity[b] $\bar{V}_o$ (cm/sec)	Superficial Velocity[b] $\bar{V}_a$ (cm/sec)	Flooding Freq (cycles/min)	Continuous Phase	Aqueous to Organic Ratio	HETS [feet (meters)]	Percent Loss U	Percent Loss Th	Zr-Nb DF U Basis	Zr-Nb DF Th Basis	% Flooding Frequency	Temp.
1A	Extraction	933 (959) (951)	0.81 (0.84) (0.83)	0.24 (0.24) (0.25)	91 (90) (90)	Organic	0.302 (0.291) (0.305)	-- -- --	0.08 (0.08) --	0 04 (0.03) (0.03)	9.17 (3.56) (9 41)	12.17 (11.42) (10.87)	80 (81) (81)	Ambient
1S	Scrub	843 (881) (867)	0.81 (0.84) (0.82)	0.14 (0.16) (0.16)	100 (96) (96)	Organic	0.178 (0.186) (0.190)	Zr-Nb = 7.2[c] (2.19) --	-- -- --	-- -- --	7.27 (5.86) (6.73)	4.35 (1.23) (0.97)	82 (85) (85)	Ambient
1BX	Partition	605 (601) (614)	0.42 (0.42) (0.44)	0.26 (0.26) (0.25)	82 82 (81)	Aqueous	0 595 (0.603) (0.579)	3 66(Th) (1.11) 3.19(Th) (0.97) 3.53(Th) (1.07)	-- -- --	0.008 (0.003) (0.01)	5.75 (15.6) (24.4)	-- -- --	73 (73) (74)	Ambient
1BS	Partition-Scrub	644 (610) (652)	0.16 (0.11) (0.17)	0.57 (0.57) (0.57)	74 (75) (73)	Aqueous	3.71 (5.04) (3.46)	1.89(U) (0.57) 1.36(U) (0.41) 1.79(U) (0.54)	0.05 (0.18) (0.03)	-- -- --	-- -- --	0.95 (0.73) (0.97)	76 (75) (77)	Ambient
1C	U-Strip	566 (565) (578)	0.43 (0.43) (0.44)	0.21 (0.21) (0.21)	85 (85) (84)	Aqueous	0.493 (0.507) (0.488)	2.63(U) (0.80) 2.80(U) (0.85) 3.85(U) (1.17)	0.10 (0.02) (0.28)	-- -- --	1.57 (1.25) (0.38)	-- -- --	85 (85) (86)	50°C

[a] The data in parentheses correspond to a second and third set of operating conditions.

[b] $\bar{V}_o + \bar{V}_a = \bar{V}_T$; volume velocity (in gallons/hr/ft^2) 885 $\bar{V}_T$, $\bar{V}_o$ is the superficial velocity of the organic phase and $\bar{V}_a$ is the aqueous phase.

[c] Average ^{95}Zr-Nb equilibrium distribution = 0.1.

TABLE 6-3
HETS, PERCENT LOSS, Zr DECONTAMINATION FACTOR, AND FLOODING DATA, RUN 50[a]

Column	Purpose	Vol Velocity (gal/hr/ft^2)	Superficial Velocity[b] $\bar{V}_o$ (cm/sec)	Superficial Velocity[b] $\bar{V}_a$ (cm/sec)	Flooding Freq (cycles/min)	Continuous Phase	Aqueous to Organic Ratio	HETS [feet (meters)]	Percent Loss U	Percent Loss Th	Zr-Nb DF U Basis	Zr-Nb DF Th Basis	% Flooding Frequency	Temp.
1A	Extraction	942 (950) (966)	0.80 (0.81) (0.83)	0.26 (0.26) (0.26)	91 (90) (89)	Organic	0.318 (0.317) (0.319)	-- -- --	0.05 (0.02) (0.01)	0.51 (0.21) (0.08)	41.6 (34.1) (31.5)	60.1 (106.5) (63)	90 (91) (92)	Ambient
1S	Scrub	840 (848) (856)	0.81 (0.81) (0.82)	0.14 (0.15) (0.15)	100 (99) (98)	Organic	0.176 (0.182) (0.188)	Zr-Nb = 13.8[c] (4.20) --	-- -- --	-- -- --	3.54 (3.84) (3.2)	1.71 (1.33) (1.91)	85 (86) (87)	Ambient
1BX	Partition	606 (608) (599)	0.43 (0.43) (0.42)	0.25 (0.26) (0.25)	82 (82) (83)	Aqueous	0.580 (0.599) (0.589)	3.33(Th) (1.01) 3.12(Th) (0.95) 3.33(Th) (1.01)	-- -- --	0.08 (0.004) (0.008)	13.9 (6.1) (5.5)	-- -- --	79 (67) (66)	Ambient
1BS	Partition-Scrub	649 (651) (630)	0.16 (0.16) (0.15)	0.57 (0.58) (0.56)	74 (74) (74)	Aqueous	3.38 (3.71) (3.84)	1.79(L) (0.54) 1.65(L) (0.50) 1.65(U) (0.50)	0.01 (0.01) (0.02)	-- -- --	-- -- --	0.82 (0.59) (1.07)	68 (68) (68)	Ambient
1C	L-Strip	567 (575) (569)	0.43 (0.43) (0.42)	0.21 (0.22) (0.22)	~85 (~85) (~85)	Aqueous	0.478 (0.513) (0.509)	2.68(L) (0.81) 2.68(U) (0.81) --	0.01 (0.01) --	-- -- --	2.02 (1.49) (204)	-- -- --	~50 ~50 ~50	46°C

[a] The data in parentheses correspond to a second and third set of operating conditions.

[b] $\bar{V}_o + \bar{V}_a = \bar{V}_I$; volume velocity (in gallons/hr/ft^2) 885 $\bar{V}_T$; $\bar{V}_o$ is the superficial velocity of the organic phase and $\bar{V}_a$ is the aqueous phase.

[c] Average ^{95}Zr-Nb equilibrium distribution = 0.1.

TABLE 6-4
CARTRIDGE DESCRIPTIONS, SOLVENT EXTRACTION RUNS 49 AND 50

Column	Column Diameter [in. (mm)]	Cartridge Height [ft (m)]	Plates			
			Nozzle Direction	Hole Size [in. (mm)]	Free Area (%)	Plate Spacing [in. (mm)]
1A extraction	2 (51)	13 (4)	Down	1/8 (3)	23	2 (51)
1A scrub	2 (51)	9 (2.7)	Down	1/8 (3)	23	2 (51)
1S scrub	2 (51)	18 (5.5)	Down	1/8 (3)	23	2 (51)
1BX	3 (76)	15 (4.6)	Up	3/16 (5)	23	Graded[a]
1BS	2 (51)	17 (5.2)	Up	3/16 (5)	23	2 (51)
1C	3 (76)	15 (4.6)	Up	3/16 (5)	23	Graded[a]

[a]Graded cartridge is, from the bottom, 8-1/2 ft (2.6 m) with 4-in. (102 mm) spacing, 1-1/2 ft (0.5 m) with 3-in. (76 mm) spacing, and 5 ft (1.5 m) with 2-in. (51 mm) spacing.

Hence, the effective aqueous-to-organic flow ratio in the 1A-1S system was increased. No significant increase in uranium and thorium losses from previous runs occurred due to this flowsheet change.

The improvement in zirconium decontamination from run 49 to run 50 is at least partially explained by the increased organic phase thorium concentration. Despite the increase in the aqueous-to-organic ratio and increased thorium concentration in the organic phase, the maximum thorium loss via the 1AW stream was only 0.51%.

The overall ^{95}Zr-Nb DF in run 49 was about 70 to 80 (thorium basis). The ^{95}Zr-Nb DF for uranium was about 600 to 800. In neither case did a decrease in decontamination occur which could be attributed to the addition of DBP. The only direct evidence of the presence of DBP was the visual change in the dispersion characteristics in the middle of the 1C column.

The overall ^{95}Zr-Nb DF in run 50 improved in comparison with run 49. The overall thorium basis DF was 100 to 150; the uranium DF was 1000 to 4000. The overall ^{95}Zr-Nb DF on a uranium basis decreased after the addition of DBP. The thorium basis DF increased slightly after DBP addition. Only very slight changes were observed in the 1C column dispersion after DBP was added during run 50.

The DBP was added to the 1A column [3 ft (0.91 m) below feed point] during runs 49 and 50 after the operation was at steady state. Impurities in the stock DBP were about 50% by volume based on the losses during purification and analytical analyses. The stock DBP, purchased to a 95% pure specification, had been used as-received in previous runs. Any large effects of the impurities in the stock DBP on zirconium decontamination in the solvent extraction system from previous runs were not apparent.

The maximum rate of DBP addition to the 1A column in run 49 corresponded to about 0.046 g per liter of 1AX solvent. The accumulative DBP added during run 49 was about 6.1 g. In run 50, the maximum addition rate

for DBP was about 0.060 g per liter of 1AX solvent. The accumulative DPB added during run 50 was about 4.6 g. The maximum DBP concentration expected to form in the solvent due to radiolysis of TBP during irradiated fuel reprocessing is about 0.08 g per liter. Effects on processing, particularly the effects which occur in the 1C column, are a function of cumulative amounts of DBP. The cumulative effects occur as a result of precipitation or buildup of DBP.

The reason for little or no effect from the DBP addition is probably the low concentration and total amount of DBP added during each run. These results are encouraging and indicate any short-term effects due to solvent radiolysis in HTGR reprocessing will not be large as long as the fluoride additions are made to the 1BX and 1CX streams.

In run 49 the 1BT stream contained 33 to 180 parts of uranium per million parts of thorium. In run 50 the 1BT contained 14 to 18 parts of uranium per million parts thorium. The solvent used for the 1AX and 1BS streams in run 50 had received ion exchange resin (Ref. 6-2). This cleanup removes residual metallic ions and degradation products. This ion exchange cleanup probably contributed to, or was responsible for, the low uranium content in the thorium product (1BT) in run 50.

Flooding tests were run on the 1BX column to test the capacity of the newly installed cartridge. Some improvement in capacity was noted with these plates with 3/16-in. (0.48 cm) holes versus the 1/8-in. (0.32 cm) holes. The new foam eliminator worked effectively in reducing foam carry-over from the 1SP headpot into the 1BX column. However, the inherent instability of the 1BX column remained. This instability, which manifests itself as cyclic flooding in the bottom third of the column, does not significantly affect column efficiency. Controlling the instability is readily accomplished by reduction of the pulse frequency in the column. The foam eliminator was made by placing a stainless steel sieve plate cartridge [1/2-in. (1.27 cm) plate spacing] into a section of glass pipe

and connecting this section horizontally into the overflow of the headpot. The sieve plates promote gas-liquid separation as the solvent flows slowly through the cartridge, thus dissipating the foam.

The HETS values were estimated using the available equilibrium data. An average equilibrium distribution for ^{95}Zr-Nb of 0.1 was assumed for the 1S column HETS calculations.

REFERENCES

6-1. "Thorium Utilization Program Quarterly Progress Report for the Period Ending November 30, 1975," ERDA Report GA-A13746, General Atomic Company, December 31, 1975.

6-2. Schutz, W. W., "Macroreticular Ion Exchange Resin Cleanup of Purex TBP Solvent," Atlantic Richfield Hanford Report ARH-SA-58, August 1, 1970.

7. OFF-GAS STUDIES

In January 1976, the off-gas studies task was added to the scope of work performed by GA under the Thorium Utilization Program. Work was initiated on a preconceptual design study for a burner and leacher off-gas treatment system to be added to the GA pilot plant facilities. The semi-volatile and particulate collection device, CO/HT oxidizer, SO_2 adsorbent, NO_x converter, iodine adsorbent, and tritium adsorbent components have been identified as probable subsystems to be studied in cold engineering-scale tests. The experimental design parameters and experimental limitations are being defined.

8. SEMIREMOTE HANDLING SYSTEMS

A number of fixtures have been designed and fabricated to aid in the construction and assembly of unit operations in the prototype line and to demonstrate techniques which will be required for remote disassembly of operating equipment in a production-scale reprocessing facility. These fixtures are actually to be employed in a semiremote fashion in which manual manipulations are presently required but for which manipulators and other remotely operated devices could be used to perform similar operations in a large-scale facility. Progress in the manufacture of these fixtures is described.

8.1. PROTOTYPE SIZE REDUCTION SYSTEM

8.1.1. Lift Fixture - Primary Pitman Assembly

This fixture will be used to engage the primary pitman assembly at its crown and to lift it vertically clear of the UNIFRAME. A feature of the mechanism is the automatic leveling system which seeks the correct attitude of the assembly regardless of the position of the load center of gravity.

Mechanical fabrication is complete. Electrical wiring of the motor and sensing devices is under way. Testing and operational checkout are scheduled for completion during the transition quarter.

8.1.2. Lift Fixture - Primary Fixed Jaw

This device adapts the primary pitman lift fixture to remove the primary fixed jaw.

All fabrication is complete. Testing and operational checkout are scheduled for completion during the transition quarter.

8.1.3. Lift Fixture - Secondary Pitman Assembly (Fig. 8-1)

The construction of this unit is very similar to that of the primary pitman fixture except for the addition of a vertical actuator to handle the toggle arm during the lift maneuver.

Mechanical fabrication is complete and electrical wiring of the two actuating motors and control equipment is under way. Testing and operational checkout are scheduled for completion during the transition quarter.

8.1.4. Removal Fixture - Secondary Fixed Jaw (Fig. 8-2)

A new design is under development for the removal fixture for the secondary fixed jaw. This jaw can not be removed vertically without first removing the primary pitman assembly. The new mechanism utilizes a single short screw jack to first lower the jaw onto a cradle and then pivot it into a near horizontal attitude for removal. The redesign simplifies the fixture as originally planned, adding reliability and improving the application to hot cell operation.

Initial concepts were approved at the design review, major components have been identified, preliminary costing is complete, and drafting is in progress.

8.1.5. Crusher Shroud Shutoff Valve (Fig. 8-3)

This valve is contained within a cylindrical communication port between the lower extremity of the crusher shroud and the screener assembly. The size of the port is approximately 44 in. in diameter and 6 in. high; the valve consists essentially of a sliding shutter plate which acts as a closure. The primary feature of the valve is a sealing sleeve on the inside surface, which is actuated axially by a helical cam. This device provides an unobstructed inside surface during crusher operation, which avoids trapping of dust or particles. The same device seals the slide valve plate and also acts as scrubber during valve opening.

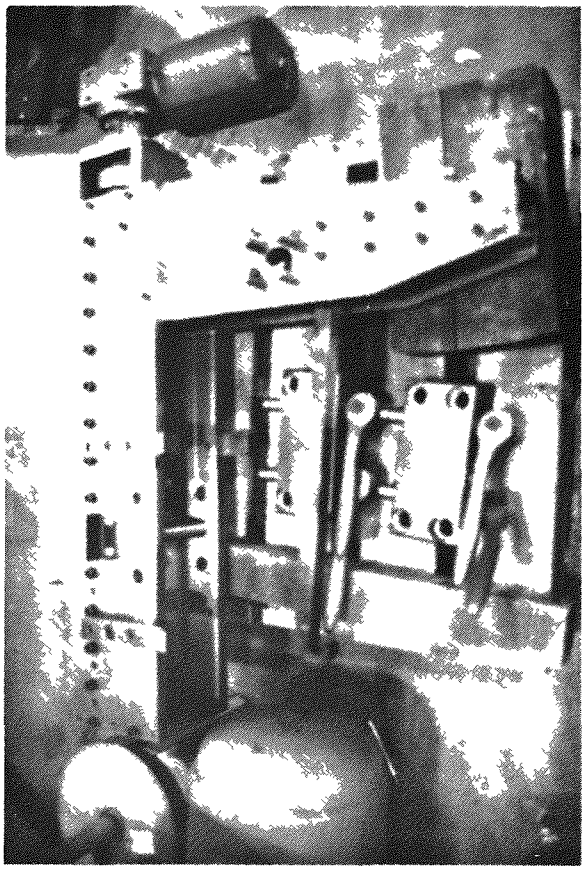

Fig. 8-1. Lift fixture, secondary pitman assembly

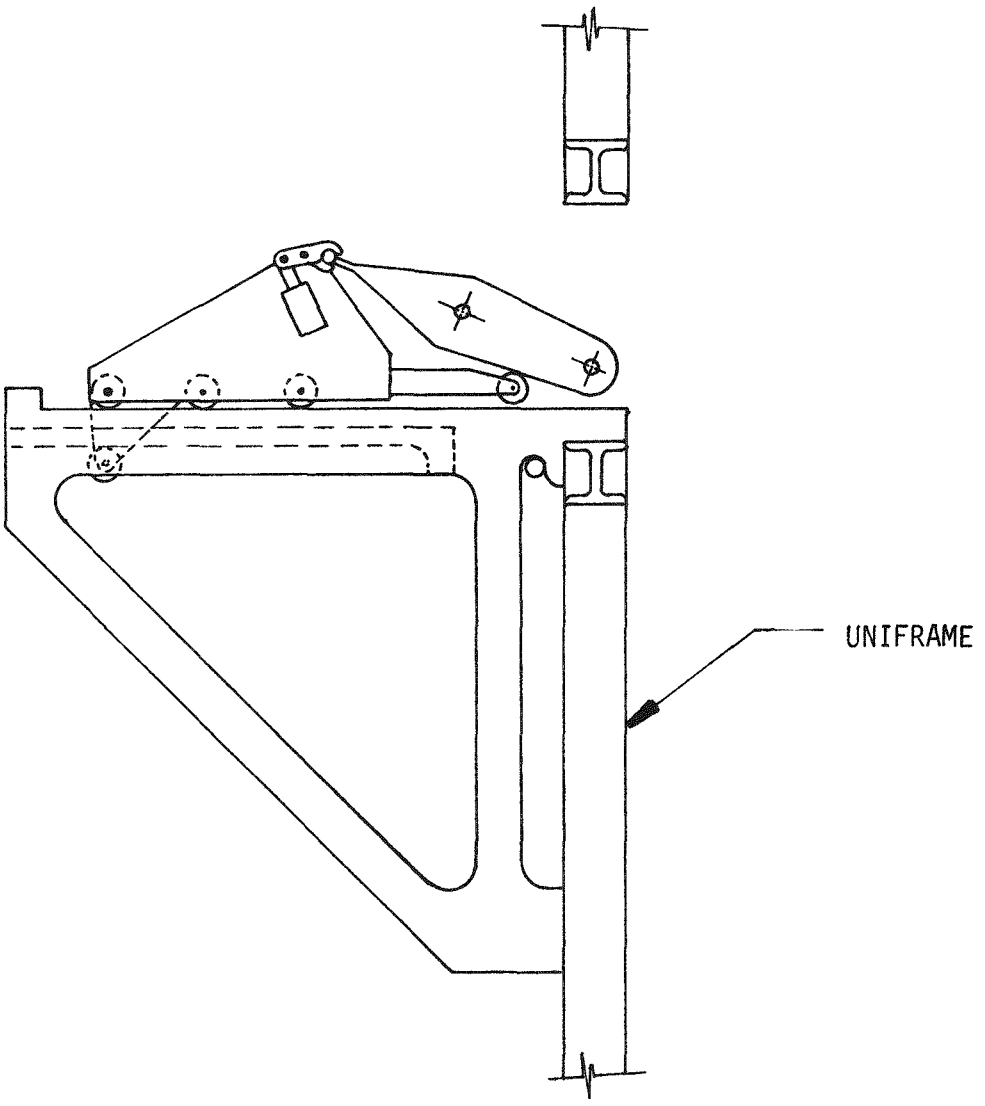

Fig. 8-2. Removal fixture, secondary fixed jaw

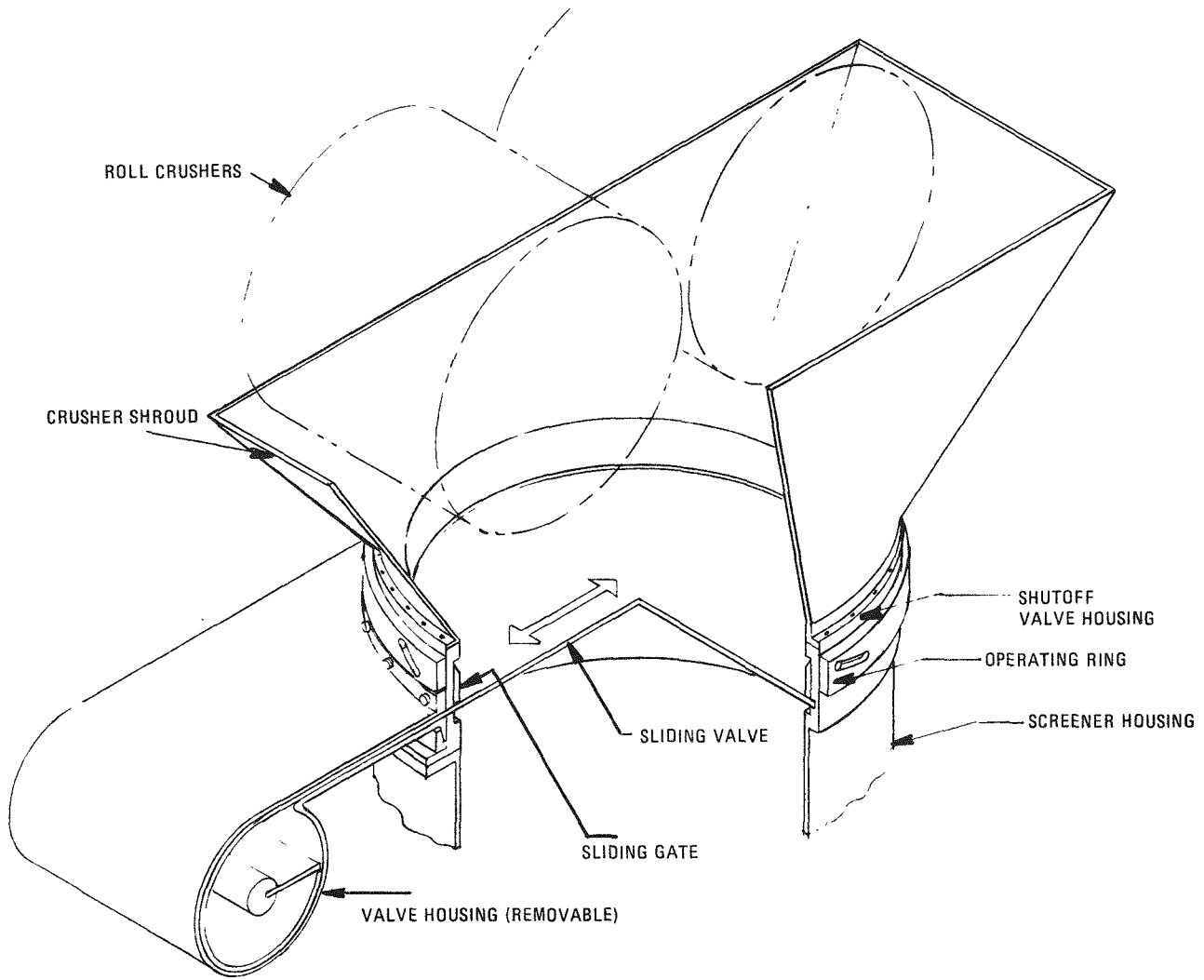

Fig. 8-3. Crusher shroud shutoff valve

The design is in an advanced stage and was accepted at the design review held January 3, 1976. Fabrication of one valve is planned for installation on the base of the crusher shroud. This valve will also adequately demonstrate the effectivity of the screener valve which may be used in a similar form for the closure of the screener top.

8.2. PROTOTYPE PRIMARY AND SECONDARY BURNERS

Installation and maintenance procedures for the plenum cart have been completed and released. Operating and test procedures for all fixtures are now being started.

All semiremote primary and secondary burner fixtures were received this quarter and are now in varying stages of operational readiness as described below.

8.2.1. Tilt-Down Fixture (Fig. 8-4)

The tilt-down fixture is complete and undergoing final painting and load testing. It is anticipated that operational readiness will be compatible with burner initial installation in mid-March 1976.

8.2.2. Tri-Beam Lift Fixture (Fig. 8-5)

The tri-beam fixture is complete including final painting and load test. The fixture will be ready for operation with the primary burner. Final center of gravity adjustments will be made during initial burner installation.

8.2.3. Susceptor and Ceramic Holding Fixture, Primary Burner (Fig. 8-6)

This fixture was received complete. Operational checkout was completed during initial assembly of the primary burner. All operations and interfaces were verified satisfactorily.

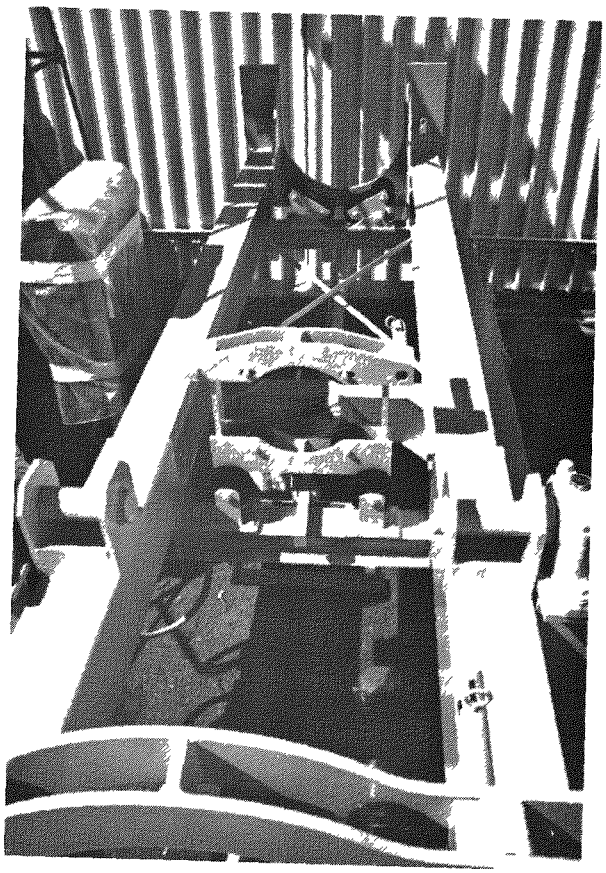

Fig. 8-4. Tilt-down fixture for primary burner

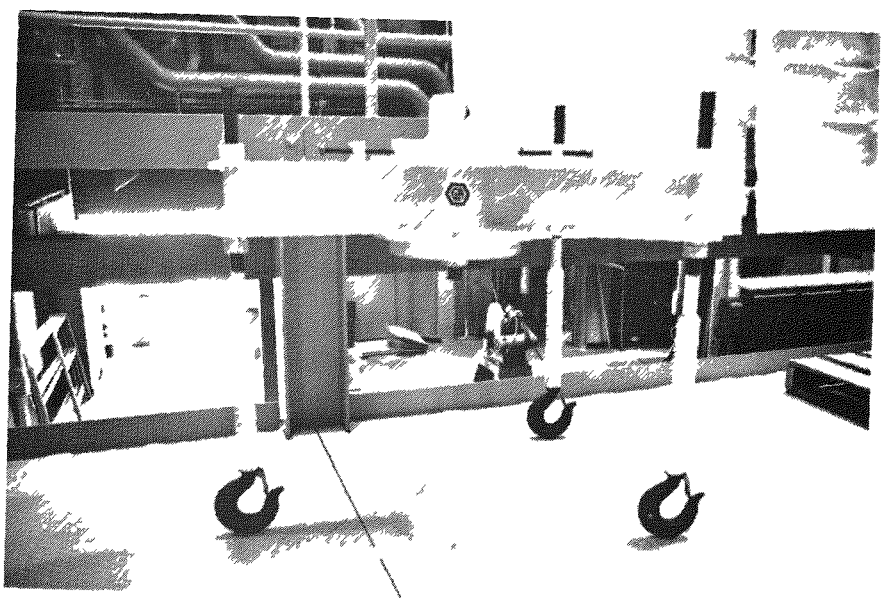

Fig. 8-5. Tri-beam lift fixture for primary burner

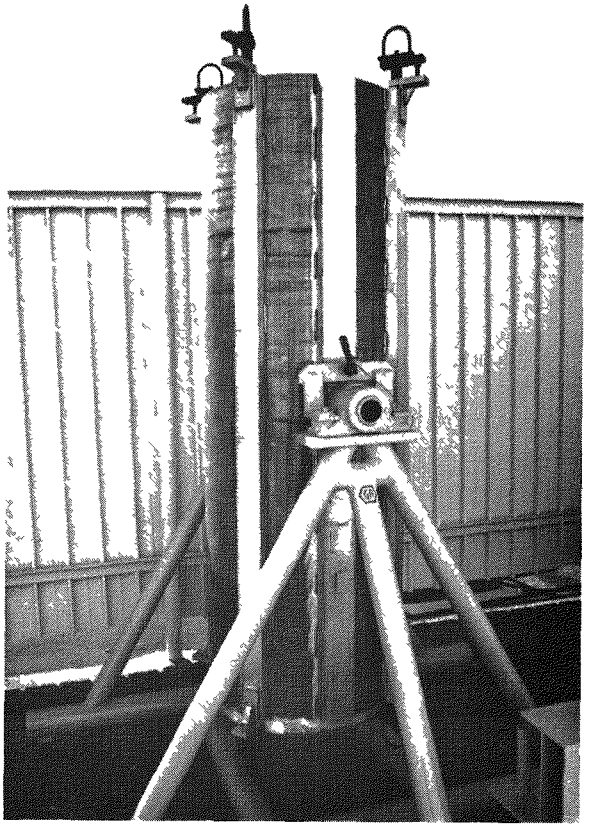

Fig. 8-6. Primary burner susceptor and ceramic holding fixture

8.2.4. Susceptor and Ceramic Removal Fixture (Fig. 8-7)

This fixture was received complete. Operational checkout was partially completed during initial assembly of the primary burner. Major interface operational checks were completed and some necessary adjustments were noted for future correction.

8.2.5. Susceptor and Ceramic Holding Fixture, Secondary Burner (Fig. 8-8)

This fixture was received and is ready for operational checkout.

8.2.6. Heater and Shroud Removal Fixture, Primary Burner (Fig. 8-9)

This fixture is required to facilitate handling the primary burner heating and cooling package. It must be moved from its operating position under the burner support platform laterally to a position which provides vertical access to permit susceptor removal. This fixture will also be used during the initial installation of the burner assembly. Definition of the requirement of this new fixture was provided early in this quarter. Design, detail drawings, procurement, and fabrication have been completed. Installation is well under way with completion planned for the end of this quarter.

8.2.7. Remote Disconnect

Preliminary conceptual design has been started. The design study is investigating various concepts for remote disconnection of a dual purpose electrical and water connector for the primary burner heating coil. Current fiscal year funding covers only conceptual design of the component.

8.3. SECONDARY BURNER

8.3.1. Lift Fixture (Fig. 8-10)

The lift fixture is complete including final painting and load testing and is ready for operation with the secondary burner.

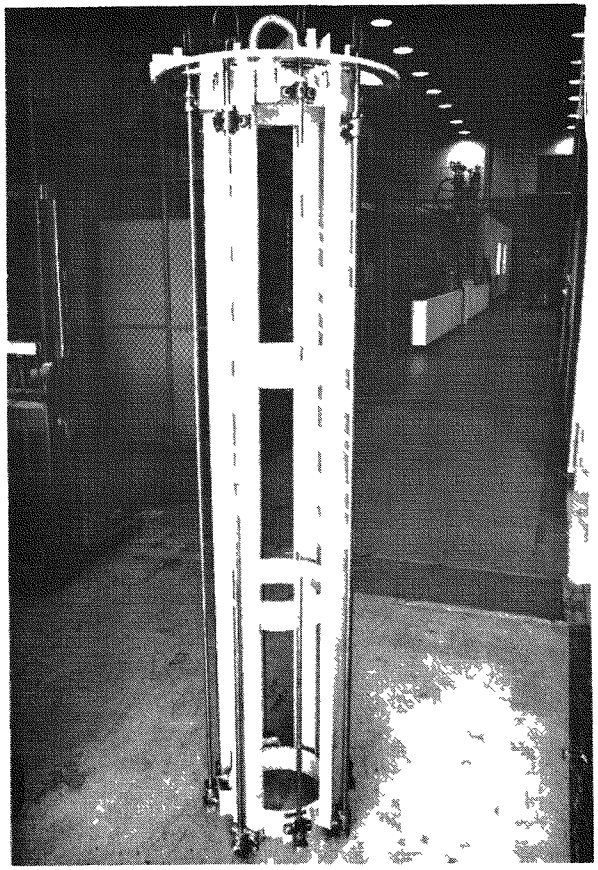

Fig. 8-7. Primary burner susceptor and ceramic removal fixture

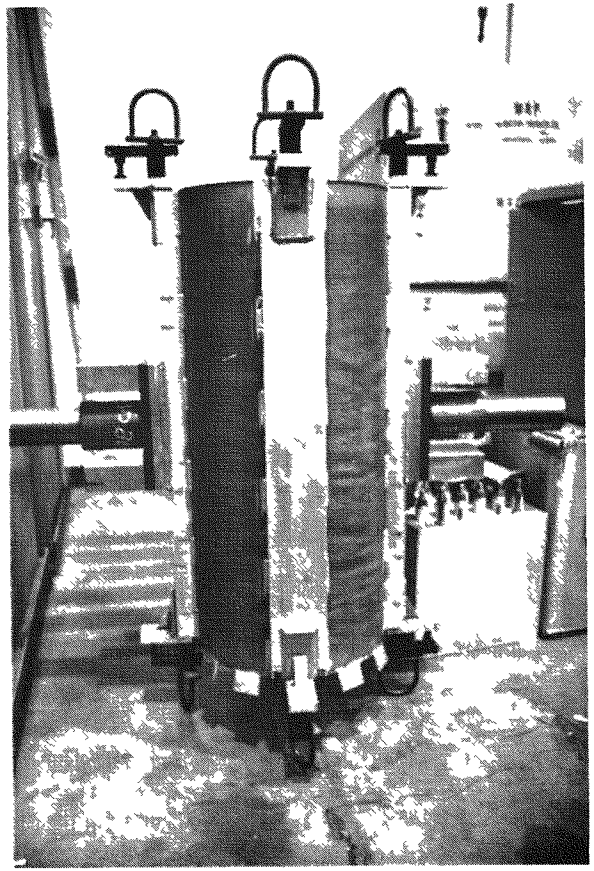

Fig. 8-8. Secondary burner susceptor and ceramic holding fixture

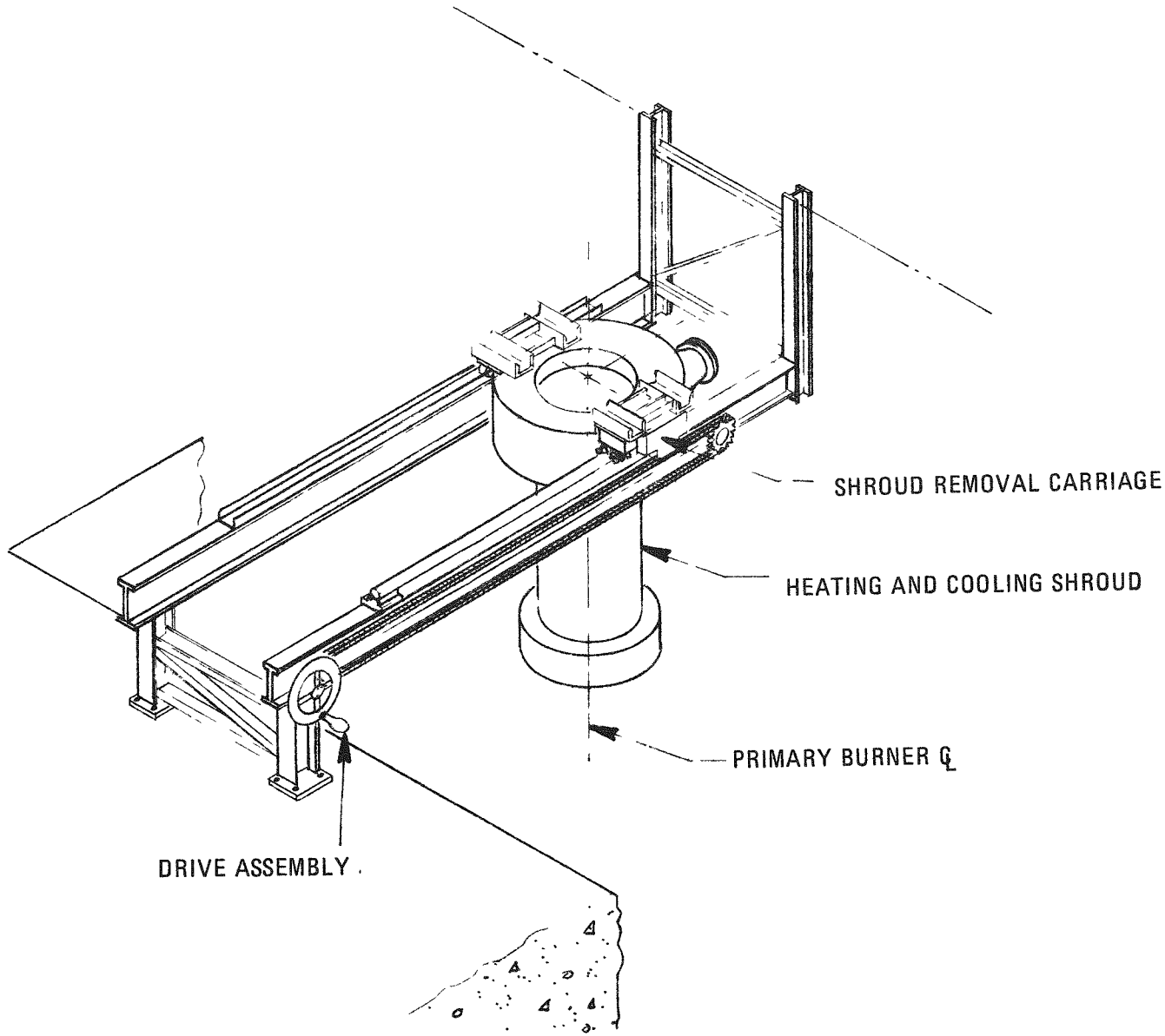

Fig. 8-9. Primary burner heater and shroud removal fixture

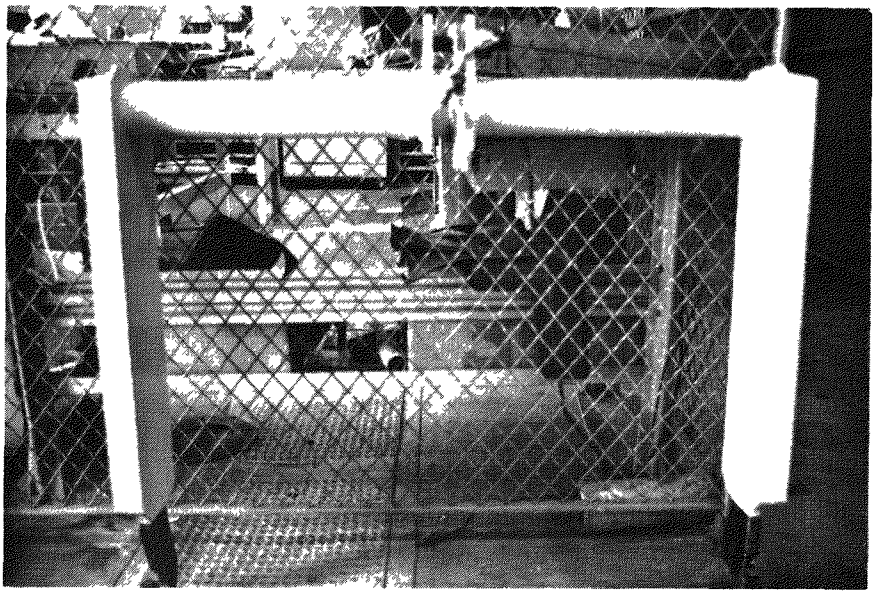

Fig. 8-10. Secondary burner lift fixture

8.4. GENERAL

8.4.1. E-Building 20-Ton Traveling Crane

The crane is now equipped with a control center for the operation of devices suspended from either hook. The facilities provided include two discrete motor control reversible starters, remote control pendant, and self-coiling cable reels. The control center provides for remote control of automatic/manual switching of the transfer functions for the lift shackle and raising features required for the crusher secondary pitman toggle.

8.4.2. Hydra-set (Fig. 8-11)

A Hydra-set auxiliary hoist control has been purchased for use with all lift fixtures. This device is basically a hydraulic cylinder equipped with an accumulator and a manual hydraulic punch. Interposed between the load and the crane hook, the Hydraset provides fine control of vertical displacement (0.001-in. steps) and lifting force to 10 tons indicated on a 6-in. dial via a load cell.

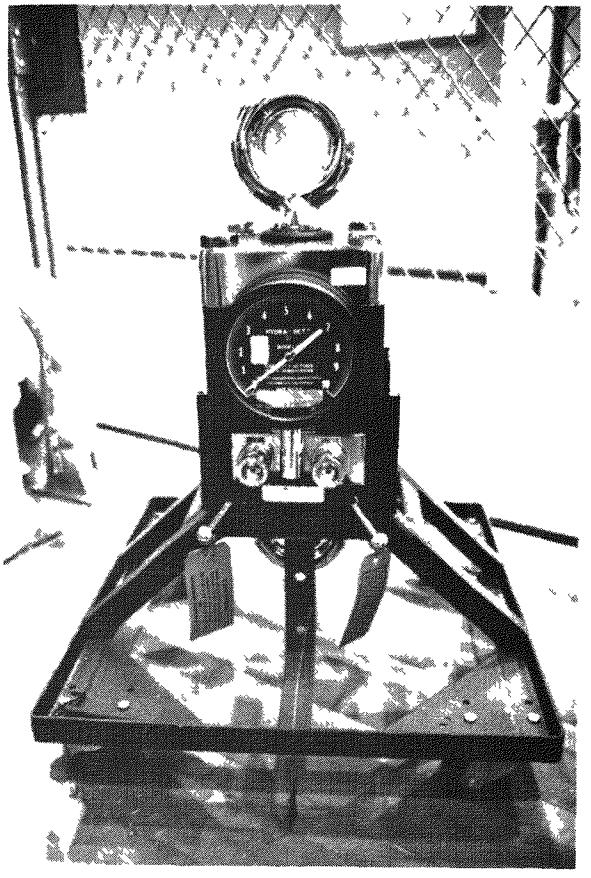

Fig. 8-11. Hydra-set for lift fixtures to provide fine control of vertical displacement

9. ALTERNATIVE HEAD-END REPROCESSING

Scoping work previously under way in this activity has been suspended due to an ERDA directive eliminating this item from the work scope.

10. FUEL RECYCLE DESIGN

10.1. ENGINEERING EVALUATION OF PROCESSES AND EQUIPMENT FOR PRODUCTION REPROCESSING AND REFABRICATION

10.1.1. Flowsheet Review for Production Reprocessing and Refabrication

A critical review of current development activities and engineering and economic studies has been completed to provide a basis for reconfirmation of the reference flowsheet for major HTGR fuel recycle processes and to identify additional development requirements. This review was performed within the context of an HTGR Recycle Demonstration Facility (HRDF), as described in objectives of the Alternate Program for HTGR Fuel Recycle prepared by the ERDA Task Force in April 1975.

Primary objectives of the HRDF are to verify recycle processes and design concepts by operation of a prototypical, integrated recycle facility; to demonstrate a technology base adequate for the design of a commercial-size production recycle plant; and to provide a processing capacity able to accommodate early HTGR fuel recycle needs. The ERDA Thorium Utilization Program is responsible for providing technology and design criteria required to construct and operate this demonstration facility. A reference flowsheet which embodies essential requirements of an operational processing facility and is representative of present technology and development activities is necessary to direct and implement a coordinated development program.

This study derived from a conceptual design of a commercial-size facility, the HTGR Target Recycle Plant (TRP), and from a recent preconceptual design prepared for the HRDF concept. The draft report entitled "Flowsheet Review for Production Reprocessing and Production

Refabrication Requirements" (Ref. 10-1) was forwarded to ERDA-Headquarters, ACC-Idaho, and ORNL for review and comment prior to publishing the report in final form.

10.1.2. Reprocessing Systems Analysis

Systems analyses of processes and equipment required in a production reprocessing facility have been initiated to further define flowsheet requirements and to assess the need for revisions. The analysis discussed below was performed to evaluate the radioactivity of recovered thorium and long-term storage requirements.

Thorium recovered from the reprocessing of spent HTGR fuel contains a significantly higher concentration of Th-228 than does natural thorium. The radioactivity of natural thorium is largely due to the decay daughters of Th-228, so the recovered thorium would have a significantly higher radioactivity level even if no residual fission products were present. Thorium-228 arises from two sources, Th-232 decay and U-232 decay. The pertinent decay chains and half-lives are shown in Fig. 10-1.

The decay daughters of Th-228 all have short half-lives, so for practical purposes the quantity of Th-228 present is a measure of the radioactivity of the thorium. Based on the decay chain shown in Fig. 10-1, the weight fraction of Th-228 in aged natural thorium is 1.334×10^{-10}. The actual weight fraction of Th-228 in fresh HTGR fuel would be somewhat less than this because the thorium purification process would remove the Th-228 parent, Ra-228. Figure 10-2 shows the relative amount of Th-228 in purified thorium as a function of time assuming complete removal of the Ra-228.

Based on the HTGR Design Criteria DC-18-9, Issue D, "Levels of Fission Product, Activation Product, and Actinide Nuclides," the weight fraction of Th-228 in thorium from spent fuel is 1.52×10^{-7} at reactor discharge. This value is three orders of magnitude greater than that in aged natural

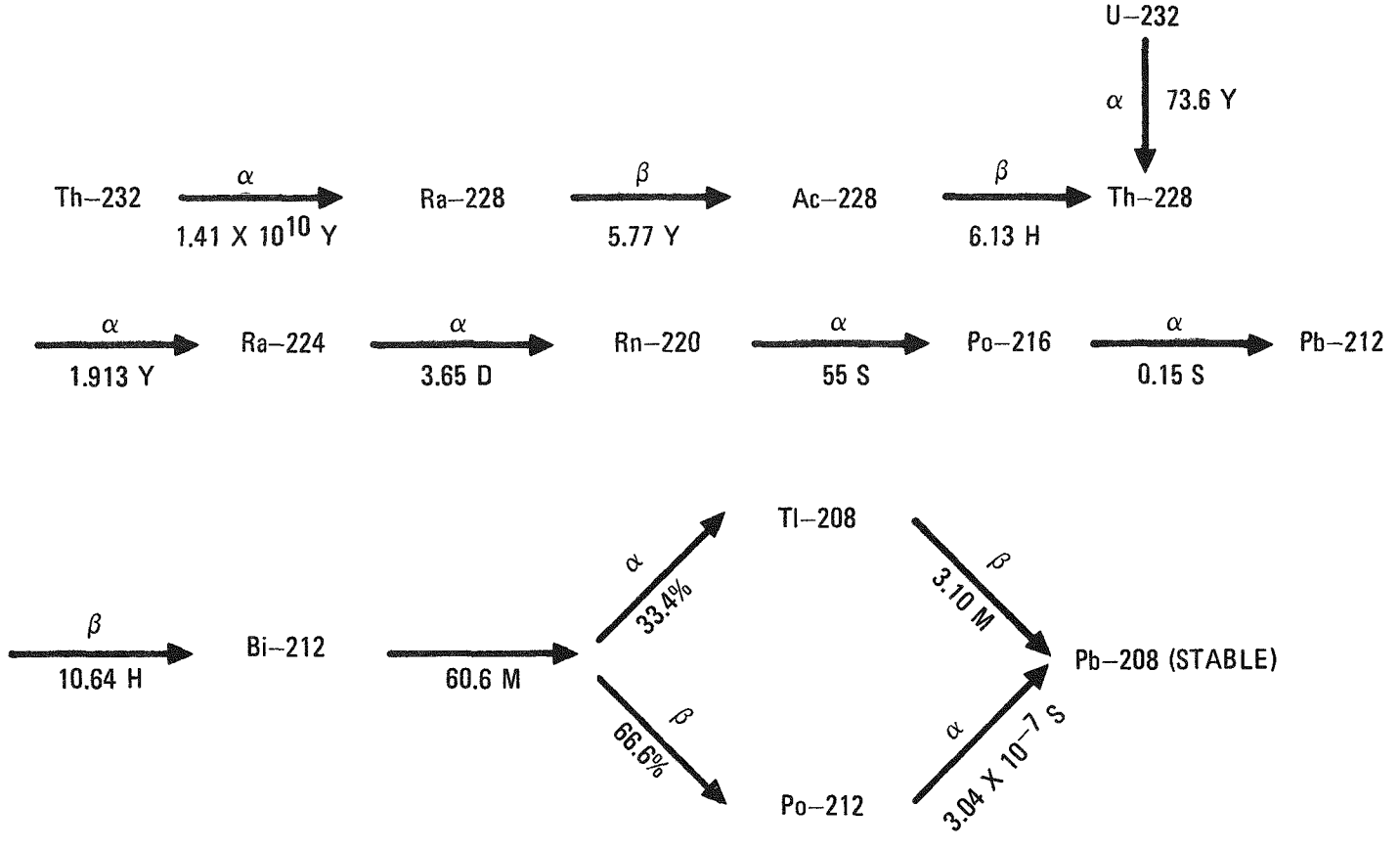

Fig. 10-1. Th-232 and U-232 decay chains

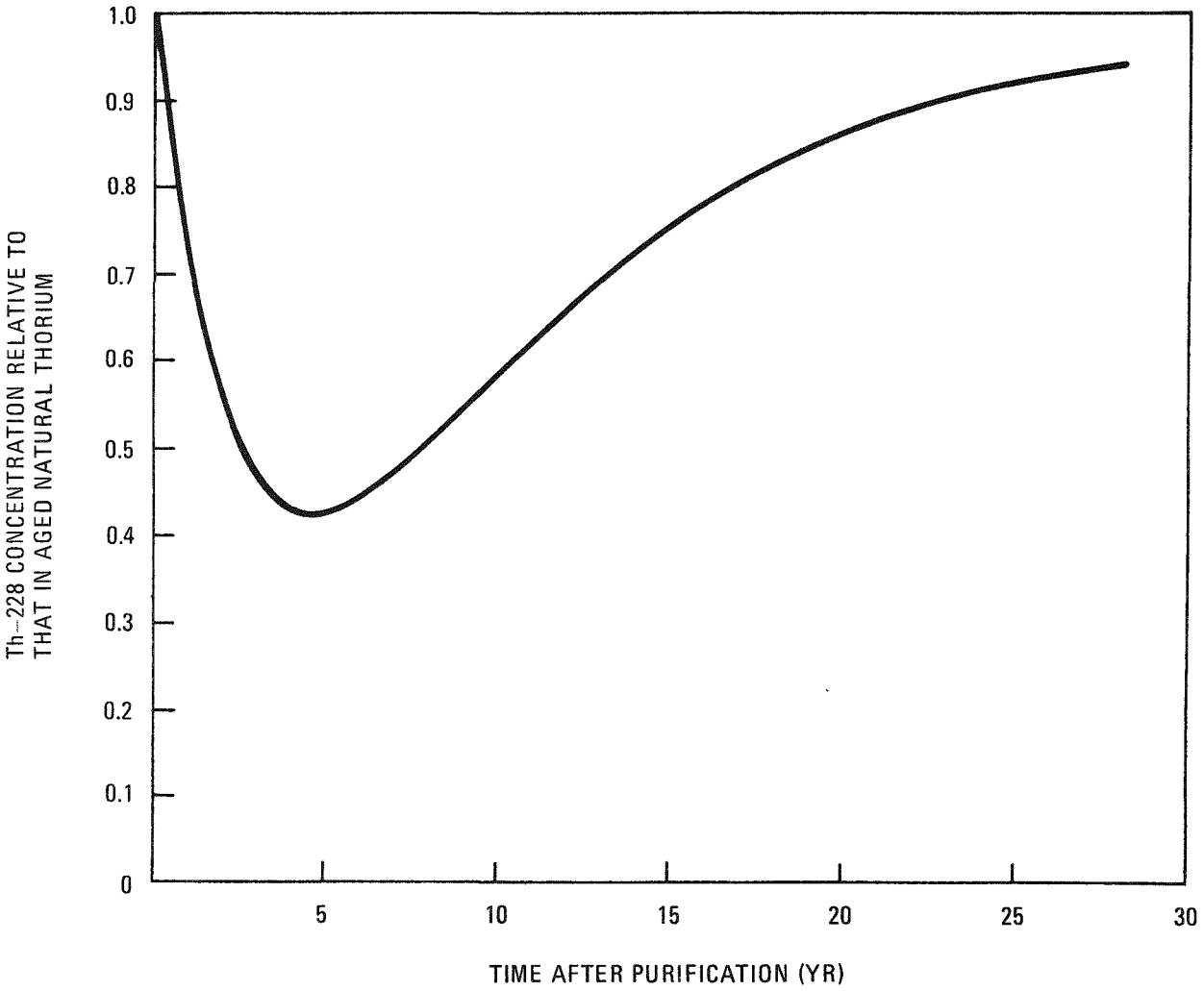

Fig. 10-2. Change in Th-228 concentration following purification of natural thorium

thorium. It would take about 30 yr for the Th-228 to decay to the level of that in natural thorium provided no U-232 is present. It is not reasonable, however, to assume a complete separation of the bred uranium from the thorium. Thus, some residual U-232 will be present in the recovered thorium. Figure 10-3 shows the weight fraction of Th-228 in the recovered thorium as a function of time for varying amounts of residual uranium. The curves are based on a U-232 content in the uranium of 1500 ppm. Figure 10-3 indicates that little additional decrease in Th-228 content occurs after 15 to 20 yr of decay.

The data used in developing the curves in Fig. 10-3 are not completely compatible. The basis for the initial Th-228 content (Design Criteria DC-18-9) assumed the fresh thorium had a Th-230 content of 10 ppm. A U-232 content of about 1500 ppm would result from the use of fresh thorium containing 100 ppm Th-230, which is the upper limit now considered as a fuel manufacturing specification. With the 10 ppm Th-230, the U-232 content in the uranium stream would be about 500 ppm. No data were available on the expected initial Th-228 content from fuel originally containing 100 ppm Th-230, but it certainly would be higher. During fuel storage the Th-228 content continues to increase due to U-232 decay, i.e., a factor of two during 2 yr of storage following reactor discharge. In order to estimate the effects of the higher Th-230 content, as well as spent fuel storage, the Th-228 content as a function of time after separation was calculated for a 2-yr decay and multiplied by three. A residual uranium content of 25 parts per million parts Th was assumed. The dashed curve in Fig. 10-3 illustrates these effects. This curve again indicates the significance of the residual uranium. For storage times of interest (15 to 20 yr), the higher initial Th-228 content increases the recovered thorium activity by a factor of about two. Core analyses with a higher initial Th-230 content are required to confirm the validity of the assumptions made in the above calculations.

Data for the 10 ppm Th-230 fuel indicate the Th-230 content in the recovered thorium is 4 ppm. Thus, the recovered thorium has a significantly lower Th-230 content than the fresh thorium.

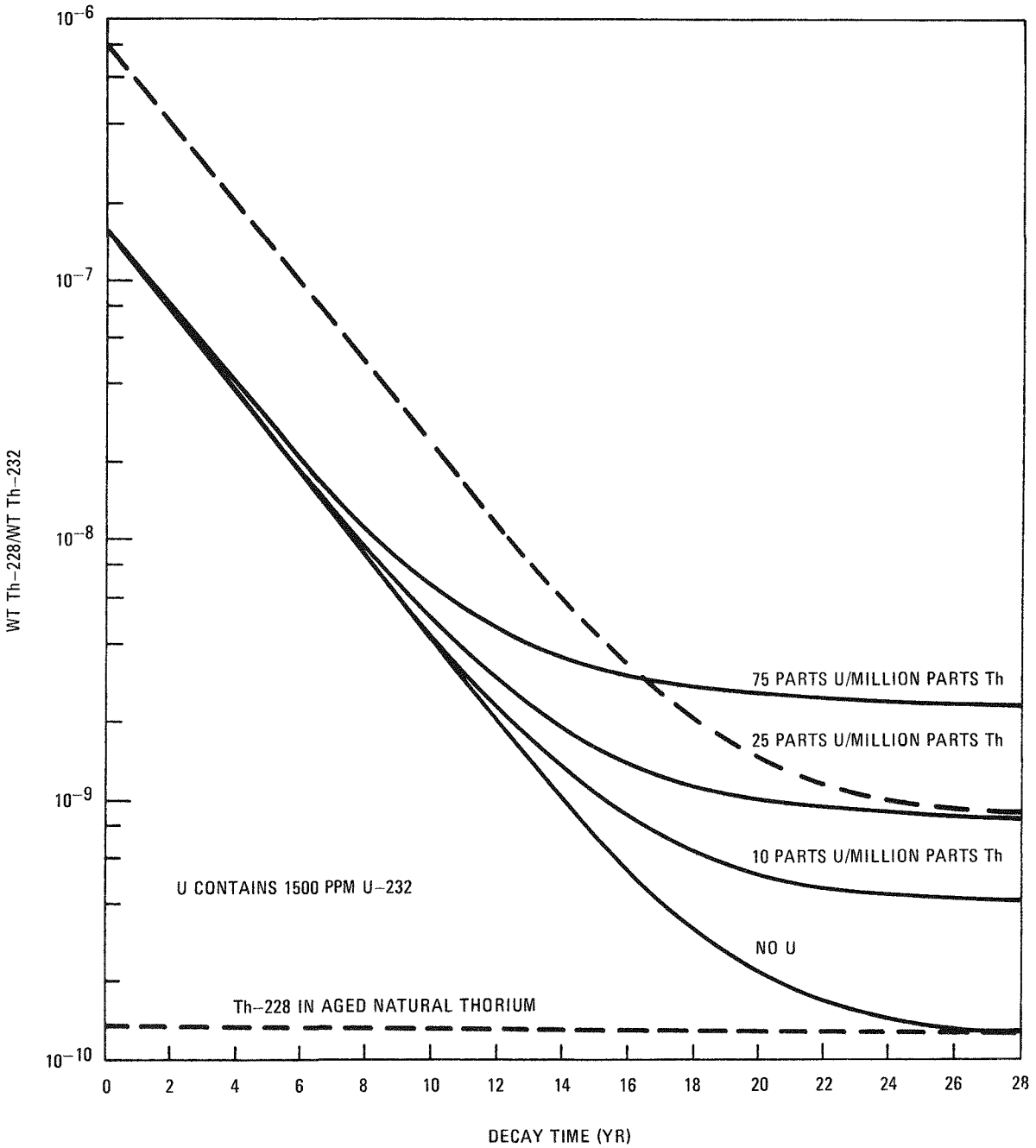

Fig. 10-3. Th-228 content of recovered thorium versus decay time

In the acid-Thorex process, it is possible to achieve a residual uranium concentration in the thorium product of 25 ppm. For this level of residual uranium, the radioactivity level of the recovered thorium would be a factor of 10 higher than that of natural thorium after 16 to 20 yr of decay storage. If this factor of 10 higher activity is the goal for thorium reuse, then the process must assure that the 25 ppm U level can be routinely achieved with a minimum of rework. It does not appear possible to do this with the present flowsheet.

In the current HRDF flowsheet, thorium-uranium partitioning occurs in the first cycle. A second thorium cycle is specified to reduce the fission product and plutonium content of the recovered thorium, but no additional uranium removal would be achieved. Separation of the uranium from the thorium relies solely on the performance of the partition columns. A process perturbation could cause the U content on the thorium stream to increase well above the 25 ppm level, but still below the level where there is a significant uranium loss (the 25 ppm level corresponds to a U loss of about 0.05%). The recycled solvent will contain some residual uranium. Its presence in the 1BS stream reduces the ability of the partition-scrub column to remove uranium from the thorium. A sufficiently high uranium content in the 1BS stream would make it impossible to achieve a 25 ppm U level in the 1BT stream. Pilot plant runs indicate uranium is present in the 100 stream, particularly when DBP is present. In the HRDF flowsheet, the solvent recovery system supplying the 1BS stream treats not only the spent solvent from the partition cycle but also that from the second U-233 cycle and from the first U-235 cycle. A perturbation causing an increased waste loss in any of these strip columns could cause an increase in the uranium content of the recovered thorium.

It is possible to modify the second thorium cycle so as to achieve some uranium removal. This could be done by modifying the operation of the 2E column so that it resembles that of a partition column. The loaded solvent from the 2D column would enter the 2E column some distance from the bottom, and a clean solvent stream (2ES) would be introduced at the bottom.

The 2EX acidity would be increased. With this arrangement uranium in the second thorium cycle would be directed to the 2EW stream. The success of this approach depends on the 2ES stream having a low uranium content. Since the second thorium cycle normally contains low levels of uranium, a separate solvent treatment system dedicated to this cycle would decrease the probability of significant uranium concentrations in the 2ES. As an alternative, the 2ES stream could receive additional treatment, such as passage through a macroreticular resin bed to maintain a low uranium content. In either event, flowsheet modification would result in increasing the acidity of the thorium product.

The higher acidity would reduce the solubility of thorium in the concentrated thorium nitrate product solution unless some product denitration is included. If the thorium is converted to the oxide form for storage, then the higher acidity would have little effect.

The ultimate need for possible flowsheet changes depends on the overall economics of fuel recycle. If the added shielding and attendant maintenance and operating complexities required for handling thorium high in Th-228 are less costly than a somewhat increased complexity of the second thorium cycle, then no flowsheet changes need be considered. A study to further explore these alternatives is planned.

10.1.3. Refabrication Systems Analysis

A technical and economic evaluation of refabrication furnace off-gas pretreatment systems has been initiated. Off-gas handling methods which are currently being developed at ORNL and GA will be evaluated for application to HRDF. The major parameters of interest to this study include (1) initial capital cost, (2) operating cost, (3) technical performance, and (4) effect of the methods on interfacing plant systems and overall plant economics.

10.2. ENGINEERING AND ECONOMIC STUDIES

10.2.1. HTGR Spent Reflector Block Disposal Study

A preliminary evaluation of alternate concepts and associated costs for the disposal of irradiated HTGR reflector blocks has been completed. The alternative methods considered in the study were: (1) burial of the reflector blocks as contaminated waste, and (2) disposal of the blocks by a crush-burn process in a reprocessing facility. The primary objective of the study was to evaluate the relative economics of the two disposal methods alternatives. All cost figures developed in this study are stated in 1976 dollars and refer to cost incurred by the processor or contractor, not cost to the utility which must pay for this service.

The HTGR reflector blocks are hexagonal graphite shapes similar to HTGR fuel elements. Replaceable reflector blocks, which form an envelope surrounding the active reactor core, are either full-length or half-length blocks identical in cross section to fuel elements. After 6, 7, and 8 yr of reactor operation, 500-block segments of reflector blocks are removed from the reactor and replaced. Typical dose rates of spent reflector blocks are given in Table 10-1.

TABLE 10-1
DOSE RATE OF SPENT REFLECTOR BLOCKS
(Bare Blocks, 100-Day Decay, 8-Yr Accumulation, Design Plateout)

	Dose Rate at 1-ft Distance (R/hr)	
Location	Side	End
Side and upper (1 full size)	7.0	4.2
Lower (1 half size)	33.0	31.6

For the purpose of this study, it was assumed that 5000 spent reflector blocks, equivalent to 3550 full-size blocks, are to be disposed of per year. This assumption is consistent with the sizing of a reprocessing plant for 20,000 spent fuel elements per year, such as the proposed HRDF.

Compared to spent fuel elements, spent reflector blocks require much less shielding and generate insignificant decay heat. It is therefore proposed that shipping casks of carbon steel construction with 51 mm of lead as shielding be used, along with carbon steel containers with a capacity of six full-size reflector blocks per container. A truck cask would carry three containers, compared to 12 containers per rail cask.

10.2.1.1. Disposal by Burial

The total cost of disposal by burial includes the transportation cost and the cost of burial. The transportation cost is dependent upon the mode of transport, e.g., special rail service, regular rail service, or truck service, and upon the distance between the reactor site and the burial site.

The burial cost is sensitive to the nature of the radioactive waste (i.e., transuranic or nontransuranic) as well as the level of activities involved. Additionally the burial cost is also dependent on whether the spent reflector blocks are to be buried in sealed containers.

For shipping cost calculation, the following key assumptions are made:

1. The rail shipping unit consisting of cask and car is estimated to cost $800,000/unit. The truck shipping unit consisting of cask and truck trailer is estimated to cost $165,000/unit. In the absence of detailed cask designs, these cost numbers represent an educated guess.

2. The carbon steel shipping container is estimated to cost $4500/unit. Container availability is assumed to be 330 days per year.

3. Cask utilization is assumed to be 300 days per year for rail casks and 330 days per year for truck casks.

4. Depreciation for shipping casks, containers, and rail cars is assumed to be 15 years straight line.

5. Transportation manpower required for project management, cask procurement liaison, customer service, and operations is estimated to be two persons plus 0.65 person per 1000 blocks shipped by rail, or two persons plus 1.3 persons per 1000 blocks shipped by truck. The average annual labor rate is $26,875 per year; an occupancy charge of $10,642 per person per year is assumed for office space, equipment, and associated services.

6. Cask unloading and decontamination labor required at the recycle plant is provided by the recycle plant operator. Cask loading at the reactor site is provided by the reactor site operator.

7. Cask maintenance is subcontracted at an annual cost of $25,000 per rail unit and $10,000 per truck unit.

8. Direct material cost is $1722/rail trip and $414/truck trip for consumable closure hardware, seals, etc.

9. Property taxes are $4133 per rail unit per year and $689 per truck unit per year. Truck license tag expense is $3400 per truck unit per year.

10. Spent reflector block shipping is assumed to be insured for nonradiological transportation accidents at a cost of $230 per rail unit per year and $1378 per truck unit per year. Insurance

for accidents of radiological consequence is assumed to be provided by the utility and/or the recycle operator.

The results of shipping cost calculations led to the conclusion that shipping by truck is the most economical mode of transportation for spent reflector blocks. Therefore, only truck shipping was considered in a subsequent parametric cost comparison study of overall disposal costs for spent HTGR reflector blocks by burial.

The cost of burial is sensitive to the nature of the radioactive waste, i.e., transuranic or nontransuranic, as well as the level of activities involved. Additionally, the cost of burial is also dependent upon the type of container required for burial. Tables 10-2 and 10-3 present costs of reflector block disposal by burial as a function of disposable container cost and shipping distance for nontransuranic waste and transuranic waste, respectively.

Figure 10-4 presents a graphical comparison of the disposal costs of transuranic and nontransuranic spent reflector blocks by burial.

10.2.1.2. Disposal by Processing

In processing the spent reflector blocks at the HRDF facility, it is assumed that a separate process line dedicated to the processing of the reflector blocks will be built. There are basically five operations associated with the spent reflector block processing: shipping from reactor site to HRDF, cask unloading and storage, reflector block crushing, crushed block burning, and off-gas treatment. Other than shipping, each of these operations will be conducted in specific cells or areas.

The spent reflector blocks will be transported in shipping casks as described in Section 10.2.1.1. Shipping by truck has been selected as the most economical mode of transportation for the spent reflector blocks.

TABLE 10-2
COST OF DISPOSAL OF HTGR SPENT REFLECTOR BLOCKS
BY BURIAL AS NONTRANSURANIC WASTE[a]

Disposable Liner Cost ($)	Disposal Cost ($/reflector block)		
	600 Miles[b]	1200 Miles[b]	1800 Miles[b]
0	318	388	465
300	368	430	515
600	418	488	865
1200	518	588	665
2400	718	788	865

[a] All costs are in 1976 dollars.

[b] Distance shipped.

TABLE 10-3
COST OF DISPOSAL OF HTGR SPENT DEFLECTOR BLOCKS
BY BURIAL AS TRANSURANIC WASTE[a]

Disposable Liner Cost ($)	Disposal Cost ($/reflector block)		
	600 Miles[b]	1200 Miles[b]	1800 Miles[b]
0	1262	1346	1438
300	1322	1406	1498
600	1382	1466	1558
1200	1502	1586	1678
2400	1742	1826	1918

[a] All costs are in 1976 dollars.

[b] Distance shipped.

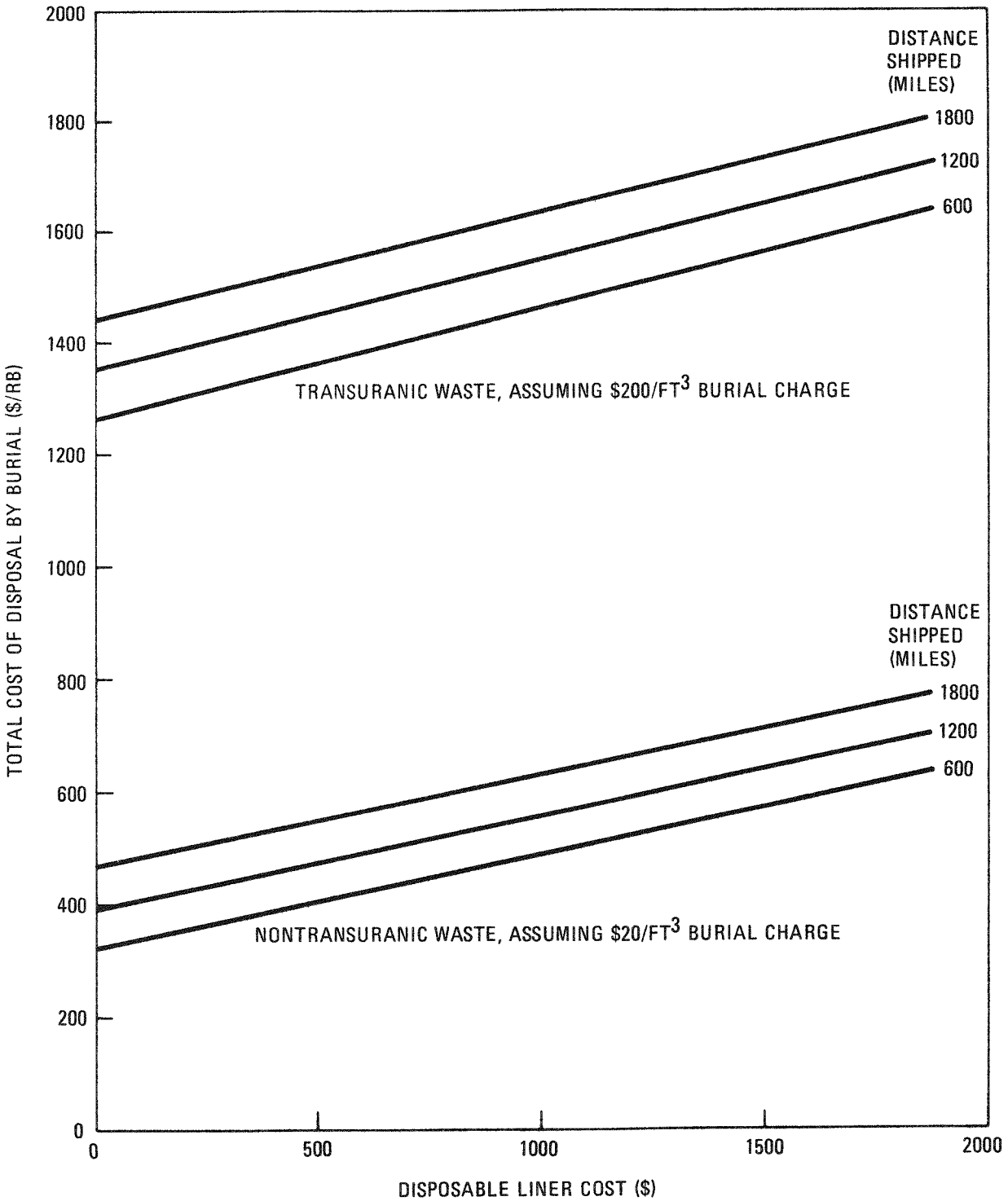

Fig. 10-4. Costs of disposal of HTGR spent reflector blocks by burial

Spent reflector blocks arriving at the HRDF will be unloaded, handled, and transferred to dedicated storage wells in the same manner as described in prior documentation relating to HRDF preconceptual design (Ref. 10-4). The storage wells are steel cylinders suspended from the storage area floor and extend into a cooling area. There are 300 wells, each accommodating two containers. Filtered outside air is circulated once-through to remove heat from the storage area.

For processing, a reflector block container is removed from storage and conveyed by monorail to a dumping bay where the reflector blocks are released from the container to a chute that feeds a UNIFRAME crusher assembly (Ref. 10-5). The UNIFRAME crushing system is designed to reduce reflector blocks to -3/16-in. particles, suitable for fluidized bed burning. Following separation of oversize particles by screening, the crusher product is discharged to a hopper for pneumatic transport to a burner feed/weigh hopper.

The fluidized bed burner, described in Ref. 10-5, has the capacity to combust one full-size reflector block per hour of operation. An inert bed of alumina spheres is used in the burner to aid in controlling the CO/CO_2 ratio in the burner off-gas and to reduce fines generation. Periodic ash removal from the burner and subsequent disposal of this solid waste material is assumed to be required. The off-gas from the burner is treated in a separate off-gas system which incorporates (1) semivolatile fission product removal, (2) iodine removal, (3) CO and tritium oxidation, and (4) tritiated water removal. Design of the components for this off-gas system is assumed to be as described in Ref. 10-4. It is further assumed that krypton and carbon-14 are not present in significant quantities in the spent reflector blocks. The potential cost impact of carbon-14 fixation is, however, reflected in the comparative disposal cost summation shown in Table 10-4.

TABLE 10-4
COST COMPARISON OF DISPOSAL OF HTGR SPENT REFLECTOR BLOCKS BY PROCESSING AND BURIAL(a)
($/Reflector Block)

	Nontransuranic		Transuranic	
	Processing	Burial(b)	Processing	Burial(c)
Without CO_2 fixation	455 - 602	368 - 515	455 - 602	1502 - 1678
With CO_2 fixation	655 - 802	368 - 515	655 - 802	1502 - 1678

(a) All costs are in 1976 dollars.

(b) Including $50/reflector block disposable liner cost.

(c) Including $240/reflector block disposable liner cost.

The cost summary for processing the spent reflector blocks is shown in Table 10-5. The capital and operating costs are broken down into their major components in Tables 10-6 and 10-7, respectively. Variation in disposal cost as a function of scale of operation is shown in Table 10-8.

10.2.1.3. Conclusions

The costs of disposing of HTGR spent reflector blocks by burial and by processing (i.e., crush/burn) have been estimated for a reactor economy requiring disposal of 3550 full-size-equivalent reflector blocks per year, and assuming an HRDF-sized reprocessing plant.

At the design capacity of 3550 full-size reflector blocks per year (i.e., 20 operating HTGRs), the overall costs of disposal are compared in Table 10-4 as a function of two key parameters. The first parameter is the nature of the radioactive waste, i.e., transuranic or nontransuranic, and the second paremeter is the inclusion of CO_2 fixation for burner off-gas treatment, i.e., converting CO_2 into $CaCO_3$. The need for CO_2 fixation arises from the possible presence of an excessive amount of C-14 in the off-gas.

The costs presented in Table 10-4 are based on truck transportation utilizing an 18-element lead-steel cask, which has been found to be more economical than either special rail or regular rail service. Each cost range represents shipping distances between 600 to 1800 miles, and within this shipping range the cost increases approximately linearly with distance.

It is clear from Table 10-4 that disposal by processing would be preferred if spent HTGR reflector blocks were to be classified as transuranic waste. Capital cost in excess of $10 million is required for processing, while less than $3 million is required for burial.

TABLE 10-5
COST COMPONENTS FOR DISPOSAL OF HTGR SPENT REFLECTOR BLOCKS BY PROCESSING[a]

Cost Components	Cost ($)		
	600 Miles[b]	1200 Miles[b]	1800 Miles[b]
Capital depreciation[c]	117	117	117
Operating	120	120	120
Shipping	218	288	365
Total	455	525	602

[a] Operating at 3550 reflector blocks per year. Costs are in 1976 dollars.

[b] Distance shipped.

[c] Capital depreciation based on 20 years straight line.

TABLE 10-6
CAPITAL COST SUMMARY FOR PROCESSING OF HTGR SPENT REFLECTOR BLOCKS[a]
($000)

Cost Components	Labor Cost	Material Cost	Total Cost
040 Site, rail yard, etc.	11	23	34
050 Process building	268	753	1021
020 Reprocessing unit operation			
Crush	110	407	517
Burn	224	1505	1730
Off-gas	319	2147	2466
045 HVAC	52	478	530
015 Storage and cask unloading	211	1810	2021
Total	1193	7123	8318

[a] Capital cost includes building, equipment, and installation costs, but no design cost or contingency is included. Capital cost represents an incremental cost over the HRDF cost. Costs are in 1976 dollars.

TABLE 10-7
OPERATING COST SUMMARY FOR PROCESSING OF HTGR SPENT REFLECTOR BLOCKS[a]

Cost Components	$/Reflector Block
Variable costs	
Direct labor	38
Variable overhead	16
Direct material	11
Fixed costs	19
Operating costs	
Utilities	7
Maintenance material	25
Operating supplies	4
Total	120

[a]Costs are in 1976 dollars.

TABLE 10-8
COSTS OF DISPOSAL OF HTGR SPENT REFLECTOR BLOCKS BY PROCESSING

Scale of Operation (reflector blocks/hr)	Disposal Cost ($/reflector block)		
	600 miles[a]	1200 miles[a]	1800 miles[a]
1000	753	823	900
2000	546	616	693
3550[b]	455	525	602
6000	407	477	554

[a]Distance shipped.

[b]Scale of operation required for twenty 1160-MW(e) HTGRs, which is the design capacity.

10.2.2. U-235 Recycle Benefit/Cost Analysis

The U-235 recycle benefit/cost analysis final report has been delayed in order to incorporate waste disposal effects based on waste quantity and disposal cost calculations currently being generated as part of a separate program, and to incorporate preliminary fuel cycle cost calculations of U-235 recycle effects being generated for a Base Program report. The addition of these two types of information will allow the U-235 recycle analysis to consider benefits of recycling U-235 to the reactor in terms of reduced fresh uranium requirements, the costs of processing U-235 in fuel recycle plants (reprocessing and refabrication), and the cost of spent fuel waste disposal as they occur over a period of time. The final report is expected to be in review by the end of March.

The costs of processing U-235 (26 million initial construction cost and $14 million annual operating cost) in a commercial-scale recycle plant have been evaluated for the effect on price to the utility (fuel cycle cost effect). The results are shown in Fig. 10-5. Reprocessing prices reflect the reduction in capital and operating costs for the deletion of U-235 processing beyond head-end as a reduction in price. However, the loss of revenue from fuel elements refabricated from the U-235 fissile material results in a refabrication price increase even though construction and operating costs are reduced (fewer fuel elements available for amortization of remaining costs). The net effect on fuel cycle cost of the recycle plant cost reduction for deletion of U-235 processing capabilities is therefore negligible.

In addition to the "no U-235 recycle" case, the costs and benefits of alternate modes of U-235 recycle are being assessed for the following cases:

1. Full recycle - all U-233 and U-235 recovered and mixed for continuous recycle.

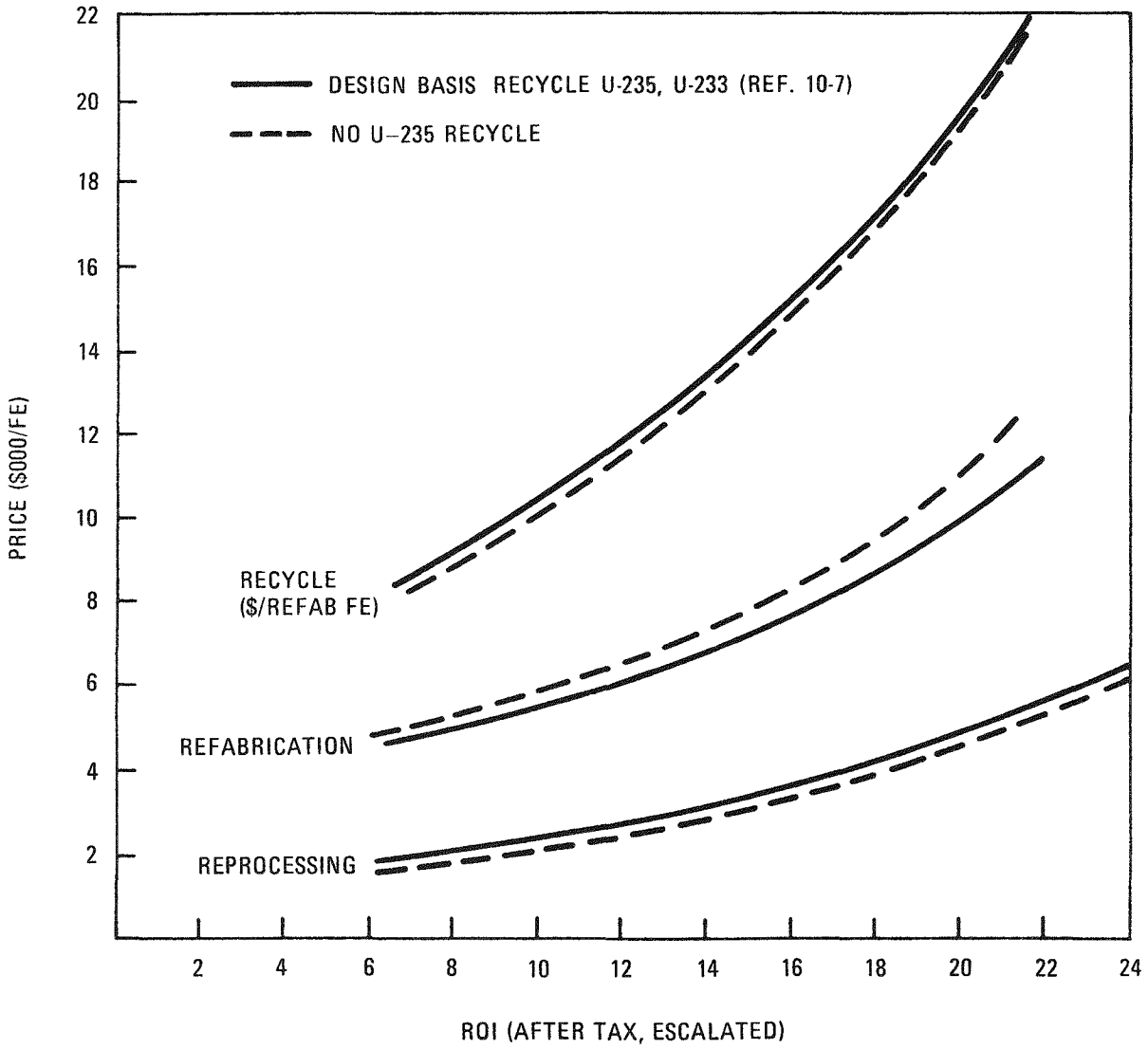

Fig. 10-5. Design basis recycle versus no U-235 recycle (Ref. 10-6)

2. Mixed recycle - U-235 fissile material recovered and mixed with U-233 fissile material for recycle. Retire mixed recycle fissile material.

3. Partial mixed recycle

   a. Variation 1 - U-235 and U-233 fissile material recovered from segments one and two, mixed for recycle, and retired when spent U-235 fissile material is retired from segments 3 and on.

   b. Variation 2 - Mix U-235 fissile material with U-233 from segments 1 and 2. Retire U-233, U-235, and mixed U-233/U-235 spent fissile material from segments 3 and on.

In addition to recycle and waste disposal cost effects, the advantages and disadvantages shown in Table 10-9 are being addressed in the analysis. Preliminary results indicate that the reduction in fresh U-235 fuel requirement significantly outweighs the disadvantages of U-235 recycle.

10.2.3. Spent Fuel Composition and Recycle Mass Flow

The initial run of the modified GARGOYLE code was completed. The core flux spectrum for an HTGR as a function of operating time was prepared and the concentrations of 108 heavy metal nuclides were calculated for one fuel particle type of one fuel element. The additional heavy metal group runs for each particle type in the initial core (I), makeup (M), recycle U-233 (23R), and recycle U-235 (25R) fuel elements were completed. GARGOYLE runs are complete for the first of the three fission product groups (108 fission product and impurity nuclides in each group) for each fuel element and fuel particle type. Calculations for the remaining two fission product groups are in progress.

TABLE 10-9
EFFECTS OF U-235 RECYCLE[a]

	Advantages	Disadvantages
Utility	Reduced fresh U-235 requirements.	Penalty for accompanying U-236.
Recycle plant	Increased plant output (costs amortized over larger number of units).	Operating two different types of processes in solvent extraction.
	Potential revenue from recovered Pu-238.	Less head-end efficiency due to accountability for three types of fuel elements.
	Benefit of early demonstration of high burnup fuel processes (reprocessing I,M fissile particles).	Necessity for separate storage and accountability for two products from refabrication.
Waste handling		Loss of coated particle containment of fission products.

[a] Assumes design basis of twice-through U-235 as compared to throwing away U-235 as fissile particles.

The activation and decay chains utilized in the modified GARGOYLE calculations are illustrated on Figs. 10-6 through 10-8 for the U-235 fissile particle, the U-233 fissile particle, and the fertile particle. Fission product and impurity nuclide activation and decay chains are shown on Figs. 10-9 through 10-11. The heavy metal and fission product nuclide concentrations for each fuel particle, fuel element type, reactor discharge, and reactor reload are written onto a data tape. Nuclide concentration data for the discharge segments are compiled at the time point of reactor shutdown. A composite reactor fuel mass flow case is being calculated to develop typical data for several HTGR fuel cycle modes. The composite cycle used will provide data for an HTGR fuel cycle using no recycle fuel, segregated recycle fuel only, and equilibrium recycle with segregated M, 23R, and 25R elements.

A decay code, NUCLIN, was written and put into production to read the GARGOYLE data tape and to calculate the nuclide concentrations at specified decay times. The code writes a data tape compiled at each decay time for the data array of fuel particle, fuel element type, and reactor discharge segment.

To perform the final compilation and prepare a report form printout, a code LOOKUP has been written. For user specified reactor reloads and decay times, the LOOKUP code reads the NUCLIN data tape, computes the nuclide concentrations in grams or curies per fuel element, and compiles data tables suitable for report printout. Report tabulations will be prepared for specified reactor discharges and reload segments. The discharge segment tabulations will be made for each decay time. Each tabulation will list the nuclides and the nuclide activity or concentration arranged by columns for the fuel element type.

The LOOKUP code is being set up to enable the user to selectively obtain the fuel element composition data in a reasonably condensed form. However, any of the data points calculated by the GARGOYLE or NUCLIN codes are preserved on the data tapes and may be called up by a user for future use to prepare report data or as a tape data file for other calculations.

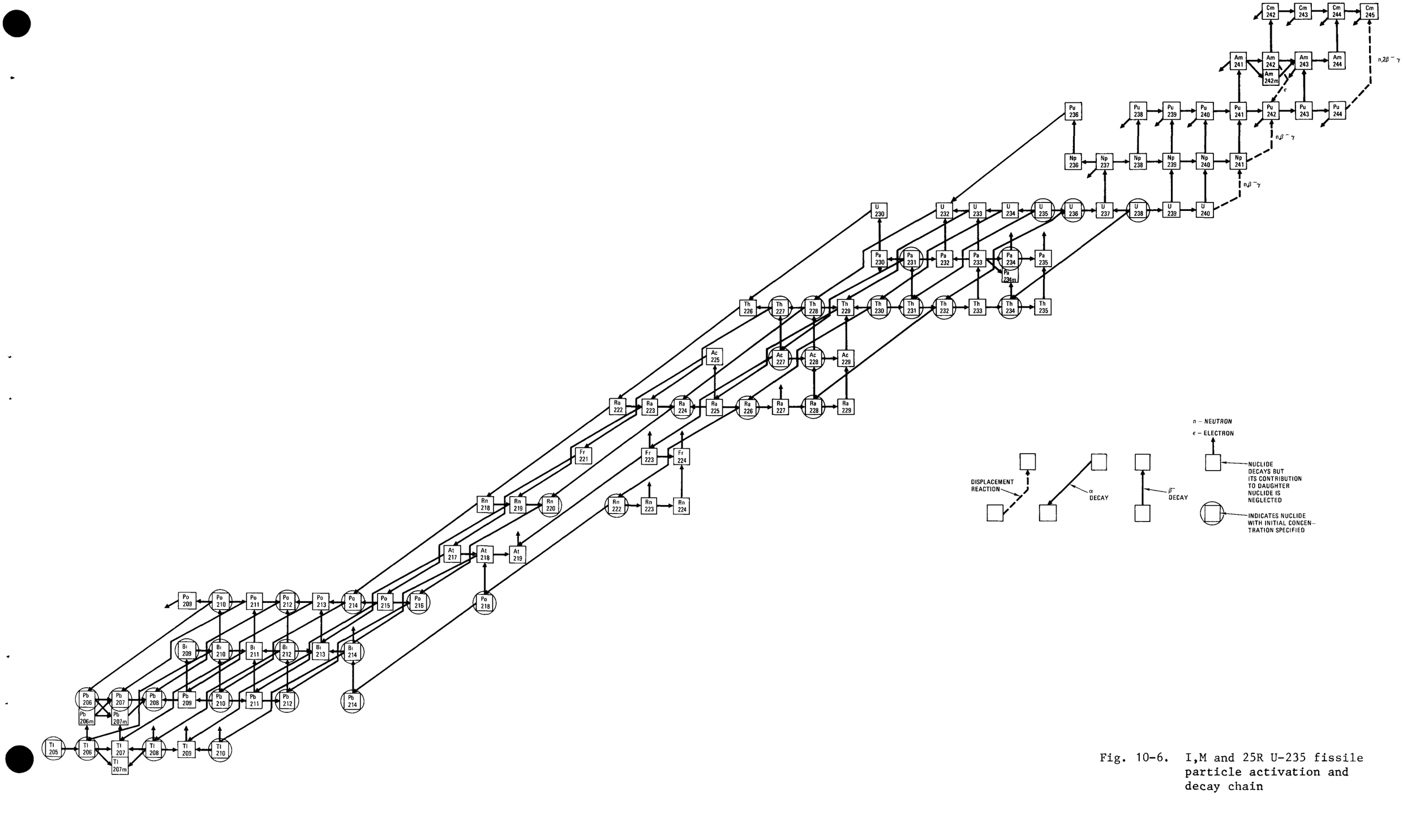

Fig. 10-6. I,M and 25R U-235 fissile particle activation and decay chain

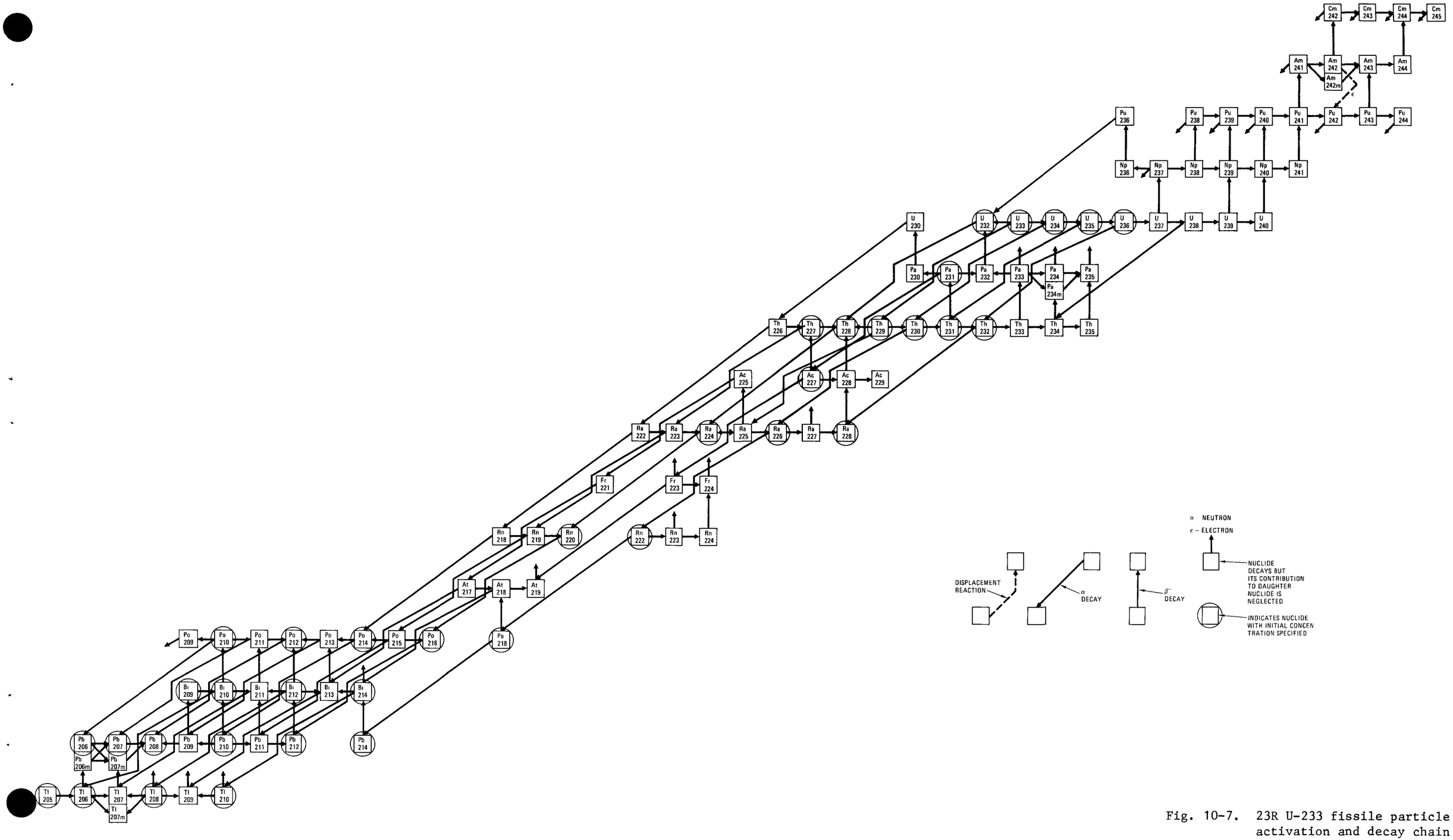

Fig. 10-7. 23R U-233 fissile particle activation and decay chain

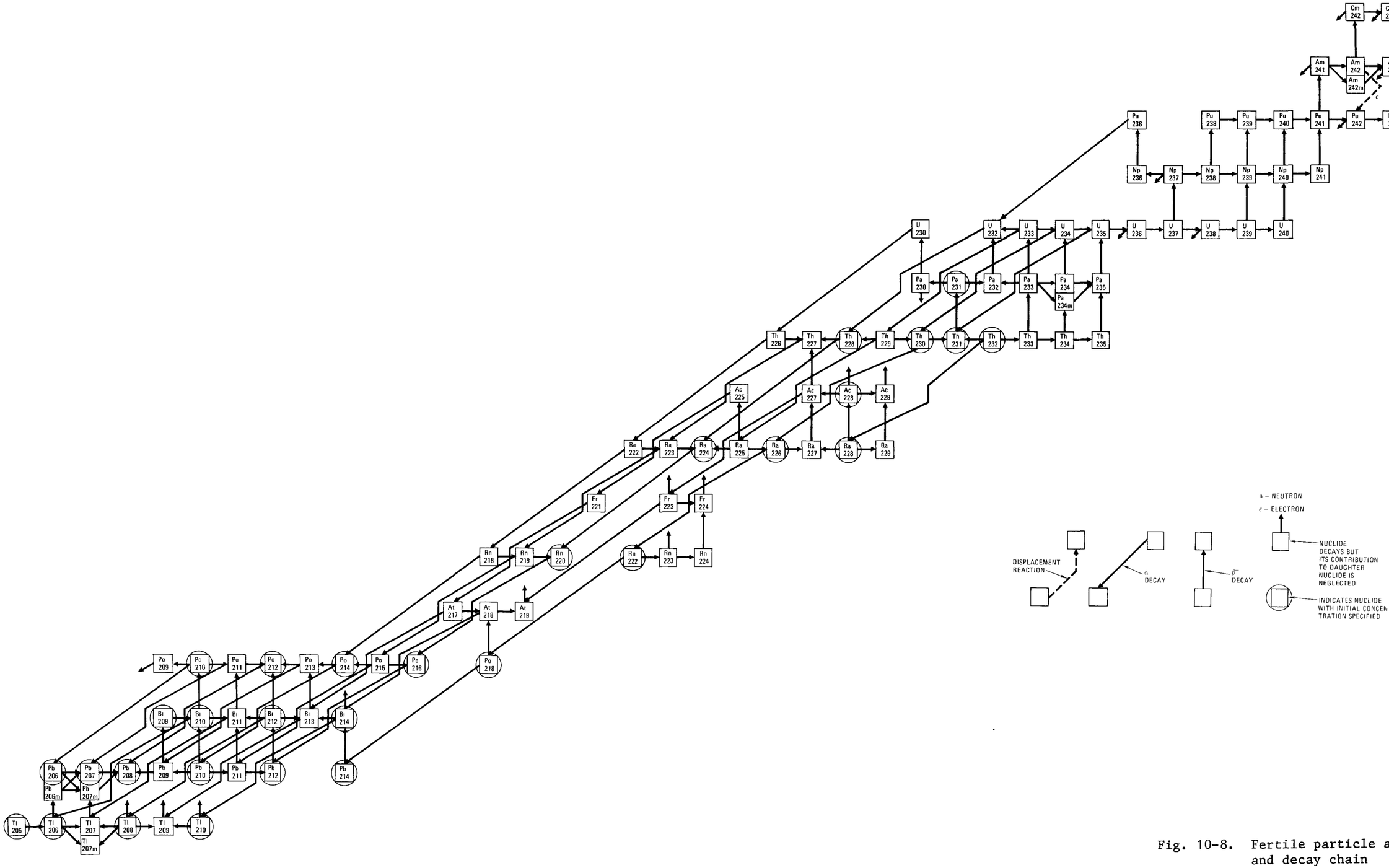

Fig. 10-8. Fertile particle activation and decay chain

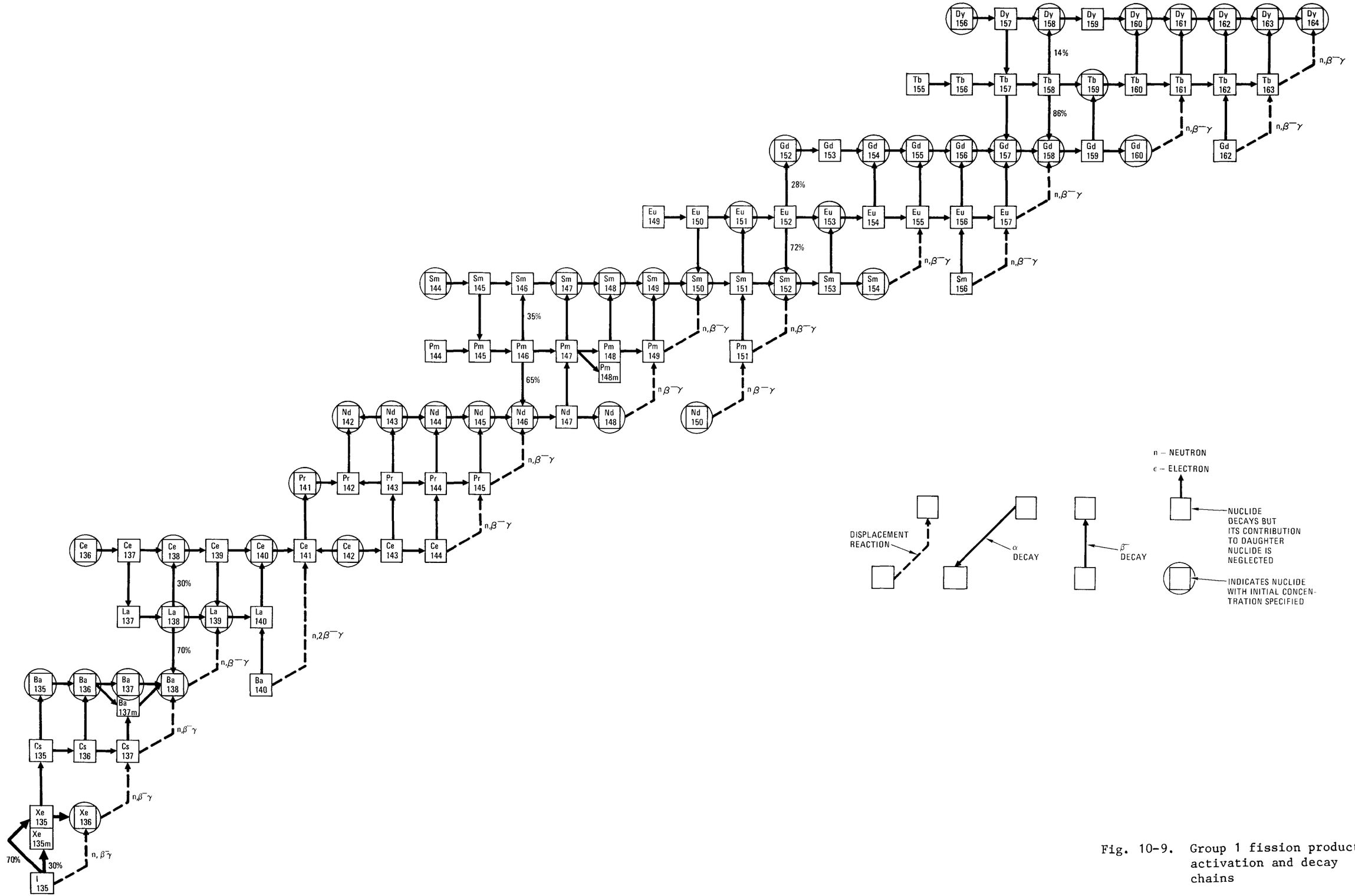

Fig. 10-9. Group 1 fission product activation and decay chains

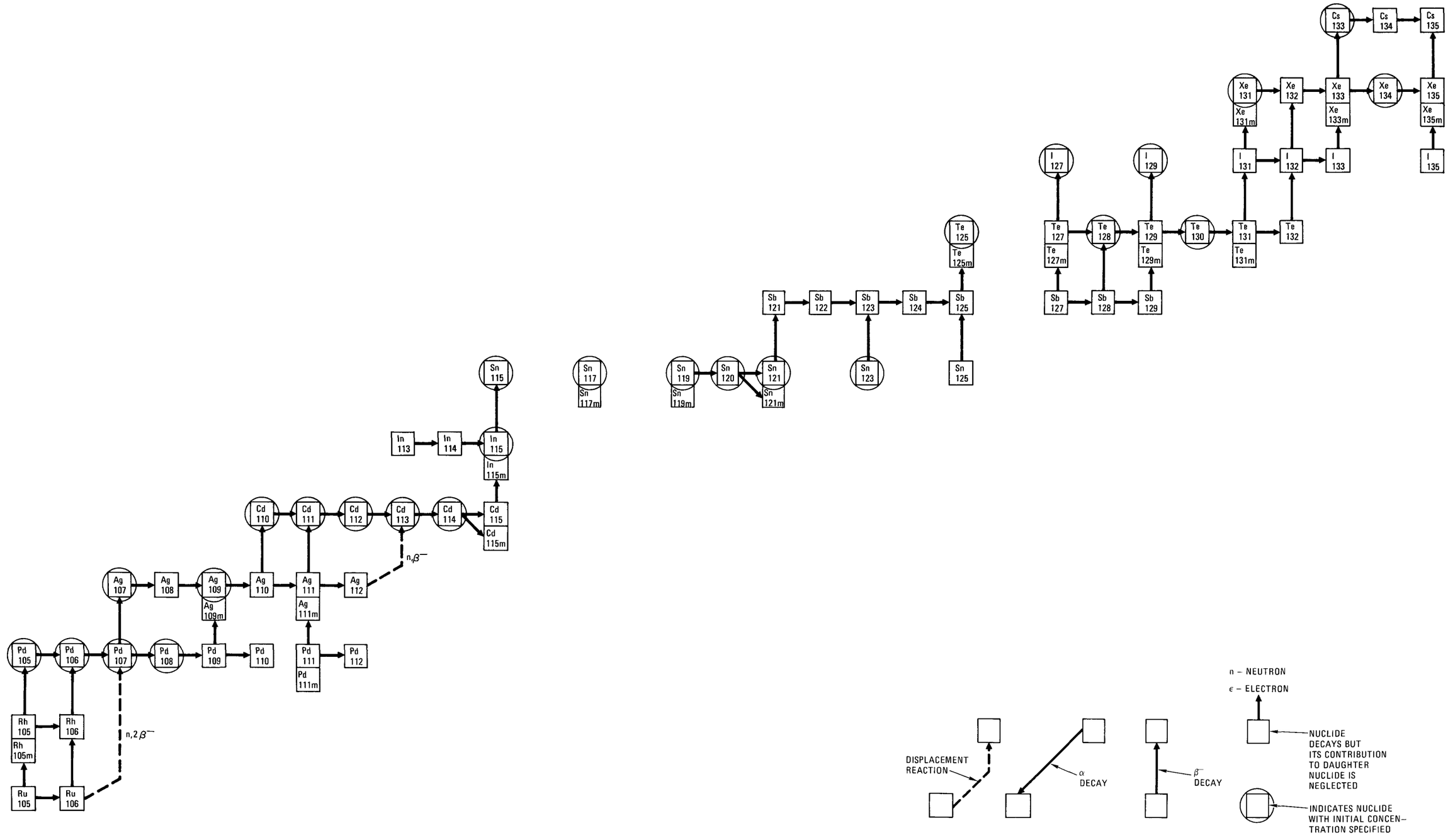

Fig. 10-10. Group 2 fission product activation and decay chains

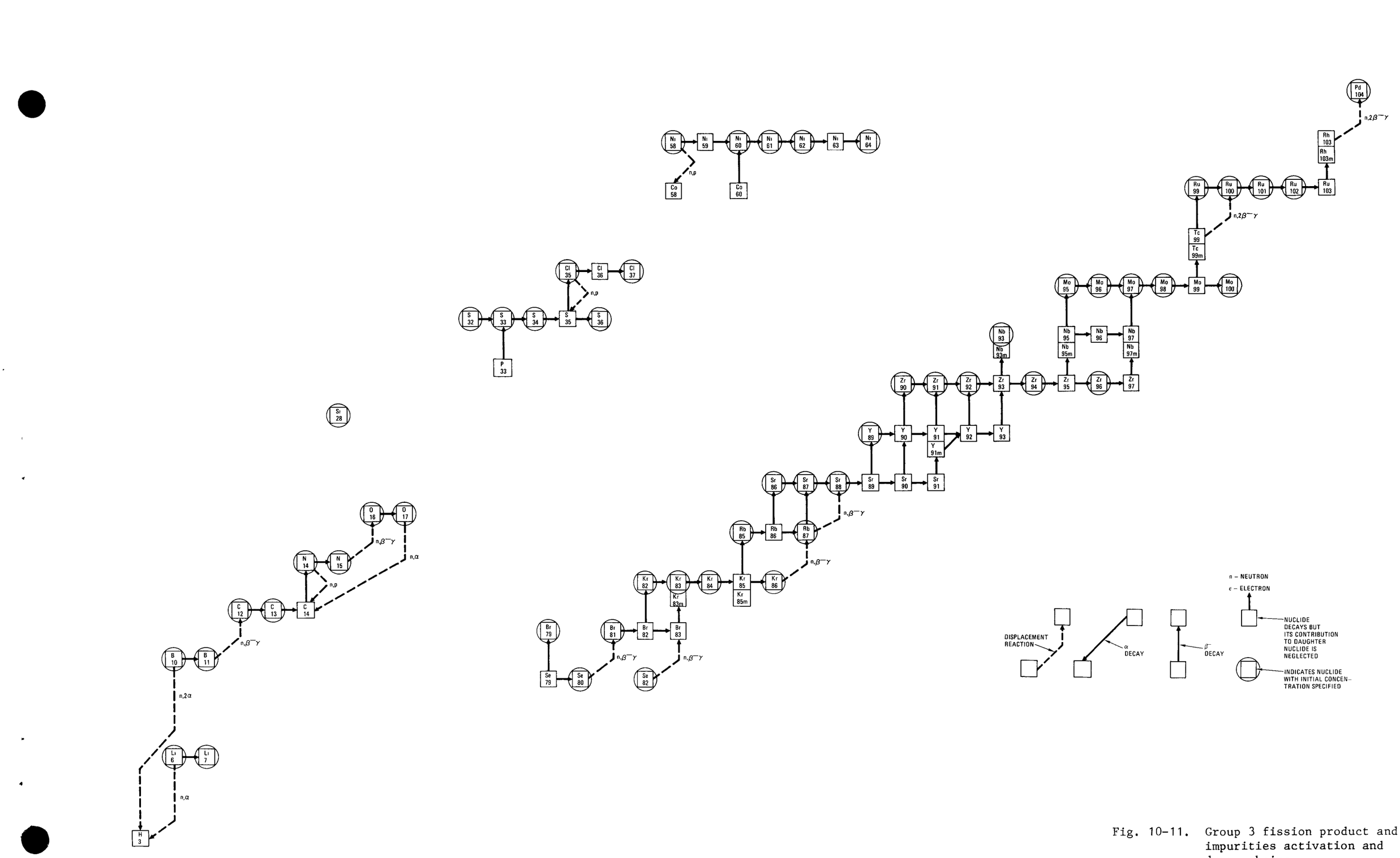

Fig. 10-11. Group 3 fission product and impurities activation and decay chains

REFERENCES

10-1. "Flowsheet Review for Production Reprocessing and Production Refabrication Requirements," General Atomic Report GA-A13751, to be published.

10-2. "High-Temperature Gas-Cooled Reactor Spent and Recycle Fuel Shipping," General Atomic Report GA-A13395, April 1975.

10-3. Engholm, B. A., General Atomic, private communication, January 1976.

10-4. "Preconceptual Design and Estimate Summary for HTGR Recycle Demonstration Facility (HRDF)," General Atomic Report GA-A13502 (Draft), July 1975.

10-5. Heath, C. A., and M. E. Spaeth, "Reprocessing Development for HTGR Fuels," General Atomic Report GA-A13279, February 15, 1975.

10-6. Rothstein, M., "U-235 Recycle Effects on Recycle Prices," General Atomic unpublished data, November 26, 1975.

10-7. "Conceptual Design Summary and Design Qualifications for HTGR Target Recycle Plant," General Atomic Report GA-A13365, April 30, 1975.

APPENDIX A

PROJECT REPORTS PUBLISHED DURING THE QUARTER

Rickman, W. J., "Interim Development Report for Secondary Burner," ERDA Report GA-A13540, General Atomic Company, December 25, 1975.

Stula, R. T., D. T. Young, and H. H. Yip, "Interim Development Report for Primary Burner," ERDA Report GA-A13546, January 5, 1976.

APPENDIX B

DISTRIBUTION LIST

J. BROIDO	E-155	J. F. WATSON	L-640
L. BROOKS	SV-101	B. BAXTER	E-177
R. C. DAHLBERG	L-503	A. E. HUTTON	E-170
G. B. ENGLE	L-364	R. D. ZIMMERMAN	E-179
W. V. GOEDDEL	SV-101	R. H. HANSEN	EA2-208
A. J. GOODJOHN	E- 217	M. H. MERRILL	L-510
T. D. GULDEN	L-444	J. HOLZGRAF	L-424
J. JAYNE	S-137	N. CARNEY	E-086
S. LANGER	TO-559	S. T. ALMODOVAR	EA2-204
C. S. LUBY	L-608	G. E. BENEDICT	E-249
D. R. MATHEWS	TO-406	R. K. KIBBE	E-170
G. B. MELESE d'HOSPITAL	TO-365	J. W. ALLEN	E-171
C. A. HEATH	E-166	H. REESER	E-172
C. L. RICKARD	L-205	R. M. BURGOYNE	E-165
O. STANSFIELD	L-440	D. T. PENCE	E-243
H. B. STEWART	L-602	A. S. BALLARD	E-160
J. J. SHEFCIK	E-244	P. L. WARNER	E-167
R. F. TURNER	L-507	F. CARPENTER	E-161

LEGAL

WASHINGTON

15 DOCUMENT CENTER

161 TIC

1 V. A. Magliano, Director, Contract Services Division
U.S. ERDA
San Francisco Operations Office
1333 Broadway
Oakland, Ca. 94612

1 J. B. Radcliffe
PMIC-SD

1 Assistant Director, Commercial Fuel Cycle Division of Nuclear Fuel Cycle and Productions
U.S. ERDA
Washington, D. C. 20545

2 Chief, HTGR Fuel Recycle Branch
Division of Nuclear Fuel Cycle and Productions
U.S. ERDA
Washington, D.C. 20545

1 Project Manager, HTGR Fuel Reprocessing Development
Allied Chemical Corp.
P. O. Box 2204
Idaho Falls, Idaho 83401

1 Director, Research and Technical Support Division
Oak Ridge Operations Office
U.S. ERDA
P. O. Box E
Oak Ridge, Tennessee 37830

1 Director, Advanced Gas-Cooled Reactor Programs
Attention: P. R. Kasten
Oak Ridge National Laboratory
P. O. Box X
Oak Ridge, Tennessee 37830

1 Office of the Manager
Idaho Operations Office
U.S. ERDA
Idaho Falls, Idaho 83401

1 G. W. Hogg
1 J. A. Rindfleisch
1 W. B. Palmer
Allied Chemical Corp.
550 Second St.
Idaho Falls, Idaho 83401

1 V.C.A. Vaughen
Chemical Technology Division
Union Carbide Co.
P. O. Box X
Oak Ridge, Tennessee 37830

1 W. D. Woods
1 E. E. Fisher
R. M. Parsons Co.
Pasadena, Ca. 91124

1 Chong Lewe
Nuclear Utility Services
4 Research Place
Rockville, Maryland 20850

1 W. G. Price
Vice President - Generation
Delmarva Power and Light
800 King St.
Wilmington, Delaware 19899

1 J. D. Hornbuckle
So. Calif. Edison
P. O. Box 351
Los Angeles, Ca.

1 G. F. Daebeler
Branch Head, Safety and Licensing
1 R. F. Manty
Branch Head, Fuel Management
1 H. D. Honan
Philadelphia Electric
2301 Market St.
Philadelphia, Penn. 19101

1 P. U. Fischer
1 R. Finkbeiner
General Atomic Europe
Weinbergstrasse 109
8006 Zurich
Switzerland

1 K. Paulovich
General Atomic International
c/o Pacific Gulf Oil, Ltd.
P. O. Box 43
Akasaka, Tokyo
Japan 107

1 J. Ganley
GAC Fuels Group
France
(via M. H. Merrill)

1 Mr. Claude Moreau
Commissariat a l'Energie Atomique
Centre d'Etudes Nucleaires de Saclay
BP No. 2
91190 Gif-sur-Yvette
France

1 J. L. McElroy
Battelle Northwest Laboratories
P.O. Box 999
Richmond, Washington 99352

1 Dr. K. Hackstein
HOBEG
6450 Hanau/Main
Postfach 787
Germany

1 Dr. D. Stoelzl
Hochtemperatur Reaktorbau Gmbh
Gottlieb-Daimler-Strasse 8
D-68 Mannheim - 1
Postfach 5360
Germany

1 K. Natz
1 J. Snider
Oak Ridge National Laboratory
Oak Ridge, Tennessee 37830